THE STUDY OF THE EFFECT ON THE TWO-PHASE LOCAL HEAT TRANSFER COEFFICIENT OF DISCONTINUITIES IN THE FLOW AREA OF A HEATED ANNULAR PASSAGE

by

Alan Watson

A thesis presented for the Degree of Doctor of Philosophy
at the University of Aston in Birmingham

May 1973

CONTAINS PULLOUTS

SUMMARY

In almost all heat transfer equipment the fluids involved must pass through changes in section of the flow passage which are generally unavoidably present because of constructional requirements.

A survey of previous work has shown that the effect of these changes in section upon the heat transfer coefficient between the heating surface and the fluid have been studied for the cases of simple geometries with a single phase fluid but not at all for the case of a two phase fluid flowing through an annular flow section with a step change in the flow area.

An experimental arrangement to measure the heat transfer to water/steam flowing through an annulus with an electrically heated inner wall, and a step change in the flow section, was constructed. Results were obtained for the effect of both a convergent and a divergent step change in section, upon the heat transfer coefficient between the heating surface and the fluid, for both single and two phase flow.

In developing this experimental equipment a new type of radiation thermocouple was constructed to provide a continuous axial temperature profile of the inner surface of the heating tube, and a computer programme was written to demonstrate that the axial conduction of heat in the heating tube was negligible.

The heat transfer results were supported by flow visualization studies using air bubbles in water and also by using a schlieren optical system with colour filters to demonstrate the behaviour of the boundary layer.

The effect of the step change was compared with results obtained by previous workers from measurements taken with water flowing through a tube of cicular section.

Additional to the step change in section the equipment was modified to measure the effect of swirl upon the heat transfer coefficient for both single and two phase flow. The results were plotted graphically and the effects explained.

ACKNOWLEDGEMENTS

The author expresses his thanks to his advisor and supervisors Professor A.J. Ede, Mr. D.C. Hickson and Mr. J.P. Bertinat for guidance and the provision of research facilities.

CONTENTS

PRESENT WORK

APPLICATION OF RESULTS

CONCLUSIONS

APPENDICES

BIBLIOGRAPHY

NOMENCLATURE

A	area	m^2
c	specific heat	kJ/kg K
d	diameter	m
G	mass velocity	kg/m^2s
h	heat transfer coefficient	kW/m^2K
h	enthalpy	kJ/kg
k	thermal conductivity	kW/mK
p	pressure	bar = 10^5 N/m^2
$q/A = \phi$	heat flux	kW/m^2
t	temperature	^oC
T	temperature	K
$\Delta t_e = t_e - t_s$	effective superheat	K
$\Delta t_{sub} = t_s - t_b$	degree of subcooling	K
$\Delta t_x = t_w - t_s$	wall superheat	K
v	specific volume	m^3/kg
V	velocity	m/s
x	dryness fraction	-
X	dT_s/dp	m^2K/N
Z	$-(\rho_f/\rho_g)/dp$	m^2/N
ρ	density	kg/m^3
σ	surface tension	N/m
μ	viscosity	kg/ms
τ	period of bubble growth/collapse cycle	s

Subscripts

b	bulk
bo	boiling
bu	bubble
c	forced convection
cal	calculated
e	effective
exp	experimental
f	liquid
fi	film
fg	liquid to gas
g	gas
i	inner
mac	macro convective single phase mechanism
nbo	non-boiling
o	outer
p	constant pressure
s	saturated
sub	subcooled
sp	single phase
tp	two phase
w	wall

Dimensionless groups

Bo boiling number $\dfrac{q/A}{G\, h_{fg}}$

Nu Nusselt number $\dfrac{hd}{k}$

Pr Prandtl number $\dfrac{c_p \mu}{k}$

Re Reynolds number $\dfrac{\rho V d}{\mu}$

St Stanton number $\dfrac{Nu}{Re \times Pr}$

X_{tt} Martinelli parameter $\left(\dfrac{\mu_f}{\mu_g}\right)^{0.1}\left(\dfrac{v_f}{v_g}\right)^{0.5}\left(\dfrac{1}{x}-1\right)^{0.9}$

ψ $\dfrac{\mu_b}{\mu_w}$

DRAWINGS

GRAPHS

PHOTOGRAPHS

TABLES

INTRODUCTION

Chapter 1.

1.1. SINGLE PHASE CONVECTIVE HEAT TRANSFER.

The mechanism of convective heat transfer has been long established as a two process mechanism where first, heat from a hot surface is transferred to the fluid boundary layer by conduction, and that there then follows a macroscopic exchange of elements of fluid between the hot boundary layer and the cooler bulk of the fluid. This interchange of mass and momentum between the stationary or slowly moving elements of fluid of the boundary layer and the faster moving elements of fluid of the main stream results in a loss of kinetic energy by the bulk of the fluid flowing over the heating surface. The fact that the heat transfer rate from the hot surface to the fluid bulk and the kinetic energy loss from the fluid bulk both depend on the same mechanism of mass and momentum transfer between the fluid boundary layer and the fluid bulk, formed the basis for Reynold's analogy between the friction factor for a fluid flowing through a heated tube and the heat transfer coefficient between the tube surface and the fluid bulk.

This two process mechanism of heat transfer between a hot surface and the fluid flowing over it means that the rate of heat transfer will be a function of the properties of the fluid, particularly conductivity and specific heat during the first process of conduction, and upon the intensity of the turbulent interchange of mass between the hot boundary layer and the bulk of the fluid during the second process of mass transfer. Dimensional analysis applied to the results of heat transfer experiments between a hot surface and a fluid flowing over it has produced the well known Dittus-Boelter equation,

$$Nu = C\, Re^{0.8}\, P_r^{0.4}$$

from this equation it can be seen that to increase the heat transfer through a given heating surface, to a given fluid, with a given surface to fluid temperature difference, it is simply a matter of increasing the velocity of the fluid over the heating surface. It can be expected that the heat transfer rate will increase by a factor proportional to $(\text{Velocity})^{0.8}$, but on the other hand it can be also expected that the kinetic energy loss from the bulk fluid and thus the frictional loss will increase by a factor proportional to $(\text{Velocity})^{2.0}$.

1.2. METHODS OF INCREASING TURBULENCE.

The aim of increasing the rate of mass exchange between the hot boundary layer and the fluid bulk can be effected by turbulence promoters attached or held near to the hot surface, for example trip wires to break up a laminar boundary layer, changes in section of the fluid flow path to induce additional turbulence in the fluid, and swirl vanes to produce an artificial gravitational field in the fluid and thus a natural convection mechanism to assist the forced convection mechanism. All of these methods are accompanied by a frictional pressure drop penalty but can be used never the less to provide a more compact heat exchange surface. Indeed the mechanical design requirements of a heat exchanger generally introduce changes in section, for example at a tube entrance,where the effect must be known and allowed for in the design.

The other mechanism which can be used under certain conditions is that of a liquid boiling on a hot surface, this effect can be additional to the forced convection heat transfer mechanism and need not incur increased frictional pressure loss.

1.3. NUCLEATE BOILING MECHANISM.

The boiling process has been used, until comparatively recently, primarily as a means of changing the phase of a liquid to a vapour, rather than as a means of increasing the rate of heat transfer to the liquid and it is only during the last thirty years that real efforts have been made to understand the mechanism of the boiling process and to produce data correlations suitable for use in designing heat exchange surfaces where boiling is present.

It has been shown that the latent heat of evaporation supplied to evaporate a bubble of vapour at the heating surface accounts for only a small part of the increased heat transfer consequent to the boiling of the liquid at the hot surface. The greater part of the heat transfer increase due to boiling is due to the additional turbulence induced in the hot fluid boundary layer by the mechanism of vapour bubbles growing on the heated surface and by their subsequent collapse or their departure from the heated surface into the cooler bulk of the liquid.

If this boiling is increased in intensity then the turbulence it introduces into the hot fluid boundary layer progressively overshadows the forced convection turbulence and the heat transfer becomes independent of the fluid velocity.

If the heat transfer rate is increased further then the vapour bubbles leaving the surface coalesce into a vapour blanket and do not allow the cold bulk fluid to reach the surface, the nucleate boiling mechanism then breaks down and the heating surface temperature rises dramatically often to the melting point or "Burn out" of the metal.

1.4. PRESENT WORK.

In the present work the aim was to investigate the effect of a change in section of the flow area upon the heat transfer coefficient using first single phase conditions and then extending the tests to conditions of subcooled nucleate boiling. This aim was later extended to include some tests on swirl flow.

The experimental equipment available for the tests which are described later was able to provide conditions for heat transfer tests from single phase forced convection to forced convection with surface nucleate boiling with water, but the tests were conducted well below the "burn-out" point.

The basic configuration of the test section was an electrically heated metal tube surrounded by a concentric glass tube providing an annular section for water to pass through. Tests were carried out with single phase and nucleate boiling conditions with a step change in the annulus section and then with swirl vanes in the annulus.

Finally, a small Freon II test circuit was constructed to attempt to visualise the flow pattern at a step change of section. In this case, the flow section was rectangular with a heating strip on one side and two sides of the section were made from glass to permit observation through the flow.

The tests performed involved combinations of turbulence induced by forced convection, turbulence induced by the nucleate boiling mechanism and turbulence induced by a change of section in the flow path. Considering the difficult progress made so far towards obtaining general correlations for boiling, without the complication of change of section, it could be reasonably thought that the information these experiments would produce would give some insight into the mechanism of the flow at the change of

section with and without boiling present, whilst it might be also useful to attempt to verify existing correlations with the data obtained from the plain sections of the test piece.

PREVIOUS WORK

2. 1. INTRODUCTION

In making a survey of previous work in the field of this research topic it became apparent that there were essentially two references which were directly relevant in that the effect of discontinuities in the flow section on the heat transfer coefficient had been studied, although only for a single phase fluid R 1, 1956 and R 2, 1962. No references to work dealing with the effect of discontinuities in two phase flow on the local heat transfer coefficient were found, although work on the pressure drop at flow section discontinuities had been carried out by a number of workers, R 3, 1958, R 4, 1966. Since the work described in this thesis did not involve the study of two phase pressure drops these references have not been included in the following survey.

The survey has been divided into sections dealing with;

2.2. Single phase heat transfer in an annulus

2.3. Boiling heat transfer mechanisms and correlations

2.4. Measurement of temperature

2.5. Photographic techniques used in the study of boiling

2.6. The effect of discontinuities in the flow path on the single phase heat transfer coefficient.

2. 2. SINGLE PHASE HEAT TRANSFER IN AN ANNULUS.

The work has been treated with reference to the case of heat transfer to a fluid flowing through a duct of circular section, so that correlations of the same form are obtained but with the ratio of the inner and outer diameter of the annulus as an additional factor. The general form of the heat transfer correlation being:

$$Nu = C\ Re^{n}\ Pr^{m}\ \psi^{p}\ \left(\frac{d_o}{d_i}\right)^{q} \qquad 2.2.1$$

Wiegand and Baker, R 5, 1942, produced a survey of work carried out from 1907 on laminar and turbulent flow and accepted the equivalent diameter defined as, $d_o - d_i$ to be used in calculating the Reynolds and Nusselt number.

Monrad and Pelton, R 6, 1942, carried out experimental work with water, and also with air flowing through an annular section. For heat transfer from the outer surface of the annulus they confirmed the use of the Dittus - Boelter equation modified to include a term involving the ratio of the inner and outer diameters.

$$Nu = 0.02\ Re^{0.8}\ Pr^{0.4}\ \left(\frac{d_o}{d_i}\right)^{0.53} \qquad 2.2.2$$

For heat transfer from the inner surface of the annulus they suggested that a constant involving the ratio of the velocity gradients at the inner and outer surfaces be used.

$$Nu = 0.023\, Re^{0.8}\, P_r^{0.4} \left\{ \frac{2 \ln\left(\frac{d_o}{d_i}\right) - \left(\frac{d_o}{d_i}\right)^2 + 1}{\frac{d_o}{d_i} - \frac{d_i}{d_o} - 2\,\frac{d_o}{d_i} \ln\left(\frac{d_o}{d_i}\right)} \right\} \qquad 2.2.3$$

Davis, R 7, 1943, took the data of several previous workers and using dimensional analysis produced a close correlation which held over a large range of diameter ratios

$$Nu = 0.031\, Re^{0.8}\, P_r^{0.33}\, \psi^{0.14} \left(\frac{d_o}{d_i}\right)^{0.15} \qquad 2.2.4$$

the diameter used in the Reynolds and Nusselt number was d_i rather than $d_o - d_i$, because it gave a tighter correlation.

McMillen and Larson, R 8, 1944, carried out a series of experiments with water flowing through an annulus. In calculating the heat transfer coefficients they did not use measured values of surface temperature but by keeping the heating fluid flowing through the inside tube at a high velocity and thus maintaining a nearly isothermal surface and a high heat transfer coefficient they were able to deduce the annulus inside wall heat transfer coefficient from the overall heat transfer coefficient. They used, d_o, in computing the Reynolds number. Their results could be expressed by the equation proposed by Davis with little error.

Carpenter, Colburn, Shoenborn and Wurster, R 9, 1946, carried out a series of tests on water flowing through an

annulus. They used the same method as McMillen and Larsen to calculate the heat transfer coefficient from the inside wall of the annulus, from the overall heat transfer coefficient between the heating water and the water flowing through an annulus. They restated the appropriate equivalent diameter to be $d_o - d_i$ since from their pressure drop results the transition from viscous to turbulent flow occurred at Re = 2000 and by using this defined equivalent diameter the friction and heat transfer correlations obtained could be compared with those existing from flow through a round tube. The heat transfer data was plotted as a comparison with correlations obtained by previous workers which were shown to be somewhat optimistic.

McAdams, R 10, 1954, has usefully summarised the correlations proposed for heat transfer from the inner wall to the fluid flowing through an annulus, all of the form;

$$St\ Pr^n = \frac{C\,\psi^p}{Re^m} \qquad 2.2.5$$

with a recommendation to use

$$St\ Pr^{0.67} = \frac{0.023\ \psi^{0.14}}{Re^{0.2}} \qquad 2.2.6$$

for design calculations.

In summary, this work has been extensively reported and at the small values of temperature difference normally used with heat transfer to water, all of these equations predict nearly the same value of heat transfer coefficient.

2.3. BOILING HEAT TRANSFER MECHANISMS AND CORRELATIONS.

When a subcooled liquid flows over a heated surface, heat is transferred through a thin liquid boundary layer by conduction to the fluid bulk. The heat flux can be plotted against the difference between the heating surface temperature and the fluid saturation temperature. G.21, section A to B, and the heat transfer can be correlated by,

$$Nu = C\, Re^{0.8}\, Pr^{0.4} \qquad 2.3.1$$

If, by increasing the heating power the temperature of the hot plate increases to a certain minimum value above the saturation temperature of the fluid then the graph will follow the path B to C. The boundary layer of liquid is superheated above the liquid saturation temperature and at nucleation centres on the hot surface surface vapour bubbles grow and collapse repeatedly, this mechanism reduces the resistance of the liquid boundary layer to heat transfer by apparently introducing micro-convection currents in it, by the growing bubbles displacing hot liquid from the heating surface, and also transfers some heat from the hot surface as the latent heat of evaporation in the bubbles.

A further power increase will increase the temperature of the hot surface still further and the bubbles form at an increasing number of nucleation sites on the hot surface and grow larger to the point where they are detached from the hot surface by their own bouyancy and the fluid bulk flowing over

them, the graph now follows a steep line C to D.

Further increase in heating power to the hot surface results in such a vapour bubble formation rate that the necessary replacement liquid flow to the hot surface is blocked and the mechanism of nucleate boiling breaks down to be replaced by film boiling, with the heating surface completely covered by vapour, then the operating condition will flip from D to E with a large temperature increase of the hot surface. This temperature at E may be sufficient to melt some heating metals and flux at point D would then be known as the burn out flux.

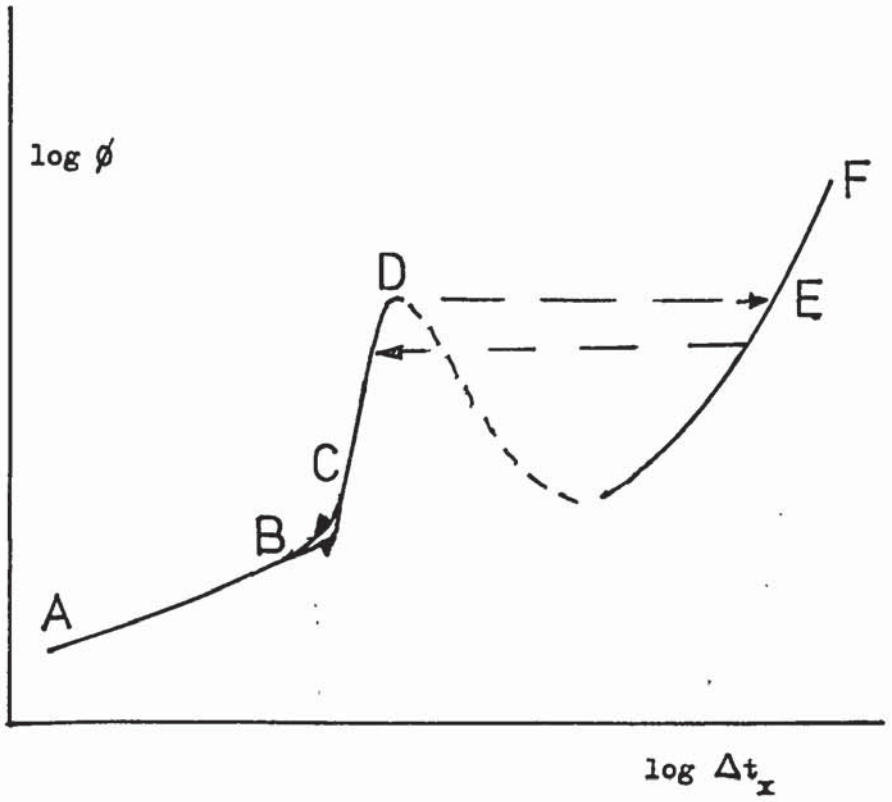

Characteristic boiling curve, log ø - log Δt_x

G 2.1

If the metal of this heating surface will stand this temperature without failure the power may be increased further, E to F, to give stable film boiling.

On reducing from the film boiling level the hot surface temperature will reduce below the burn-out point before the operating condition flips back to the nucleate boiling curve.

A second hysteresis effect is also present when reducing the power from the subcooled boiling level to that for single phase, in that nucleate boiling will persist to a lower level of heat flux than that with the increasing power.

The dotted line is an unstable condition in that a reduction of heat flux may be accompanied by an increase in temperature.

In the experimental work presented here the operating conditions ranged from single phase to nucleate boiling in an almost saturated fluid and in the following survey only this area of the boiling curve will be considered in detail.

The existence of subcooled pool boiling and the accompanying high rate of heat transfer has been long known in the process of quenching hot metal in water, where the rate of cooling increased as the metal temperature was reduced, that is as the initial film boiling was replaced by subcooled nucleate boiling before finally reducing to single phase cooling. However, the main experimental work has been concerned with

steady state conditions, Mosciki and Broder R 11, 1926, performed some experiments with electrically heated wires in water and compared the heat fluxes obtainable with boiling against single phase values.

Nukiyama R 12, 1934, used an electrically heated platinum wire in saturated water to explore the boiling modes and demonstrated saturated nucleate boiling, film boiling and conditions for burn-out. He gradually increased the temperature of a platinum wire immersed in a pool of saturated water and observed the rapid increase in the heat flux until, at a limiting value, the mechanism of nucleate boiling broke down and the wire was completely surrounded by a vapour blanket. The temperature of the wire having increased suddenly by approximately 700 K.

Farber and Scorah, R 13, 1947, carried out experimental work on subcooled pool boiling of water. They refined their equipment to measure the surface finish of the heating wire and used a number of different metals for comparison purposes. Also the experiments were carried out at a number of different pressures. The results confirmed the existance of a characteristic boiling curve which can vary with the pressure level and can show variations with different heating surfaces. In these experiments the temperature of the heating wire was measured by spot welding a Chromel/Alumel thermocouple junction to the surface. The leads from the surface would interfere with the liquid flow pattern and also cool the heating surface at the point of attachment with the effect that the

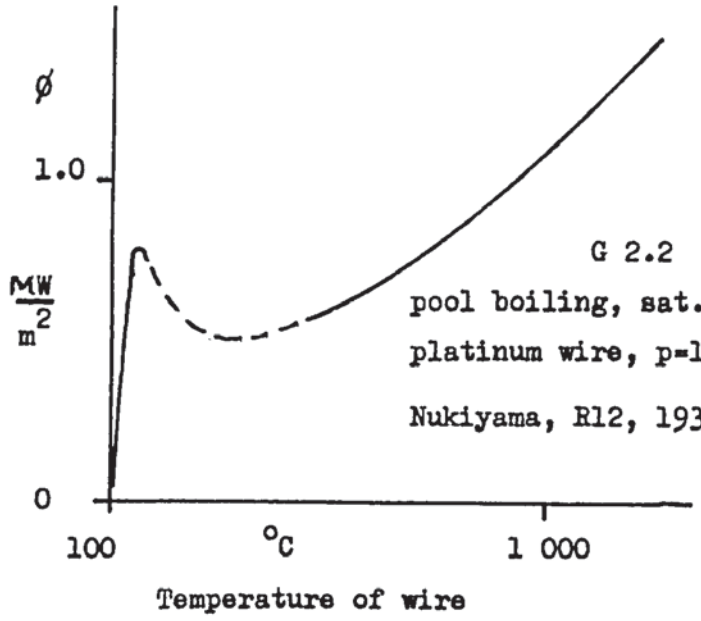

G 2.2
pool boiling, sat. water
platinum wire, p=1bar.
Nukiyama, R12, 1934.

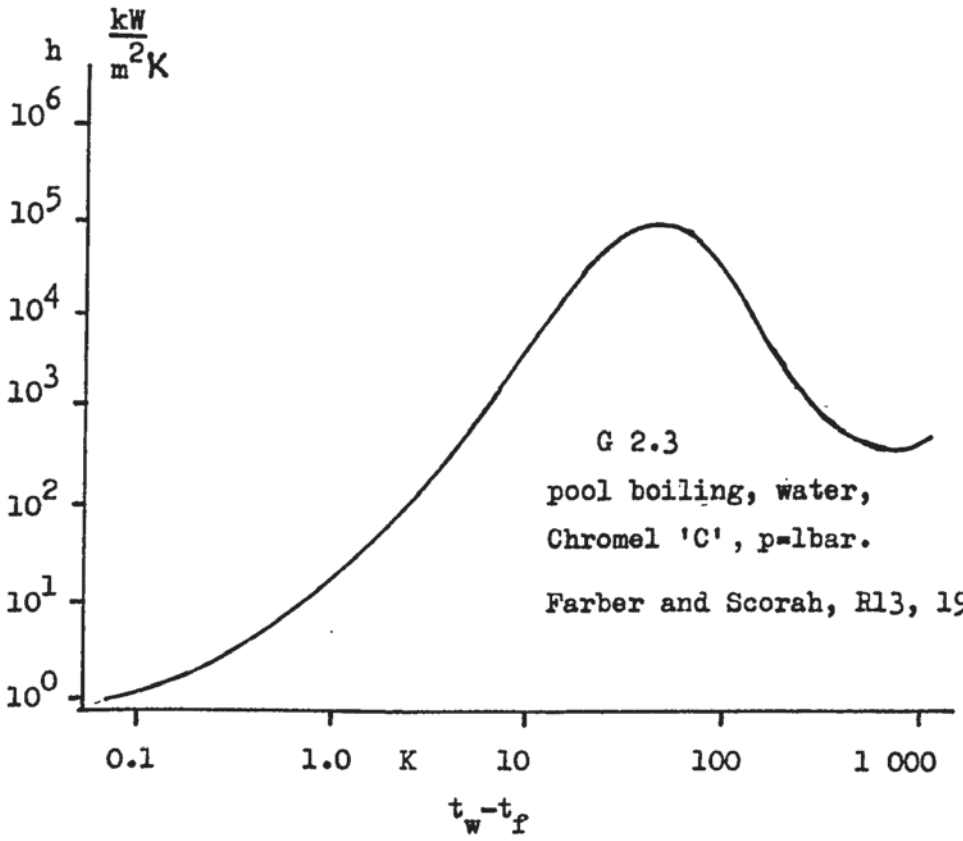

G 2.3
pool boiling, water,
Chromel 'C', p=1bar.
Farber and Scorah, R13, 1947.

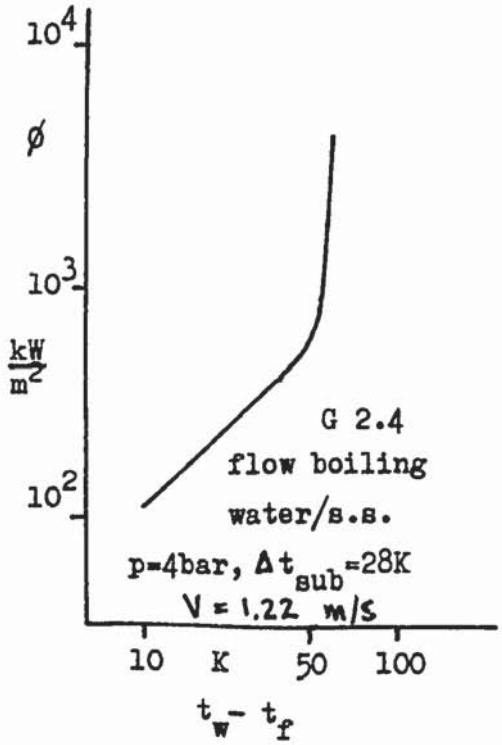

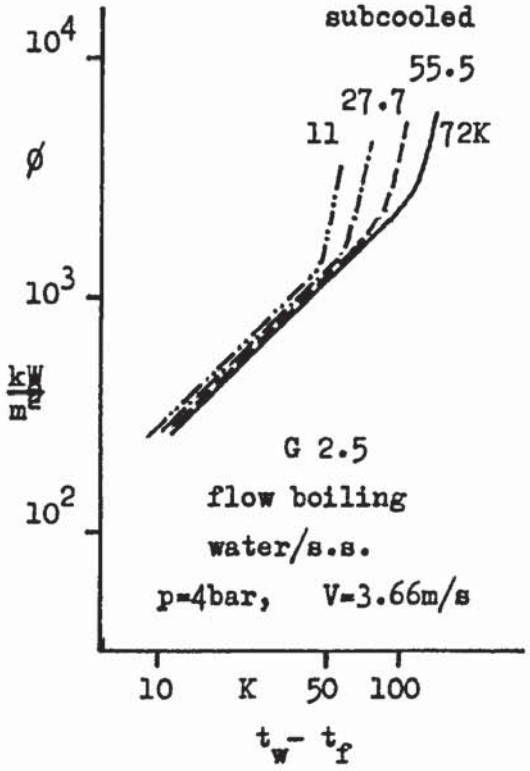

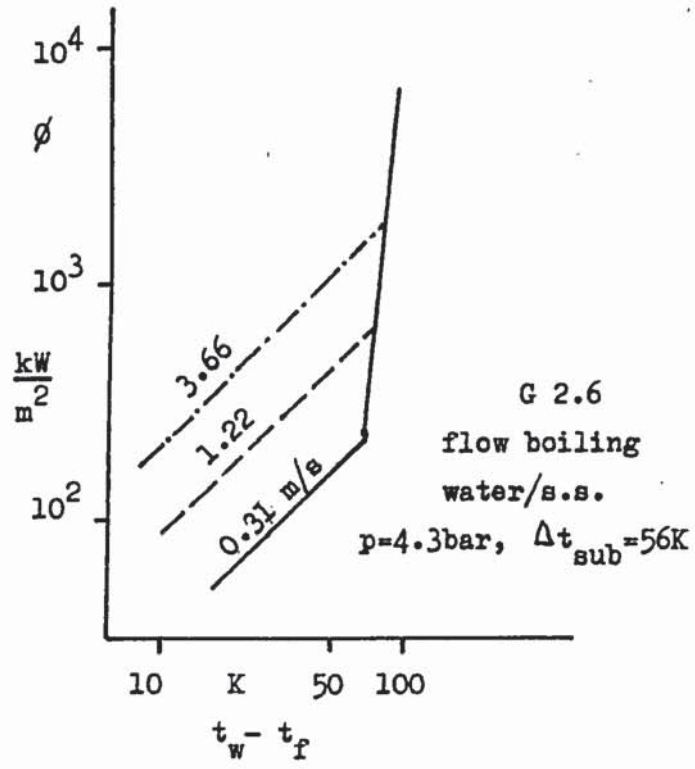

Flow through annulus, McAdams et al, R14, 1949.

temperatures given could well be below the true surface temperatures.

McAdams et al, R 14, 1949, carried out experimental work with subcooled nucleate boiling of water flowing through an annulus, electrically heated at the inner wall. They plotted their data as log ϕ against log $(t_w - t_f)$ and measured the effect of fluid velocity and subcooling. Assuming the driving force behind the boiling heat transfer process to be the boiling potential, $t_w - t_s = \Delta t_x$, they replotted their data as log ϕ against log Δt_x and thus obtained an approximate correlation which was independent of velocity and subcooling.

$$\phi = C \Delta t_x^{3.86} \qquad 2.3.2$$

They showed that the transition between single phase and subcooled nucleate boiling heat transfer was not a sudden step but that a transition area existed.

In these experiments the surface temperature of the tube was measured on the dry side, a calculated correction being applied for the temperature drop through the tube wall, and can thus be expected to be accurate.

Krieth and Summerfield, R 15, 1950, R 16, 1949, carried out experimental work with water, aniline and n-butyl alcohol flowing through an electrically heated stainless steel tube, to further confirm the boiling characteristics.

Whilst the heat transfer characteristics of the boiling process were confidently known for the range of parameters employed, further work towards obtaining a correlation was seen to depend on a detailed knowledge of the mechanism of vapour bubble formation in a liquid on a heated surface, and Rohsenow and Clark, R 17, 1951, studied the high speed ciné record of the boiling process produced by McAdams et al, R 14, by measuring the bubble sizes and the frequency of bubble formation. The heat required to produce a vapour bubble can be expressed with fair approximation as,

$$q = \frac{\frac{4}{3}\pi r^3}{v_g} h_{fg} \qquad 2.3.3$$

this by counting the rate of bubble formation on a given area of heating surface and by considering the heat required by each, the heat transfer due to bubble formation alone was calculated. This amounted to only a small fraction of the power input to the heating surface, thus it could be said that the latent heat of evaporation of the liquid played only a small part in the heat transfer process and that the physical agitation of the fluid boundary layer by the forming and departing bubbles was probably the reason for the high heat transfer rates associated with boiling. Again using the results of McAdams for heat transfer with aerated water, the increase in the heat flux compared with that from dearated water under the same conditions was accompanied by the appearance of air bubbles coming out of solution at the heating surface. Here no latent heat was involved and the observed increase would seem to confirm

that the boundary layer is subject to turbulence caused by the forming air bubbles.

Gunther, R 18, 1950, Gunther and Kreith, R 19, 1950 used a Kerr cell in conjunction with a high speed film transport to photograph flow boiling at 20 000 frames a second. From the analysis of the films taken they were able to present graphs showing the variation of bubble radius with time and of the effect of subcooling, fluid velocity, and heat transfer rate, on bubble population, size, and lifetime. They also observed that with a large subcooling the bubbles would slide along the heating surface rather than detach from it. The results confirmed the idea of boundary layer turbulence due to bubble growth as the main mechanism augmenting the heat transfer, with quantitative figures to support it.

A further empirical correlation of flow boiling heat transfer data after the manner of McAdams, was produced by Jens and Lottes, R 20, 1951, using collected data for water over the pressure range 34 to 136 bar,

$$\Delta t_x = 4.46\, e^{-\frac{p}{62.1}}\, \phi^{0.25} \qquad 2.3.4$$

Rohsenow, R 21, 1952, sought to extend the dimensionless correlation used for conditions of single phase forced convection heat transfer,

$$Nu = f(Re, Pr) \qquad 2.3.5$$

to the case of pool boiling by arguing that the heat transfer was still dependent on liquid properties and liquid velocity but that in the case of boiling the velocity could be related to the boundary layer conditions rather than the free stream velocity of single phase forced convection heat transfer,

$$Nu_{bu} = f\left(Re_{bu}, Pr\right) \qquad 2.3.6$$

where Nu_{bu} and Re_{bu} are appropriate numbers.

Using the work of Jacobs, R 22, 1949, the heat transfer to bubbles of vapour on the surface can be expressed as,

$$\phi_{bu} = n f \left(\frac{\pi d_{bu}^3}{6}\right) \rho_g h_{fg} \qquad 2.3.7$$

The diameter of the bubble as it leaves the surface is given by Fritz, R 23, 1935 as,

$$d_{bu} = C_d \beta \sqrt{\frac{2\sigma}{g(\rho_f - \rho_g)}} \qquad 2.3.8$$

where β is the liquid/vapour surface angle

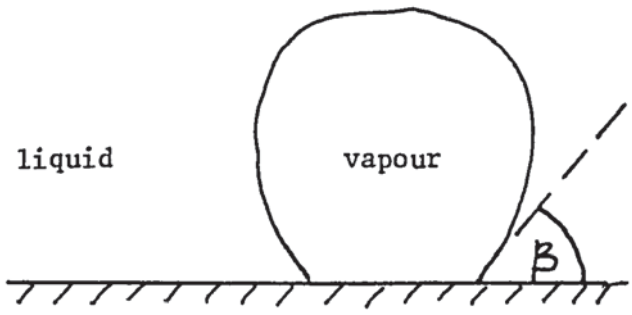

It was shown by Jacob that for water and carbon tetrachloride the product of bubble diameter and frequency is approximately constant,

$$f\ d_{bu} = \text{Constant} \qquad 2.3.9$$

Inspection of these equations showed that for a given operating pressure,

$$\phi_{bu} \propto n \qquad 2.3.10$$

since all other quantities were constant or a function of saturation pressure.

It had been previously observed that the rate of heat transfer to a boiling liquid is proportional to the number of vapour columns leaving the surface. This was later confirmed by Donald and Haslam, R 24, 1958, who measured the percentage of the area of a heating surface which was covered with bubbles, by measuring the change in conductivity from the surface to a fixed electrode through water with a small addition of hydrochloric acid to improve the conductivity of the water.

Thus,

$$\phi \propto \phi_{bu} = C n f \left(\frac{\pi d_{bu}^3}{6}\right) \rho_g h_{fg} \qquad 2.3.11$$

where C is a function of pressure.

The mass velocity of the vapour bubbles leaving the surface was,

$$G_{bu} = n f \rho_g \left(\frac{\pi d_{bu}^3}{6}\right) \qquad 2.3.12$$

Thus the bubble Reynolds Number was defined as

$$Re_{bu} = \frac{G_{bu} d_{bu}}{\mu_F} = C' \beta \frac{\phi}{\mu_F h_{fg} \sqrt{g(\rho_F - \rho_g)}} \sqrt{\frac{2\sigma}{}} \qquad 2.3.13$$

The bubble Nusselt number,

$$Nu_{bu} = \frac{h d_{bu}}{k_f} \qquad 2.3.14$$

which became by using equation 2.3.8,

$$Nu_{bu} = C_d \beta \frac{h}{k_f} \sqrt{\frac{2\sigma}{g(\rho_f - \rho_g)}} \qquad 2.3.15$$

and the correlation proposed was,

$$Nu_{bu} = f(Re_{bu}, P_r) \qquad 2.3.16$$

where, C_f, μ_f, σ, ρ_f, ρ_g, were all evaluated at the saturation temperature corresponding to the local pressure, and to account for the effects of subcooling,

$$h = h_s = \frac{\phi}{\Delta t_x} \qquad 2.3.17$$

Since both Re_{bu} and Nu_{bu} embodied the term ϕ, the group,

$$\frac{Re_{bu} P_r}{Nu_{bu}} = \frac{c_f \Delta t_x}{h_{fg}} \qquad 2.3.18$$

was used to give,

$$Re_{bu} = f\left(\frac{c_f \Delta t_x}{h_{fg}}, P_r\right) \qquad 2.3.19$$

This correlation was applied to pool boiling data obtained by Addoms, R 25, 1948, (water on platinum), Cichelli and Bonilla, R 25, 1945, (ethyl alcohol on chromium, benzene on chromium, and n-pentane on chromium) and Cryder and Finalborgo, R 27, 1937, (water on brass) to give,

$$\frac{c_f \Delta t_x}{h_{fg}} = C_{wf}\left(\frac{\phi}{\mu_f h_{fg}} \sqrt{\frac{\sigma}{g(\rho_f - \rho_g)}}\right)^{0.33} \left(\frac{c\mu}{k}\right)_f^{1.7} \qquad 2.3.20$$

where C_{wf} had a value which was characteristic of the surface/fluid combination.

The correlation when arranged to the form for single phase heat transfer

i.e. $$Nu = C\, Re^{0.8}\, P_r^{0.4} \qquad 2.3.21$$

gave $$Nu_b = \frac{1}{C_{wf}}\, Re_b^{0.667}\, P_r^{-0.7} \qquad 2.3.22$$

The value of C_{wf} ranging from 0.0027 to 0.015 for ethyl alcohol and n-pentane respectively when boiling on a chromium surface, showed that further information was needed on the effect of surface/fluid combinations and pressure on the value of the bubble angle β.

It was found, R 21, 1952, that for the forced convection boiling of water at high pressure, 100-140 bar, this correlation for pool boiling could be used additively with the single phase forced convection heat transfer correlation to give the total heat transfer due to the combination of boiling effects and forced convection effects.

$$\phi_{total} = \phi_{\substack{convective \\ single\ phase}} + \phi_{\substack{pool \\ boiling}}$$

in the subcooled or low quality regimes.

Forster and Zuber, R 28, 1955, developed an analytical expression for the growth rate of a vapour bubble in a heated fluid, from the Rayleigh equation. The growth rates predicted were compared with the experimental results for bubble growth

obtained by Dergarabedian, R 29, 1953, and showed close agreement.

They proposed an equation of the form,

$$Nu = C\, Re_b^a\, Pr^b \qquad 2.3.23$$

to describe the boiling process, but whereas Rohsenow in his correlation had taken the characteristic length as the diameter of the vapour bubble leaving the heating surface, and this diameter multiplied by the bubble frequency as the characteristic velocity, Forster and Zuber took the bubble radius and the radial velocity of the growing bubble as the characteristic length and velocity respectively.

The correlation was produced as,

$$Nu = 0.0015\, Re_b^{0.62}\, Pr^{0.32} \qquad 2.3.24$$

which closely fitted the data of Cichelli and Bonilla for pool boiling for n-pentane, benzene and ethyl alcohol all on chromium, and water on brass. The correlation did not include a factor for surface conditions and cannot be said to have been tested against a range of surface/fluid combinations.

The derivation of bubble growth rate assumed a free nucleus in a volume of liquid rather than at a solid/liquid interface. However the predictions compared closely with the measured growth of a vapour bubble on a surface, R 18.

The selection of the bubble surface radial velocity as the characteristic velocity would seem more realistic than

using the bubble velocity particularly at a lower heat flux or a high degree of subcooling where the bubble could grow and then collapse without leaving the surface. The experimentally substantiated predictions for the bubble growth velocity had values of the order of 3 m/s which demonstrated the intense turbulence caused in the thin boundary layer by ebullition.

Griffith, R 30, 1958, and Bankoff and Mikesell, R 37, 1958, subsequently extended the analysis of the formation of a vapour bubble to that of a bubble forming on a flat heating surface.

Levy, R 32, 1959, presented a correlation for pool boiling which was based on the bubble growth equations derived by Forster and Zuber.

The equation produced gave the heat flux in explicit form,

$$\phi = \frac{k_f c_f \rho_f^2}{\sigma t_s (\rho_f - \rho_g)} \cdot \frac{1}{B_f} (\Delta t_x)^3 \qquad 2.3.25$$

where $\frac{1}{B_f}$ varied with pressure and was shown to be a complex function of $\frac{1}{\rho_g \cdot h_{fg}}$ which it was suggested had a physical significance as the vapour escape velocity from the heated surface. The equation gave a satisfactory correlation of data for pool boiling, from a number of previous workers.

The various previously proposed mechanisms to explain the high heat flux obtained with boiling,

Micro-convection in the boundary layer

Bubbles acting as surface roughness

Latent heat transport by vapour bubbles

Vapour-liquid exchange action

were critically compared against the experimental evidence available, Engelberg-Forster and Grief, R 33, 1959. The vapour-liquid exchange mechanism was shown to be the most probable since it could completely fit the experimental facts. The experimental values of heat flux could be accounted for if the forming vapour bubble could displace its own volume of hot liquid from the heating surface.

When the liquid was subcooled then the heat flux,

$$\phi \propto \frac{1}{J}\left(t_w - t_f\right) c_f \left(\frac{t^3_{max}}{v_f}\right) \qquad 2.3.26$$

if the degree of subcooling is increased then,

1. The temperature difference increases
2. The bubble period decreases
3. The maximum bubble radius decreases

by using the data of Ellion, R 34, 1954, for pool boiling, they were able to show that the effect of these variations on the heat transfer were very nearly self cancelling. Thus the high flux and insensitivity to subcooling could be theoretically accounted for with the vapour-liquid exchange model.

Ivey and Morris, R 35, 1962, showed that although the liquid-vapour exchange mechanism could well explain the magnitude of the heat flux obtained in subcooled boiling in water at atmospheric

pressures it could not be extended to high pressures. They used the dimensionless ratio,

$$M = \frac{\text{Vapour-liquid exchange heat transport}}{\text{Latent heat transport}} = \frac{C_f \rho_f \Delta t_{mean}}{h_{fg} \rho_v}$$

where $\Delta t_{mean} = \frac{t_w - t_f}{2}$ 2.3.27

as a measure of the importance of the liquid-vapour exchange mechanism and showed that it reduced from a value of, $3_x \Delta T_{mean}$, at atmospheric pressure to, $0.075 \times \Delta T_{mean}$, at 70 bar. Using experimental data from Cichelli and Bonilla, R 26, Addoms, R 25, and Averin, R 36, they showed this to represent a reduction in the value of M from 80 to 1.1.

Schrock and Grossman, R 37, 1962, carried out experimental work with water flowing through an electrically heated tube and used dimensionless groups, based on the analysis of Sterman, R 38, 1953, to correlate their data.

$$Nu_{tp} = f\left(Re, Pr, X_{tt}, Bo\right) \quad 2.3.28$$

where the Nu, Re and Pr numbers were evaluated using saturated liquid properties at the local pressure.

They presented their results as a plot of,

$$\frac{Nu}{Re^{0.8} Pr^{0.33}} \text{ against } X_{tt}$$

for a series of fixed value of Bo. The ordinate was alternatively expressed as the ratio between the two-phase and single phase heat transfer coefficient.

$$\frac{h_{tp}}{h_{sp}} = \frac{h_{tp}}{0.023 \frac{k}{d} Re^{0.8} Pr^{0.33}} = \frac{Nu_{tp}}{0.023 Re^{0.8} Pr^{0.33}} \qquad 2.3.29$$

From the curves it could be seen that at low values of the Bo number the heat transfer was a function. of the flow parameter X_{tt} whilst at high values of Bo number the heat transfer was independent of X_{tt} and depended solely on the Bo number. This they explained by assuming that for low values of the Bo number the flow pattern in the pipe was annular with a vapour core and a thin layer of liquid on the wall. This being so then the liquid could sustain a temperature which was enough to account for the heat transfer by conduction and then surface vapourisation, but not sufficient to produce nucleate boiling. As the heat flux and the Bo number were increased then nucleate boiling developed and at high heat flux to mass flow ratios it predominated as the heat transfer mechanism and thus the heat transfer coefficient became essentially independent of X_{tt}.

The final correlation fitted their experimental results to within $\pm$ 35%

$$\frac{Nu}{Re^{0.8} Pr^{0.33}} = 170 \left[Bo + \frac{1.5 \times 10^{-4}}{X_{tt}^{0.66}} \right] \qquad 2.3.30$$

Hsu and Graham, R 39, 1961, used a high speed ciné camera, 5 000 frames a second, to photograph vapour bubbles forming in

water, pool boiling on an electrically heated strip of metal. They used both Schlieren and shadowgraph systems to show the movement of the hot boundary layer from the heating surface by the forming bubble.

Bennett et al, R 40, 1961, used an annular flow section with electrical heating of the inner surface, to measure heat transfer coefficients to water/steam mixtures. When the flow was high enough to suppress nucleate boiling they correlated their results by using the Martinelli two-phase flow parameter X_{tt}

$$\frac{h_{tp}}{h_{sp}} \phi^{-0.11} = 0.64 \left(\frac{1}{X_{tt}} \right)^{0.74} \qquad 2.3.31$$

which was similar to the form proposed by Dengler and Addoms, R 64, 1953, and by Schrock and Grossman, R 37. For the tests using low quality mixtures of steam and water they found that the pool boiling correlation of Rohsenow, R 17, was adequate.

Papell, R 41, 1963, carried out non-boiling and boiling heat transfer tests with water flowing through an electrically heated Inconel X tube. The data obtained was used together with data from previous workers to test a boiling heat transfer correlation, which was presented as the ratio of the Nu numbers for boiling and non-boiling conditions against dimensionless groups, relevant to the boiling process, as proposed by Sterman, R 38.

The ratio of the Nu numbers was first plotted against the Bo number and then two additional groups were added to compensate for pressure level and the degree of subcooling.

The final form of the correlation was,

$$\frac{Nu_{bo}}{Nu_{nbo}} = 90.0\left[\left(\frac{\phi}{h_{fg}\rho_g V}\right)\left(\frac{h_{fg}}{c_p \Delta t_{sub}}\right)^{1.2}\left(\frac{\rho_g}{\rho_F}\right)^{1.08}\right]^{0.7} \qquad 2.3.32$$

where the Nu_{nbo} number was calculated from the usual single phase heat transfer correlation,

$$Nu_{nbo} = C\, Re^{0.8}\, Pr^{0.4} \qquad 2.3.33$$

The correlation was restricted to subcooled boiling since the second parameter became infinite at saturation conditions.

The range of the experimental data was used to produce this correlation was, pressure 1 - 150 bar, heat flux 42 - 91 000 kW/m^2, bulk fluid velocity 0.4 - 62 m/s, degree of subcooling 3 - 187 K. The data was correlated with a spread of $\pm$ 12%. Sharp, R 42, 1964, conducted an experiment seeking to demonstrate the micro-layer of liquid existing below a forming vapour bubble on a heating surface, and by measuring the reduction in thickness of this liquid micro-layer with time, to calculate the heat flux from the surface required to achieve this evaporation rate and thus give support to the idea of the evaporation of the liquid film under the base of the bubble accounting for a substantial part of the heat transfer associated with nucleate boiling.

Essentially the apparatus consisted of a methanol or water boiling on a glass plate which was heated by a jet of

hot air on its dry side. A beam of monochromatic light was directed down through the bubble and reflected back both at the top and bottom surface of the liquid micro-layer, thus producing interference fringes which were measured to deduce the thickness of the liquid micro-layer. The experimental results recorded by a high speed ciné camera demonstrated this micro-layer but the large bubble formed in the low pressure fluid flattended by a transparent cover plate above it was far from a typical bubble both in size and shape.

Blatt and Adt, R 43, 1964, used Rohsenow's additive correlation, R 21, for heat transfer data obtained from boiling Freon 11 and also Freon 113, flowing through a tube heated externally by hot water. The experimental points showed a maximum deviation of $\pm$ 30%.

Bergles and Rohsenow, R 44, 1964, carried out boiling heat transfer experiments with water using the same metal heating surface for both pool boiling and flow boiling tests.

One of the objects of the tests was to ascertain whether the fully developed flow boiling heat transfer curve could be regarded as an extension of the pool boiling curve, G 2.7. The results G 2.8, showed that the shape, slope and intercept of the pool boiling curve varied with the degree of subcooling and the idea of extending the slope of the curve upwards to represent fully developed flow boiling was shown to be untenable.

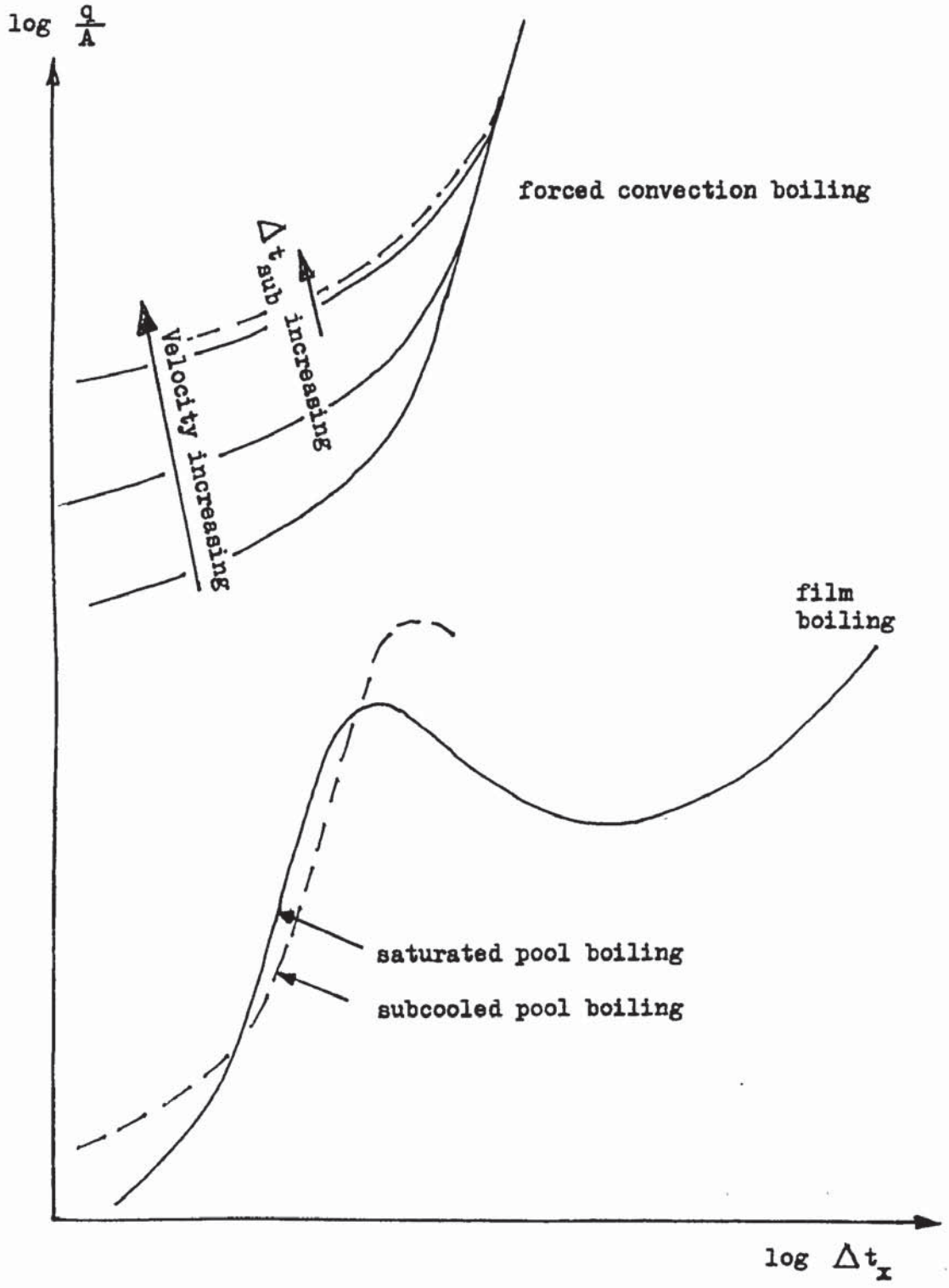

Regimes in boiling heat transfer, Rohsenow. G 2.7

Forced convection surface boiling and pool boiling data for stainless steel tube, Bergles and Rohsenow 1964.

G 2.8

Chen, R 45, 1966, in considering upward two-phase flow with net generation of vapour, proposed a correlation based on the idea previously suggested by Rohsenow, R 21, of the additive effect of the single phase heat transfer mechanism and the boiling heat transfer mechanism for pool boiling, thus,

$$h_{tp} = h_{bo} + h_{mac} \qquad 2.3.34$$

Considering the contribution of the macro-convective single-phase mechanism, Chen postulated that the Dittus-Boelter equation modified to use two-phase values could be used,

$$h_{mac} = 0.023 \left(Re\right)_{tp}^{0.8} \left(Pr\right)_{tp}^{0.4} \left(\frac{k}{d}\right)_{tp} \qquad 2.3.35$$

and since for fluids normally encountered in heat transfer applications other than liquid metals, the Pr numbers for the liquid and the vapour were of the same order of magnitude,

$$Pr_{tp} \simeq Pr_{sp} \qquad 2.3.36$$

The heat from the hot surface was assumed to be transferred through a thin film of liquid so that the value of k for the liquid would be appropriate.

If the ratio of the Re numbers for two-phase flow to that for single-phase flow be designated as F,

$$F = \left(\frac{Re_{tp}}{Re_{sp}}\right)^{0.8} \qquad 2.3.37$$

Temperature profiles for pool boiling and convective boiling with the same total superheat, Chen 1966. G 2.9

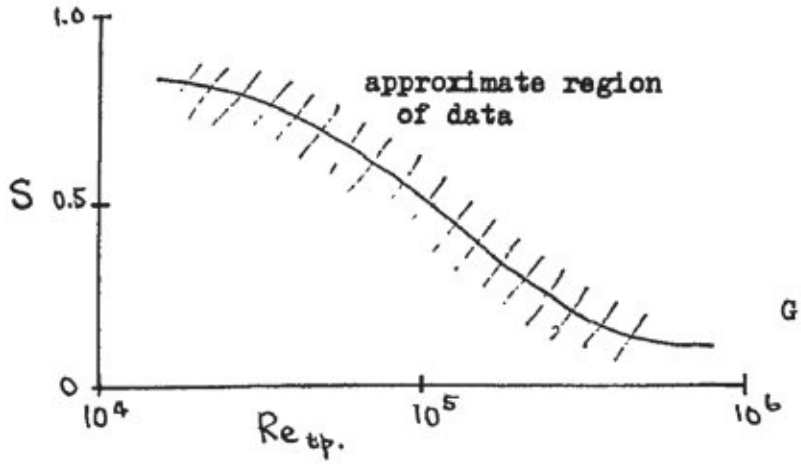

G 2.10

Variation of the bubble growth supression factor

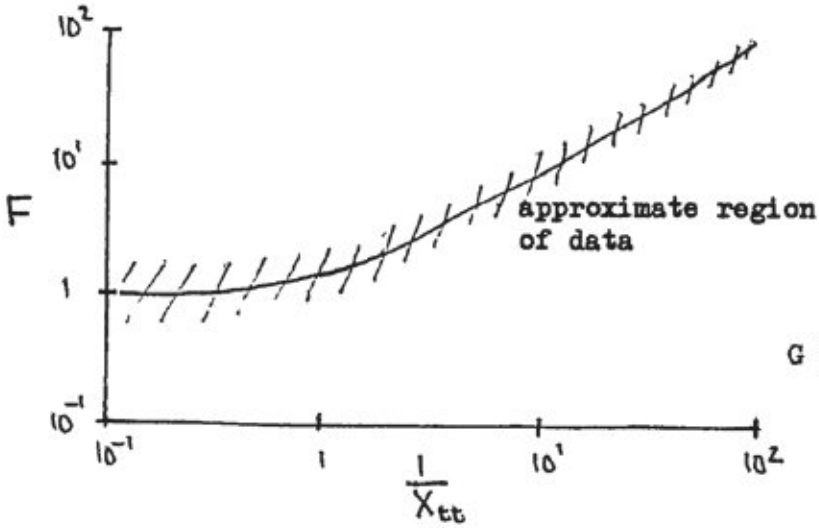

G 2.11

Variation of the two-phase Reynolds number function

then,

$$h_{mac} = 0.023 \left(Re\right)_{sp}^{0.8} \left(P_r\right)^{0.4} \left(\frac{k_f}{d}\right) F \qquad 2.3.38$$

The value of F , the only unknown in the equation was shown by experiment to be a function of the Martinelli parameter X_{tt}.

The contribution of the micro-convective heat transfer due to boiling was based on the analysis of Forster and Zuber, R 28, for the case of pool boiling but modified to take account of the more severe boundary layer temperature gradient which would be present with flow boiling conditions.

In their analysis of pool boiling, Forster and Zuber had assumed that the liquid surrounding the growing vapour bubble was at the temperature of the heating surface and while this was a reasonable approximation for pool boiling, it would not hold for flow boiling G 2.9, where the temperature of the liquid surrounding the bubble was at a value appreciably below the heating surface temperature and was controlled by the bulk flow rate.

From Forster and Zuber, using effective values of superheat and vapour pressure difference,

$$h_{bo} = 0.00122 \left(\frac{k_f^{0.79} \, c_f^{0.45} \, \rho_f^{0.49}}{\sigma^{0.5} \, \mu_f^{0.29} \, h_{fg}^{0.24} \, \rho_g^{0.24}} \right) \Delta t_e^{0.24} \, \Delta p_e^{0.75} \qquad 2.3.39$$

Chen defined a suppression factor S as the ratio of the mean effective superheat to the heating surface superheat,

$$S = \left(\frac{\Delta t_e}{\Delta t_x}\right)^{0.99} \qquad 2.3.40$$

The power of 0.99 being included so that after the subsequent analysis S would be expressed to the first power in the final equation.

Using the Clausius-Clapeyron equation,

$$S = \left(\frac{\Delta t_e}{\Delta t_x}\right)^{0.24} \left(\frac{\Delta p_e}{\Delta p_s}\right)^{0.75} \qquad 2.3.41$$

and,

$$h_{bo} = 0.00122 \left(\frac{k_f^{0.79}\, c_f^{0.45}\, \rho_f^{0.49}}{\sigma^{0.5}\, \mu_f^{0.29}\, h_{fg}^{0.24}\, \rho_g^{0.24}}\right) \Delta t_x^{0.24}\, \Delta p_s^{0.75}\, S \qquad 2.3.42$$

S was expressed as a function of the two-phase Re number and F was determined empirically from experimental data.

The final correlation was tested against a wide range of experimental data from different sources, using water, methanol, cyclohexane, pentane, heptane and benzene, and produced a close fit.

This correlation was extended subsequently for use in the subcooled region, R 46, 1972, with satisfactory results.

Hodgson, R 47, 1968 obtained experimental subcooled boiling heat transfer data for water flowing through an electrically heated tube and applied dimensionless analysis to correlate his results. The essential parameters he selected were,

tube diameter

degree of subcooling

liquid specific heat

liquid viscosity

liquid thermal conductivity

latent heat

heat flux

and also two terms,

$$Z = \frac{dt_s}{dp} \qquad X = \frac{-d\left(\frac{\rho_f}{\rho_g}\right)}{dp}$$

to fully describe the effect of pressure.

The resulting dimensionless equation was,

$$St \propto Re^a Pr^b \left[\frac{\Delta t_{sub}\, C}{h_{fg}}\right]^f \left[\frac{\phi}{h_{fg}\, G}\right]^s \left[\frac{Z h_{fg}}{X c}\right]^t \qquad 2.3.43$$

and assuming that the exponents of the Reynolds number and the Prandtl number are the same for boiling and non-boiling, the equation was re-arranged as,

$$\frac{St_{bo}}{St_{nbo}} = \text{function}\left[\frac{\phi}{h_{fg}.G} : \frac{\Delta t_{sub}.C}{h_{fg}} : \frac{Z.h_{fg}}{X.c}\right] \qquad 2.3.44$$

Using the experimental data to determine the group exponents gave,

$$\frac{St_{bo}}{St_{nbo}} = 141 \left(\frac{\emptyset}{h_{fg} G}\right)^{0.7} \left(\frac{\Delta t_{sub} C}{h_{fg}}\right)^{-0.55} \left(\frac{Z \cdot h_{fg}}{X c}\right)^{-0.08}$$

2.3.45

This equation correlated the data within 20%. The low value of the exponent assigned to the last group would indicate that it was of little significance.

Robin and Snyder, R 48, 1970, following on previous work developed an analytical equation for the mass transfer rate across a vapour bubble from evaporation at the base to condensation at the crown. They showed that the bubble growth prediction compared well with the experimental results obtained by Gunther, R 18, and that this mass transfer mechanism could account for the high heat transfer rates present with subcooled boiling at low pressures.

Jacobs and Shade, R 49, 1969, used a Schlieren optical system to visualise the bubble formation in pool boiling of carbon tetrachloride. They positioned a micro chromel/alumel thermocouple, 0.012 mm wire diameter, so that the rising vapour bubbles sliced through it and showed that except for very large degrees of subcooling the vapour contained by the bubbles remained superheated until bubble collapse was well advanced.

In summary, the high heat transfer rates associated with nucleate boiling with flow, have been explained in a satisfactory manner by different possible mechanisms,

(i) The mass exchange mechanism with the detaching hot vapour bubble being replaced by its volume of cool liquid, (Rohsenow).

(ii) The mass exhange mechanism with the growing bubble acting as a liquid pump forcing the hot boundary layer into the bulk fluid. (Engelberg and Greif).

(ii) The mass exchange mechanism with the transfer of heat from the superheated liquid at the base of the bubble to the cool liquid at the crown of the bubble by evaporation and condensation respectively, the bubble acting as a heat pump. (Robin and Snyder).

Other workers have observed hot jets of liquid leaving the heating surface following bubble collapse, an effect which may yet be quantified to provide an additional mechanism, (Villeneuve ,R 50, 1964.

These mechanisms are the basis of a number of design correlations, the most recent being that of Chen, R 45, for saturated boiling. This correlation was shown by Moles, R 51, 1973, to be limited to saturated boilings, but more recently Collier, R 46, has stated that this correlation can be modified to extend to subcooled boiling conditions.

The alternative approach to producing boiling heat transfer design correlations, has been to use dimensionless analysis on a range of variables chosen for their probable significance in the boiling process. This has resulted in useful equations, Papell, R 41, and Moles and Shaw, R 51, but care is needed to verify the range of fluids and operating conditions for which they are valid. Moles has usefully reviewed these correlations.

2.4. MEASUREMENT OF TEMPERATURE.

The difficult temperature to measure in boiling heat transfer experiments is the temperature of the heating surface, and since the driving potential for the boiling process, $\Delta t_x = t_w - t_s$, is usually the small difference between two large quantities a small error in the measurement of surface temperature can result in a magnified error in the value of Δt_x.

Early workers used the heating tube as a resistance thermometer or attached a thermocouple directly to the heating surface on the fluid side, R 13, 1947. Subsequent workers found that to obtain an accurate surface temperature without disturbing the flow pattern it was necessary to measure the heating tube temperature on the dry side, and to correct this to the wet side value by subtracting the calculated radial temperature drop through the tube wall.

The two experimental arrangements used in previous work are, with few exceptions, fluid flowing through a heated tube, or fluid flowing over an inner heated tube in an annular flow section. The ohmic heating in both cases was provided by either a D.C. or A.C. electrical supply. Since the tube dimensions, the electrical and thermal resistance of the tube material, and the value of the heating current could all be accurately measured, then a precise temperature correction could be made if the heating surface remained clean during the

experiment. When deposits were built up on the heating surface during the experimental programme then the value of the radial temperature drop through the heating tube wall was greatly dependent on the deposit thickness, R 15, 1950.

The method of measuring the dry side temperature of the heating tube has been to use a thermocouple attached to the surface, but electrically insulated from it to avoid voltage pick up from the heating supply, this being particularly important when a D.C. supply was used. The method of drilling holes in the heating tube and brazing thermocouples in position has been used, R 52, 1965, but the accuracy of temperatures obtained in this way must be suspect.

The accuracy of the thermocouple temperature measurement of the heating tube outer surface depended on the maintainance of a good surrounding insulation or better still a guard heater to maintain an adiabatic surface, R 47, 1968.

In the case of the annular flow geometry with an inside heating tube the attachment of thermocouples to the inside of the heating tube was mechanically difficult to achieve, and a radiation thermocouple probe has been used successfully for this application, R 40, 1961. This had the added advantage of axial movement which enabled an axial temperature traverse to be taken. The time constant of the thermocouple would restrict the speed at which the traverse could be taken.

Some work on measuring the response time of thermocouples attached to a heating tube has been carried out, R 53, 1964, but since most measurements were made in the steady state condition, thermocouple response time was not a limiting factor.

The metal thermocouple has been used to the virtual exclusion of all other temperature sensors because of its accuracy, very small size e.g. wire diameters of 0.025 mm, repeatability and cheapness. The availability of high stability, high input impedance, sensitive digital voltmeters has confirmed this practice and led to data logging systems to record temperatures, since thermocouples can be used to measure all temperatures in an experimental system.

Other forms of temperature sensor have been used only for particular applications, e.g. temperature sensitive crystals used to show the local cooling spots on a heating surface due to the formation of vapour bubbles during boiling, R 54, 1971.

2.5. PHOTOGRAPHIC TECHNIQUES USED IN THE STUDY OF THE BOILING PROCESS.

Photographs of the boiling process have been used;

(i) To indicate the fluid flow patterns.

(ii) To show the manner of bubble formation and to permit bubble growth rates to be accurately measured.

(iii) In conjunction with a Schlieren system to show the interaction of the heated fluid boundary layer and the forming bubbles.

To indicate the fluid flow patterns a single black and white photograph with an exposure time determined by the fluid velocity, that is not so short as to "freeze" the bubble motion but just of sufficient duration to allow the bubbles a small movement and thus to produce elongated images which serve as a vector portrayal of the flow pattern, has been found satisfactory.

To show the manner of bubble formation a high speed framing camera, 5 000 frames/s, has been employed, R 39, 1961. The problem has always been to anticipate exactly the location of an individual bubble just as it begins to form and to then film its life history at high speed against a scaled grid background for subsequent frame by frame analysis. For very high speeds a Kerr cell was used as the camera shutter, R 55, 1948, R 56, 1949. This depended on the fact that some chemical solutions would polarize light when an electric field was applied to them. This polarization effect was used

with an additional polarizing filter to give a combination filter which was normally opaque, but which became clear during the application of a microsecond electrical impulse to the solution. With this device exposure rates of 14 000/s were achieved with individual exposure times of 3 μs. Since the film transport accelerated from standstill to operating speed, only the last 10% of the film length was running at a speed high enough to accommodate the exposure rate, R 18, 1950.

An important point in high speed photography was the duration of the exposure as well as the number of exposures per second, since it was the duration of the exposure which was important in obtaining a "frozen" image. Flash synchronised cameras were used as an improvement on the normal shutter arrangement, as an example if a camera was running at 1 000 frames/s then each framing time could be 1 ms, however if an illuminating stroboscope was triggered to flash at each exposure, then at the same 1 000 frames/s the exposure time was 4 μs, that is the duration of the stroboscope flash. This would give a sharpness of image equivalent to a normal framing speed of 250 000 frames/s if such a speed were possible.

The initial high speed of vapour bubble growth rate made demands on camera speed beyond the reach of a normal framing camera and some success in measuring bubble growth rates was achieved by simply dispensing with the camera shutter and allowing only a thin slit of the image to focus on the film,

the width of the line image giving a continuous record of the bubble diameter, R 57, 1969.

An interesting application of photography to the boiling process was the interference method of measuring the thickness of the liquid layer beneath the forming vapour bubble, R 42, 1964. Here monochromatic light was projected through the bubble to the heating surface and reflected back from both the top and the bottom of the thin liquid layer beneath the bubble. The two reflections combined to give interference rings and thus an accurate measure of the liquid thickness. The bubble growth period was recorded by a high speed camera so as to produce a time record of events.

The previous methods provided data on bubble formation but were not able to show the interaction of the forming bubble with the surrounding liquid. To demonstrate this a Schlieren optical system, R 57, 1963, in conjunction with a high speed camera was used with both black and white, R 39, 1961, and colour film, R 50, 1964. The colour Schlieren system had the significant advantage that it could be roughly calibrated, colour against temperature, and it thus carried more information than the black and white system which indicated flow patterns only. Against this, black and white film was cheaper and had a very much higher emulsion speed than colour film for which the camera speed was limited by the light available.

The light source for a Schlieren system must be as near a point source as possible, this requirement has been met by a point source mercury vapour lamp with either a smoothed D.C. supply or used as a pulsed point light source with a thyratron repeatedly discharging a capacitor bank through the lamp, R 58, 1969. More recently Xenon point source lamps have been used.

2.8. THE EFFECT OF DISCONTINUITIES IN THE FLOW PATH ON THE HEAT TRANSFER COEFFICIENT.

The work carried out by Ede, Hislop and Morris, R 1, and by Ede Morris and Birch, R 2, was concerned with the flow of water through a step convergence, and a step divergence, in the flow section.

At the values of heat flux used, 38 kW/m^2 maximum, the flow was at all times single phase. The heat release was constant over the length of the pipe, which was heated by the passage of direct current through it.

The approach length to the step discontinuity was greater than 100 pipe diameters for both the step convergence and the step divergence and the effect of the step change persisted for approximately 30 pipe diameters downstream in each case.

The variation in the pipe wall temperature and thus the heat transfer coefficient was plotted from values measured at a number of discrete points along the axis, spaced by one diameter near the change on section, but more widely spaced away from the change in section.

Taking the accepted correlation for turbulent flow through a straight pipe.

$$Nu = 0.023\ Re^{0.8}\ Pr^{0.4}$$

this can be arranged as

$$N = \frac{Nu}{Re^{0.8} Pr^{0.4}}$$

where the constant N should be independant of Re number and Pr number.

Results of the variation in heat transfer coefficient along the axis of the tube were plotted as a variation in the local value of N. By using this method all results for turbulent flow could have been reasonably expected to follow one curve but the authors found that the results were too scattered for this to be useful and in fact plotted the results for particular Re numbers on separate graphs. The abscissae was scaled in pipe diameters.

For each Re number used a number of tests were carried out, each with a particular heat flux. From the results an attempt was made to graphically estimate the variation of N for the zero heat flux condition.

The results for the converging flowwere plotted as the ratio

$$\frac{N_{\text{local measured}}}{N_{\text{fully developed plain pipe}}}$$

against axial distance scaled in pipe diameters and shown to have the same form as those of previous workers.

The Re numbers used extended from the turbulent through the transition region into the laminar region where a similar

experimental method was used.

A typical plot of the heat transfer coefficient variation against axial distance is shown, G 2.1, transferred from the data, R 1, for comparison with the results of the present work.

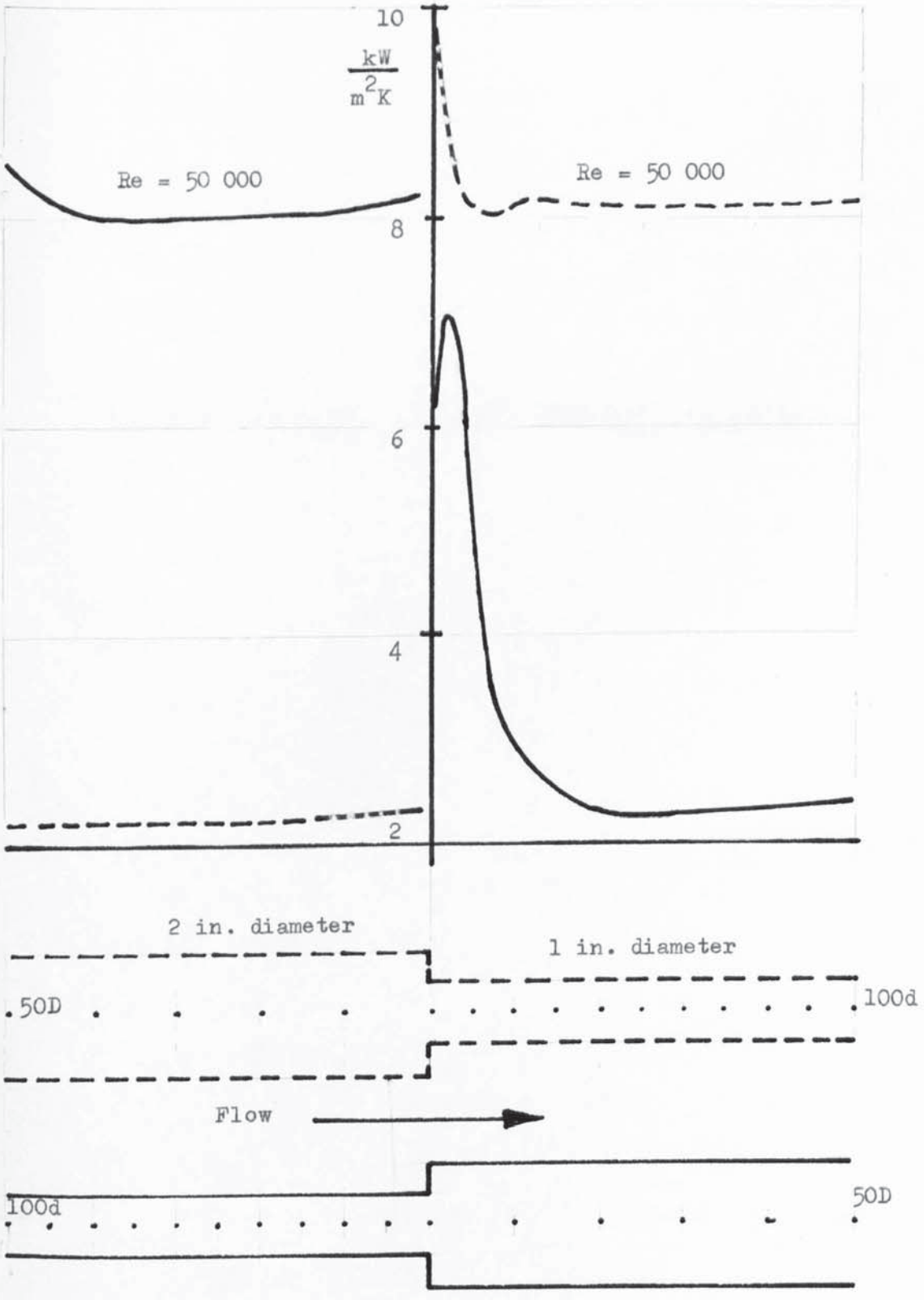

VARIATION OF THE HEAT TRANSFER COEFFICIENT ALONG THE AXIS OF A STEPPED PIPE
Taken from data from Ede, Hislop and Morris, R 1.

G 2.12

APPARATUS AND PROCEDURE

Chapter 3.

3.1. INTRODUCTION.

It was thought at the outset that in studying two-phase flow with heat transfer, particularly at discontinuities in the flow path, that a visual picture of the flow would be extremely valuable. Consequently the preferred geometry of the test section would be an annular duct with the outside wall constructed of glass.

The simplest possible discontinuity, a step in the diameter, was planned, and this led to the choice of having a step in the inner heating tube, or in the outer glass wall, being aware that the two alternative geometries would produce different effects on the heat transfer coefficient and the pressure drop. Wary of the differential expansion problems likely to be encountered in a fabricated stepped glass tube it did seem that a stepped heating element would provide the easier solution to the problem, and the construction of a stepped heating element was attempted, D 3.12 but later abandoned due to the difficulties experienced in placing thermocouples inside the element. A stepped glass outer tube D 3.13 was then attempted and after some initial failures a successful tube was constructed.

Electrical heating of the inner tube was employed as the most convenient and easily measured heat source and in practice it presented no difficulties except that at the point of attachment of the leads to the heating element regular cleaning was required to maintain the required low resistance joint, D 3.3.

The upper limit to the temperature of the water leaving the test section was set by the commencement of boiling in the reservoir tank, D 3.1 where the water was at a lower pressure than that in the test section. The water circuit was modified to include a

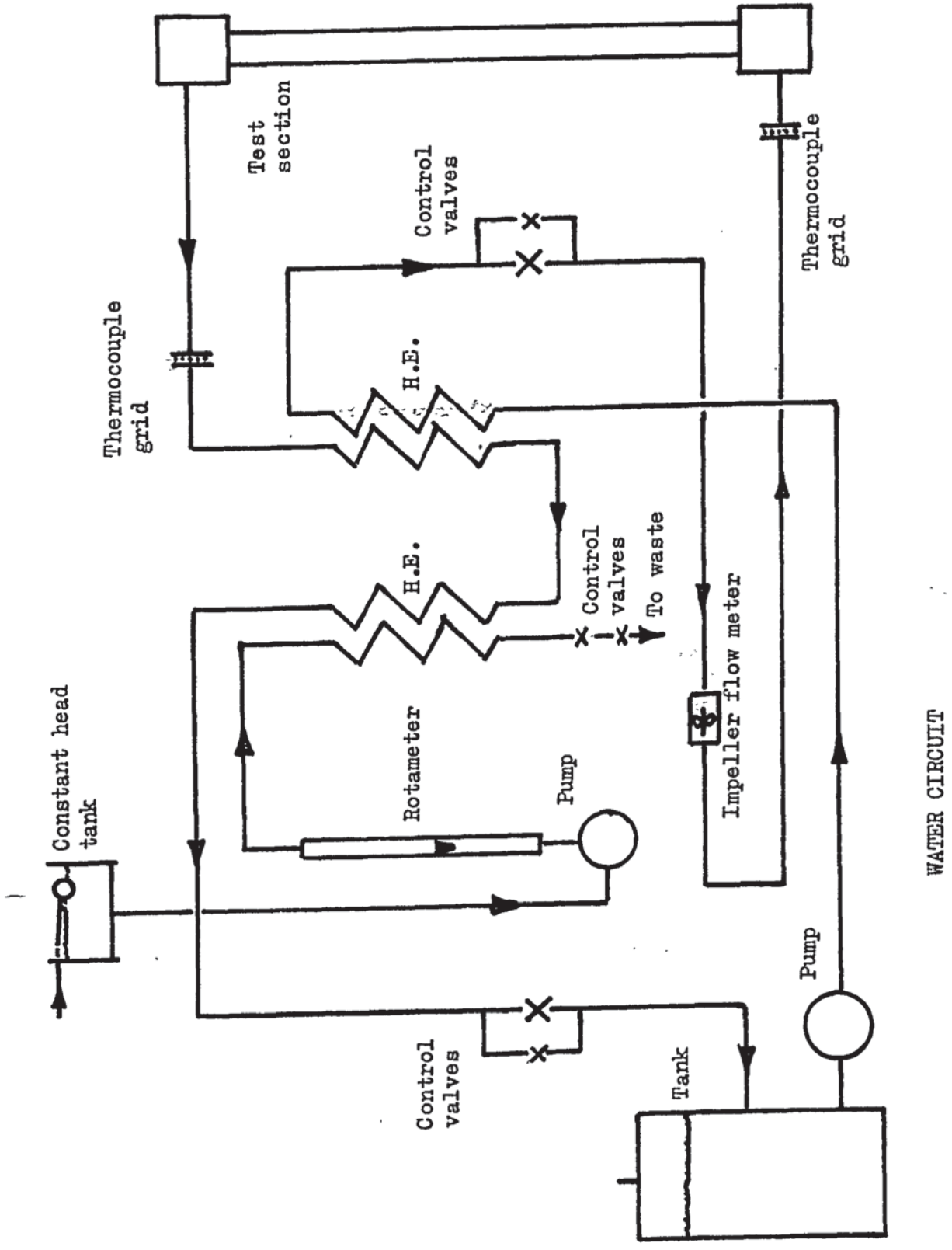
Test section
Control valves
Thermocouple grid
Thermocouple grid
H.E.
H.E.
Control valves
To waste
Impeller flow meter
Constant head tank
Rotameter
Pump
Pump
Control valves
Tank
WATER CIRCUIT

D 3.1

recuperative heat exchanger which transferred heat from the heated water leaving the test section to the cooler water entering the test section. This modification effectively raised the upper limit of the temperature at the test section.

All temperatures in the circuit were measured by Chromel-Alumel thermocouples referenced to an ice point provided by a "Frigistor" solid state heat pump. The outputs from the thermocouples were measured by a digital voltmeter controlled by a high speed data logger which recorded the data on eight hole paper tape. This arrangement was planned to achieve almost simultaneous readings of the temperature round the circuit and to permit the use of a computer programme to convert the millivolt output from the thermocouples to temperature values.

The flow rate of water round the circuit was measured by a rotating impeller type of flow meter coupled electrically to a digital frequency meter. This type of flow meter was used as it offered the possibility of having its output connected into the data logger and a computer programme was used to convert the output reading into the flow rate for use in subsequent calculations.

The use of a computer programme to process the data was eventually not proceeded with as it proved too inflexible for the various tests carried out, and a calculating machine proved adequate to process the results.

Later in the programme it was thought that a test channel could be made up with glass sides to represent a section through the annulus and at the same time permit the flow to be viewed in a direction tangential to the circular annulus. This section when manufactured was used with schlieren equipment to visualize the boundary layer.

3.2. SERVICES FOR ANNULAR TEST SECTION.

WATER CIRCUIT.

The design of the water circuit to support the investigation was governed by two limitations. One was the maximum electrical power available to heat the test piece and the other was the maximum flow rate of water which would suppress boiling when the test piece was operating at maximum power.

The maximum electrical power available was accurately known but the maximum water flow requirement was estimated and subsequently proved to be adequate. Since it was intended to carry out the investigations at near atmospheric pressure no pressurising system was necessary and the circuit was planned as a simple, reservoir tank, pump, test piece, cooler, circuit, D 3.1. This was entirely satisfactory for the initial tests which were conducted with water temperatures appreciably below saturation temperature but since, because of the frictional pressure drop in the cooler, the saturation temperature in the test piece was some 8 K above the saturation temperature in the reservoir it was not possible to have a liquid subcooling of less than 8 K in the test section without boiling taking place in the reservoir tank.

One solution would have been to have a larger cooler and at the same time an electrical pre-heating section in the circuit downstream of the pump but the additional electrical power was not available and to achieve the same effect a recuperative heat exchanger was fitted into the circuit, D 3.1, and this modification enabled the liquid subcooling in the test section to be reduced almost to zero.

FLOW MEASUREMENT.

The flow through the main circuit was measured initially by a B.S. orifice plate and manometer but this was replaced by a rotating

impeller type of flow meter which was calibrated, as installed, both with hot and cold water. The impulses from the meter were totalized by an electronic digital counter.

The flow of cooling water through the cooler was measured by a rotameter calibrated in the installed position.

ELECTRICAL HEATING EQUIPMENT.

The electrical heating supply was taken from a single phase, 250 v supply through a variable transformer and a step down transformer D 3.2. The control given by the variable transformer proved to be too coarse and an additional boost transformer was added to the circuit to give a fine control to the power supplied. Two voltage output ranges were available from the step down transformers, 0 - 20 volts at 1250 amps or 0 - 10 volts at 0 - 2500 amps. Ideally the test piece resistance should have matched one of the alternative output ranges, i.e. 0.004 Ω or 0.016 Ω, and this fully utilized the power available. However in practice it was not possible to do this exactly due to the limited range of metal wall thicknesses available in the size of tube used for the construction of the test element. It was found in carrying out the tests that the transformer was conservatively rated and would accept a 25% overload for thee hours without showing an excessive temperature rise.

The connection between the busbars and the test piece had to be capable of carrying up to 2.0 kA and at the same time to permit some mechanical flexibility. Heavy duty flexible copper braid was used and it was attached to the test piece by wrapping it round the copper ends and clamping it.

A point by point voltage drop round the circuit was taken to check the electrical soundness of the connections particularly the connection between the flexible copper braid and the test piece, D 3.3. The clamps here demonstrated a tendency to relax over a

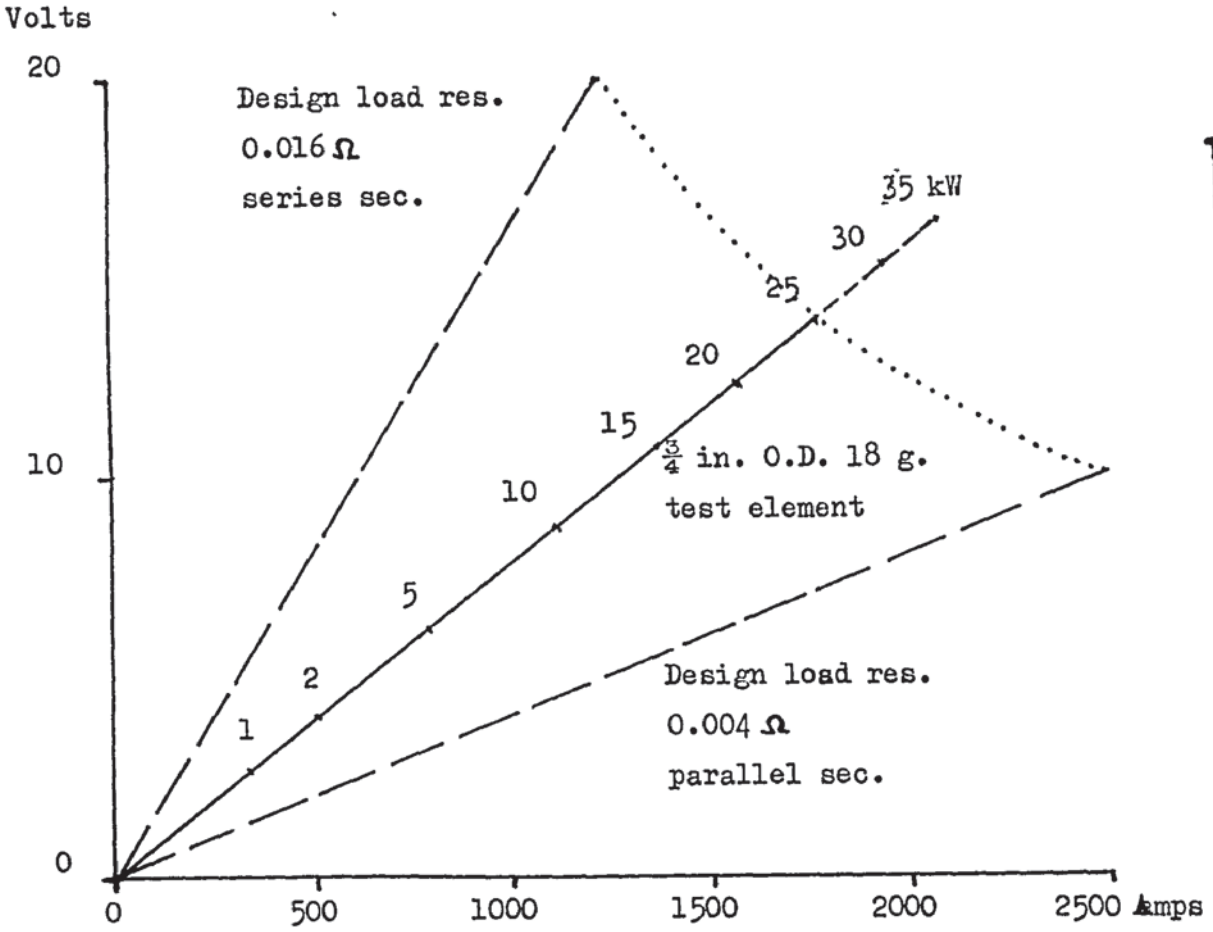

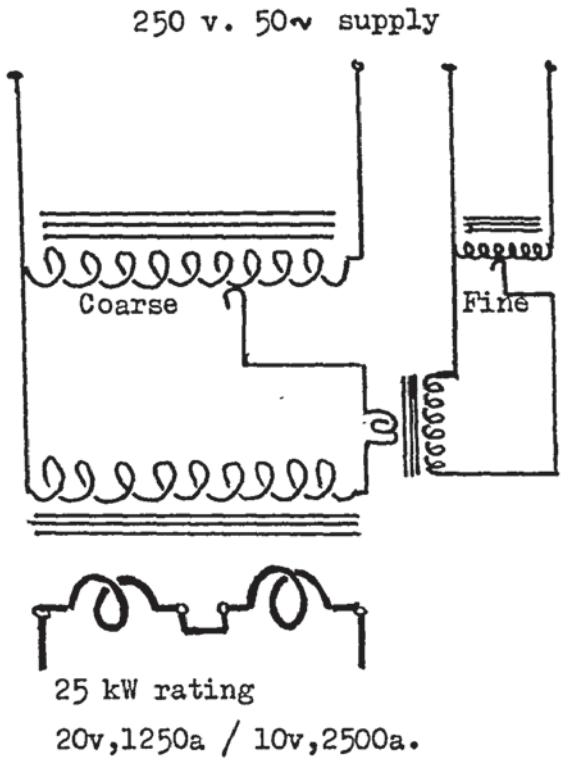

ELECTRICAL HEATING CIRCUIT

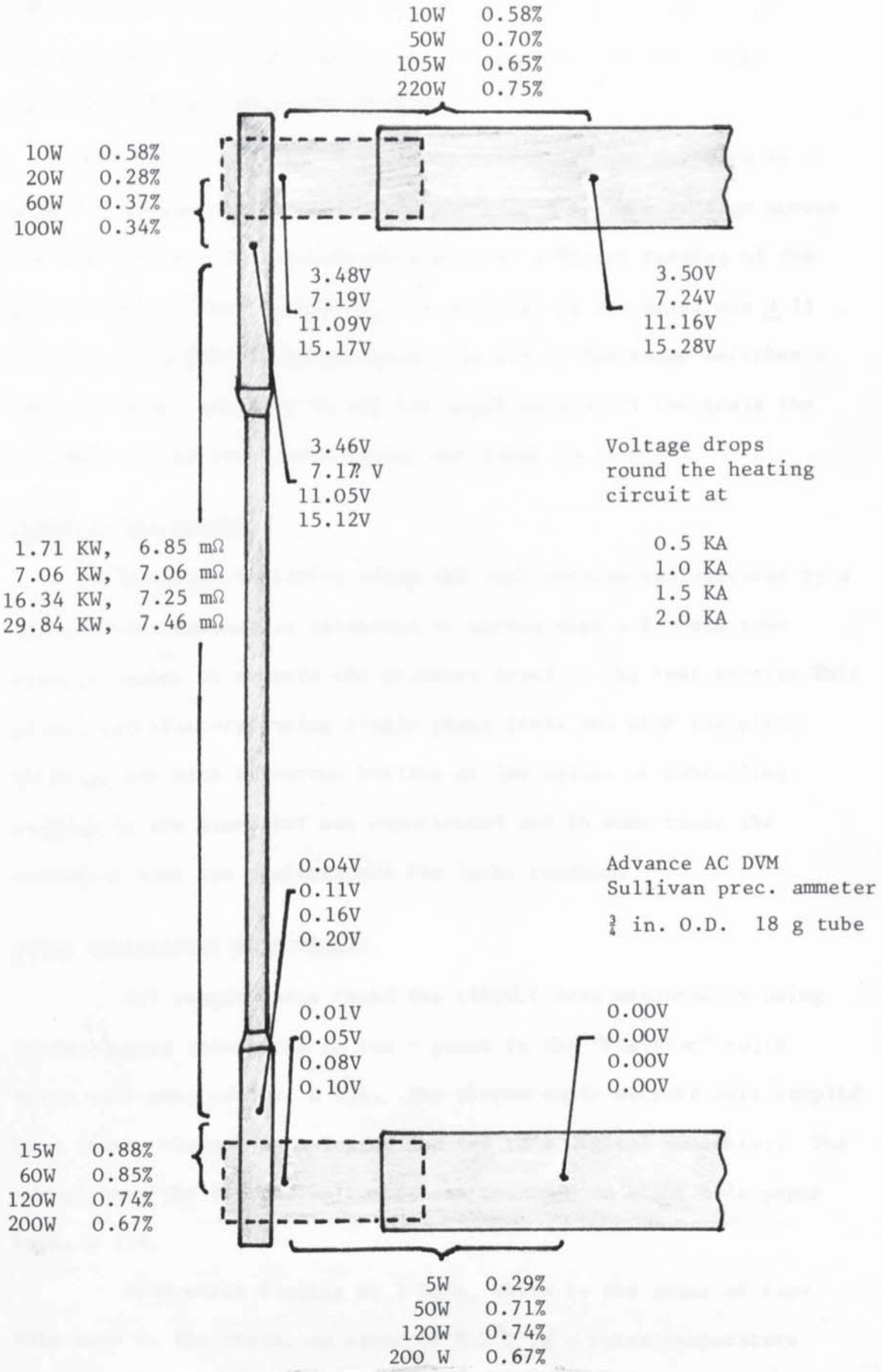

VOLTAGE DROP ROUND THE CIRCUIT

D·3.3

period of time and subsequently two sensitive A.C. milli-voltmeters were connected across these joints to continuously monitor the voltage drop and give warning of any slackness in the clamps.

INPUT ELECTRICAL POWER MEASUREMENT.

The current passing through the test piece was measured by a multi-range precision multi-purpose meter as was the voltage across the test piece. The same meter also gave a direct reading of the power input to the test piece, the accuracy of the meter was $\pm$ 1% of full scale deflection and since the use of the range switches made it always possible to use the upper portion of the scale the accuracy of the power measurement was taken to be $\pm$ 2%.

PRESSURE MEASUREMENT.

The pressure variation along the test section was measured by a row of water manometers connected in series with a Bourdon tube pressure gauge to measure the pressure level in the test section. This proved satisfactory during single phase tests and with incipient boiling, but with vigourous boiling at low values of subcooling, surging in the manometer was experienced and in some cases the manometer bank was photographed for later reading.

WATER TEMPERATURE MEASUREMENT.

All temperatures round the circuit were measured by using thermocouples referenced to ice - point in the "Frigistor" solid state heat pump cooler, D 3.4. The thermocouple outputs were sampled by a twenty channel data logger and fed to a digital voltmeter. The output from the digital voltmeter was recorded on eight hole paper tape, D 3.5.

With water flowing at 1 Kg/s, which is the order of flow rate used in the tests, an error of 0.2^{o}C in a water temperature difference reading would result in an error of approximately 0.8 kW

in the heat balance. This is typically 5% of the power supplied to the test piece and for this reason care was taken to achieve an accurate measurement of the temperature of the water entering and leaving the test section.

Assuming that the flow was symmetrical about the axis of the pipe a five point sampling grid was arranged across one diameter, D 3.6, D 3.7, this had been used successfully by Ede, R 21, As a further improvement a wire mesh was placed upstream of the thermocouple grid which had the effect of giving an extremely flat water temperature profile at the grid location, P 3.1, D 3.6 over the range of flowrates encountered in the tests. The maximum error in read out from the digital voltmeter was $\pm$ 0.002 mV which with Chromel/Alumel thermocouples was equivalent to a maximum temperature error of $\pm$ 0.05°C, A 3 . This value of maximum error on an individual temperature reading meant that the temperature difference between the water entering and leaving the test section was known within an error of $\pm$ 0.1 K.

The temperature of the water at any point along the axis of the test section was calculated from the inlet temperature by considering the heat added to the water from the heating element, to the point in question

$$t = t_{inlet} + \frac{q}{\dot{m} C_p}$$

account being taken of the variation in the specific heat of water with temperature. Although the impeller flow meter had been calibrated in a given time, it was felt that this could be judged to be not better than $\pm$ 2% of the true value. In considering the equation for calculating the temperature at any point along the heater axis, the second term was typically 15 K with small flows and 3 K with large flows, this would indicate a maximum possible error in the temperature of the water along the test section axis of

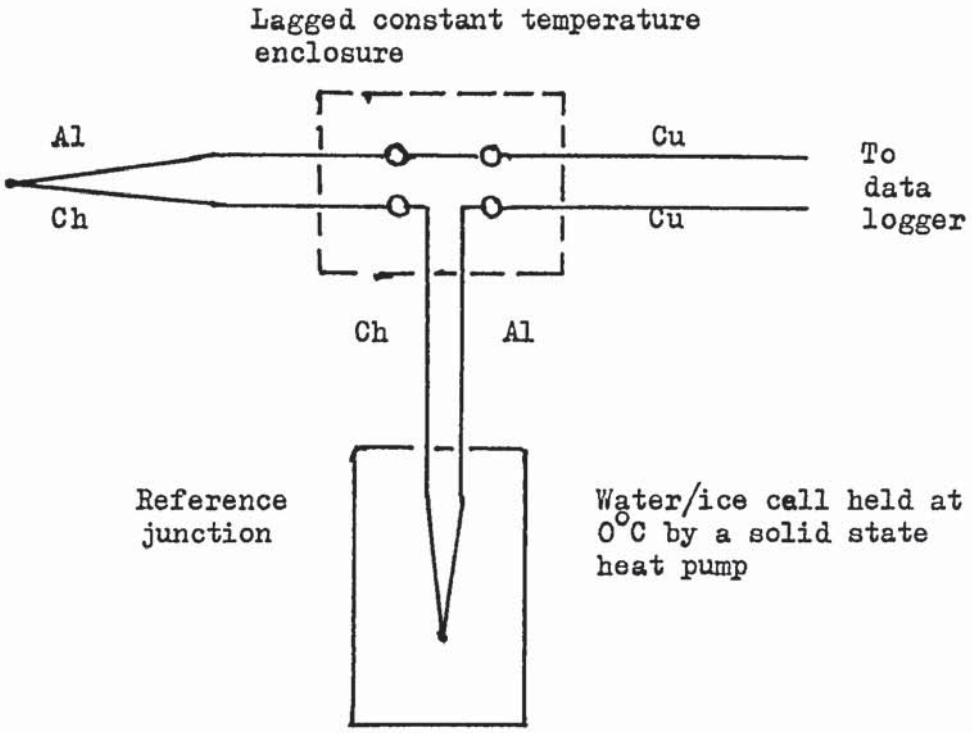

THERMOCOUPLE CIRCUIT (One junction only) D 3.4

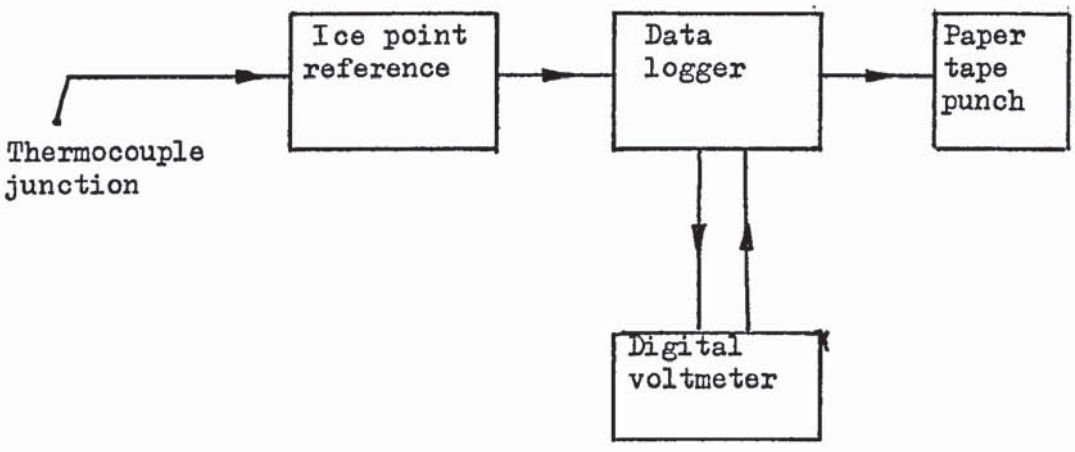

ARRANGEMENT OF DATA LOGGING EQUIPMENT
(Only one thermocouple junction shown) D 3.5

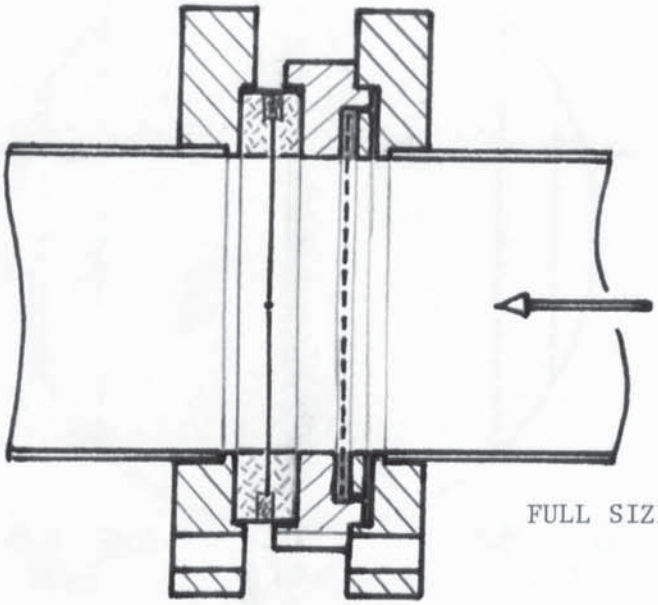

FULL SIZE

D 3.6

Detail of a thermocouple grid with upstream mesh, used to measure the water temperatures at inlet to and outlet from the test section.

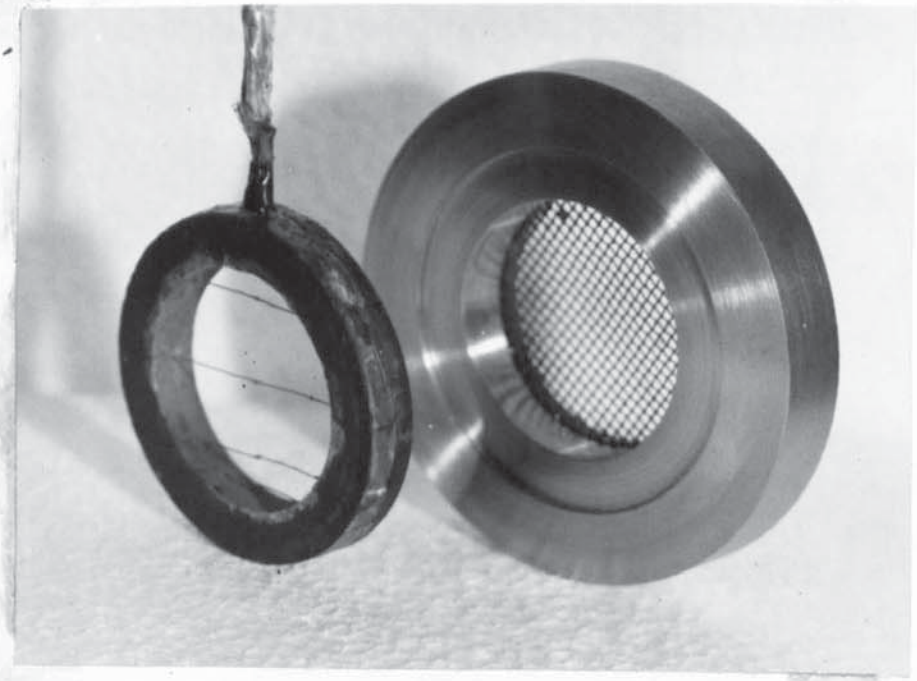

THERMOCOUPLE GRID WITH MESH

P 3.1

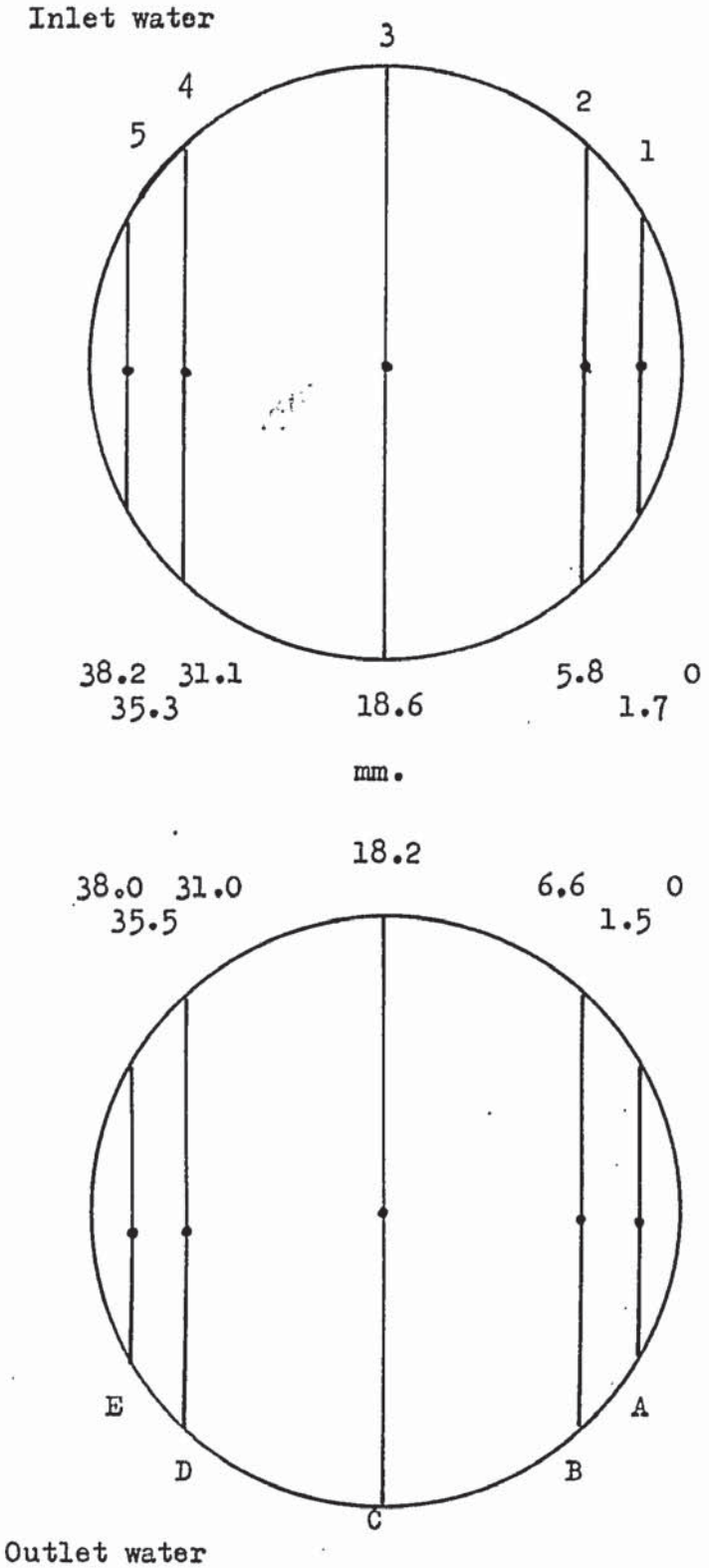

THERMOCOUPLE GRID SPACING

± 0.65 K and ± 0.17 K for minimum and maximum flow rates respectively.

The temperature of the cooling water flowing through the cooler was measured at inlet and outlet by a single thermocouple situated centrally in the highly turbulent inlet and exit flow paths.

3.3. SERVICES FOR RECTANGULAR TEST SECTION.

WATER/FREON CIRCUIT.

The circuit was designed to give comparable flow velocities to those encountered in the annular test section. A centrifugal pump was used to circulate the fluid through the test section and an air cooled heat exchanger in parallel, this arrangement permitted full flow to be maintained in the heat exchanger even at low flow velocities in the test section and thus its effectiveness was maintained. D 3.8 and P 3.2 show the layout.

FLOW MEASUREMENT.

A rotameter was used with calibration curves supplied by the manufacturer.

ELECTRICAL HEATING CIRCUIT.

This was single phase, 250 v with coarse and fine control as shown, D 3.11. The power was measured by assuming unity power factor and multiplying the measured voltage and current.

WATER/FREON TEMPERATURE MEASUREMENT.

The temperature of the fluid was measured at the entry to, and exit from, the test section by single Chromel/Alumel thermocouple junctions immersed in the fluid. It was assumed that with the small bore connection, 15 mmID, and the change of section, no temperature stratification would exist in the fluid and that the thermocouples would effectively measure the mean values of the fluid

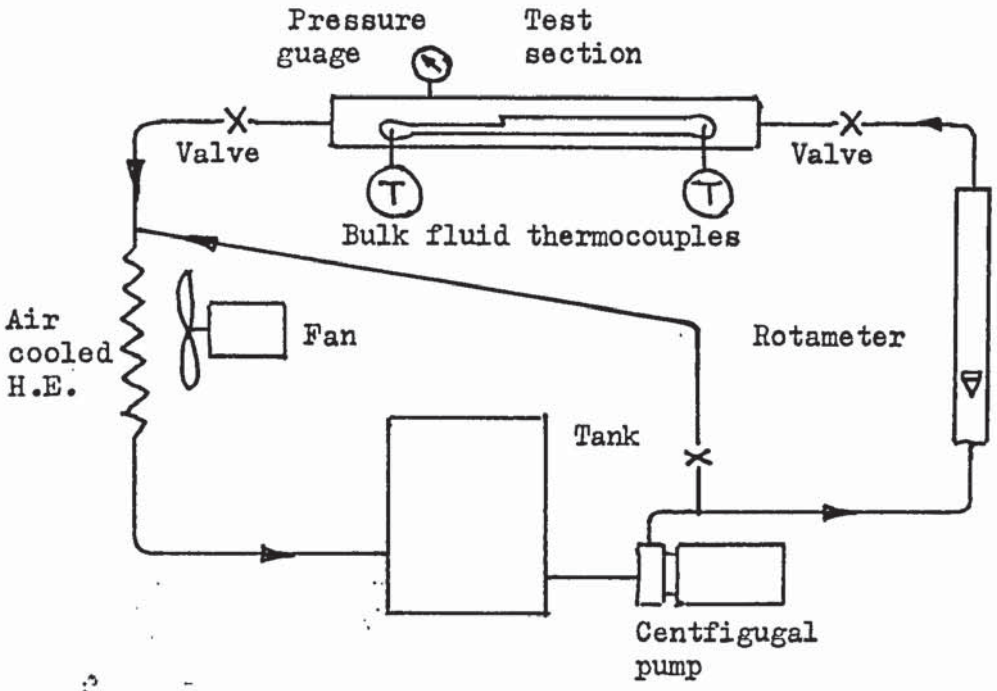

WATER/FREON CIRCUIT FOR THE TEST SECTION. D 3.8

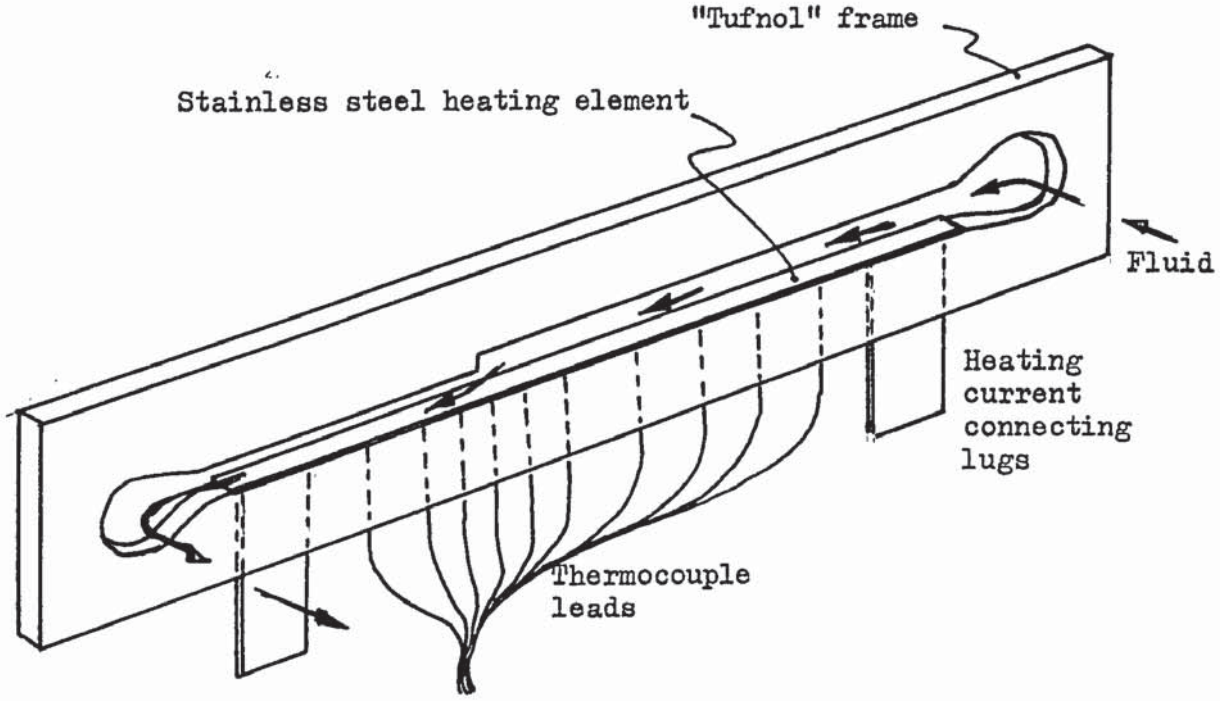

F , ARRANGEMENT OF TEST SECTION (Glass sides ommitted)

D 3.9

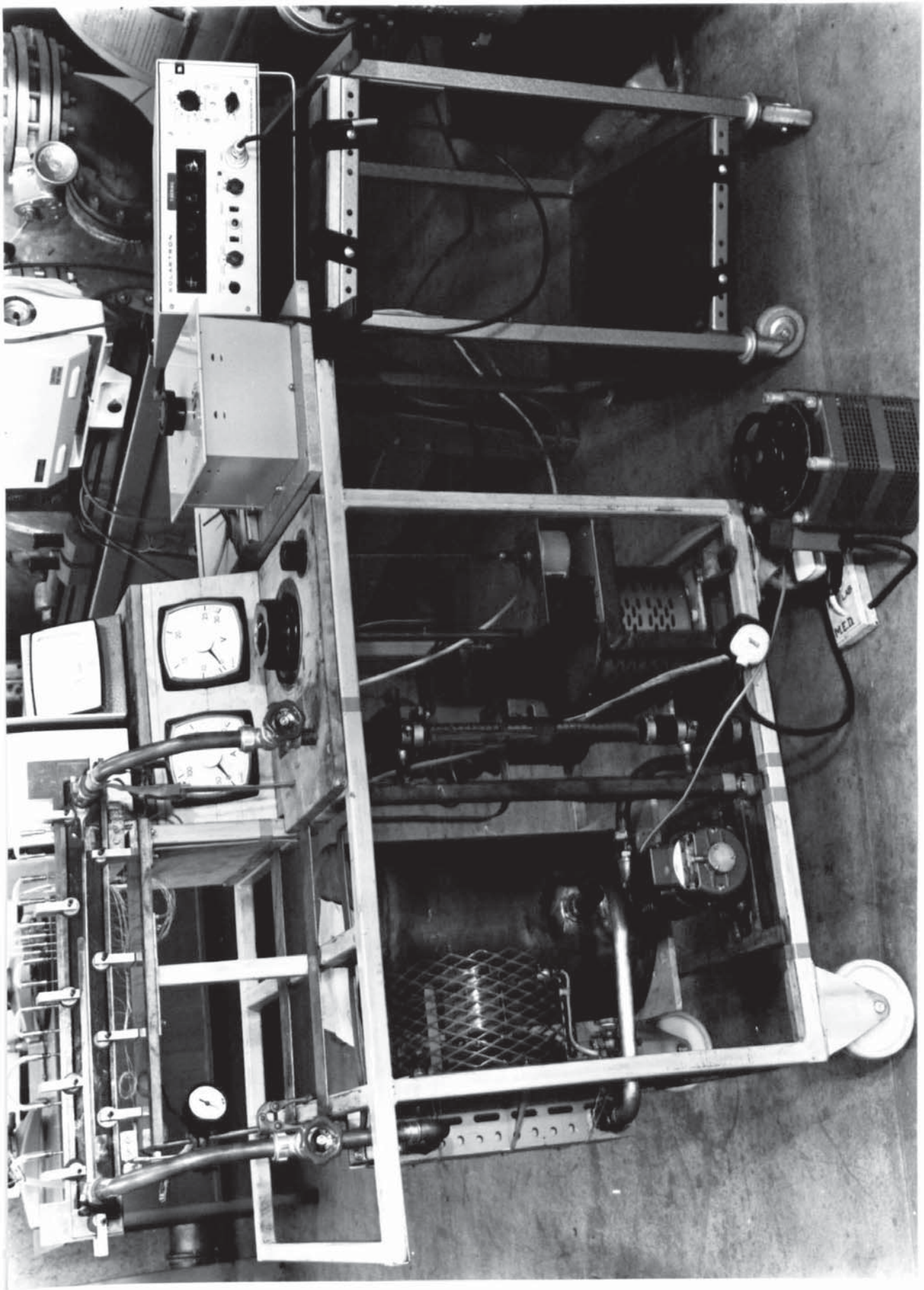

WATER/FREON CIRCUIT P 3.2

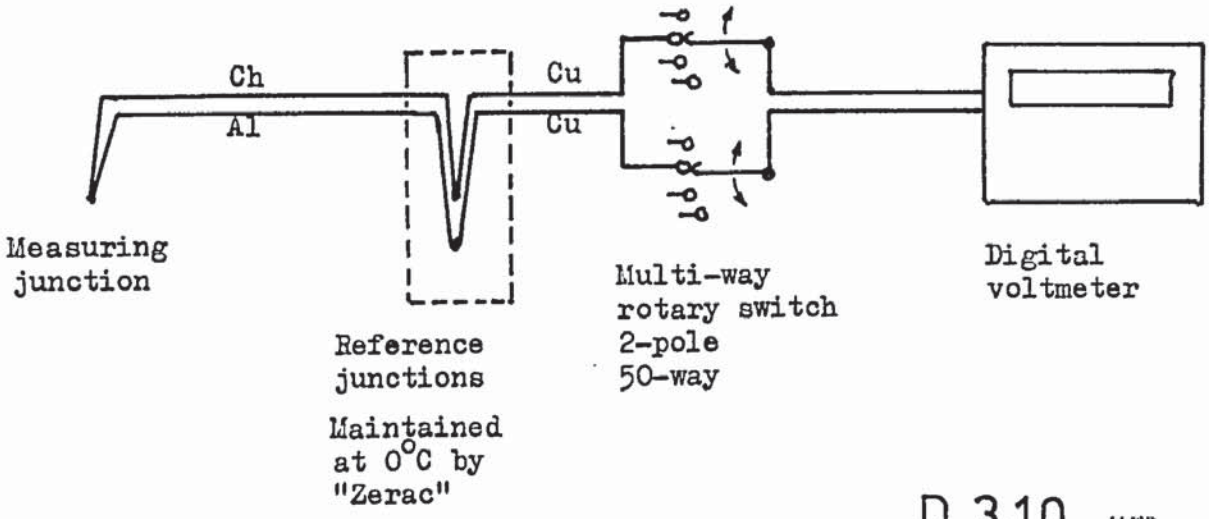

D 3.10

THERMOCOUPLE CONNECTIONS (For one junction only)

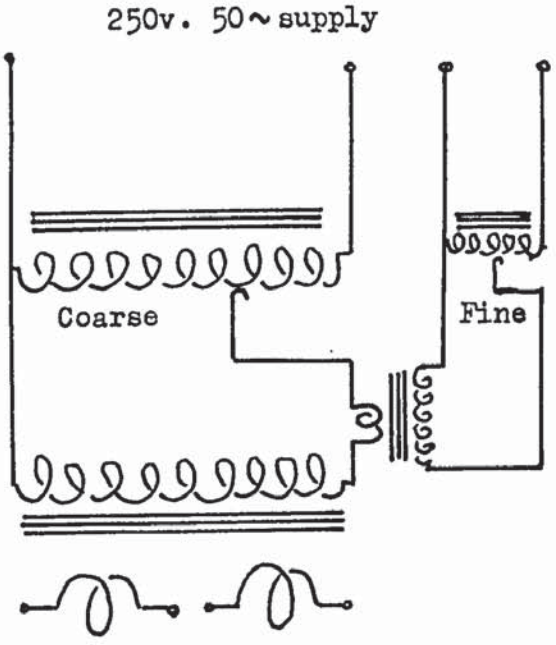

D 3.11

ELECTRICAL HEATING CIRCUIT

temperature.

PRESSURE MEASUREMENT.

Although it was initially planned to measure the static fluid pressure at a number of points along the test section this did not prove to be constructionally possible and the test section static pressure level was monitored at one point only by a small tube pressure gauge.

3.4. ANNULAR TEST SECTION.

TEST PIECE CONSTRUCTION.

The aim in constructing the test piece was to provide an annular flow section with the inner surface heated electrically and the outer wall transparent to provide a visual picture of the flow pattern with a two-phase fluid flowing through it. The annular flow section was to be made with a step discontinuity and it was essential to be able to measure the axial variation in the heating surface temperature in the region of the discontinuity. The provision of a step change in the annular section could have been achieved by having a stepped heating element or a stepped outer tube. In considering this choice and bearing in mind that the outer tube had to be made from glass, to enable the flow to be observed, it was thought that the stepped heating element would be the easier solution, D 3.12.

A lin.outside diameter tube and a 0.5 in. outside diameter tube were chosen with gauge thickness to give them the same cross sectional area and thus achieve uniform ohmic heating along the axis of the stepped heating element D 3.12. The problem of instrumenting the combined tubes with thermocouples to measure the variation in the outer surface temperature along the axis was to be solved by welding the thermocouple to the inside of the tube and calculating the radial temperature drop in the tubes to correct the

inside surface temperature to the outside surface temperature. An alternative method of fixing thermocouples to the heating element by drilling and silver soldering, was rejected, for although other workers, R 52 , had employed this construction the precise point of temperature measurement was not known and the presence of the thermocouple hole would distort the heating current locally. The actual tube was successfully built with a minimal change of resistance at the joint between the 1 in. and 0.5 in. diameter tubes P 3.5. A long reach vice was constructed to place the thermocouples accurately in position in the tube for welding but the results were disappointing for despite a lot of time being spent in trying to establish a set of optimum conditions, contact pressure, capacitance value, and changing voltage of the capacitance discharge welder, the thermocouples could not be attached with any degree of consistency. Failing to weld the thermocouples in position it was decided to devise a clamp to hold them in position and a "Circlip" with three "Tufnol" shoes was first constructed to hold the junctions in contact with the tube, P 3.3, and then an improvement was developed in the form of a cast epoxy resin 'Circlip', P 3.4, with integral thermocouples, however this still needed a backing steel circlip. The 'Circlips' were slid into position in the heating element where a minimum axial spacing of 20 mm was achieved, but after repeated temperature cycling an X-ray photograph, P 3.5, showed that the 'Circlips' were creeping out of position. In view of this it was thought that a single thermocouple 'Circlip' mounted on a sliding rod would provide a more satisfactory solution for although it would not permit simultaneous readings of the temperature along the heating element axis it would provide infinite resolution. Consequent to this decision it was further decided to use a single diameter tube

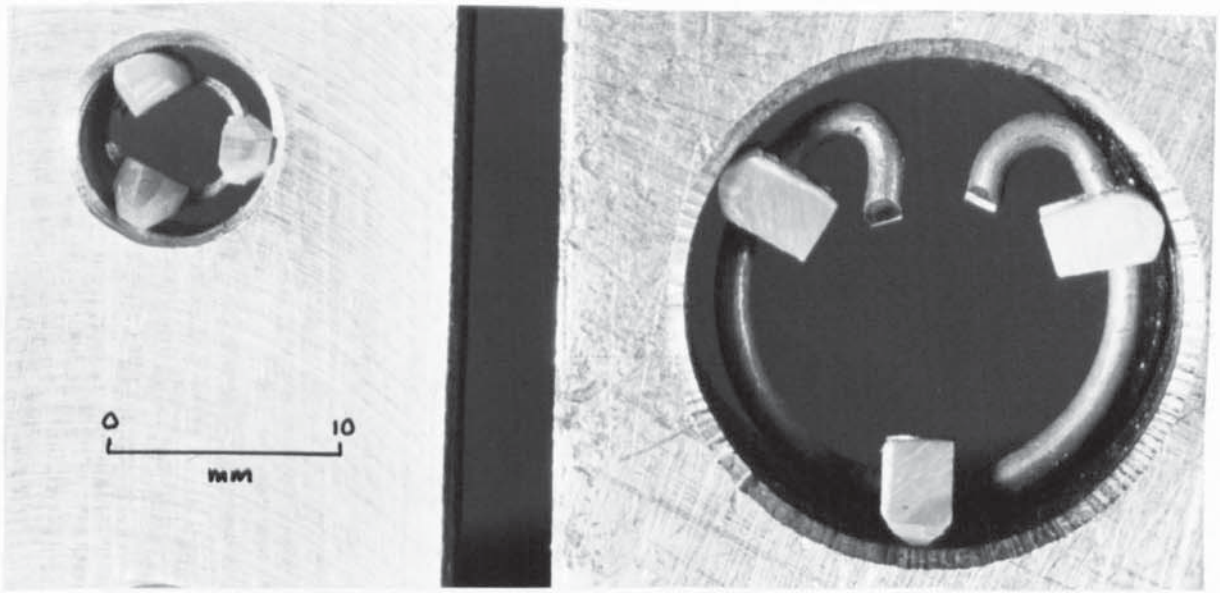

"CIRCLIP" THERMOCOUPLE HOLDER P 3.3

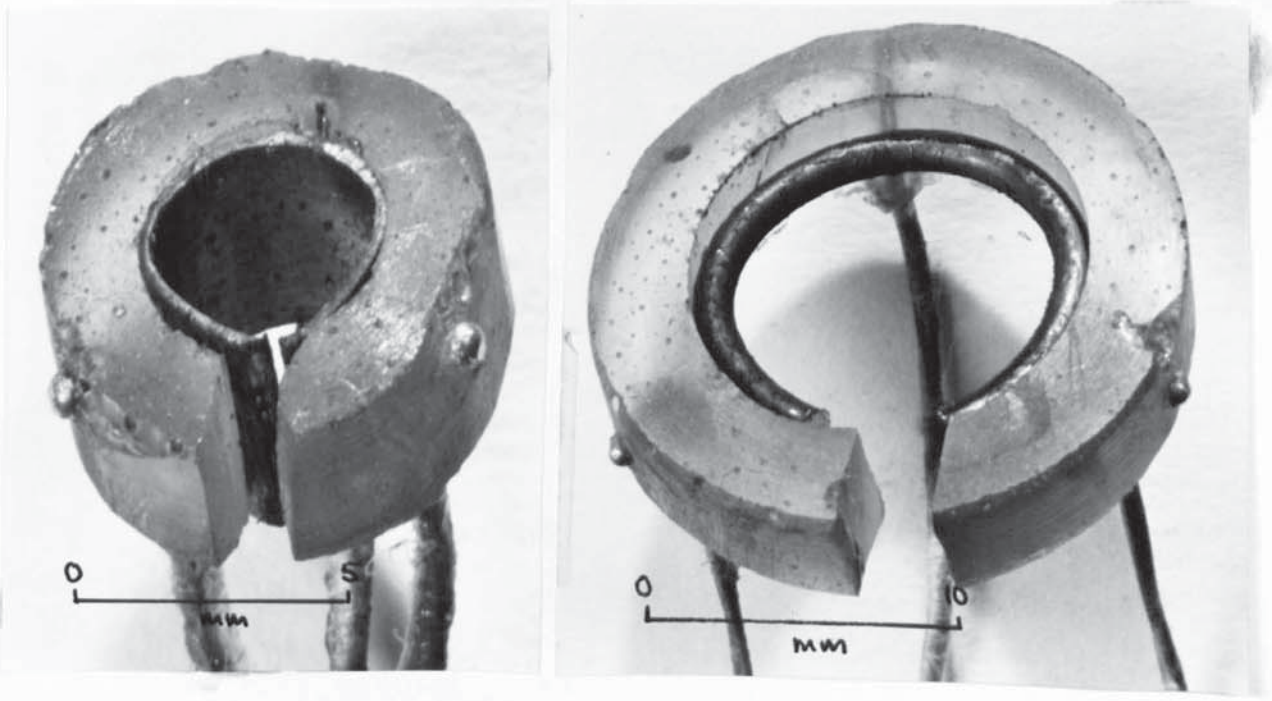

CAST EPOXY RESIN THERMOCOUPLE HOLDER P 3.4

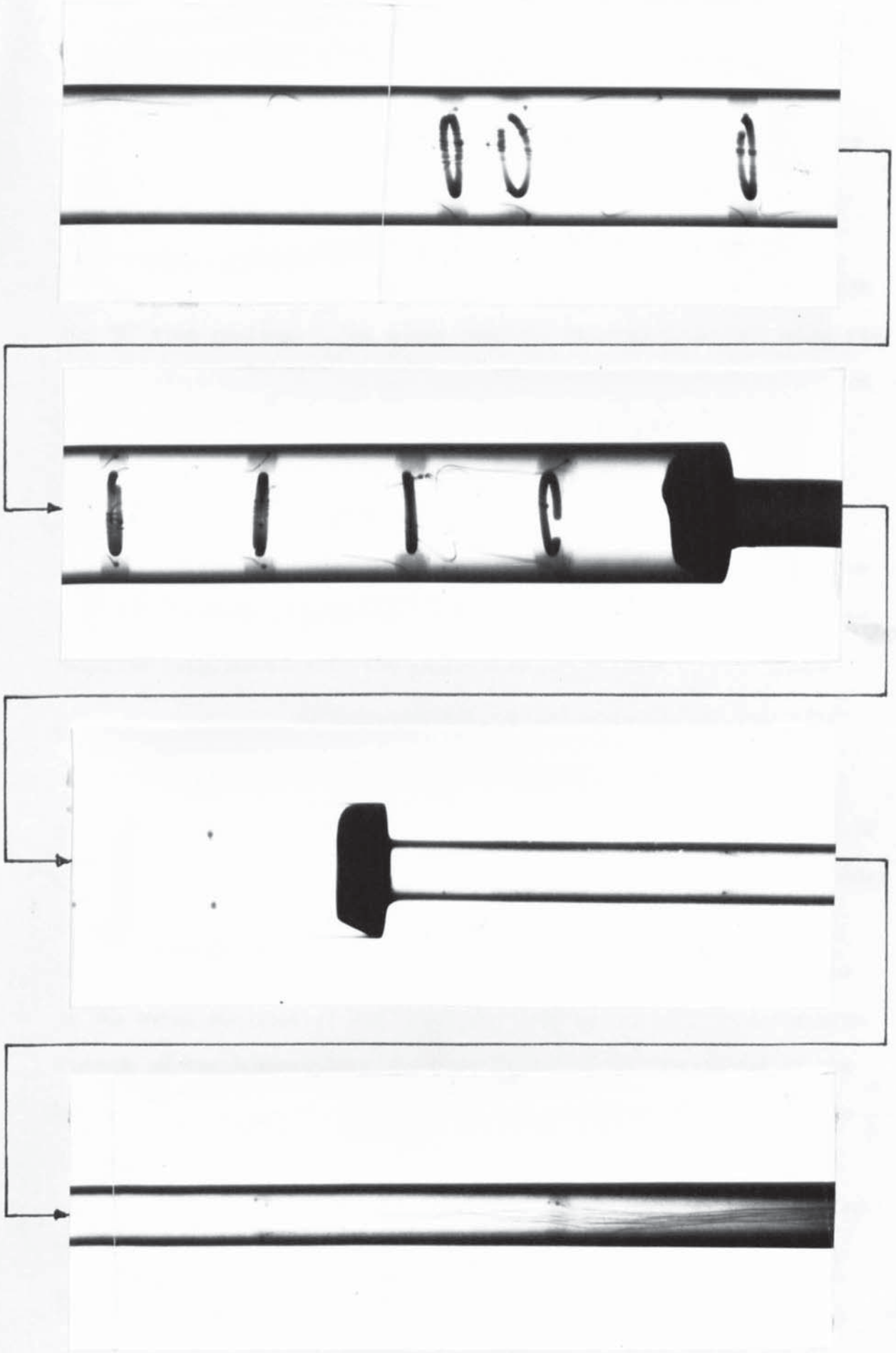

X-RAY PHOTOGRAPHS OF "CIRCLIPS" IN HEATING TUBE

P 3.5

as the heating element and to provide a step in the diameter of the outer glass tube. The section of the step in the glass tube diameter is shown in D 3.13 where the overiding consideration was to avoid imposing any tensile stress on the glass. A joint piece was cast in "Araldite" on to the end of the small glass tube and then bonded into position in the large glass tube leaving an expansion gap and "O" ring sealing. The glass tube was drilled at points along its axis to accommodate pressure tappings which were bonded into position with "Araldite".

It was appreciated that a thermocouple junction in sliding contact with a metal surface would not necessarily reach the true temperature of the surface and to determine the correction needed an investigation was carried out which compared the sliding thermocouple junction temperature with the known true metal surface temperature.

EFFECT OF THE THERMAL RESISTANCE OF A SLIDING CONTACT.

A thick walled brass tube was constructed in two halves and thermocouple junctions were embedded along a radius on the end face of one half, D 3.14. The two halves were tinned and then offered together on a centering mandrel and soldered into one composite tube. The thermocouple junctions were then effectively embedded along a radius at the axial midpoint of the composite tube and by extrapolating from a graph of the temperatures at these junctions to the surface of the bore of the composite tube, the surface temperature of the tube bore could be very accurately determined.

The tube was reamed to give a smooth bore and was then mounted in an asbestos box and provision was made to circulate hot air over the outer surface of the tube, D 3.15.

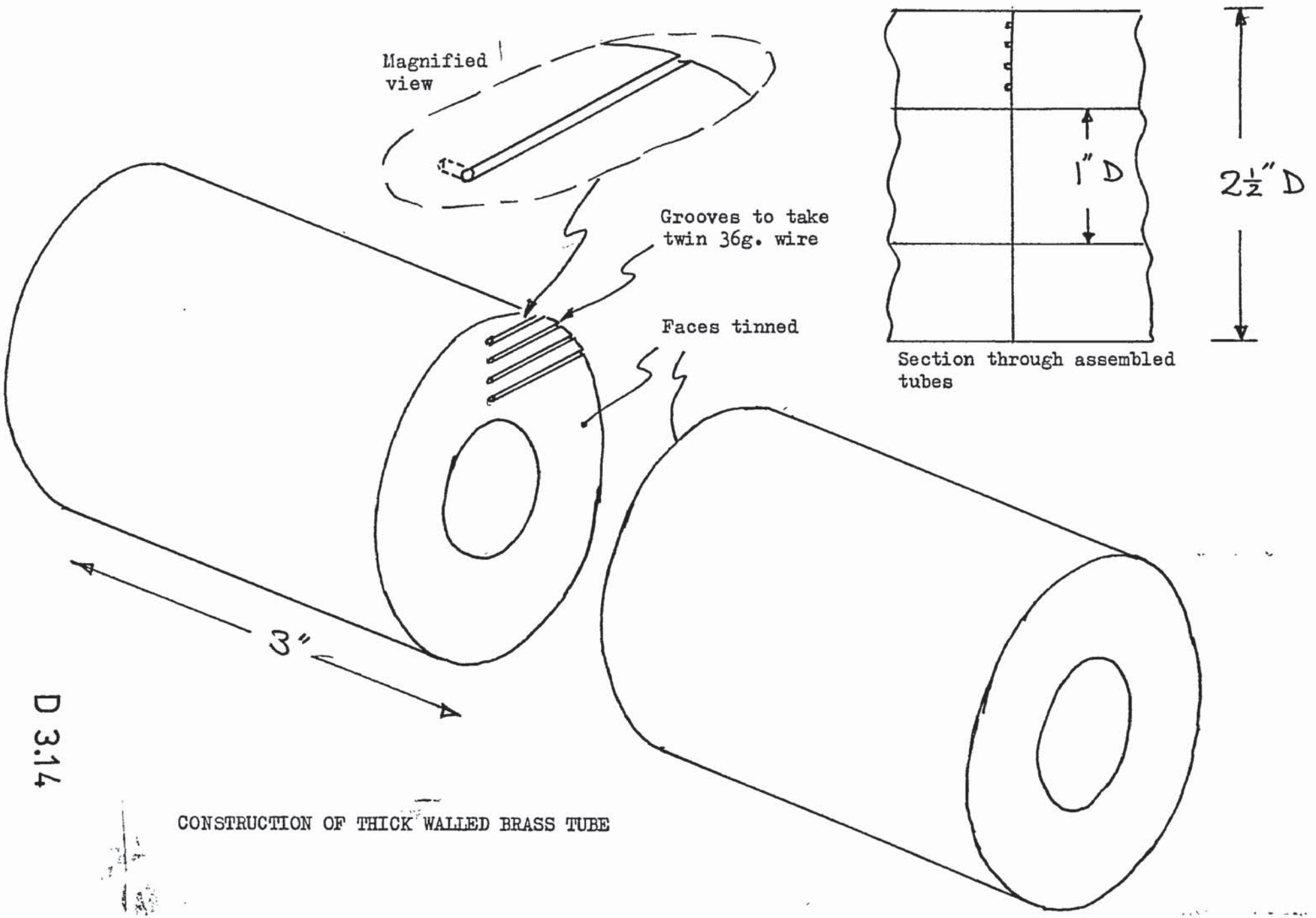

D 3.14

CONSTRUCTION OF THICK WALLED BRASS TUBE

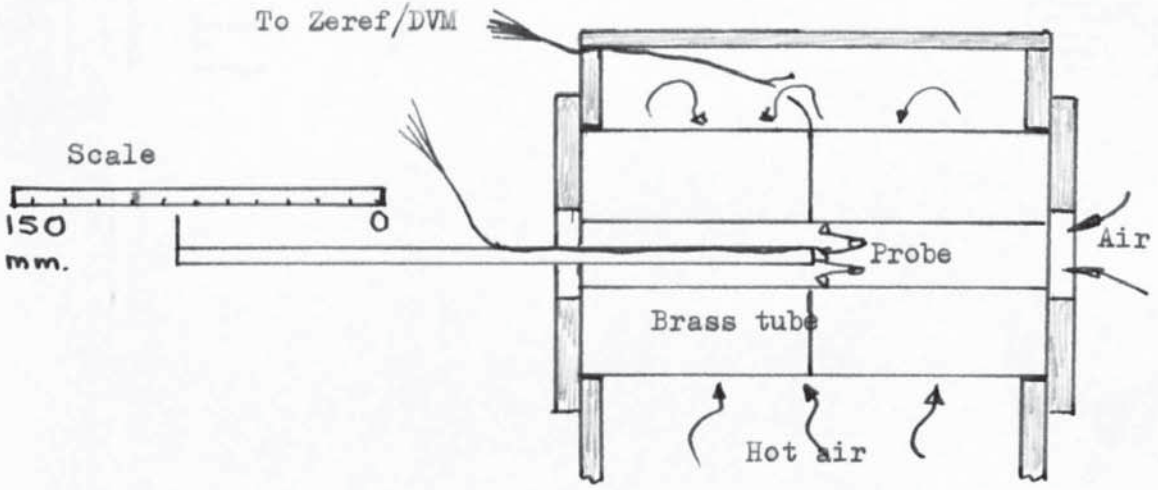

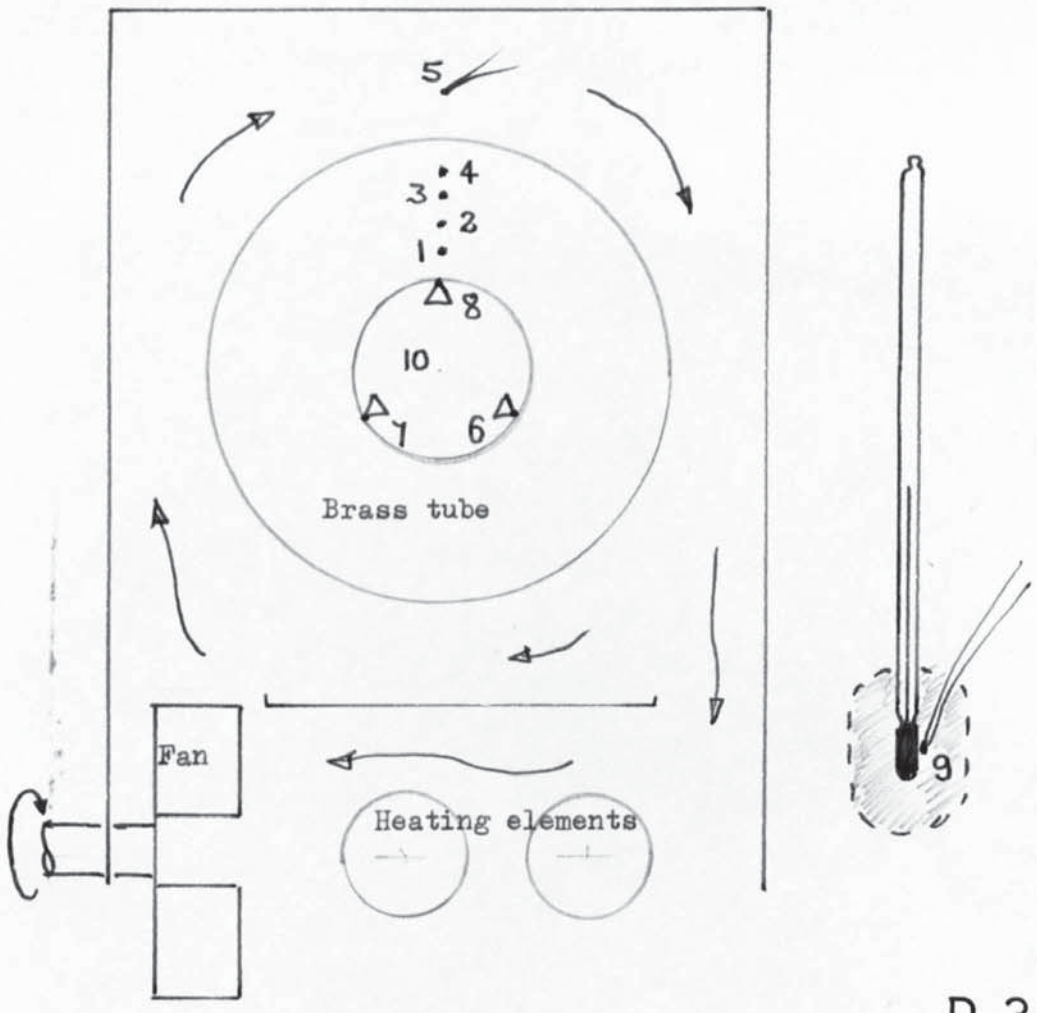

D 3.15

ARRANGEMENT OF SLIDING PROBE IN BRASS TUBE

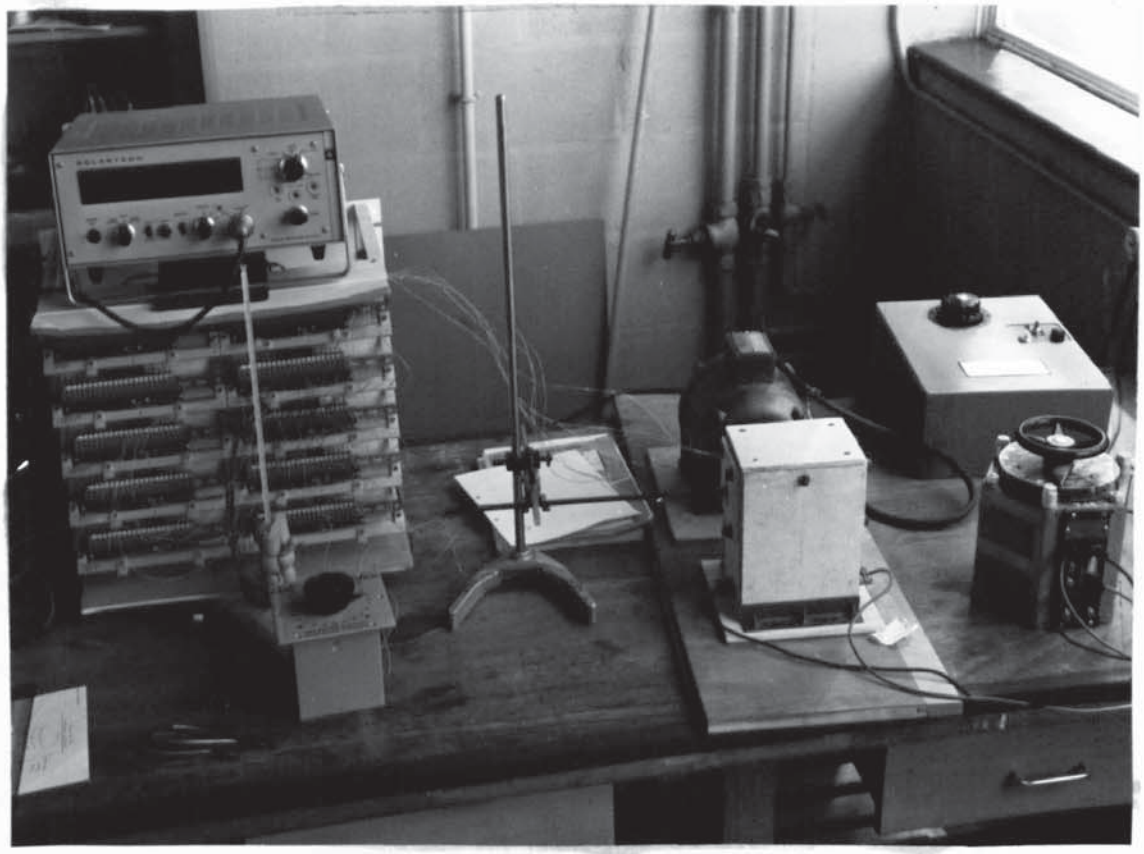

THICK WALLED BRASS TUBE EXPERIMENT P 3.6

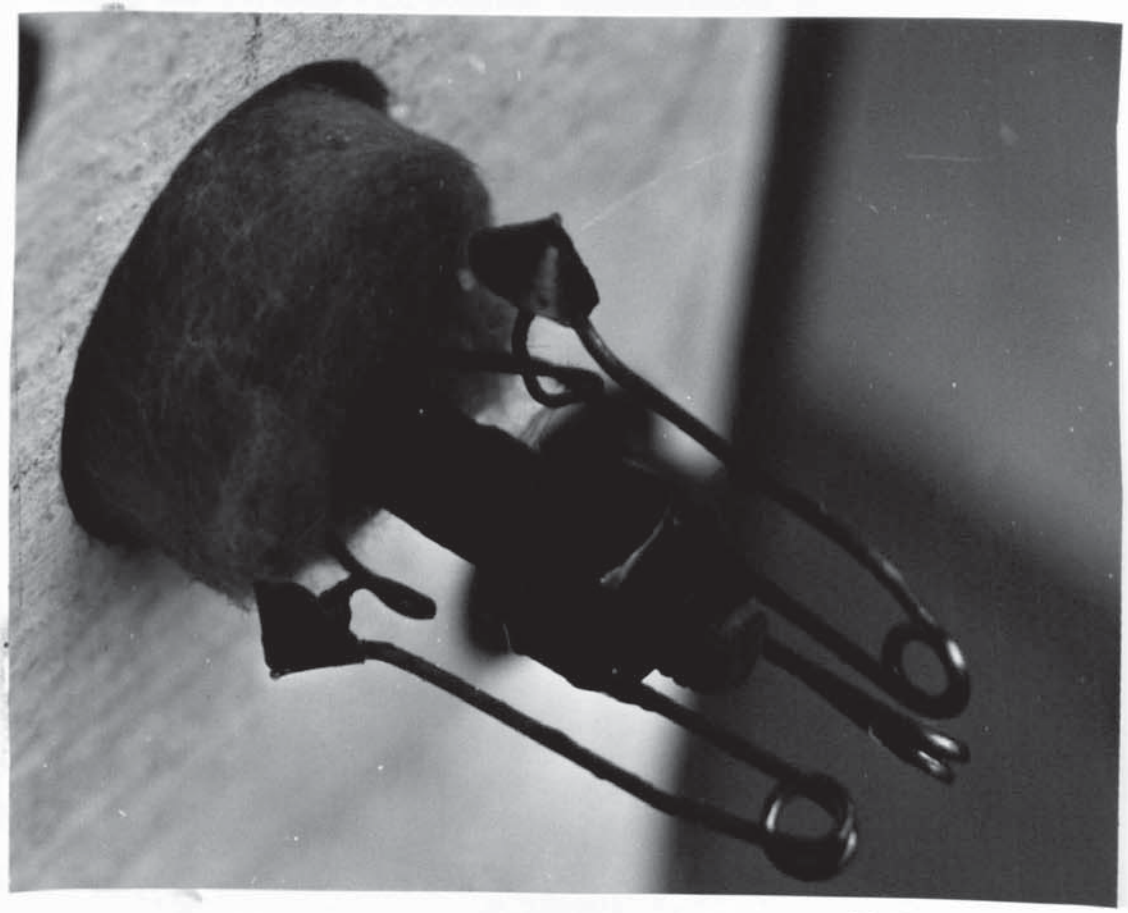

SLIDING PROBE FOR THICK WALLED BRASS TUBE P 3.7

A three prong sliding junction thermocouple probe was made to carry out an axial traverse along the bore of the tube. All thermocouple output voltages were referenced to ice-point and directed to a digital voltmeter by a multipoint switch, P 3.6. Two evaluation tests were carried out to attempt to obtain a correction factor to convert the thermocouple junction temperature to the true surface temperature.

EVALUATION TESTS.

Evaluation test 1.

The probe was traversed axially along the tube with the bore open ended to allow a flow of cooling air through it. The tube metal temperature was kept approximately constant.

The object was to compare the three thermocouple outputs from the probe and to check that the contact thermal resistance did not vary during the sliding.

Results from test 1.

Referring to G 3.1, the metal temperature is that measured at the centre section. The cooling air was very slow moving, less than 0.1 m/s. The air temperature given is that at the outlet. The thermocouple contact loading was approximately 1 N. The brass tube had a smooth reamed finish and the thermocouple a polished head which had been fused in an argon atmosphere.

It can be seen in G 3.1, that the difference between the measured surface temperature and the true surface temperature was surprisingly large, typically 200°C less 150°C giving a difference of 50 K. Also the difference between the individual thermocouple readings was large, typically 30 K. The output of each thermocouple in the probe varied with axial position.

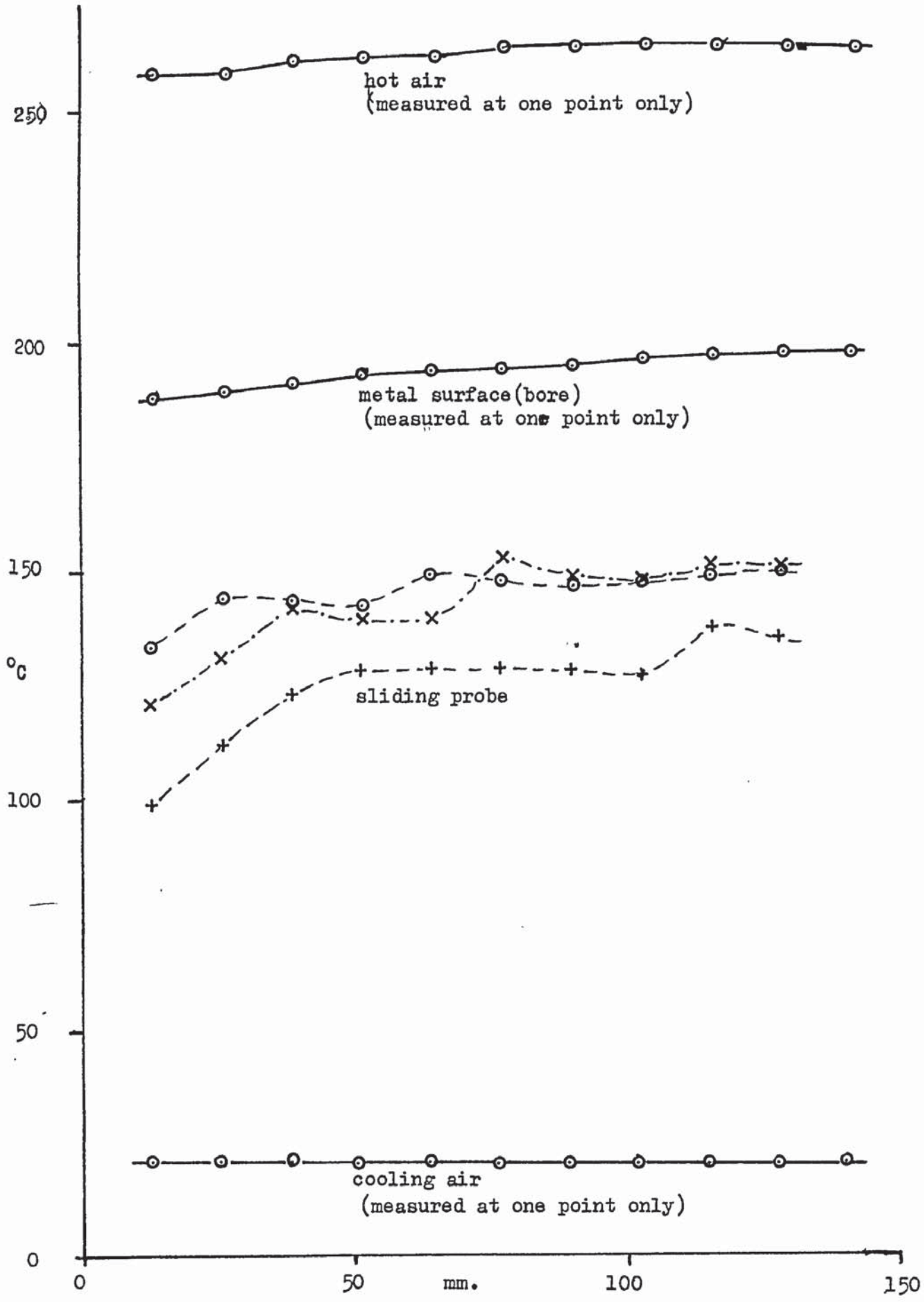

PLOT OF TEMPERATURES AGAINST AXIAL DISTANCE ALONG THE HEATED TUBE

G 3.1

Conclusions from test 1.

There is a heat flow from the metal surface to the thermocouple bead and thus to the leads, the point of contact being an important barrier to this heat flow. In a preliminary experiment one thermocouple indicated a temperature only 10 K below the metal surface temperature the other two being 30 K below, and this was found to be due to a small blob of molten solder which had been picked up, from the soldered joint in the brass tube, which was giving a much improved thermal contact between the thermocouple and the tube.

Referring to D 3.16, and accepting that in any thermocouple of finite size there is a flow of heat through the point of contact and along the thermocouple wires. The resistance of the point of contact and the thermocouple wires can be represented by two electrical resistances in series and the heat flow by the current through them. The voltage across this combination represented the temperature drop and three curves are shown which represents the form of the temperature variation with three metal temperatures but with the same air temperature in each case. Here the point Z is the required surface temperature the point Y is the indicated temperature while the point X is the surrounding air temperature. If the points X, Y and Z can be measured at any one metal surface temperature then for any other metal surface temperature the point Z can be calculated from the measured X and Y. To achieve an accurate correction, the condition of the air surrounding the thermocouples should be constant (temperature, velocity) and preferably stagnant.

Evaluation test 2.

The probe was modified to include an extra thermocouple to measure the air temperature of the air surrounding the contact thermocouples. The brass tube was loosely packed with slag wool to

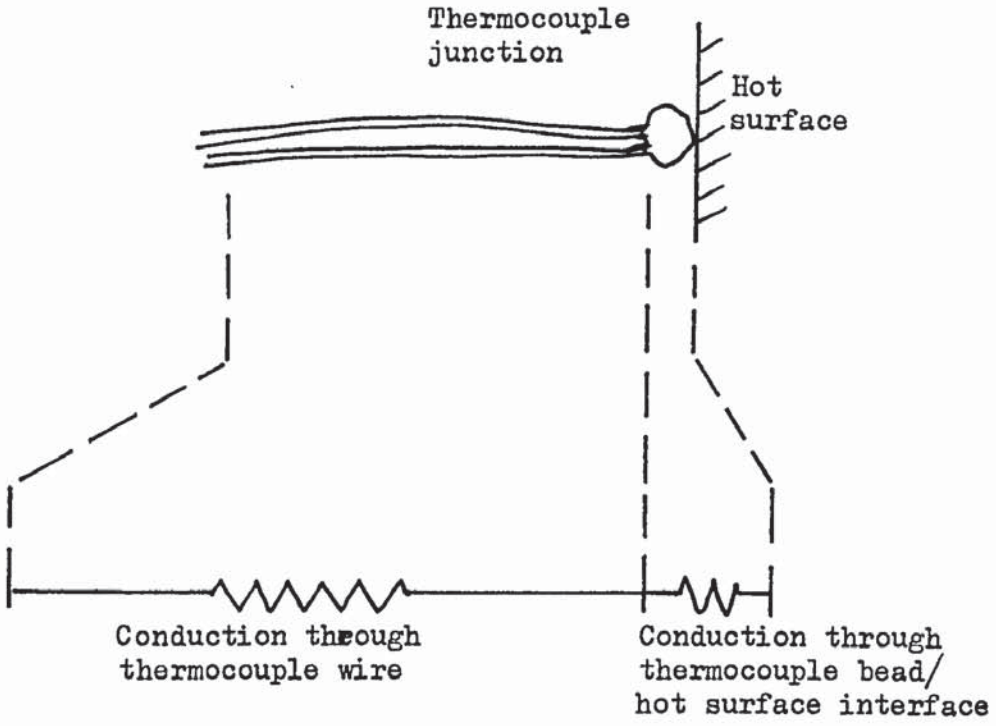

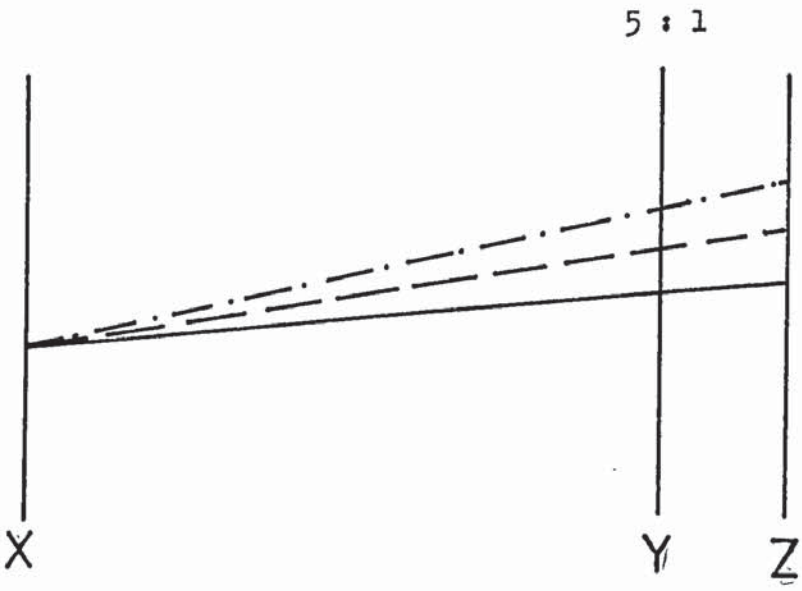

SERIES RESISTANCE ANALOGUE

give near stagnation of the internal air. The probe was not traversed axially but was given a small movement, 1 mm, up and down the bore at regular intervals to check on any change in thermal contact resistance during the experiment. The tube metal temperature was cycled over the intended working temperature range of the probe.

The object was to check whether or not the temperature indicated by the thermocouple could be accurately corrected by using a measurement of the inside air temperature.

Thermocouple output, mV Chromel/Alumel referenced to $0^{o}C$.

Time.	1	2	3	4	5	6	7	8	9	10
12.25	6.20	6.19	6.18	6.18	4.47	6.26	6.33	6.26	0.76	6.62
12.30	5.58	5.58	5.57	5.57	3.93	5.65	5.70	5.66	0.75	6.04
12.35	4.99	4.99	4.99	4.99	3.51	5.07	5.10	5.05	0.75	5.47
12.40	4.42	4.42	4.42	4.42	3.12	4.50	4.51	4.48	0.74	4.88
12.48	3.67	3.67	3.67	3.67	2.65	3.73	3.73	3.72	0.74	4.07
12.52	3.62	3.62	3.62	3.63	6.16	3.64	3.67	3.67	0.75	3.84
12.54	4.40	4.41	4.41	4.42	9.81	4.34	4.40	4.41	0.75	4.03
12.57	5.43	5.43	5.44	5.45	9.37	5.27	5.36	5.35	0.76	4.65
13.00	6.00	6.00	6.01	6.01	9.71	5.85	5.95	5.92	0.77	5.15
13.03	6.97	6.97	6.97	6.98	10.31	6.82	6.93	6.88	0.77	6.10
13.08	7.80	7.80	7.80	7.81	10.15	7.66	7.76	7.71	0.77	7.05
13.11	8.27	8.27	8.27	8.28	10.02	8.17	8.26	8.20	0.77	7.70
13.14	8.33	8.32	8.31	8.30	5.40	8.28	8.36	8.25	0.77	8.06
13.15	8.11	8.10	8.09	8.08	4.47	8.08	8.15	8.04	0.77	8.05
13.18	7.12	7.11	7.11	7.10	2.85	7.20	7.28	7.15	0.76	7.64
13.21	6.41	6.40	6.39	6.38	2.34	6.53	6.60	6.48	0.76	7.16
13.24	5.73	5.71	5.70	5.69	2.00	5.86	5.92	5.82	0.76	6.60
13.26	5.14	5.13	5.13	5.12	1.78	5.29	5.33	5.25	0.76	6.06
13.29	4.89	4.90	4.90	4.91	6.63	4.98	5.04	5.00	0.77	5.51
13.31	6.16	6.17	6.19	6.20	10.45	6.06	6.17	6.12	0.78	5.70

TEMPERATURE - TIME VARIATIONS.

T.3.1

Thermocouple output, mV from Chromel/Alumel referenced to °C.

Time	1	2	3	4	5	6	7	8	9	10
10.22	0.67	0.67	0.67	0.67	0.71	0.67	0.67	0.67	0.70	0.67
10.25	1.51	1.51	1.52	1.52	3.19	1.46	1.44	1.45	0.71	1.08
10.33	1.94	1.95	1.95	1.96	3.62	1.88	1.86	1.86	0.70	1.43
10.40	2.25	2.25	2.26	2.27	3.87	2.18	2.16	2.16	0.70	1.69
10.45	2.77	2.78	2.79	2.79	4.26	2.71	2.68	2.69	0.70	2.20
10.50	3.21	3.21	3.22	3.23	4.55	3.15	3.12	3.13	0.71	2.66
10.55	3.71	3.71	3.71	3.72	4.97	3.65	3.64	3.63	0.71	3.22
10.59	4.23	4.24	4.24	4.25	5.89	4.16	4.17	4.15	0.71	3.72
11.07	5.15	5.16	5.16	5.17	6.68	5.07	5.12	5.07	0.72	4.65
11.13	5.69	5.69	5.70	5.71	7.05	5.63	5.69	5.62	0.72	5.27
11.19	6.17	6.17	6.18	6.18	7.36	6.10	6.19	6.10	0.72	5.77
11.25	6.56	6.56	6.56	6.56	7.58	6.49	6.59	6.50	0.72	6.22
11.34	7.06	7.06	7.06	7.06	7.89	7.01	7.11	7.01	0.73	6.82
11.45	7.73	7.73	7.73	7.73	8.79	7.68	7.78	7.69	0.74	7.50
11.53	7.90	7.90	7.90	7.89	7.89	7.89	7.98	7.89	0.75	7.87
12.00	7.75	7.74	7.74	7.74	7.58	7.75	7.84	7.75	0.76	7.81
12.08	7.58	7.58	7.58	7.58	7.45	7.59	7.68	7.59	0.76	7.67
12.15	7.31	7.30	7.30	7.30	6.67	7.32	7.41	7.33	0.76	7.46
12.20	6.93	6.92	6.91	6.91	5.46	6.96	7.04	6.96	0.76	7.19

T 3.1 cont'd.

Thermocouple output, mV Chromel/Alumel referenced to $0^{o}C$.

Time	1	2	3	4	5	6	7	8	9	10
13.34	6.16	6.17	6.19	6.20	10.45	6.06	6.17	6.12	0.78	5.70
13.38	6.96	6.97	6.97	6.98	8.76	6.86	6.95	6.89	0.79	6.38
13.40	7.20	7.20	7.20	7.20	8.34	7.12	7.21	7.14	0.79	6.33
13.45	7.77	7.78	7.78	7.79	9.93	7.68	7.78	7.72	0.80	7.32
13.48	8.16	8.16	8.17	8.17	8.98	8.08	8.17	8.11	0.80	7.75

T 3.1 cont'd.

Time	True metal temperature	Mean Thermocouple output	Low to High 6,7,8	Heating or Cooling	Differences. Mean thermo less metal.	Differences. Inside air less Mean thermo.	Formula Corrected Mean thermo.	Error.
10.25	1.51	1.45	786	H	- 0.06	- 0.37	1.524	+ 0.014
10.33	1.94	1.87	786	H	- 0.07	- 0.44	1.958	+ 0.018
10.40	2.25	2.17	786	H	- 0.08	- 0.48	2.266	+ 0.016
10.45	2.77	2.69	786	H	- 0.08	- 0.49	2.788	+ 0.018
10.50	3.21	3.13	786	H	- 0.08	- 0.42	3.224	+ 0.014
10.55	3.71	3.64	876	H	- 0.07	- 0.42	3.724	+ 0.014
10.59	4.23	4.16	876	H	- 0.07	- 0.44	4.248	+ 0.018
11.07	5.15	5.09	876	H	- 0.06	- 0.44	5.178	+ 0.028
11.13	5.69	5.65	867	H	- 0.04	- 0.38	5.726	+ 0.036
11.19	6.17	6.13	867	H	- 0.04	- 0.36	6.202	+ 0.032
11.25	6.56	6.53	687	H	- 0.03	- 0.31	6.592	+ 0.032
11.34	7.06	7.04	687	H	- 0.02	- 0.22	7.084	+ 0.024
11.45	7.73	7.72	687	H	- 0.01	- 0.22	7.764	+ 0.034
11.53	7.90	7.92	687	H	+ 0.02	- 0.05	7.930	+ 0.030
12.00	7.75	7.78	687	C	+ 0.03	+ 0.03	7.774	+ 0.024
12.08	7.58	7.62	687	C	+ 0.04	+ 0.05	7.610	+ 0.030
12.15	7.31	7.35	687	C	+ 0.04	+ 0.11	7.328	+ 0.018

TEMPERATURE ERROR - TIME mV output from Chromel/Alumel referenced to $0^{\circ}C$.

T 3.2

12.20	6.93	6.98	687	C	+0.05	+ 0.21	6.938	+ 0.008
12.25	6.20	6.28	687	C	+ 0.08	+ 0.34	6.212	+ 0.012
12.30	5.58	5.67	687	C	+ 0.09	+ 0.37	5.596	+ 0.016
12.35	4.99	5.07	867	C	+ 0.08	+ 0.40	4.990	0.000
12.40	4.42	4.50	867	C	+ 0.08	+ 0.38	4.424	+ 0.004
12.48	3.67	3.73	867	C	+ 0.06	+ 0.34	3.662	+ 0.008
12.52	3.62	3.66	678	C	+ 0.04	+ 0.18	3.624	+ 0.004
12.54	4.40	4.38	678	H	− 0.02	− 0.35	4.450	+ 0.050
12.57	5.43	5.33	687	H	− 0.10	− 0.68	5.466	+ 0.036
13.00	6.00	5.91	687	H	− 0.09	− 0.76	6.062	+ 0.062
13.03	6.97	6.88	687	H	− 0.09	− 0.78	7.036	+ 0.066
13.08	7.80	7.71	687	H	− 0.09	− 0.66	7.842	+ 0.042
13.11	8.27	8.21	687	H	− 0.06	− 0.51	8.312	+ 0.042
13.14	8.33	8.29	867	H	− 0.04	− 0.23	8.336	+ 0.006
13.15	8.11	8.09	867	C	− 0.02	− 0.04	8.098	− 0.012
13.18	7.12	7.21	867	C	+ 0.09	− 0.43	7.124	+ 0.004
13.21	6.41	6.54	867	C	+ 0.13	+ 0.62	6.416	+ 0.006

T 3.2. cont'd.

13.24	5.73	5.86	867	C	+ 0.13	+ 0.74	5.712	- 0.018
13.26	5.14	5.29	867	C	+ 0.15	+ 0.77	5.136	- 0.004
13.29	4.89	5.00	687	C	+ 0.11	+ 0.51	4.898	+ 0.008
13.31	5.39	5.42	687	H	+ 0.03	+ 0.03	5.414	+ 0.024
13.34	6.16	6.12	687	H	0.04	- 0.42	6.204	+ 0.044
13.38	6.96	6.90	687	H	- 0.06	- 0.52	7.004	+ 0.044
13.40	7.20	7.16	687	H	- 0.04	- 0.43	7.246	+ 0.046
13.45	7.77	7.72	687	H	- 0.05	0.40	7.800	+ 0.030
13.48	8.16	8.12	687	H	- 0.04	0.37	8.194	+ 0.034

T 3.2 cont'd.

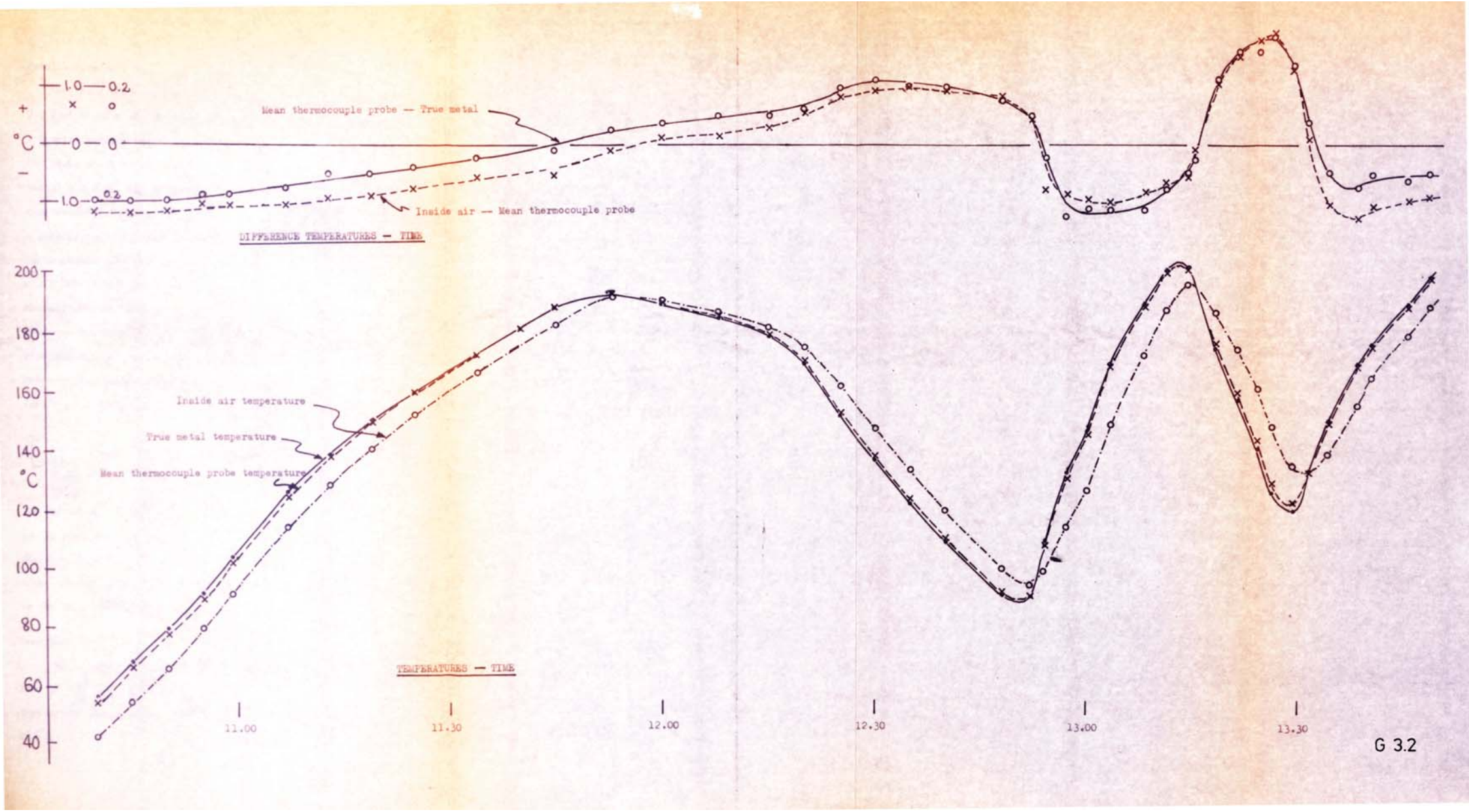
1.0 — 0.2
+
°C
0 — 0
−
1.0 — 0.2
Mean thermocouple probe — True metal
Inside air — Mean thermocouple probe
DIFFERENCE TEMPERATURES — TIME
200
180
160
140
°C
120
100
80
60
40
Inside air temperature
True metal temperature
Mean thermocouple probe temperature
TEMPERATURES — TIME
11.00
11.30
12.00
12.30
13.00
13.30

G 3.2

Results from test 2.

The three thermocouple junctions gave almost identical outputs, G 3.2, within 2 K and the mean of these three outputs followed the true metal surface temperature within 2 K. A small axial movement of the probe produced no change in the thermocouple output. It can be seen G 3.2 that the inside air temperature follows the true metal temperature in the same fashion as the contact thermocouples but with a greater time lag. If the difference temperatures between mean thermocouple less true metal are plotted and on the same graph, G 3.2, the difference temperatures between inside air less mean thermocouple are plotted using a constant reducing scaling factor then two nearly identical curves result. From this it appears possible to correct the contact thermocouple outputs to give the true metal surface temperature with a high degree of accuracy. In this case with a scale ratio of 1:5 the formula would be,

$$t_{\text{true metal temp.}} = t_{\text{contact thermo.}} + 0.2\left(t_{\text{contact thermo.}} - t_{\text{inside air}}\right)$$

The corrected thermocouple readings are tabulated, T 3.2, where it can be seen that the maximum error between the corrected reading and the true metal surface temperature is slightly greater than 1 K and this at a severe rate of rise of metal surface temperature, considered in the light of what may be expected experimentally.

Conclusions from test 2.

The accuracy of measurement was a result of reducing the heat flow through the thermocouple to metal interface by keeping the air inside the tube stagnant and allowing it to vary in temperature with the metal.

In a preliminary experiment the accuracy of temperature measurement was substantially reduced when the probe was mounted on a steel rod instead of a "Tufnol" tube, as the rod conducted heat away from the trapped air surrounding the thermocouples.

It was thought that during the alternative heating and cooling periods the thermocouple with the better thermal contact would have the highest output of the three during heating and the lowest during cooling. Looking at the low to high column in T 3.2, it would appear that junction 8 had the best thermal contact and 6 the worst while 7 being at the top of the section is subjected to an internal convection current in the section.

In the actual boiling water test rig the heated tube had a vertical axis and the internal convection currents shown to be present, despite slag wool packing, would affect the accuracy much more and it was thought that it would be an advantage to eliminate them by working in a vacuum and thus, at a low Grashof number. It would also reduce any tendency for the tube to form an insulating layer of oxide during the heat test runs.

THREE POINT SLIDING THERMOCOUPLE PROBE.

Following the evaluation of the sliding thermocouple, a test piece was constructed to contain a sliding thermocouple probe designed to work in a vacuum, D 3.17, P 3.8, P 3.9. The probe had three junctions spring loaded against the inside wall of the heating tube and a glass tube moving through a multi 'O' ring seal was used to traverse the thermocouple axially along the heating tube. The inside surface of the heating tube was cleaned and polished to provide a good thermal contact with the thermocouple junctions and the inside of the heating tube was continuously evacuated by an oil sealed vacuum pump to a vacuum better than - 0.95 bar. To prevent

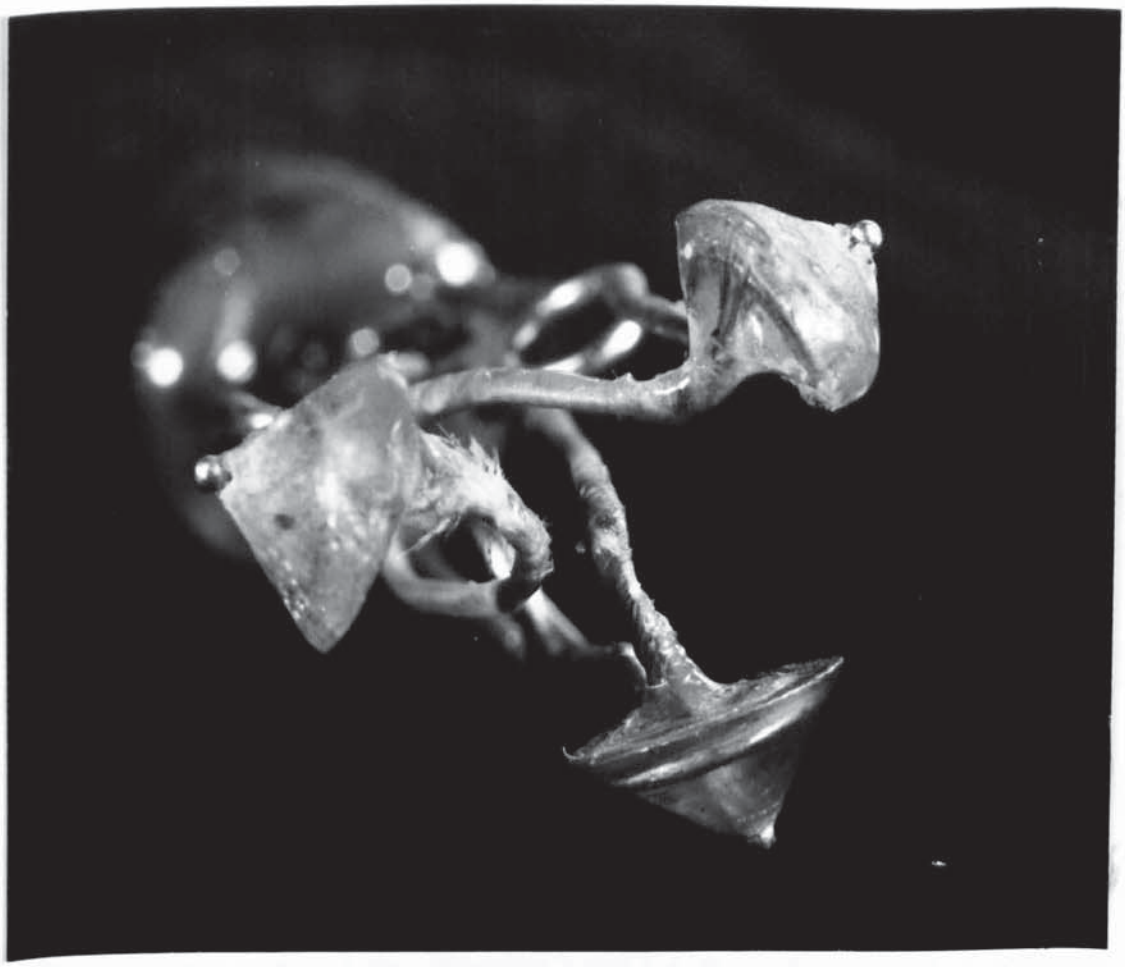

THREE POINT SLIDING CONTACT THERMOCOUPLE PROBE (End view) P 3.8

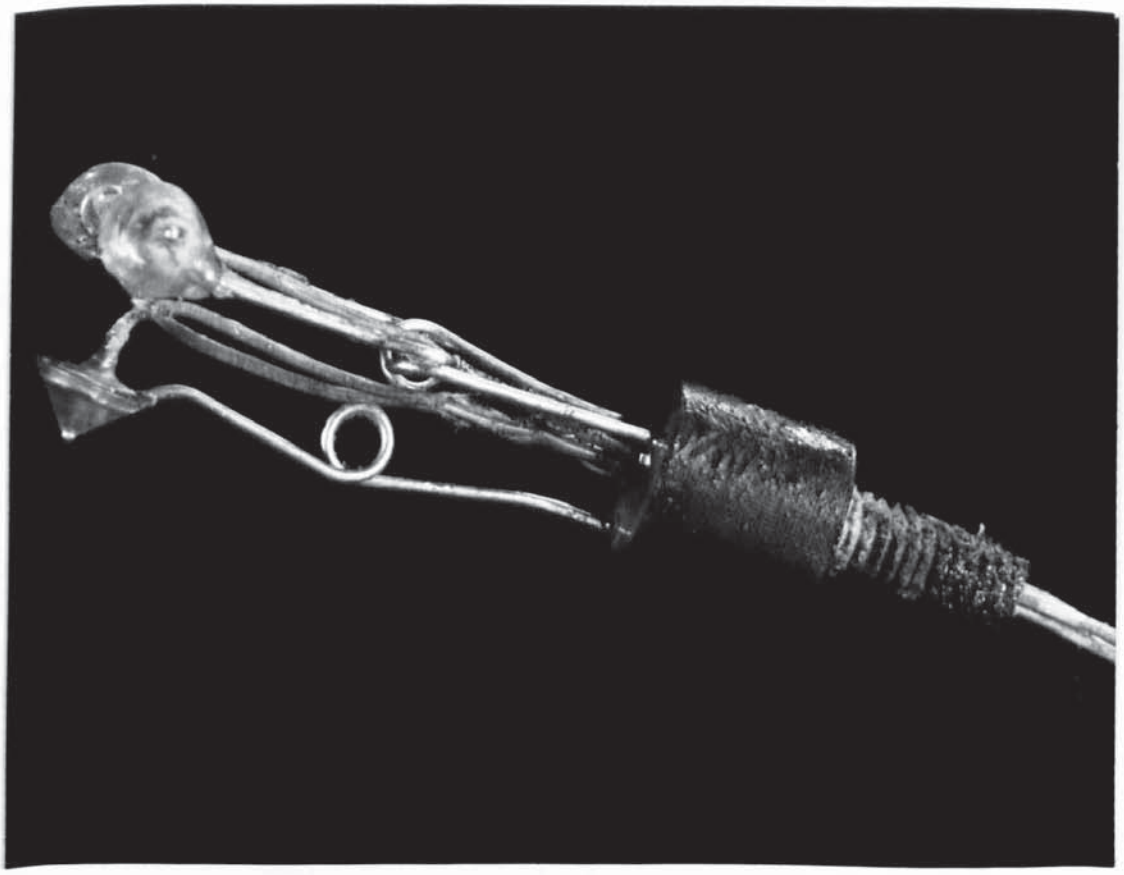

THREE POINT SLIDING CONTACT THERMOCOUPLE PROBE (Side view) P 3.9

oxidation of the inner surface of the heating tube during operation the sliding gland was packed with Argon.

In using this probe it became apparent that as two of the three junctions were giving near identical outputs and the remaining junction was giving a somewhat different output, that the probe was not remaining central in the tube and that one junction was not making contact with the tube inner wall because of this. It was apparent that a modification to ensure probe concentricity within the tube was required.

SIX POINT SLIDING THERMOCOUPLE PROBE.

The end of the sliding glass tube was modified to carry a six point probe which was fully floating D 3.18, P 3.10 - P 3.13. The connection between the glass tube and the probe was a 1 mm bore 34 gauge stainless steel tube which though rigid in the axial direction permitted the probe to float freely in the radial direction. The argon packing of the sliding gland was discontinued as the inner surface temperatures were low enough to preclude any appreciable oxidation at this low partial pressure of oxygen in the tube. In addition to two groups of three sliding thermocouples a free thermocouple was fixed to each end of the probe on the axis. In operation this probe was successful in producing consistent readings and although at some test conditions some differences in the outputs from the three junctions were observed, the mean output from the three junctions closely coincided with the output from the free thermocouple on the axis of the probe.

This fact led to two questions, i.e. was the difference in output due to variations in heating tube wall thickness or asymmetry in the flow pattern of the water passing over the heating tube? and secondly would it be advantageous to use only the central free

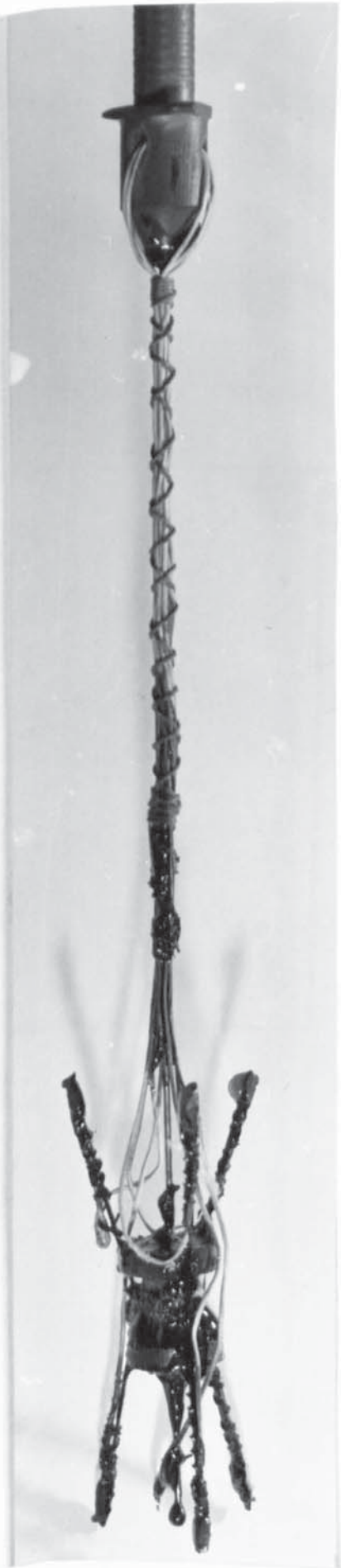

SIX POINT THERMOCOUPLE PROBE MOUNTING

P 3.10

CLOSE UP OF SLIDING CONTACT

P 3.11

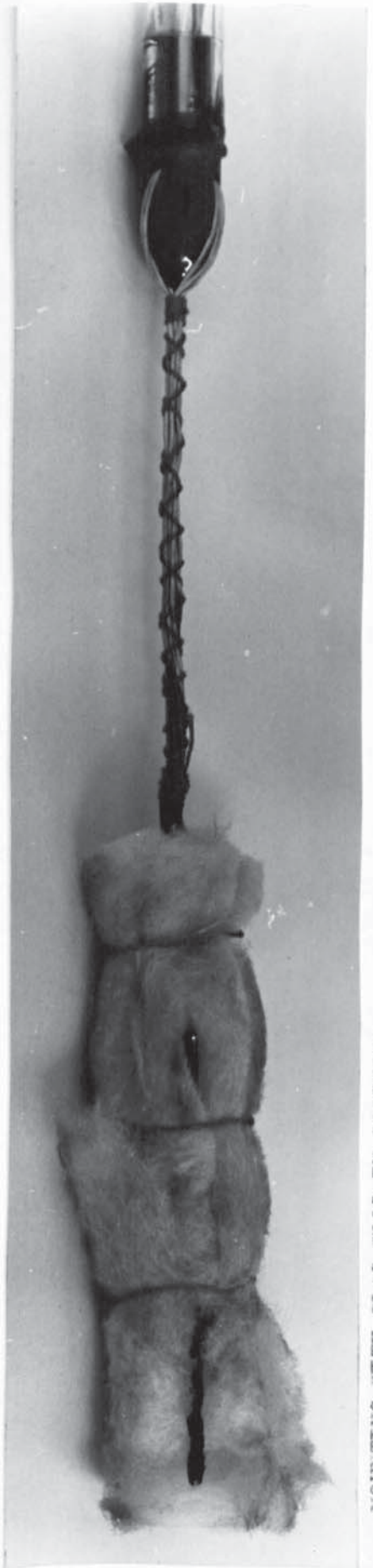

MOUNTING WITH SLAG WOOL IN POSITION

P 3.12

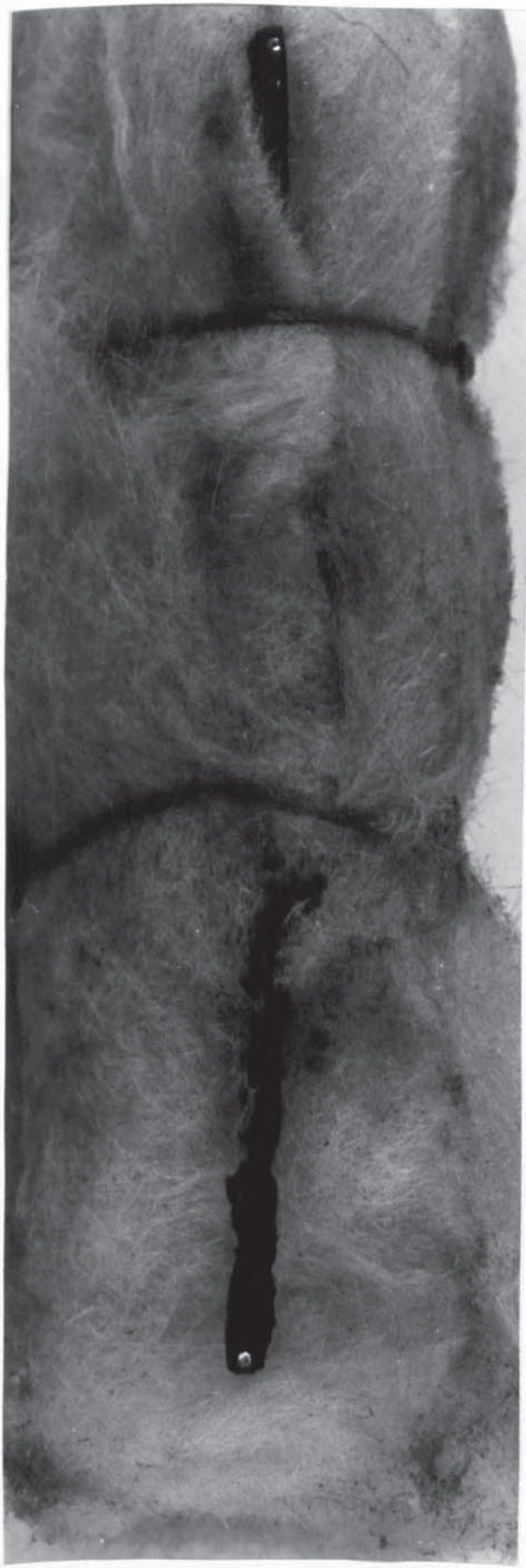

CLOSE UP OF SLIDING CONTACT WITH SLAG WOOL IN POSITION

P 3.13

thermocouple which would give a mean wall temperature directly?

A test was run to provide the answer to the first question.

CIRCUMFERENTIAL TEMPERATURE VARIATIONS.

The test rig was run under steady state conditions at a typical power level and water flow rate, 18.75 kW, 0.89 kg/s. The six point sliding thermocouple probe was rotated sequentially into three angular positions, 120° apart, with adequate time allowed between each position to allow thermal equilibrium to be reached, D 3.19. During this time the probe was kept in a constant axial position.

The probe was then moved axially upwards to that the lower ring of three thermocouples occupied the same axial position formerly occupied by the upper ring of three thermocouples, D 3.20. The probe was then again rotated sequentially into three angular positions 120° apart. The outputs from the thermocouples recorded at the positions detailed were converted to °C and presented in tabular form T 3.3.

Looking at this table the following conclusions can be drawn.

(i) The circumferential variation in surface temperature of the inside of the tube does exist, it is not altered by rotating the thermocouples, and this is thus due to either a circumferential variation in the composition of the heating tube material, a circumferential variation in the wall thickness of the heating tube material or a circumferential variation in the flow of the cooling water over the outside of the heating tube.

(ii) The temperature indicated by the free thermocouple positioned on the axis of the tube was in all cases within 0.23°C of the mean of the temperature indicated by the three sliding contact thermocouples at the same axial position.

Considering conclusion (i), it was thought that due to the method of manufacturing the tube, by piercing and drawing, a

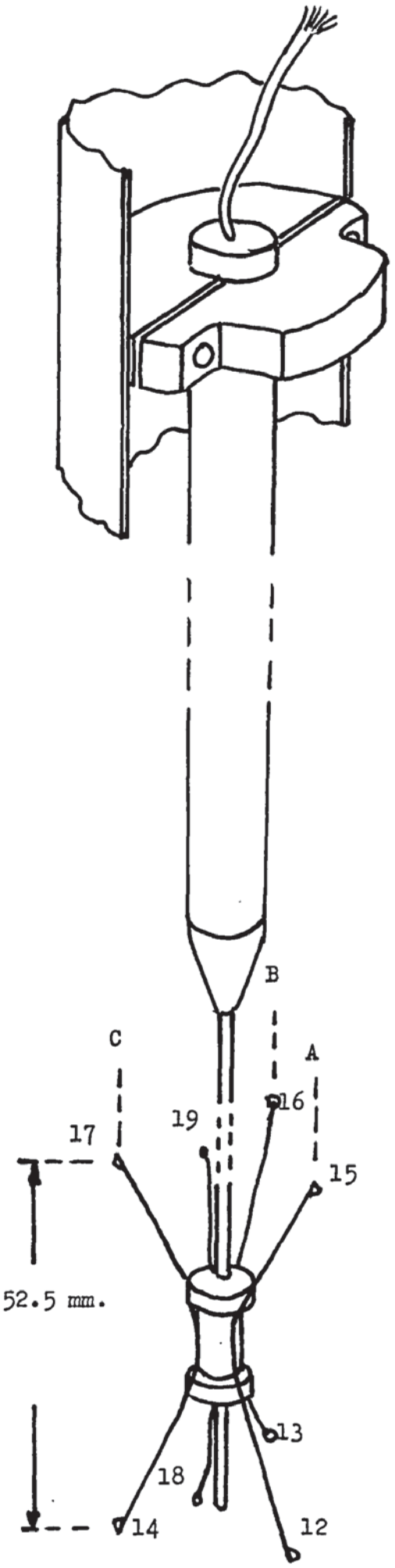

Plan view
240° clockwise

position A
read by 17 and 14

position B
read by 15 and 12

position C
read by 16 and 13

Plan view
120° clockwise

position A
read by 16 and 13

position B
read by 17 and 14

position C
read by 15 and 12

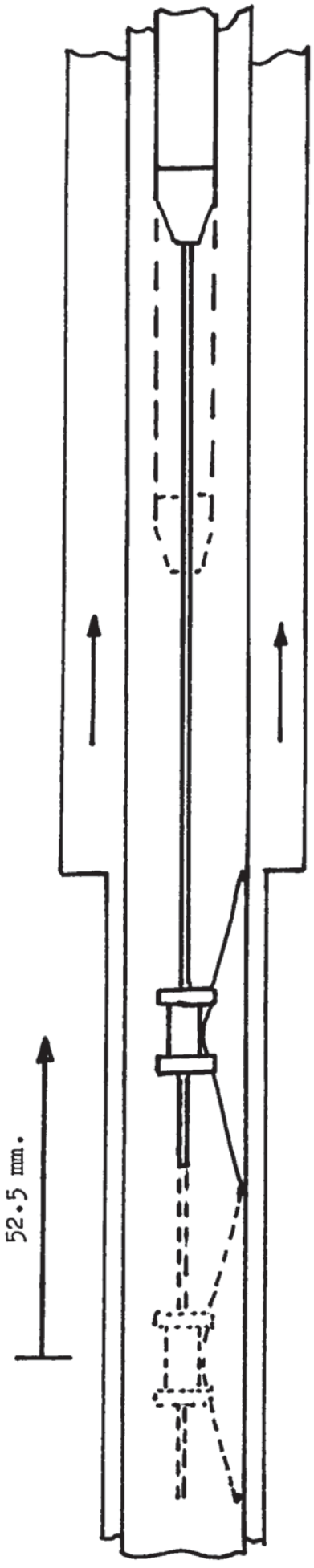

Measurement of the circumferential temperature variation in the heating element

Second probe position

First probe position

Measurement of the circumferential temperature variation in the heating element —— thermocouple outputs given in °C

Probe angular position	Angular reference line on the heating element A	B	C	free	
T	114.2	113.6	111.3	113.1	— +52.5 — upper thermocouples
↙	114.0	113.0	110.8	113.0	
↘	113.8	113.9	110.9	112.1	
point mean →	114.0	113.5	111.0	112.7	
circumferential mean →	112.8				
T	114.8	113.2	111.4	113.45	— 0 — upper thermocouples
↙	114.4	113.1	111.4	113.20	
↘	114.6	113.2	111.2	112.50	
point mean →	114.6	113.17	111.33	113.05	
circumferential mean →	113.03				
T	—	113.7	111.6	114.05	— +52.5 — lower thermocouples
↙	114.6	—	111.5	113.2	
↘	114.6	113.6	—	113.2	
point mean →	114.6	113.65	111.55	113.48	
circumferential mean →	113.3				
T	—	113.3	112.0	114.20	— 0 — lower thermocouples
↙	114.8	—	111.9	113.45	
↘	115.3	113.8	—	113.60	
point mean →	115.05	113.55	111.95	113.75	
circumferential mean →	113.52				

CIRCUMFERENTIAL TEMPERATURE VARIATIONS

circumferential variation in the composition of the metal was not a possibility. A sample length cut from the same tube was carefully measured to show any variations in wall thickness, D 3.21, they were negligible.

The tests were repeated with six angular positions of the thermocouple probe to verify this asymmetry of flow and get a precise measure of the circumferential temperature variation, T 3.4, T 3.5, G 3.3, which was shown to be greater than 2 K.

Considering conclusion (ii) it was considered that this proved that the selection of a good insulator (glass tube) for the thermocouple probe mounting rod, the use of 36 gauge wire for the thermocouple leads and the operation of the thermocouple in a vacuum reduced the predicted correction, to a negligible value and indeed the thermocouple mounted on the axis of the tube would provide a simple and accurate temperature probe without the need for sliding contact and a probe based on this idea was manufactured.

The implied asymmetry of flow of the water in the annulus surrounding the heating tube was reduced to a low level by an improved construction of the test section which allowed exact centering of the element in the outer tube.

RADIATION THERMOCOUPLE PROBE.

The probe was constructed as shown, D 3.18, P 3.14, P3.15, with three pairs of thermocouple junctions to give more rapid readings and to give a check. The response time required was checked by moving the probe rapidly from a hot region to a cool region and then back to the hot region and on each test the time taken for the thermocouple to give a constant reading was noted. The results were plotted for use in all subsequent tests G 3.4, G 3.5. The spaces between the junction pairs was filled with glass wool to

Stainless steel '321' heating tube

Wall thickness as measured by using a micrometer, at two sections

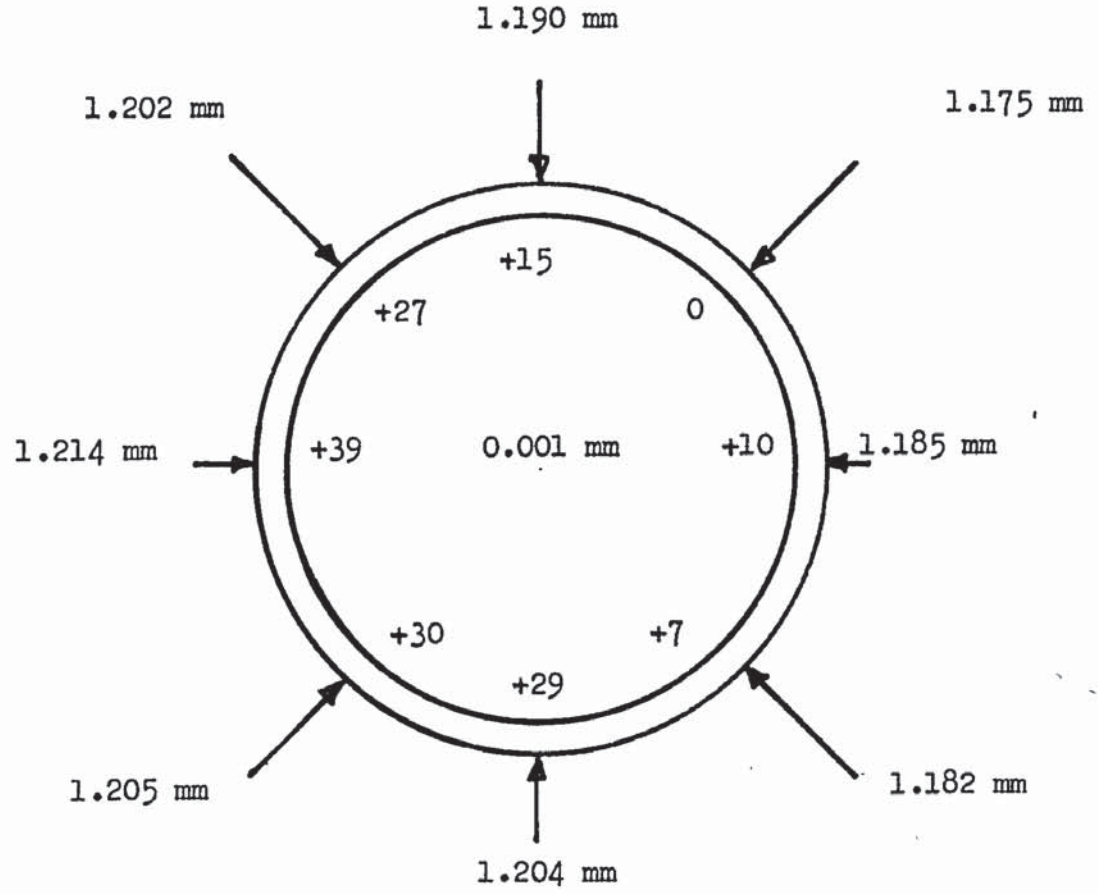

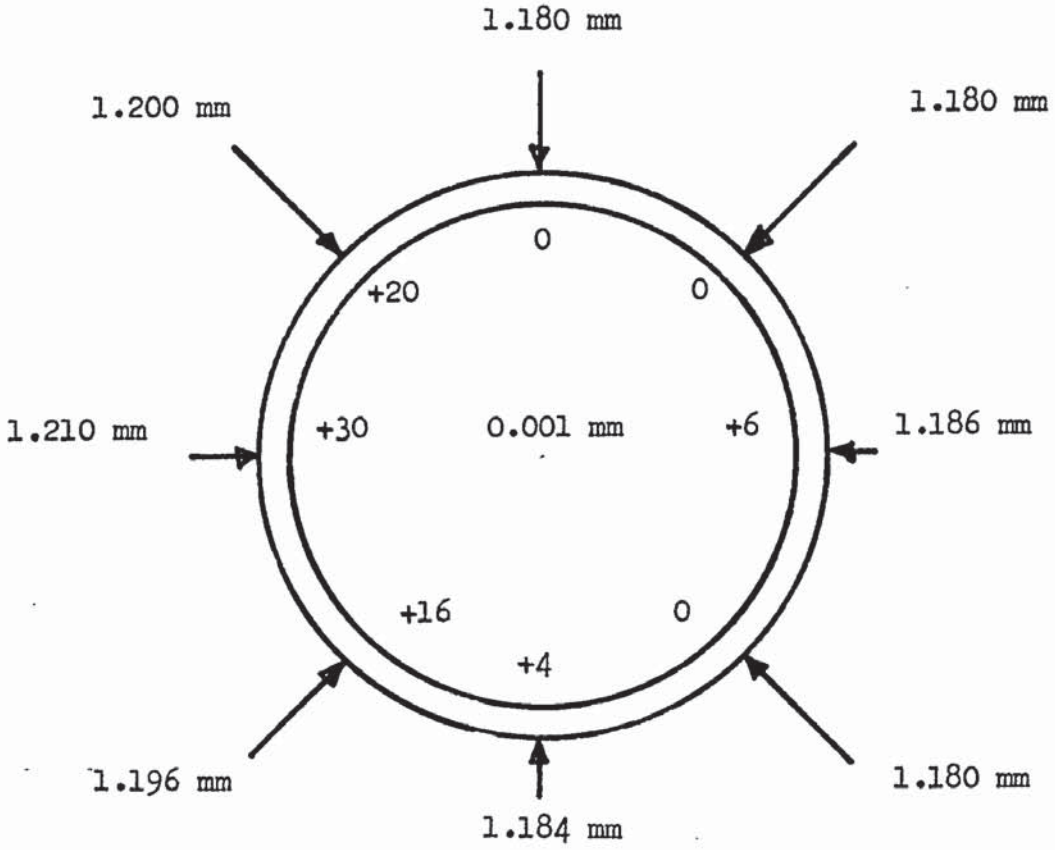

HEATING TUBE WALL THICKNESS VARIATIONS

D 3.21

PROBE EVALUATION TESTS

18.75 kW, 13.8 V, 1.353 kA.
Test section pressure 0.38 bar
Flow count 200
All readings in mV × 2 from Chromel/Alumel

*170240	T − 50														
00	+00491	1	01	+00489	1	02	+00489	1	03	+00487	1	04	+00490	1
05	+00528	1	06	+00527	1	07	+00526	1	08	+00528	1	09	+00527	1
10	+00064	1	11	+00297	1	12	+00754	1	13	+00745	1	14	+00731	1
15	+03794	1	16	-00752	1	17	-00733	1	18	-00748	1	19	-00753	1
*170520		− 50													
00	-00490	1	01	-00489	1	02	-00488	1	03	-00486	1	04	-00489	1
05	-00526	1	06	-00527	1	07	-00527	1	08	-00527	1	09	-00527	1
10	-00064	1	11	-00296	1	12	-00745	1	13	-00731	1	14	-00752	1
15	-02978	1	16	-00735	1	17	-00756	1	18	-00746	1	19	-00745	1
*170735		− 50													
00	-00491	1	01	-00489	1	02	-00488	1	03	-00487	1	04	-00489	1
05	-00528	1	06	-00527	1	07	-00527	1	08	-00527	1	09	-00527	1
10	-00064	1	11	-00298	1	12	-00732	1	13	-00752	1	14	-00745	1
15	-03663	1	16	+00759	1	17	+00753	1	18	+00740	1	19	+00747	1
*171005	T	− 50													
00	+00491	1	01	+00489	1	02	+00488	1	03	+00487	1	04	+00489	1
05	+00527	1	06	+00527	1	07	+00527	1	08	+00527	1	09	+00528	1
10	+00064	1	11	+00297	1	12	+00754	1	13	+00745	1	14	+00732	1
15	+02982	1	16	+00750	1	17	+00735	1	18	+00747	1	19	+00751	1
*171231		− 50													
00	+00490	1	01	+00489	1	02	+00488	1	03	+00486	1	04	+00489	1
05	+00527	1	06	+00527	1	07	+00527	1	08	+00526	1	09	+00528	1
10	+00064	1	11	+00297	1	12	+00754	1	13	+00733	1	14	+00742	1
15	+03188	1	16	-00734	1	17	-00744	1	18	-00748	1	19	-00748	1
*171505		− 50													
00	-00491	1	01	-00489	1	02	-00488	1	03	-00486	1	04	-00489	1
05	-00527	1	06	-00526	1	07	-00526	1	08	-00527	1	09	-00527	1
10	-00064	1	11	-00296	1	12	-00734	1	13	-00742	1	14	-00755	1
15	-03312	1	16	+00746	1	17	+00763	1	18	+00741	1	19	+00744	1
*171806		− 50													
00	+00490	1	01	+00489	1	02	+00488	1	03	+00486	1	04	+00489	1
05	+00527	1	06	+00526	1	07	+00527	1	08	+00526	1	09	+00528	1
10	+00064	1	11	+00297	1	12	+00742	1	13	+00755	1	14	+00730	1
15	+03634	1	16	-00762	1	17	-00732	1	18	-00743	1	19	-00751	1
*172133	T	− 50													
00	-00491	1	01	-00489	1	02	-00488	1	03	-00487	1	04	-00488	1
05	-00527	1	06	-00526	1	07	-00526	1	08	-00528	1	09	-00527	1
10	-00064	1	11	-00298	1	12	-00752	1	13	-00747	1	14	-00733	1
15	-03401	1	16	+00753	1	17	+00734	1	18	+00747	1	19	+00752	1
*172514	T	− 50	1% drop in power												
00	+00490	1	01	+00488	1	02	+00488	1	03	+00487	1	04	+00487	1
05	+00526	1	06	+00527	1	07	+00525	1	08	+00527	1	09	+00526	1
10	+00064	1	11	+00296	1	12	+00751	1	13	+00742	1	14	+00729	1
15	+03372	1	16	-00748	1	17	-00732	1	18	-00744	1	19	-00749	1

Note: test''173123' to test '172514' no change in angular and axial position, has a 1% reduction in power which results in a 0.5% reduction in the inner surface temperature readings.

PROBE EVALUATION TESTS (continued)

```
*172815   T -102.5
00 -00490 1  01 -00489 1  02 -00488 1  03 -00487 1  04 -00488 1
05 -00526 1  06 -00527 1  07 -00526 1  08 -00527 1  09 -00527 1
10 -00064 1  11 -00298 1  12 -00761 1  13 -00752 1  14 -00737 1
15 -01539 1  16 -00754 1  17 -00738 1  18 -00752 1  19 -00756 1
*173042   K -102.5
00 -00490 1  01 -00489 1  02 -00488 1  03 -00488 1  04 -00488 1
05 -00527 1  06 -00528 1  07 -00526 1  08 -00526 1  09 -00527 1
10 -00064 1  11 -00298 1  12 -00762 1  13 -00738 1  14 -00749 1
15 -03126 1  16 +00742 1  17 +00749 1  18 +00753 1  19 +00754 1
*173318   J -102.5
00 +00490 1  01 +00490 1  02 +00488 1  03 +00488 1  04 +00489 1
05 +00527 1  06 +00526 1  07 +00527 1  08 +00527 1  09 +00526 1
10 +00064 1  11 +00297 1  12 +00753 1  13 +00734 1  14 +00760 1
15 +03086 1  16 -00739 1  17 -00764 1  18 -00751 1  19 -00751 1
*173513   L -102.5
00 -00490 1  01 -00490 1  02 -00489 1  03 -00488 1  04 -00489 1
05 -00528 1  06 -00527 1  07 -00528 1  08 -00528 1  09 -00527 1
10 -00064 1  11 -00297 1  12 -00738 1  13 -00746 1  14 -00763 1
15 -00763 1  16 -00750 1  17 -00770 1  18 -00746 1  19 -00749 1
*173744   Y -102.5
00 -00490 1  01 -00490 1  02 -00489 1  03 -00488 1  04 -00489 1
05 -00528 1  06 -00528 1  07 -00528 1  08 -00528 1  09 -00527 1
10 -00064 1  11 -00297 1  12 -00734 1  13 -00760 1  14 -00754 1
15 -00850 1  16 -00766 1  17 -00758 1  18 -00745 1  19 -00752 1
*174009   P -102.5
00 -00491 1  01 -00490 1  02 -00489 1  03 -00488 1  04 -00490 1
05 -00528 1  06 -00529 1  07 -00528 1  08 -00528 1  09 -00528 1
10 -00064 1  11 -00298 1  12 -00748 1  13 -00764 1  14 -00735 1
15 -02981 1  16 -00771 1  17 -00741 1  18 -00748 1  19 -00757 1
*174305   T -102.5
00 -00491 1  01 -00490 1  02 -00489 1  03 -00488 1  04 -00490 1
05 -00528 1  06 -00528 1  07 -00528 1  08 -00528 1  09 -00528 1
10 -00064 1  11 -00298 1  12 -00759 1  13 -00756 1  14 -00736 1
15 -00783 1  16 -00759 1  17 -00739 1  18 -00753 1  19 -00758 1
```

Channel identification

00 — 04	Inlet water
05 — 09	Outlet water
10/11	In/Out coolong water
12,13,14	Upper sliding thermocouples
15,16,17	Lower sliding thermocouples
18	Upper free thermocouple
19	Lower free thermocouple

T 3.4 cont.

Measurements of the circumferential temperature variation in the heating element —— thermocouple outputs given in mv.×2 Ch/Al (2-12-72)

Probe angular position	A	B	C	D	E	F	free	
	——		7.54		7.38		7.56	+52.5 (upper thermocouples)
		——		7.42		7.49	7.54	
	7.64		——		7.39		7.51	
		7.70		——		7.50	7.49	
	7.66		7.58		——		7.52	
		7.71		7.41		——	7.57	
point mean →	7.650	7.705	7.560	7.415	7.385	7.495	7.532	
circumferential mean →	7.535							
	7.54		7.45		7.31		7.48	0 (upper thermocouples)
		7.54		7.33		7.42	7.48	
	7.52		7.45		7.31		7.46	
		7.55		7.34		7.42	7.41	
	7.52		7.45		7.32		7.40	
		7.55		7.30		7.42	7.43	
point mean →	7.527	7.547	7.450	7.327	7.313	7.420	7.443	
circumferential mean →	7.431							
	7.61		7.52		7.37		7.52	+52.5 (lower thermocouples)
		7.62		7.38		7.49	7.53	
	7.60		7.53		7.34		7.51	
		7.63		7.38		7.46	7.46	
	7.60		7.54		7.34		7.45	
		7.64		7.35		7.48	7.48	
point mean →	7.603	7.630	7.530	7.370	7.350	7.477	7.491	
circumferential mean →	7.493							
	——		7.52		7.33		7.53	0 (lower thermocouples)
		——		7.34		7.44	7.48	
	7.56		——		7.35		7.45	
		7.63		——		7.46	7.44	
	7.59		7.53		——		7.47	
		7.62		7.32		——	7.51	
point mean →	7.575	7.625	7.525	7.330	7.340	7.450	7.48	
circumferential mean →	7.474							

The circumferential temperature variation of the inside surface of the heating element.

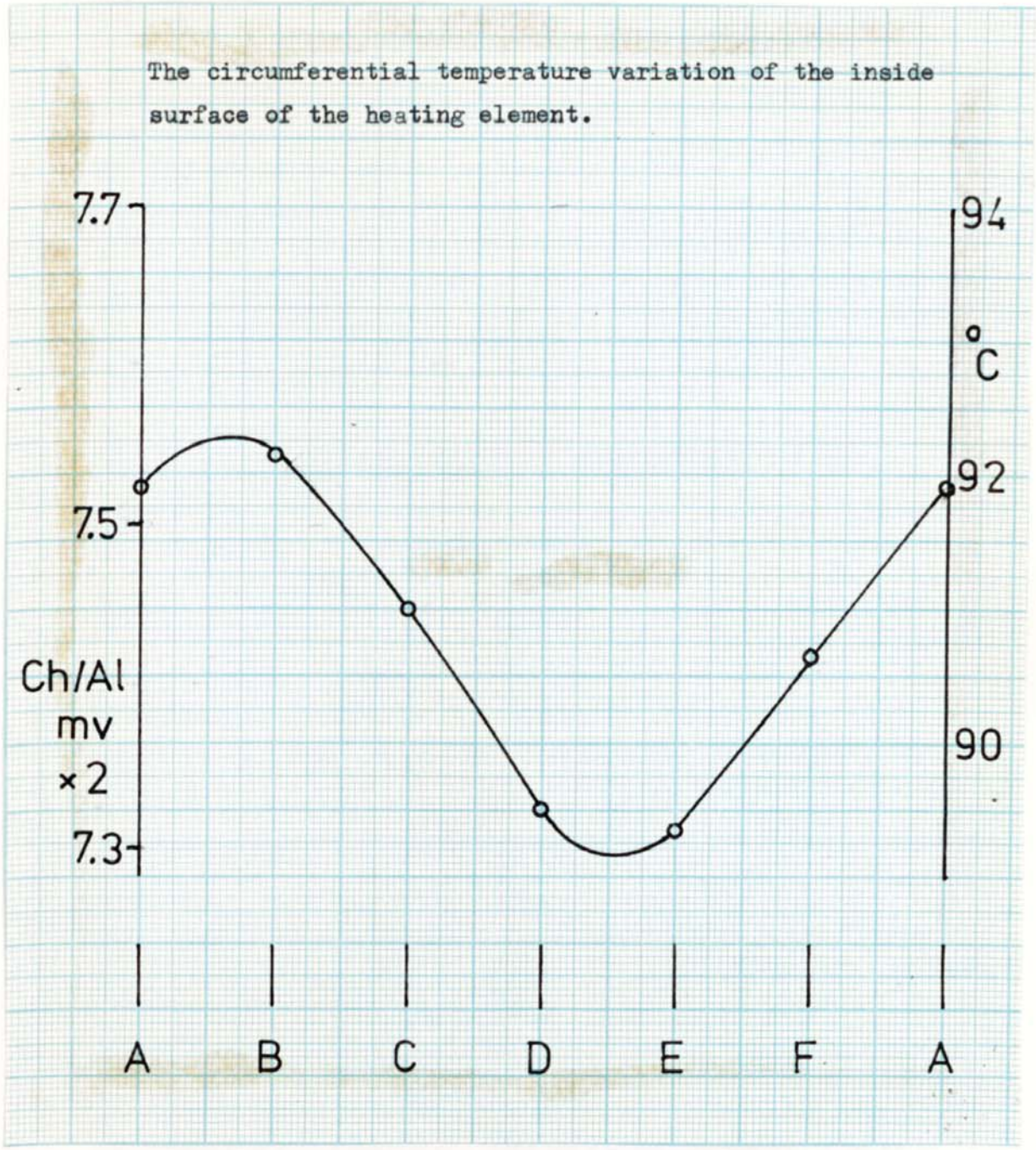

CIRCUMFERENTIAL TEMPERATURE VARIATION

RADIATION THERMOCOUPLE MOUNTING

P 3.14

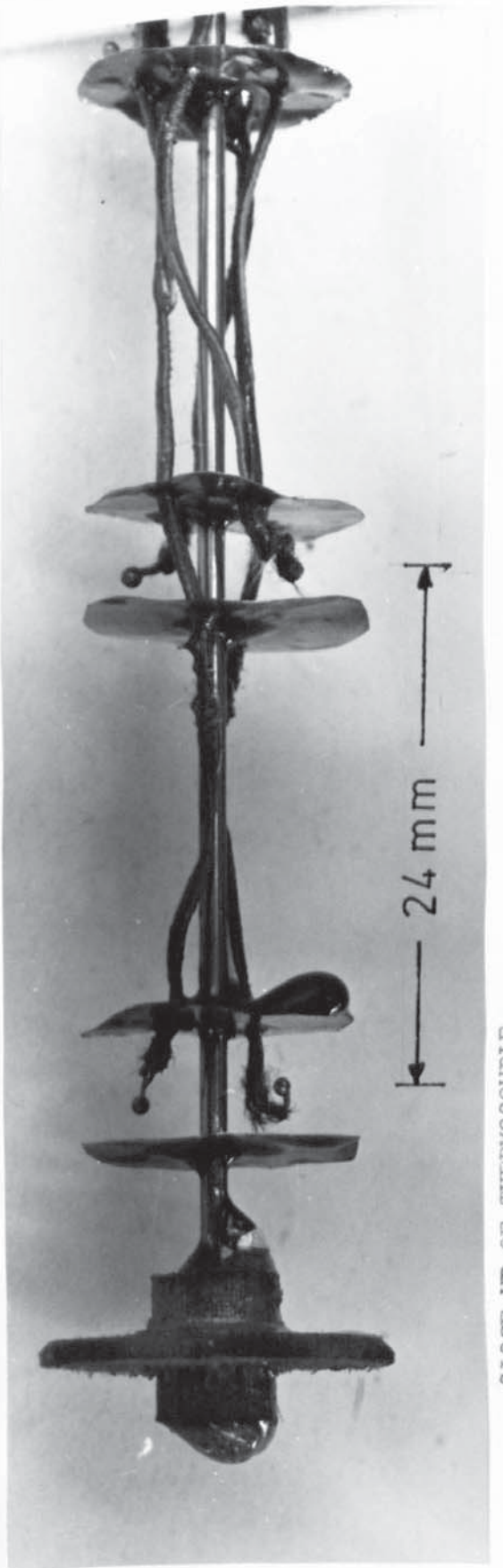

CLOSE UP OF THERMOCOUPLE

P 3.15

The change in thermocouple output is plotted against time from a sudden movement of the probe into a new axial position where the tube wall temperature has a different value.

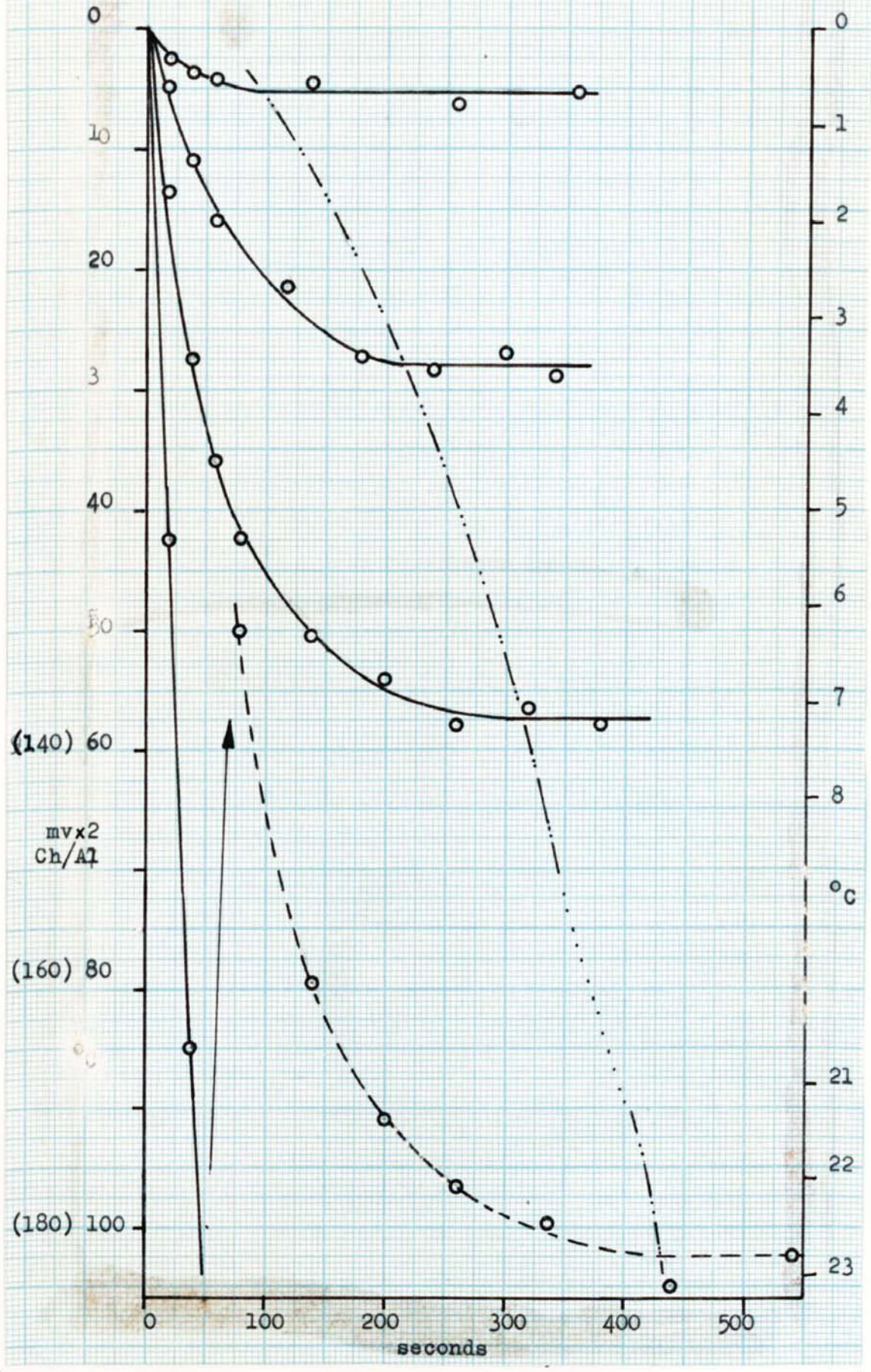

THE RESPONSE TIMES OF THE RADIATION THERMOCOUPLE PROBE TO STEP CHANGES IN THE TUBE WALL TEMPERATURE

G 3.4

The change in thermocouple output is plotted against time from a sudden movement of the probe into a new axial position where the tube wall temperature has a different value.

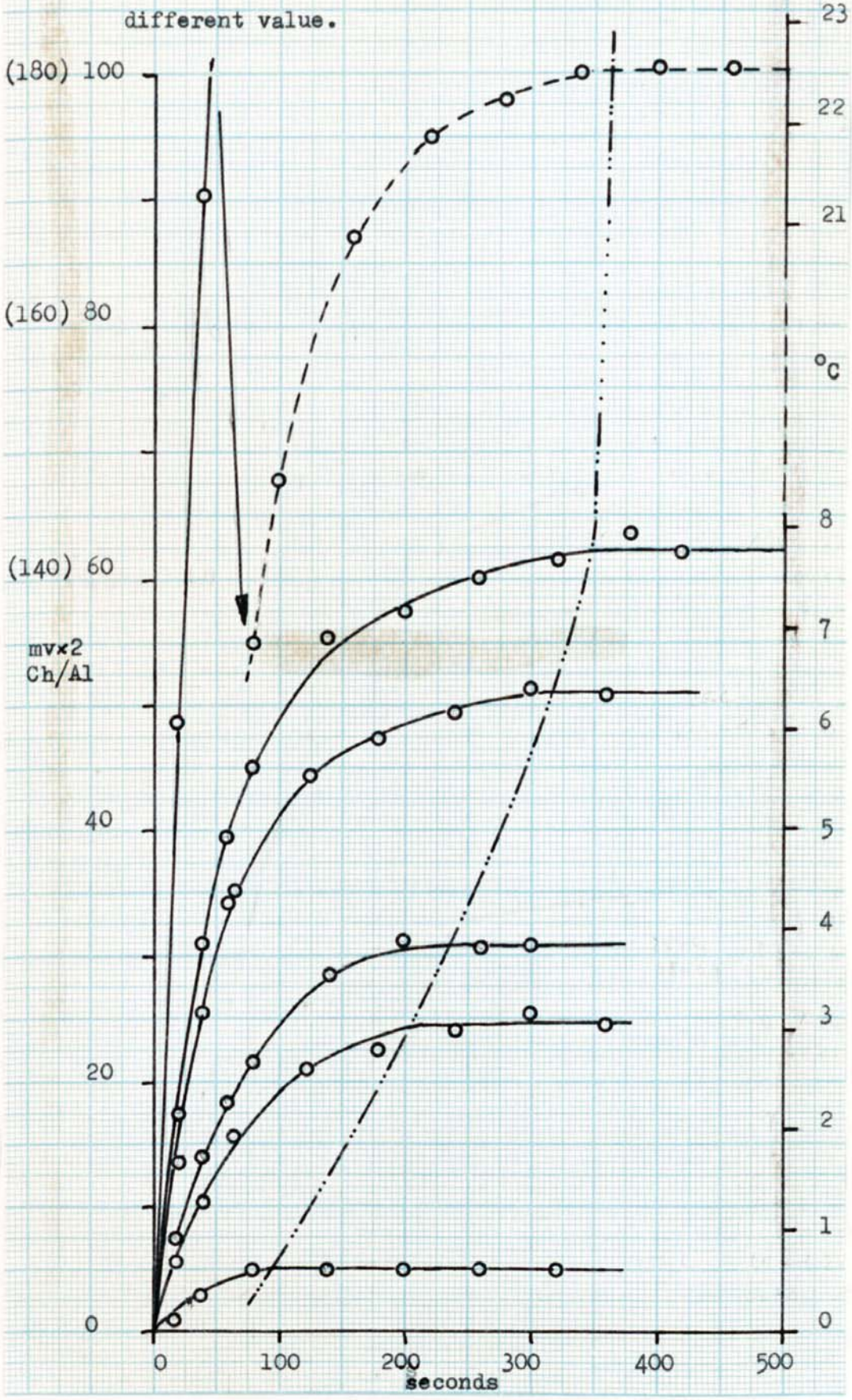

THE RESPONSE TIMES OF THE RADIATION THERMOCOUPLE PROBE TO STEP CHANGES IN THE TUBE WALL TEMPERATURE

G 3.5

minimise any possible convective heat transfer between junctions.

THE CALCULATION OF THE VALUE OF THE OUTER SURFACE TEMPERATURE OF THE HEATING TUBE.

It can be shown, A 5 , that for a tube with internal heat generation and outside cooling the radial temperature drop can be simply calculated providing that no axial or circumferential condition of heat takes place.

Uncertain of the likely axial temperature to be encountered during the tests, a computer programme was developed to predict the outer surface temperature of the metal tube without the assumption of no axial conduction, A 6 . The programme was run with a severe axial temperature gradient of 1.5 K/mm and showed that the effect on the radial temperature drop calculation was negligible. The basic calculation only, A 5 , was used during the subsequent tests.

CONSTRUCTION OF SWIRL VANES.

In designing vanes to produce swirl in the flow of water over the heating tube, metal construction was ruled out because of the possibility of electrically shorting of the heating tube. This left some form of "plastic" as the constructional material and an epoxy resin "Ciba Type 750/209" was chosen as having the necessary resistance to temperature and water and at the same time it was castable. The vanes were produced by spiral milling on an aluminium bar to give a female form, and then casting the resin in the mould formed by the milled bar and a copper foil sheath. A good deal of trial and error was involved in arriving at a suitable mixture of hard and flexible resins, 70% and 30% respectively and a suitable curing time of 2 hours at 85^{o}C, but finally this technique produced accurately formed straight and spiral vanes which were wrapped round the heating tube to

give a swirl to the flow of water passing up the annulus D 3.22, P 4.23 .

In considering the comparisons to be made between the heat transfer rates achieved with different degrees of swirl in the cooling water it was thought that the sectional shape of the flow channels normal to the direction of flow should be similar and that the velocity of flow measured in the direction of the vanes should have the same value for each test. In the construction the flow channel sectional areas and shapes were kept very nearly identical, D 3.23, and during the comparative tests with different vanes the water flow rate was adjusted to give the same flow velocity in the direction of the vanes.

The variation in static pressure along the annulus was measured by the same pressure sampling tube used in previous tests, D 3.24.

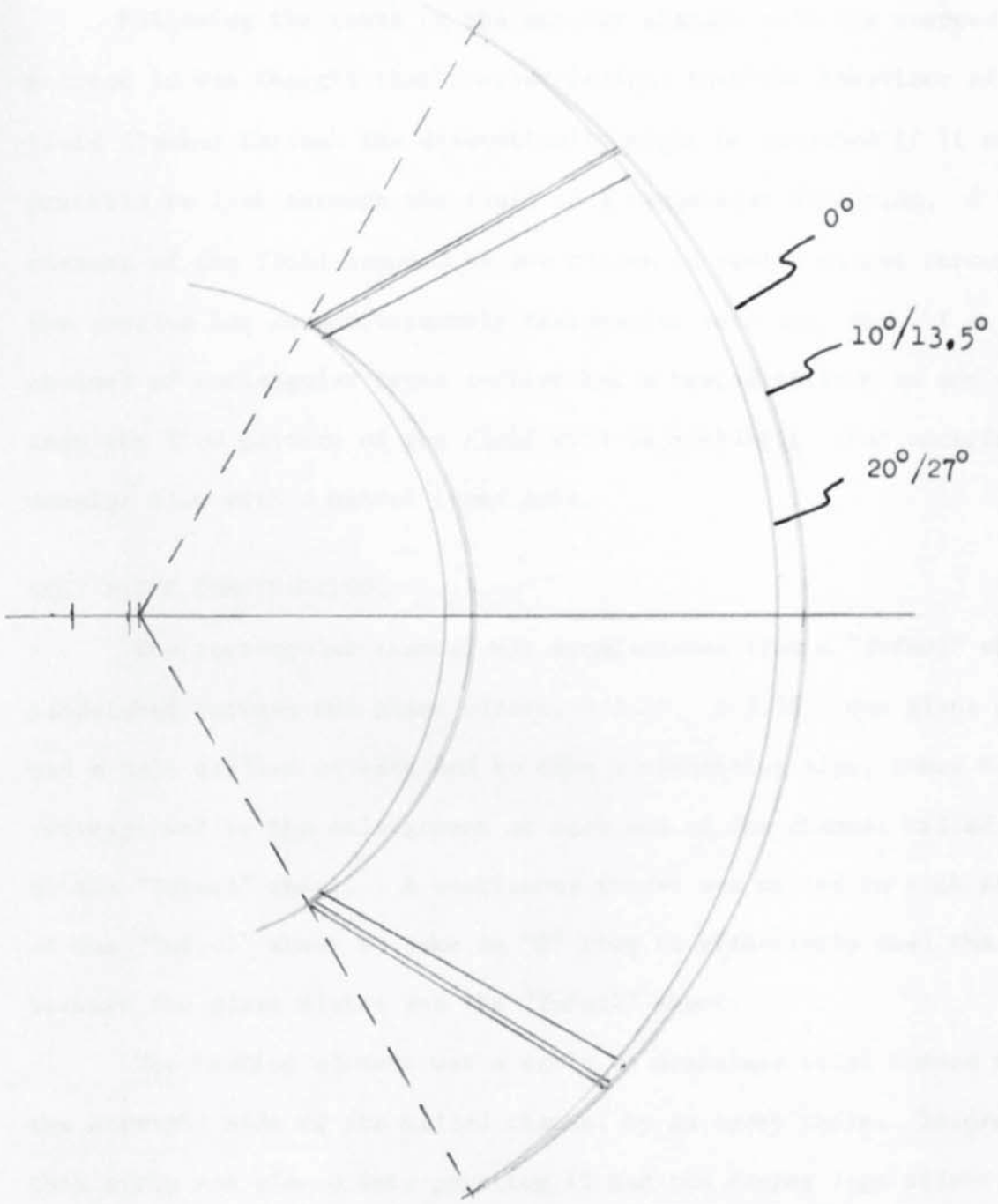

The near identical general shape of the flow channels shown for helix angles of 0°(straight axial vanes), 10°/13.5°, and 20°/27°

SECTION THROUGH ONE FLOW CHANNEL

D 3.23

3.5. RECTANGULAR TEST SECTION.

Following the tests on the annular channel with the stepped section it was thought that further insight into the behaviour of the fluid flowing through the discontinuity might be obtained if it was possible to look through the fluid in a tangential direction. A thin element of the fluid bounded by two slices in radial planes through the annulus has an approximately rectangular section. Thus if a channel of rectangular cross section has a heated surface on one side, then the flow pattern of the fluid will be similar to that occuring in annular flow with a heated inner tube.

TEST PIECE CONSTRUCTION.

The rectangular channel was manufactured from a "Tufnol" sheet sandwiched between two glass plates, D 3.25, P 3.16. One glass plate had a hole drilled at each end to take a connecting pipe, these holes corresponded to the enlargement at each end of the channel milled out of the "Tufnol" sheet. A continuous groove was milled in each side of the "Tufnol" sheet to take an "O" ring to effectively seal the gap between the glass plates and the "Tufnol" sheet.

The heating element was a strip of stainless steel bonded to the straight side of the milled channel by an epoxy resin. Before this strip was placed into position it had two copper lugs silver soldered to it, one at each end to connect electrically to the heating power supply. Also, 36 gauge Chromel/Alumel thermocouples were spot welded to the back of the strip along its length. The two glass plates were held against each side of the "Tufnol" sheet by minature "G" clamps which were tightened until it could be seen that the "O" rings were sealing against the glass plates, P 3.16. The complete assembly stood on the lower row of "G" clamps with the heating strip on the floor of the flow channel.

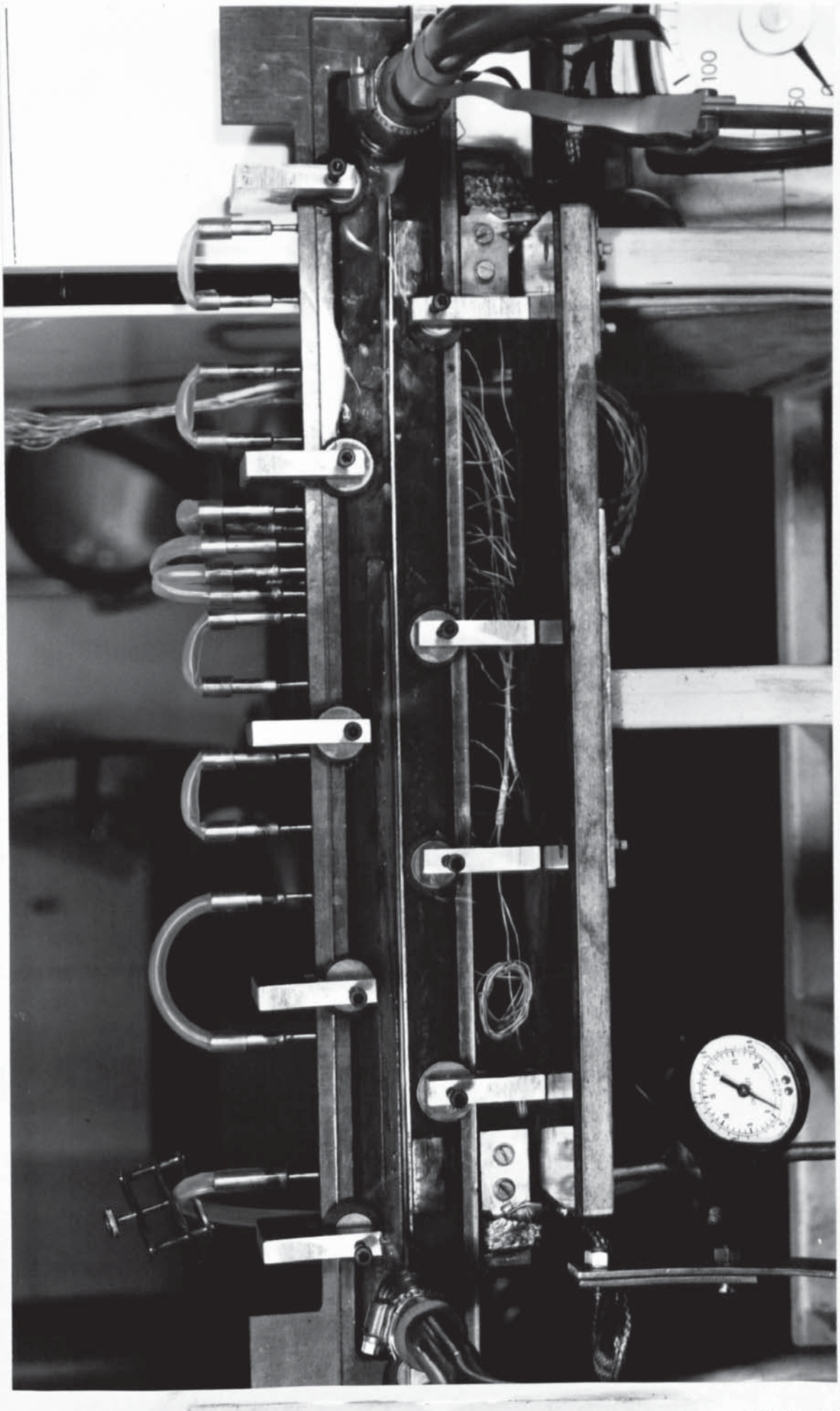

ARRANGEMENT OF GLASS SIDED TEST SECTION P 3.16

TEMPERATURE MEASUREMENT.

The outputs from the Chromel/Alumel thermocouples were referenced to 0°C, by cold junctions in a "Zeref" solid state heat pump ice point unit, and then fed to a digital voltmeter by a two pole multipoint switch, D 3.10. The last digit on the digital voltmeter represented a step of 10 μV.

CALCULATION OF THE OUTER SURFACE TEMPERATURE OF THE HEATING STRIP.

It was assumed that no conduction of heat took place along the length of the heated strip, all conduction being normal to the direction of current flow, with the values of electrical and thermal conductivity taken from manufacturers data the temperature drop across the thickness of the strip was calculated as a function of the heating current, A 4 .

3.6. FLOW VISUALIZATION.

USE OF AIR BUBBLES IN ANNULAR STEPPED SECTION.

At the point immediately following the enlargement in the annular section some flow recirculation had been observed with boiling. It was thought that air bubbles injected into the water flow upstream of this point would provide a clearer picture of any recirculation taking place. The heating element was replaced by a plain brass tube for this test and fine holes were drilled round the periphery of the tube, D 3.24, to allow air injection into the water flow upstream of the change in section. The flow was photographed and by using a range of exposures the fluid flow pattern could be visualized.

USE OF VAPOUR BUBBLES IN PARALLEL ANNULAR SECTION WITH SWIRL FLOW.

To gain an insight into the pattern flow of the water between the swirl vanes the flow was photographed at boiling conditions using both micro second flash exposure and a time exposure. The former showing the bubble size and distribution, the latter giving a vector indication of the direction of bubble travel.

USE OF SCHLIEREN SYSTEM TO SHOW THE BOUNDARY LAYER IN THE RECTANGULAR SECTION.

To investigate the possible disturbance of the heated boundary layer as a result of the change in section, the flow path was set up in the light path of a Schlieren system, D 3.26, and the changes in density of the fluid due to heating were used to produce both black and white and coloured representations of the flow pattern. The light source needed to be of very short duration in order to "freeze" the fluid movement. To achieve this a microsecond spark discharge through an argon jet between two electrodes, P 3.17, was used when photographs were required. Otherwise for live obversation a filament lamp was used.

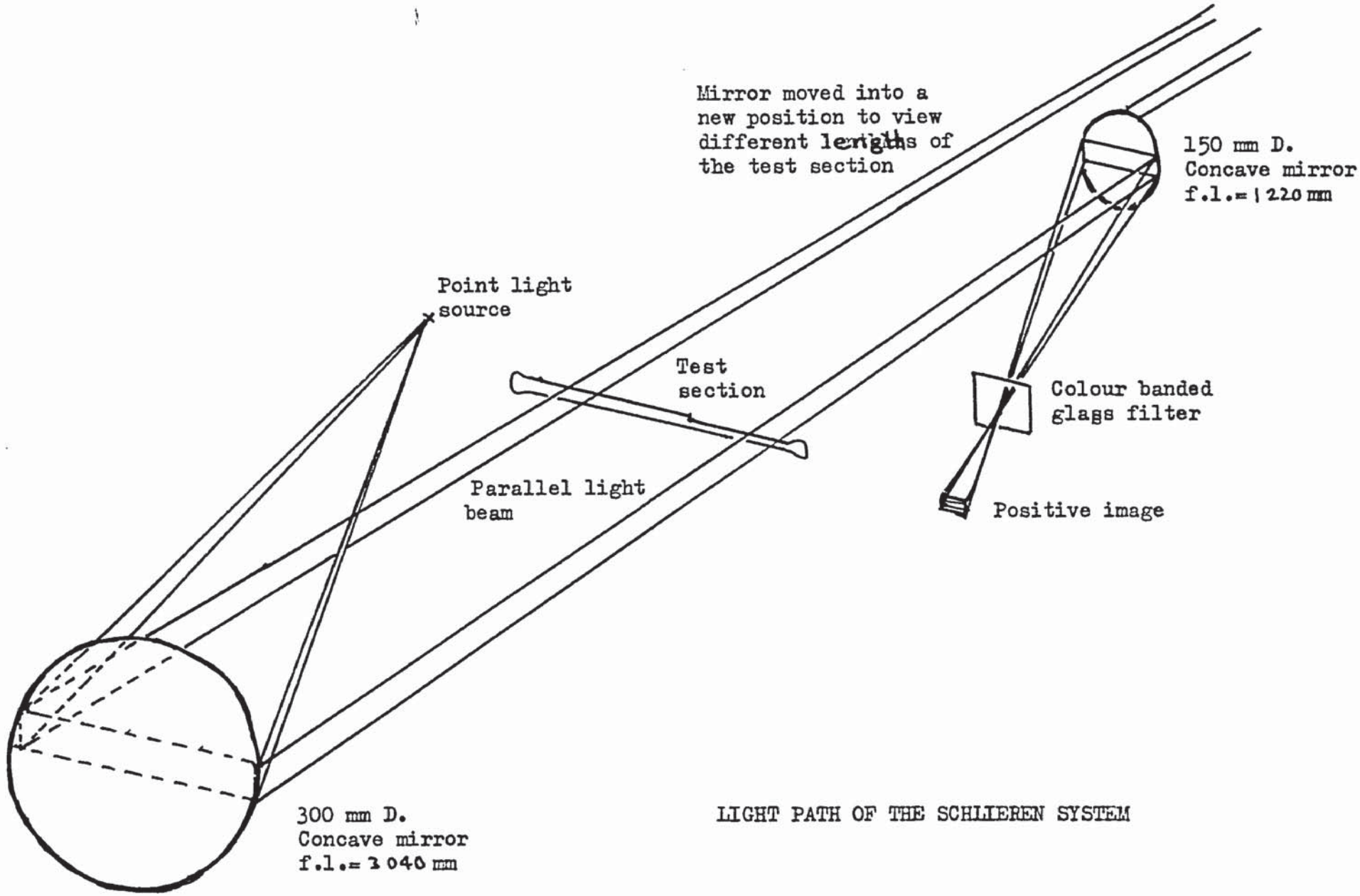

LIGHT PATH OF THE SCHLIEREN SYSTEM

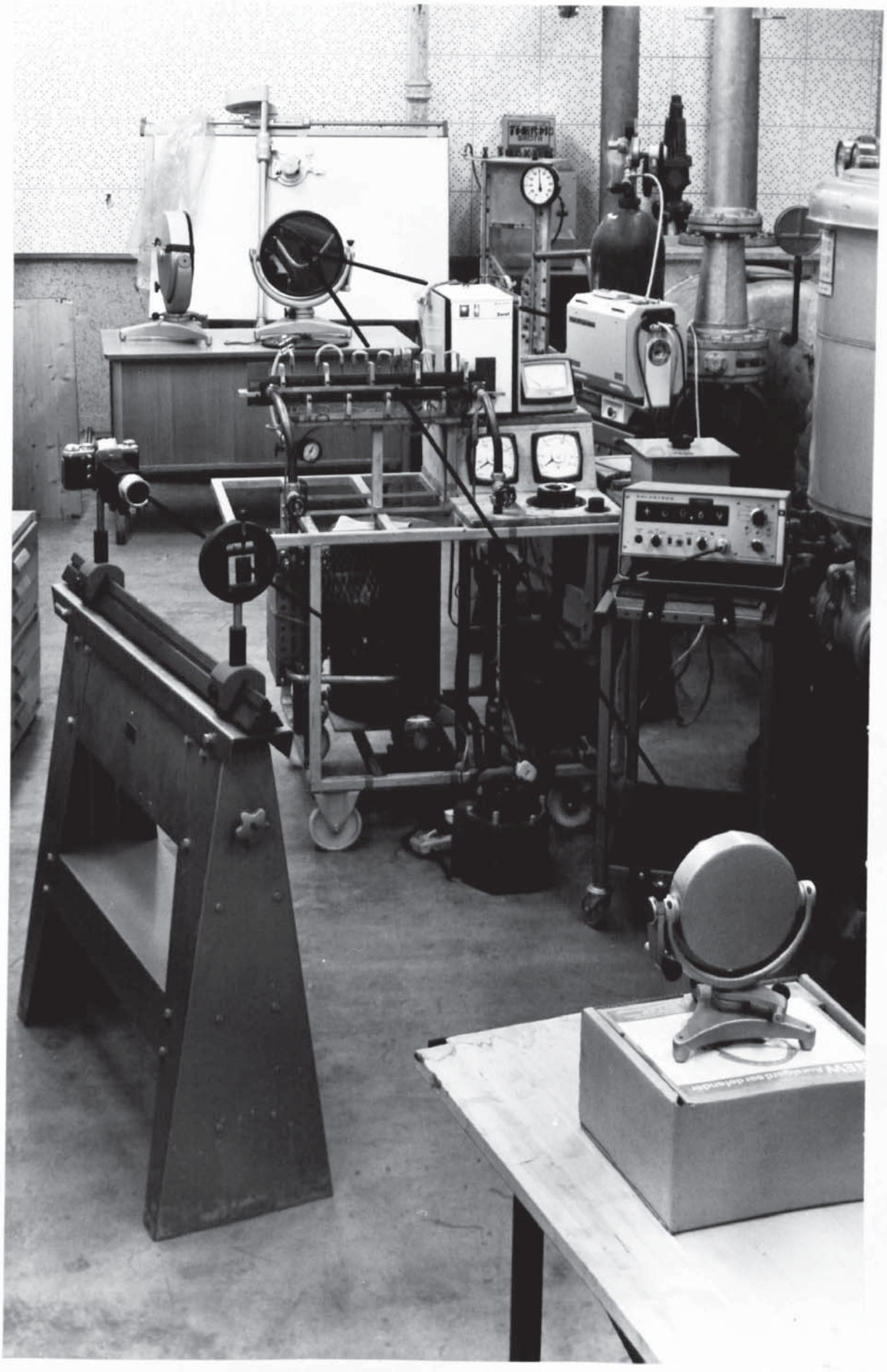

LIGHT PATH OF SCHLIEREN SYSTEM

P 3.17

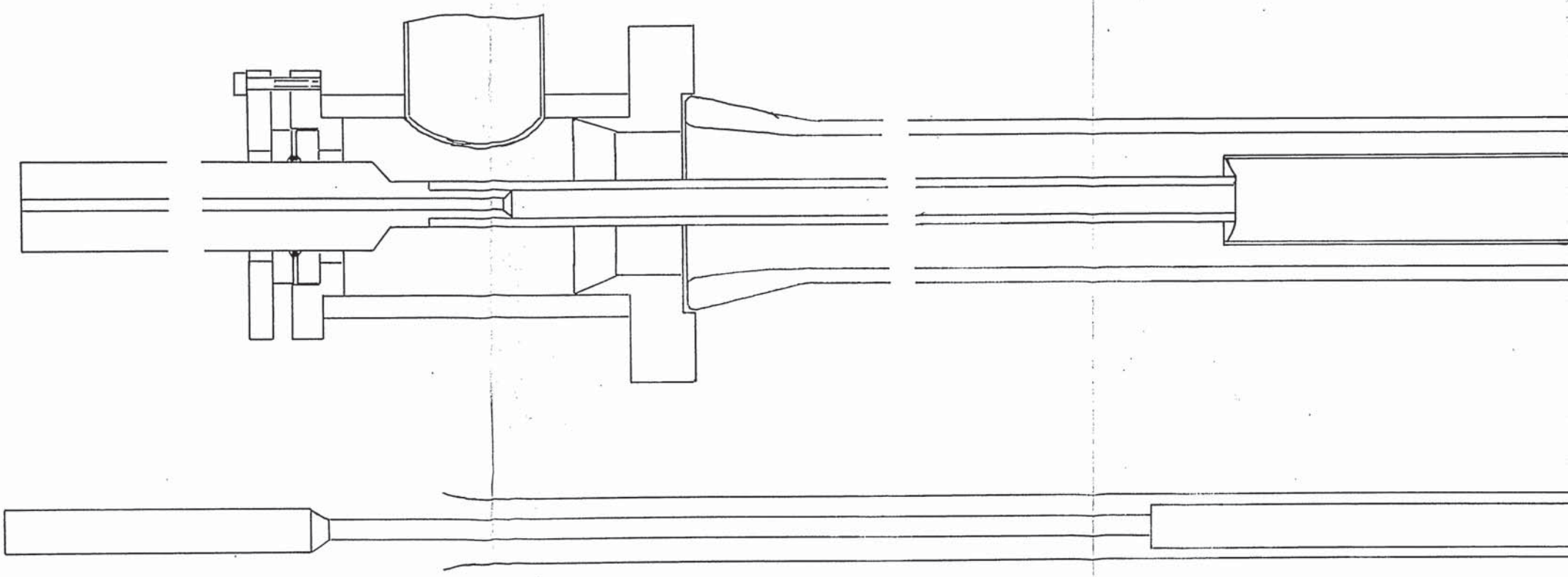

TEST SECTION

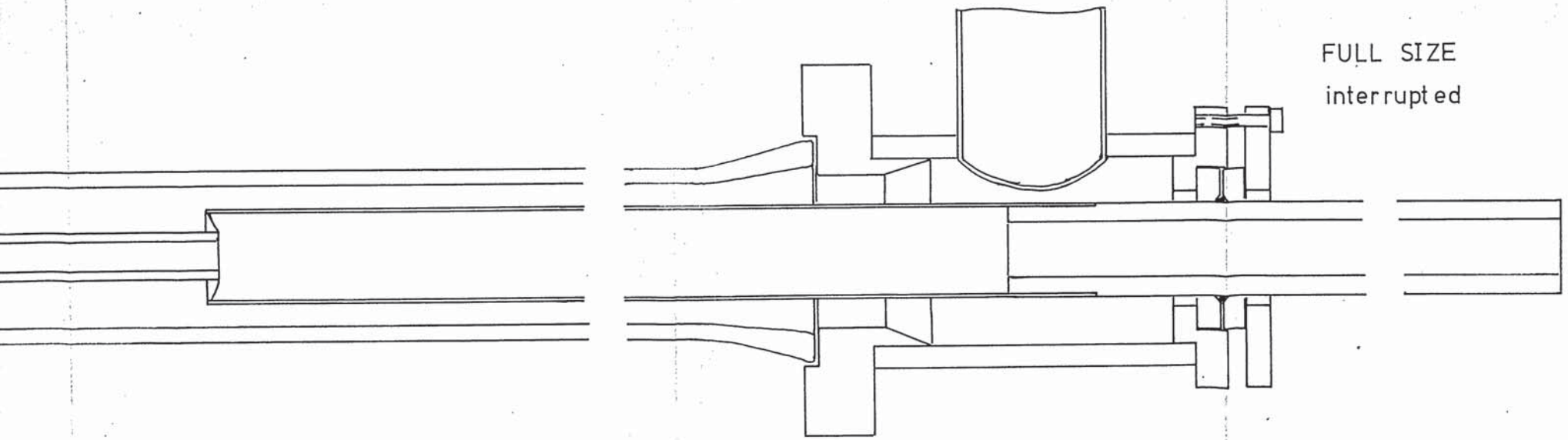

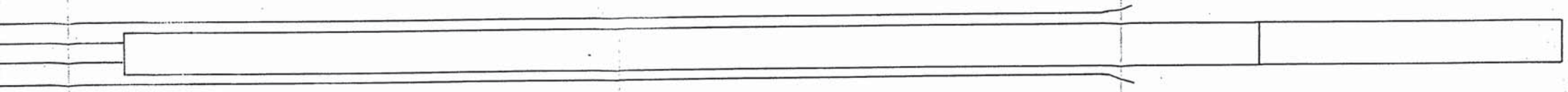

TEST SECTION

TEST SECTION

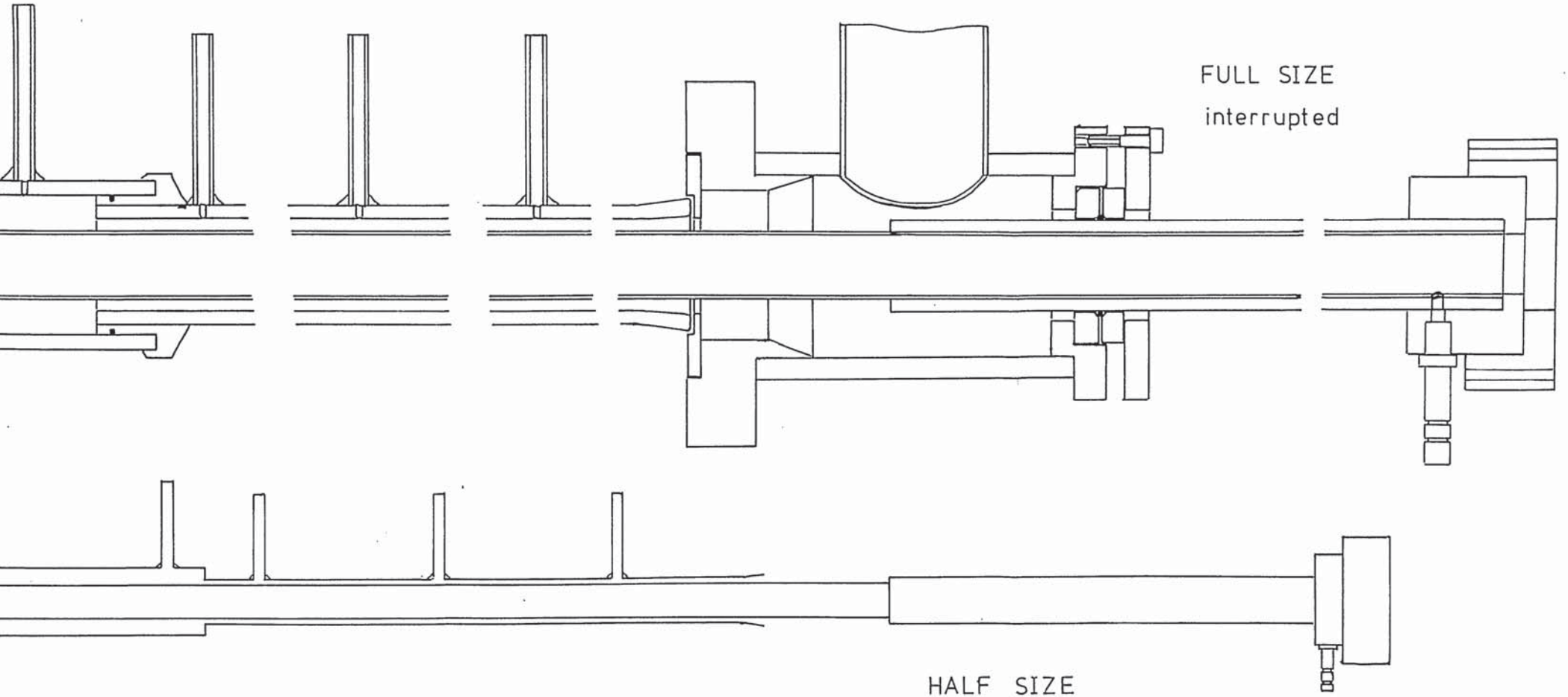

TEST SECTION

D3.13

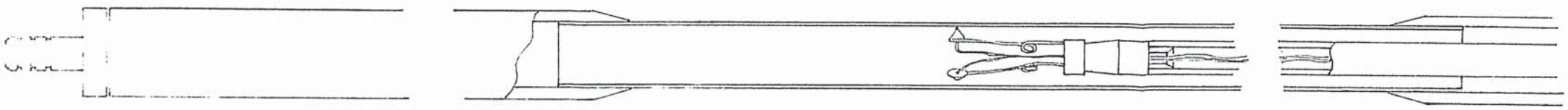

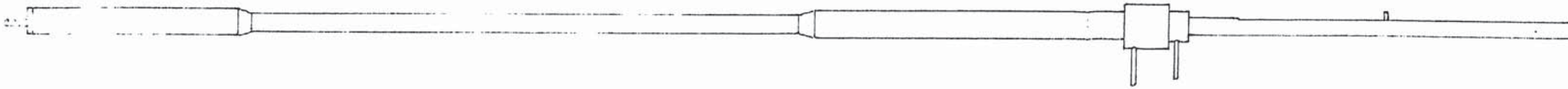

QUA

COMPLETE HEATING ELEMENT

FULL SIZE
interrupted

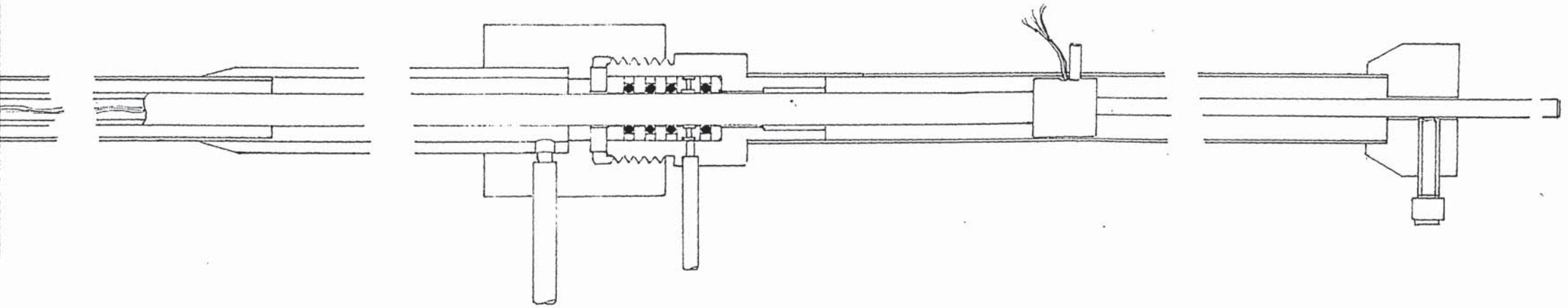

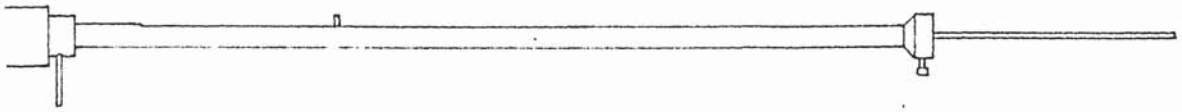

QUARTER SIZE

IPLETE HEATING ELEMENT

COMPLETE HEATING ELEMENT

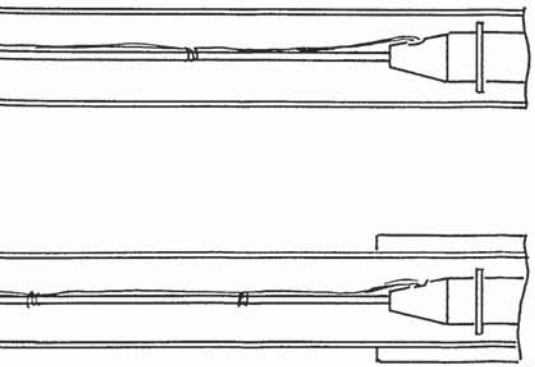

FULL SIZE
interrupted

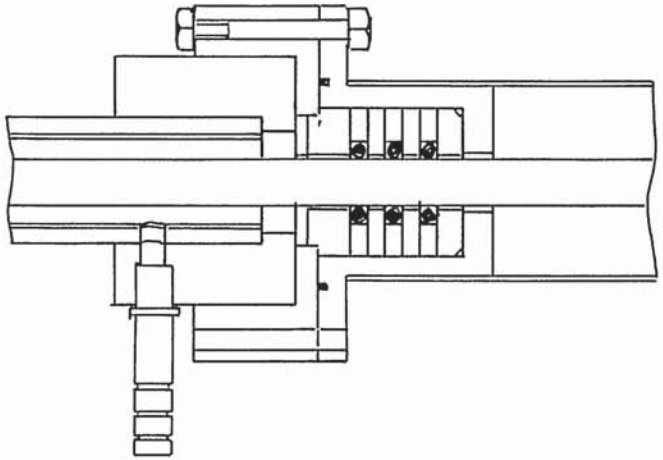

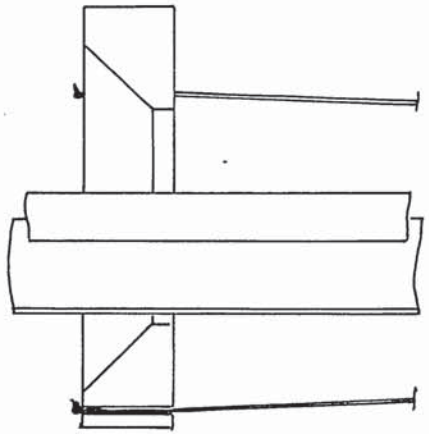

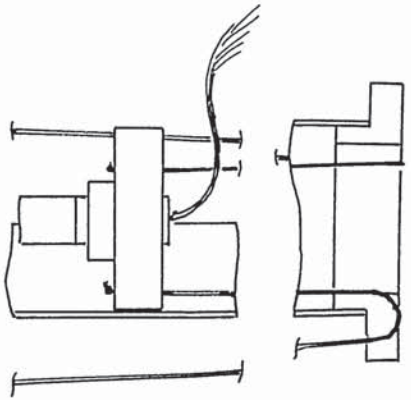

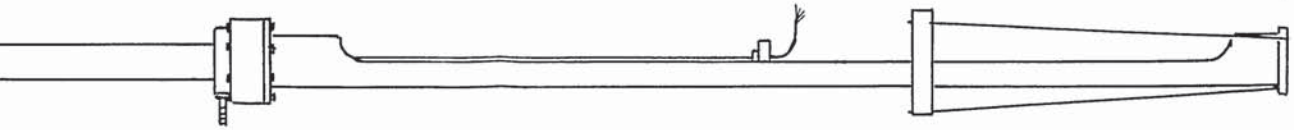

QUARTER SIZE

HEATING ELEMENT

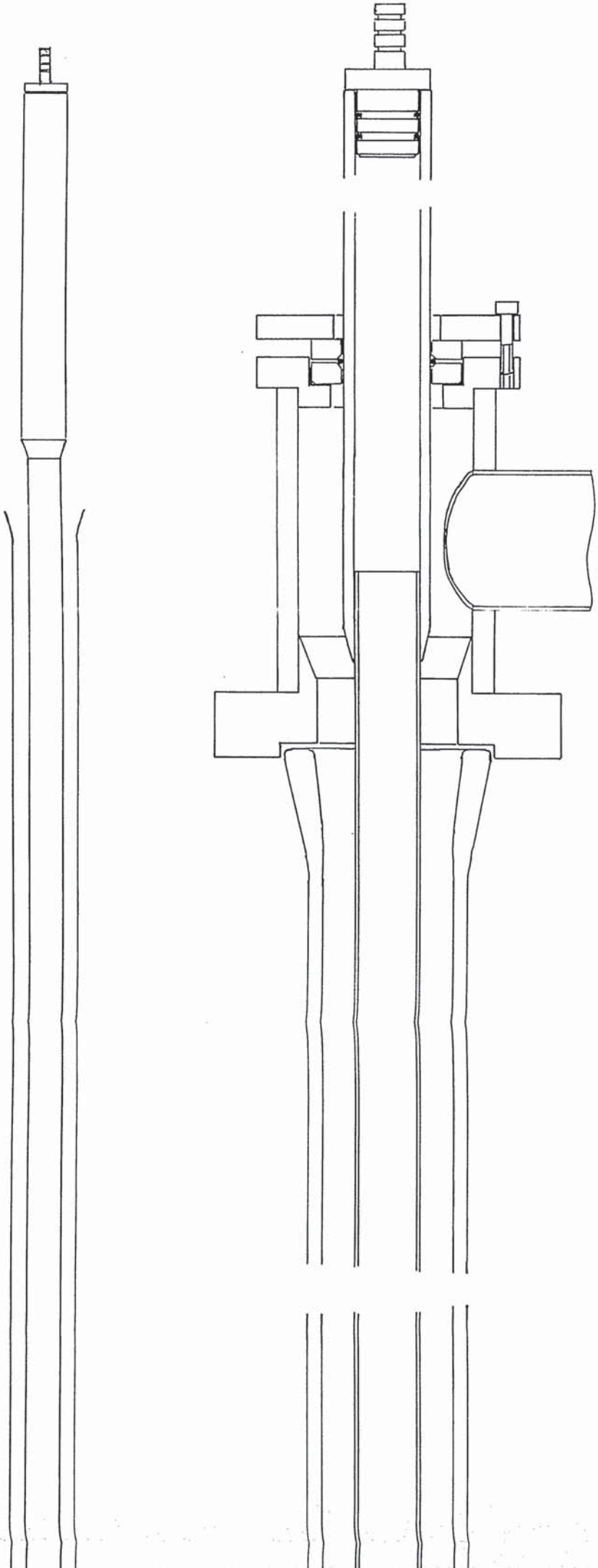

TEST SECTION

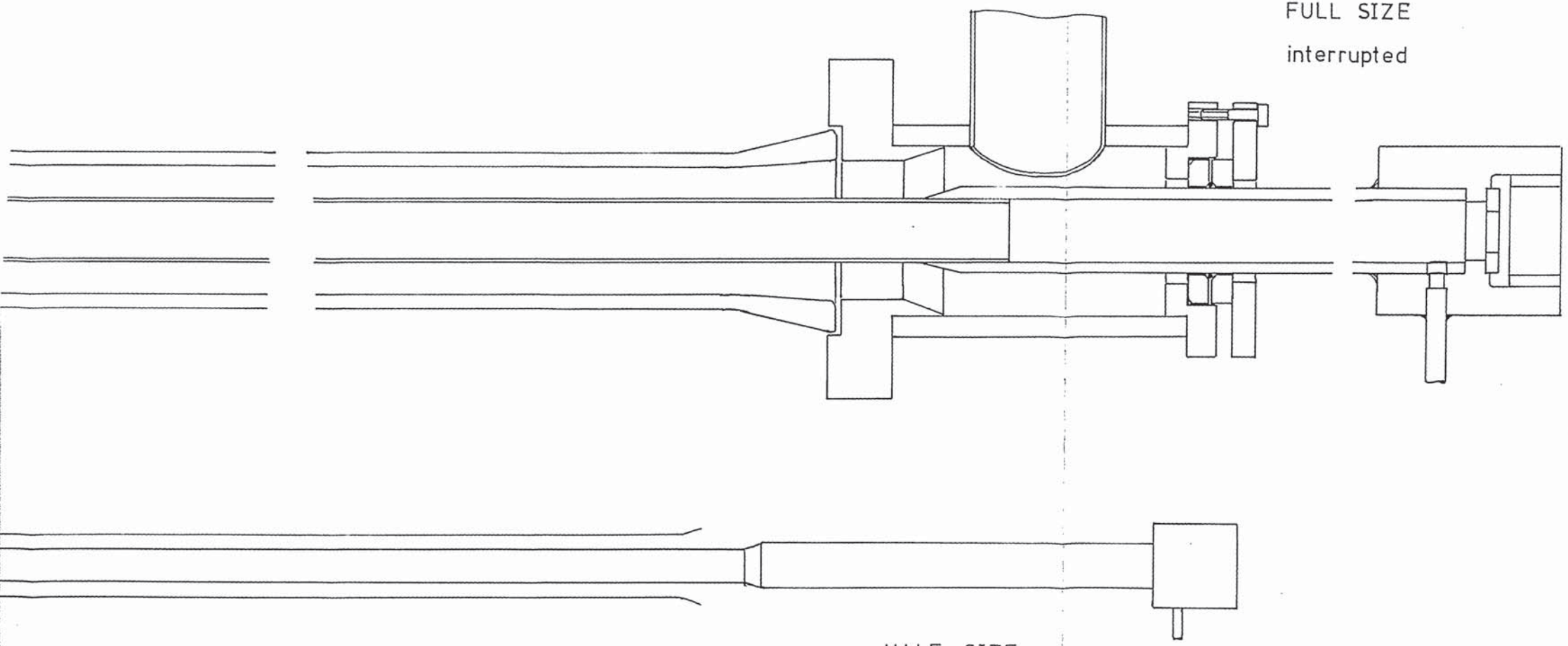

TEST SECTION

D 3.2.2

PRESSURE TRAVERSE TUBE WITH A

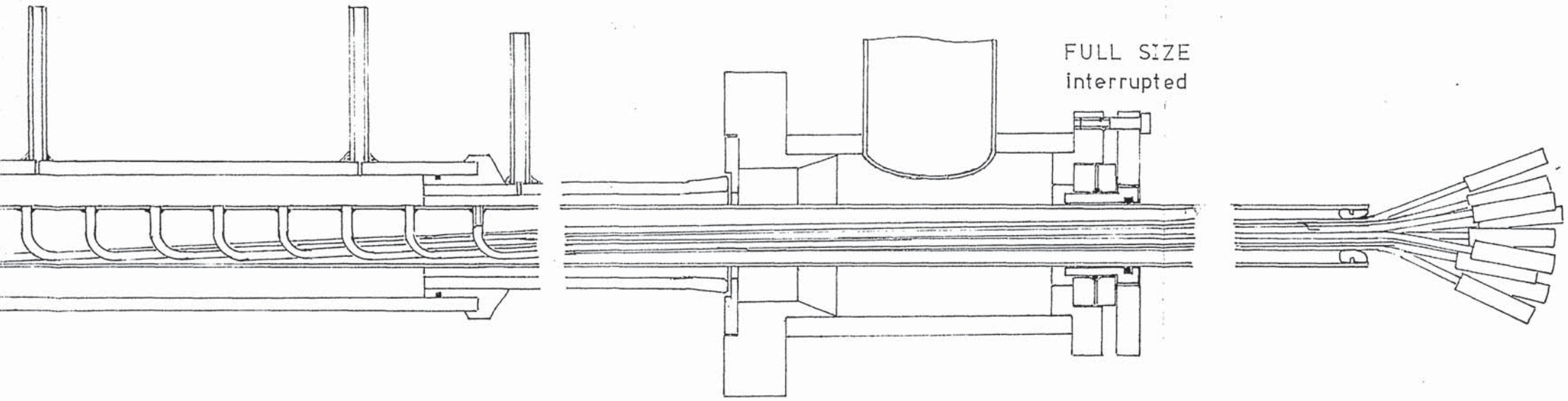

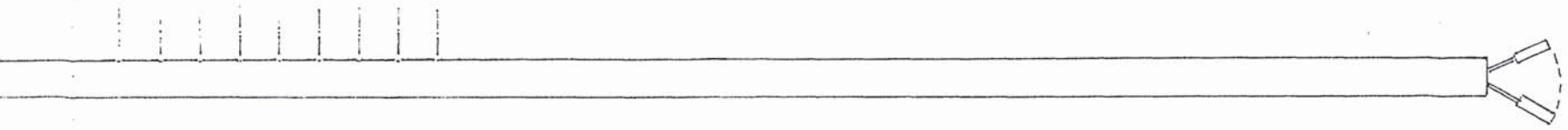

HALF SIZE

PRESSURE TRAVERSE TUBE WITH AIR INJECTION

D 3.24

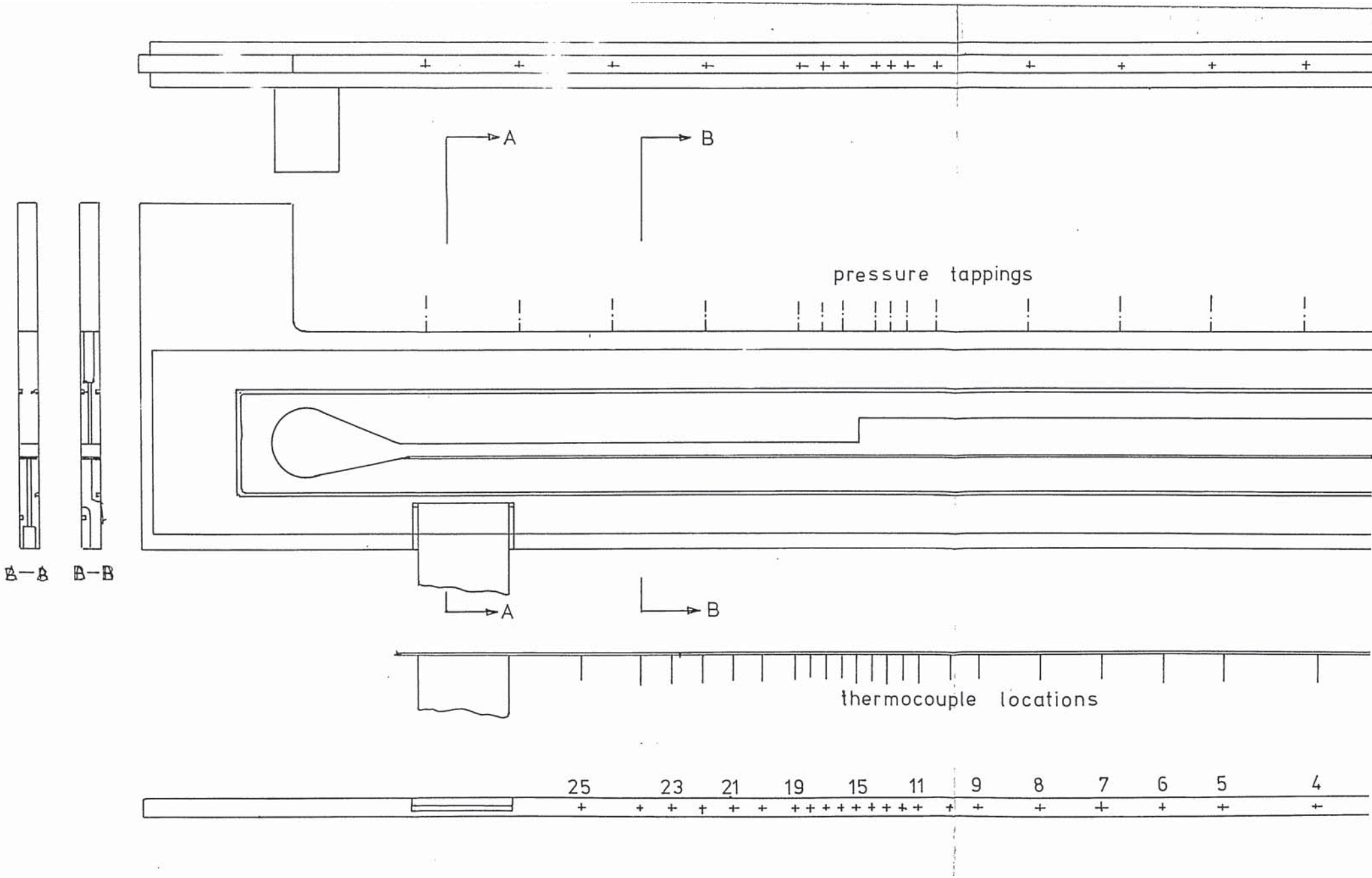
A
B
pressure tappings
B–B
B–B
A
B
thermocouple locations
25
23
21
19
15
11
9
8
7
6
5
4

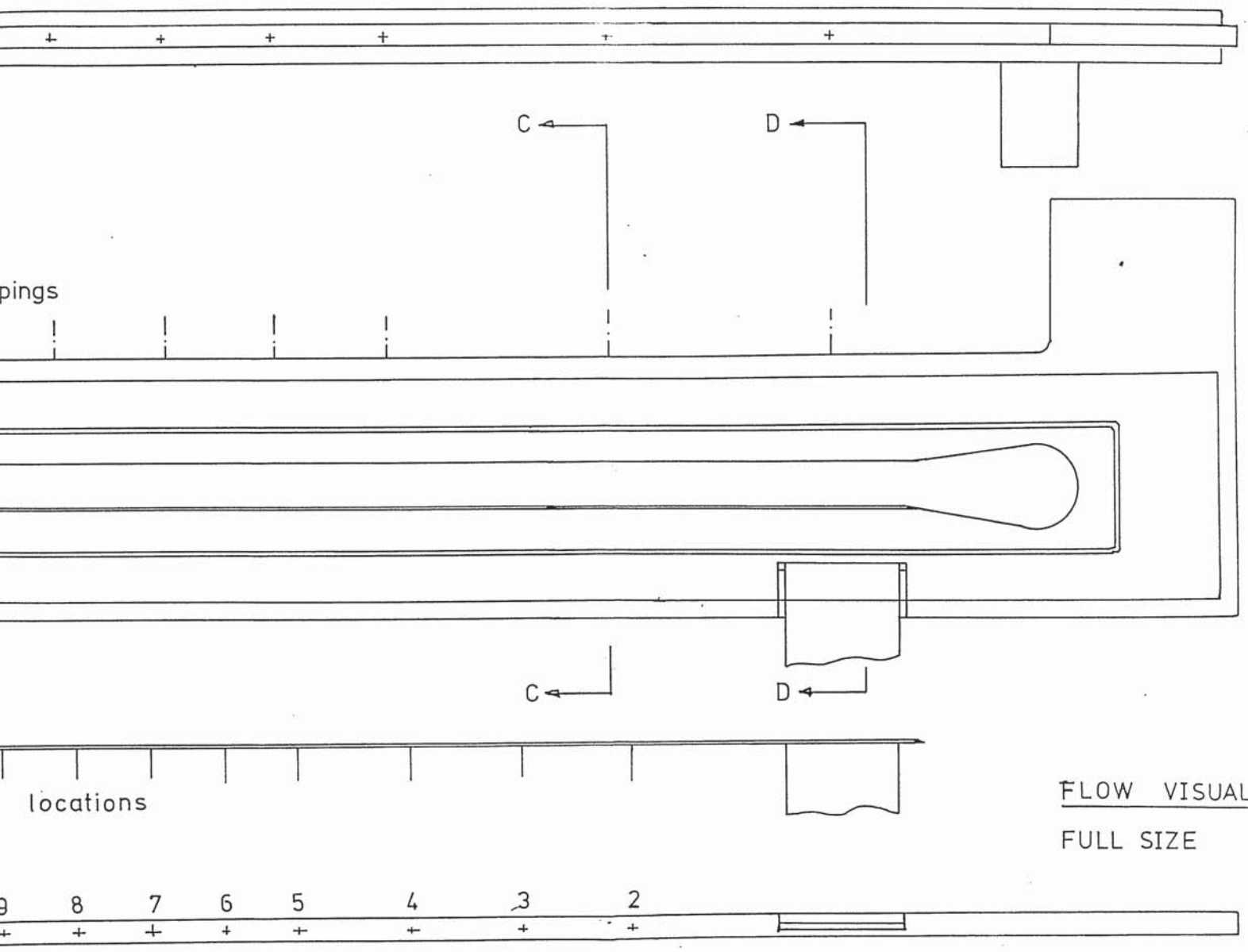

100

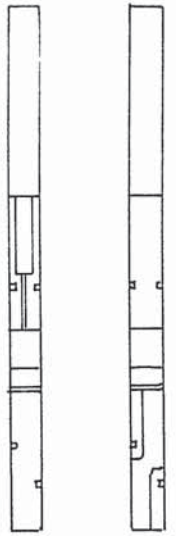

FLOW VISUALIZATION CHANNEL

FULL SIZE

D 3.25

D 3.25

PRESENT WORK

4.1 INTRODUCION.

The present work covers an investigation of the heat transfer processes for a fluid flowing through an annulus with a heated inner wall. The tests cover both single phase and nucleate boiling conditions in the fluid and are concerned principally with the effect of a change in the annulus geometry on the heat transfer coefficient. Two aspects of annulus geometry variation were explored, first a step change in section, and then the introduction of helical guide vanes to produce swirl in the fluid. The work was supported by flow visualization techniques used to attempt to gain some understanding of the effect of these annulus geometry changes on the heat transfer mechanism.

4.2 SINGLE PHASE HEAT TRANSFER CORRELATION FOR WATER FLOWING THROUGH AN ANNULUS WITH HEATED INNER WALL.

INTRODUCTION.

As a starting point in the programme of tests it was decided to use a plain annulus with single phase conditions and obtain a correlation between Re, St and Pr numbers to compare with existing data published by other workers, R6, R10. These tests would also serve to prove the instrumentation on the rig by observing how closely and consistently heat balances could be obtained.

PROCEDURE.

The 19.05 mm outside diameter stainless steel heating tube was surrounded by a 38.1 mm bore "Pyrex" glass tube for these tests, and the heat added to the water in the test section was removed in a counter flow heat exchange immediately after the test section, D 4.1.

The twenty temperatures measured by Chromel/Alumel thermocouples were recorded by the data logger in less than ten seconds and a heat balance was calculated for each test.

The three point sliding thermocouple probe, D 3.17. was used to measure the heating tube inside surface temperature at an axial position which provided the water with an approach length of thirty equivalent diameters. It was assumed that entrance effects would be negligible at this point, D 4.20.

If the heat balance, T 4.1, T 4.2, was satisfactory (within $\pm$ 4.5%) the water bulk temperature and the heating tube surface temperature were calculated at the measuring point and thus for each test the Re, Pr, and St, numbers were calculated.

The column of results, T 4.3, showed that they could be formed into four groups, each group having a virtually constant 'Pr' number. By plotting log St against log Re for constant Pr and then plotting log St against log Pr for constant Re a correlation was obtained between St, Pr, and Re numbers as follows.

Assuming an equation of the form

$$St.Pr^{a} = C_1 Re^{-b}$$

for 'Pr' = constant

$$\log (St) = -b \log (Re) + \log (C/Pr^{a})$$

c.F. $y = -mx + C$

Groups of results with nearly constant 'Pr' were plotted as log (St) against log (Re).

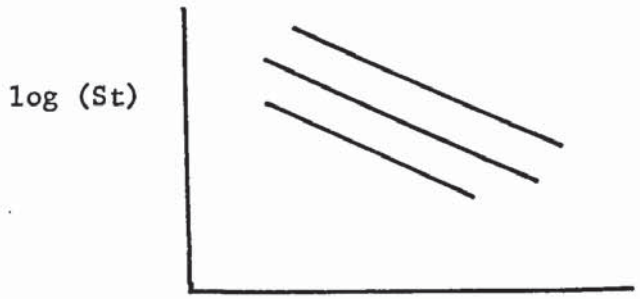

groups of results with almost constant 'Pr'

The slope of the line gave the index 'b'

For a constant 'Re',

$$St.Pr^{a} = C_1.C_2$$

$$\log (St) = -a \log (Pr) + \log (C_1 C_2)$$

$$y = -mx + C$$

From points taken from the initial graph at constant 'Re', log (St) was plotted against log (Pr).

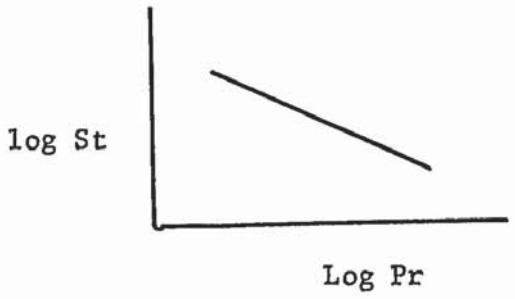

The slope of the line gave the value of the exponent 'a'.

With 'a' and 'b' determined as 0.6 and -0.2 respectively

$$St.Pr^{0.6} = C_1 Re^{-0.2}$$

$$\log (St.Pr^{0.6}) = -0.2 \log (Re) + \log C_1$$

$\log (St.Pr^{0.6})$ was plotted against log (Re)

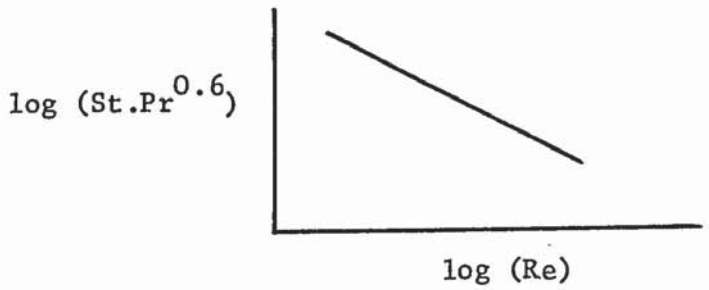

Any point on this line can be used to give co-ordinate values to substitute back into the equation

$$\log (St.Pr^{0.6}) = -0.2 \log (Re) + \log C_1$$

and thus give the value of C_1.

The complete equation was evaluated graphically as,

$$St.Pr^{0.6} = 0.0254\ Re^{-0.2}.$$

The experimental data obtained was fed into a computer to obtained the best least squares straight line fit, T 4.4. This produced the correlation

$$St.Pr^{0.6} = 0.02516\ Re^{-0.1992}$$

This result was compared with correlations of the same form produced by previous workers.

TYPICAL HEAT BALANCE, Test 3, 11.2.71

Electrical Power Supplied = 4.925 kW

Main Circuit Water

Flow rate ($\dot{m}$) = 0.20 kg/s

Specific heat (cp) = 4.18 kJ/kg K

Inlet temperature = 37.01 °C

Outlet temperature = 36.58 °C

Heat loss = ($\dot{m}$. Cp. ΔT) = 0.359 kW

Cooling Water

Flow rate (in) = 0.046 kg/s

Specific heat (cp) = 4.184 kJ/kg K

Inlet temperature = 8.40 °C

Outlet temperature = 35.40 °C

Heat extracted ($\dot{m}$. Cp. ΔT) = 5.219 k W

Heat in busbars

Upper $= k.A.\frac{dt}{dx} = 380 \times \frac{1}{1544} \times \frac{0.48}{0.20}$

Lower $= k.A.\frac{dt}{dx} = 380 \times \frac{1}{1544} = \frac{3.00}{0.20}$

$\Big\}$ = 0.004 kW

Net Input = 4.925 + 0.359 = 5.284 kW

Net Output = 5.219 + 0.004 = 5.223 kW

Misc. losses = 5.284 − 5.223 = 0.061 kW

= 1.2% of electrical power input.

SINGLE PHASE CORRELATION DATA.

Test	Water inlet °C	Wall inner °C	Wall ΔT K	Wall outer °C	m kg/s	c_p
1	35.35	81.02	4.9	76.1	0.52	4.18
2	36.29	105.03	5.7	79.3	0.34	4.18
3	37.01	112.06	4.8	107.3	0.20	4.18
4	39.44	74.49	4.7	69.8	0.64	4.18
5	40.00	71.26	4.75	66.5	0.75	4.18
6	40.37	68.01	4.75	63.2	0.87	4.18
7	40.74	65.78	4.8	63.0	1.00	4.18
8	41.35	64.04	4.75	59.3	1.18	4.18
10	41.96	62.60	4.8	57.8	1.33	4.18
11	41.68	111.52	7.3	104.2	0.41	4.18
12	41.44	100.08	8.1	92.0	0.58	4.18
13	42.12	89.19	8.1	81.1	0.81	4.18
14	42.68	86.35	8.1	78.3	0.88	4.18
15	42.92	82.49	8.1	74.4	1.03	4.18
16	42.57	79.02	8.1	70.9	1.17	4.18
17	42.57	75.82	8.25	67.6	1.33	4.18
18	43.27	74.50	8.25	66.2	1.46	4.18
19	43.63	73.40	8.25	65.2	1.59	4.18
20	44.13	71.70	8.20	63.5	8.81	4.18
21	44.43	71.15	8.20	63.0	1.94	4.18
A	58.44	104.90	10.0	94.9	1.10	4.19
B	59.25	109.86	10.1	99.8	0.96	4.19
C	57.84	111.24	9.5	101.7	0.86	4.19
D	64.10	119.52	8.9	110.6	0.74	4.19
E	63.49	122.22	8.8	113.4	0.64	4.19
F	74.35	120.62	8.6	112.0	0.88	4.20
G	74.52	114.74	8.6	106.1	1.10	4.20
H	74.65	111.82	8.5	103.3	1.24	4.20
I	74.80	109.27	8.7	100.6	1.40	4.20
J	75.04	107.24	8.8	98.4	1.61	4.20

T 4.3

SINGLE PHASE CORRELATION DATA.

Test	kW	$\Delta T = \frac{kW}{\dot{m}c_p}$	Water bulk °C	$T_w - T_b$ K	Heat Balance error, %.	G_2 kg/m^{2}s.
1.	5.00	2.30	37.55	38.55	2.2	608.1
2	4.95	3.51	39.80	39.50	3.5	395.2
3	4.93	5.89	42.90	64.40	1.2	233.9
4	4.88	1.82	41.26	28.54	4.5	748.4
5	4.90	1.56	41.56	24.94	3.2	877
6	4.90	1.34	41.71	21.49	3.5	1020
7	4.92	1.17	41.91	21.09	1.5	1172
8	4.91	0.99	41.36	17.94	1.4	1383
10	4.91	0.88	42.84	14.96	- 0.8	1555
11	7.52	4.44	46.12	58.08	1.6	473.6
12	7.90	3.24	44.68	47.32	2.4	682.9
13	7.94	2.34	44.46	36.64	- 4.2	947.2
14	7.95	2.17	44.85	33.45	0.7	1023
15	7.97	1.85	44.77	29.63	- 0.1	1204
16	7.97	1.63	44.20	26.33	1.1	1368
17	8.02	1.44	44.01	23.59	- 0.5	1707
18	8.03	1.31	44.58	21.62	2.4	1708
19	8.03	1.21	44.84	20.36	- 3.2	1859
20	8.00	1.06	45.19	18.31	3.0	2117
21	8.02	0.99	45.42	17.58	- 1.8	2264
A	10.88	2.36	60.80	34.10	- 0.3	1286
B	10.95	2.73	61.98	37.82	1.5	1123
C	10.63	2.95	60.79	40.91	2.7	1006
D	10.25	3.29	67.39	43.21	0.5	870
E	10.20	3.83	67.32	46.08	1.9	743.7
F	10.10	2.73	77.08	34.92	0.5	1031
G	10.07	2.18	76.70	29.40	3.0	1286
H	10.05	1.93	76.48	26.82	2.5	1450
I	10.16	1.73	76.53	24.07	1.0	1642
J	10.20	1.17	76.21	22.19	1.1	1883

T 4.3

SINGLE PHASE CORRELATION DATA.

Test	$\mu b \times 10^6$	Re_b	Pr_b	$\frac{kW}{m^2K} = h$	$St = \frac{h}{G c_p}$	$St \times Pr^{0.6}$
1	682	16 986	4.50	3.329	0.00131	0.00322
2	652	11 547	4.30	3.217	0.00195	0.00467
3	618	7 210	4.02	1.963	0.00201	0.00462
4	635	22 452	4.17	4.385	0.00140	0.00330
5	631	26 477	4.14	5.043	0.00138	0.00323
6	632	30 745	4.13	5.853	0.00137	0.00321
7	629	35 495	4.11	5.988	0.00122	0.00285
8	634	41 555	4.15	7.025	0.00122	0.00286
10	619	47 856	4.03	8.425	0.00130	0.00300
11	581	15 529	3.89	3.324	0.00168	0.00379
12	598	21 755	3.91	4.285	0.00150	0.00340
13	600	30 074	3.91	5.559	0.00140	0.00317
14	595	32 753	3.90	6.101	0.00143	0.00323
15	598	38 355	3.90	6.905	0.00137	0.00310
16	602	43 290	3.92	7.765	0.00136	0.00309
17	605	53 749	3.94	8.727	0.00122	0.00277
18	600	54 217	3.91	9.528	0.00133	0.00302
19	597	59 320	3.90	10.118	0.00130	0.00294
20	591	68 238	3.87	11.215	0.00127	0.00286
21	590	73 100	3.84	11.703	0.00124	0.00278
A	459	53 373	2.92	8.190	0.00152	0.00289
B	450	47 540	2.88	7.432	0.00158	0.00298
C	460	41 612	2.92	6.667	0.00158	0.00300
D	417	39 745	2.64	6.089	0.00167	0.00299
E	418	33 894	2.64	5.682	0.00182	0.00326
F	365	53 810	2.30	7.424	0.00172	0.00284
G	367	66 753	2.31	8.788	0.00163	0.00269
H	368	75 061	2.31	9.619	0.00158	0.00261
I	368	85 000	2.31	10.835	0.00157	0.00260
J	369	97 212	2.31	11.799	0.00149	0.00246

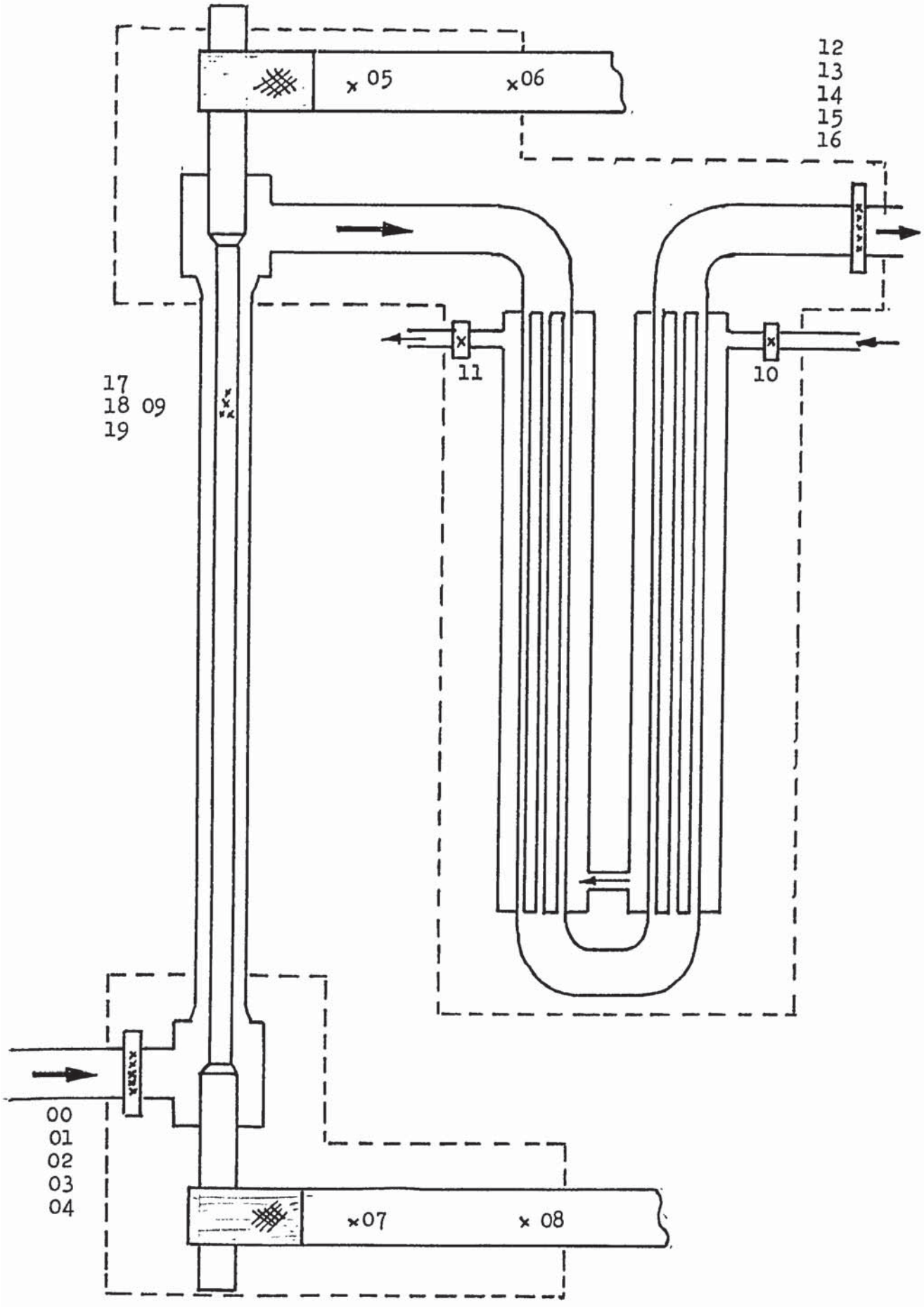

CIRCUIT FOR SINGLE PHASE TESTS (With thermocouple locations)

D 4.1

DATA LOGGER OUTPUT, Test 3, 11-2-71.

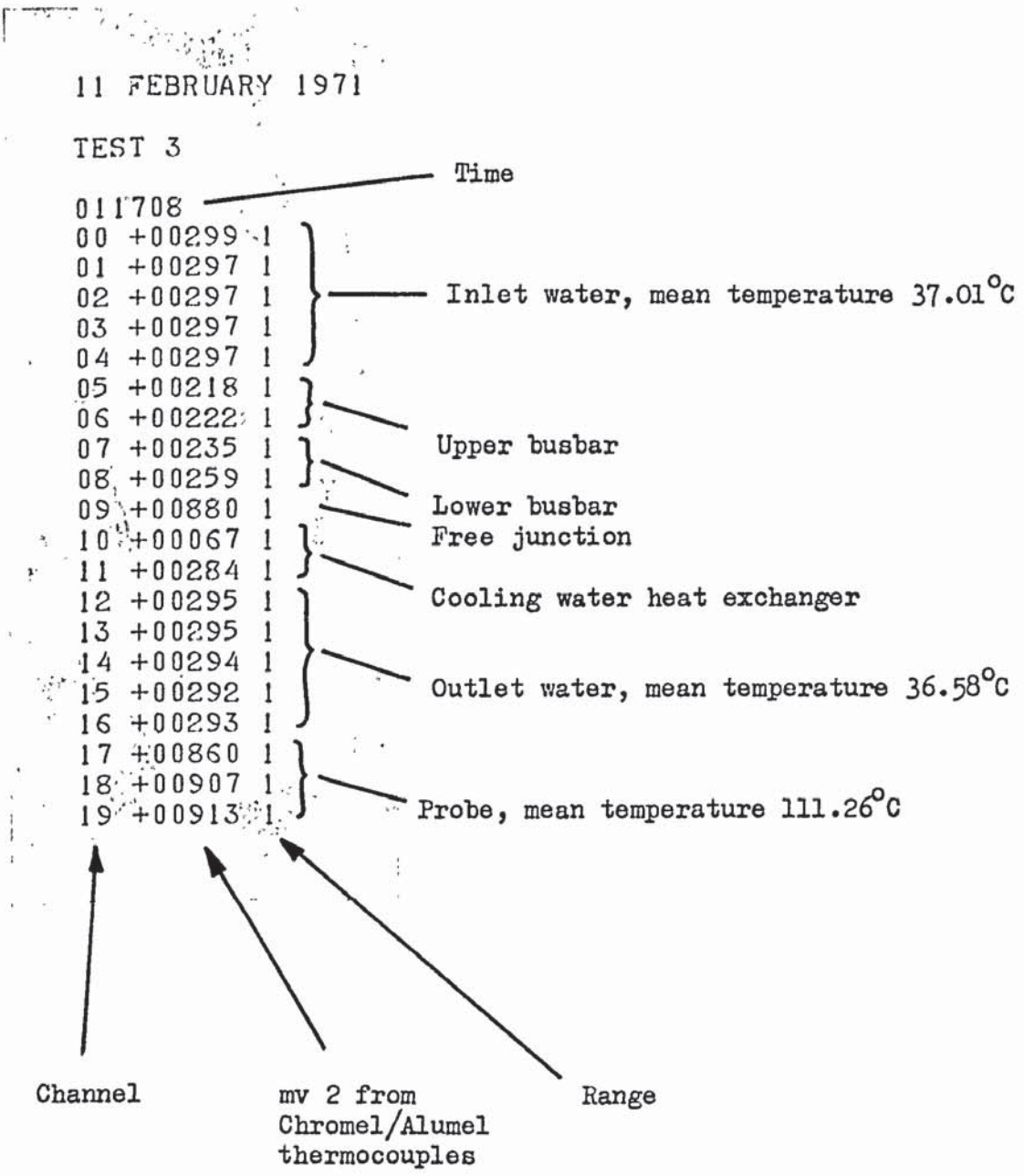

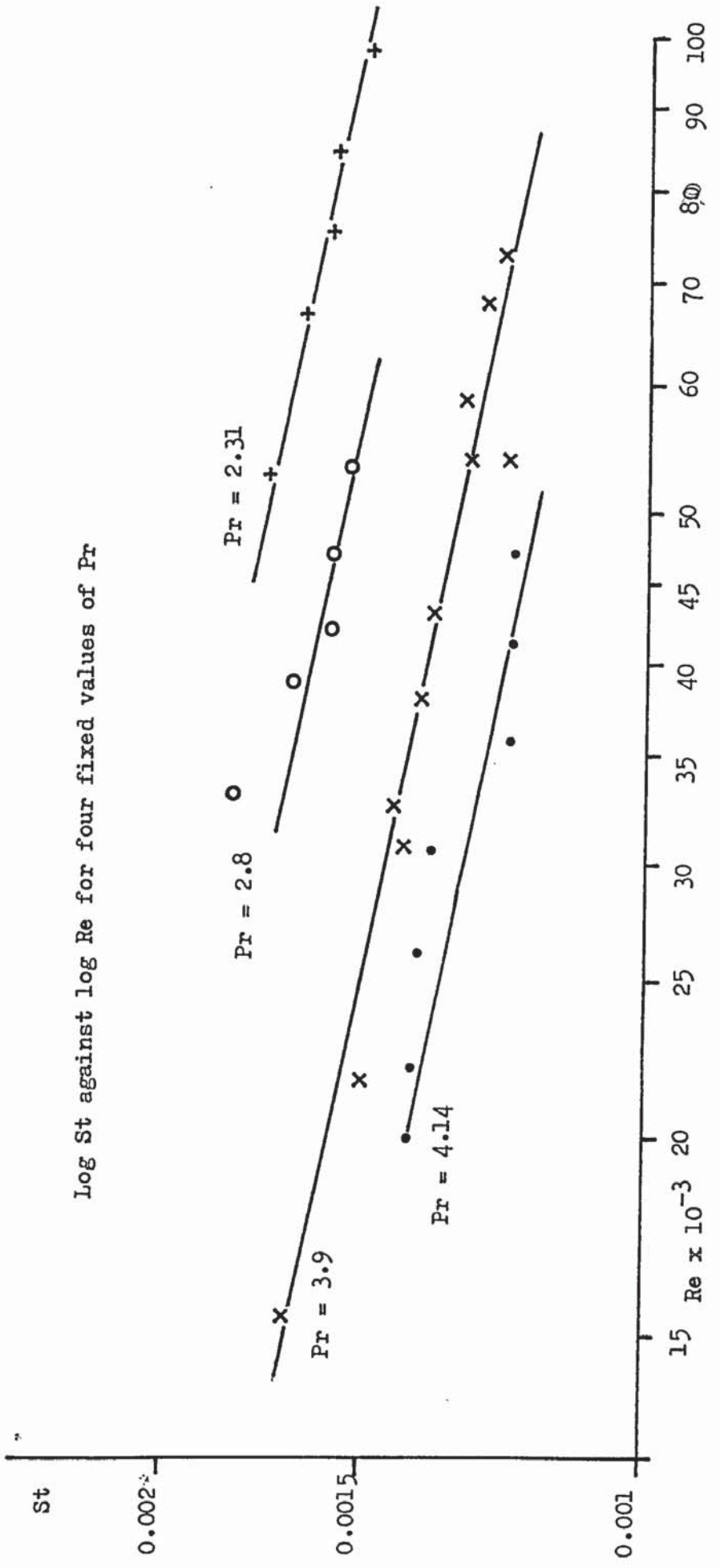
Log St against log Re for four fixed values of Pr
St
0.002
0.0015
0.001
15
20
25
30
35
40
45
50
60
70
80
90
100
Re x 10^{-3}
Pr = 2.31
Pr = 2.8
Pr = 3.9
Pr = 4.14

G 4.1

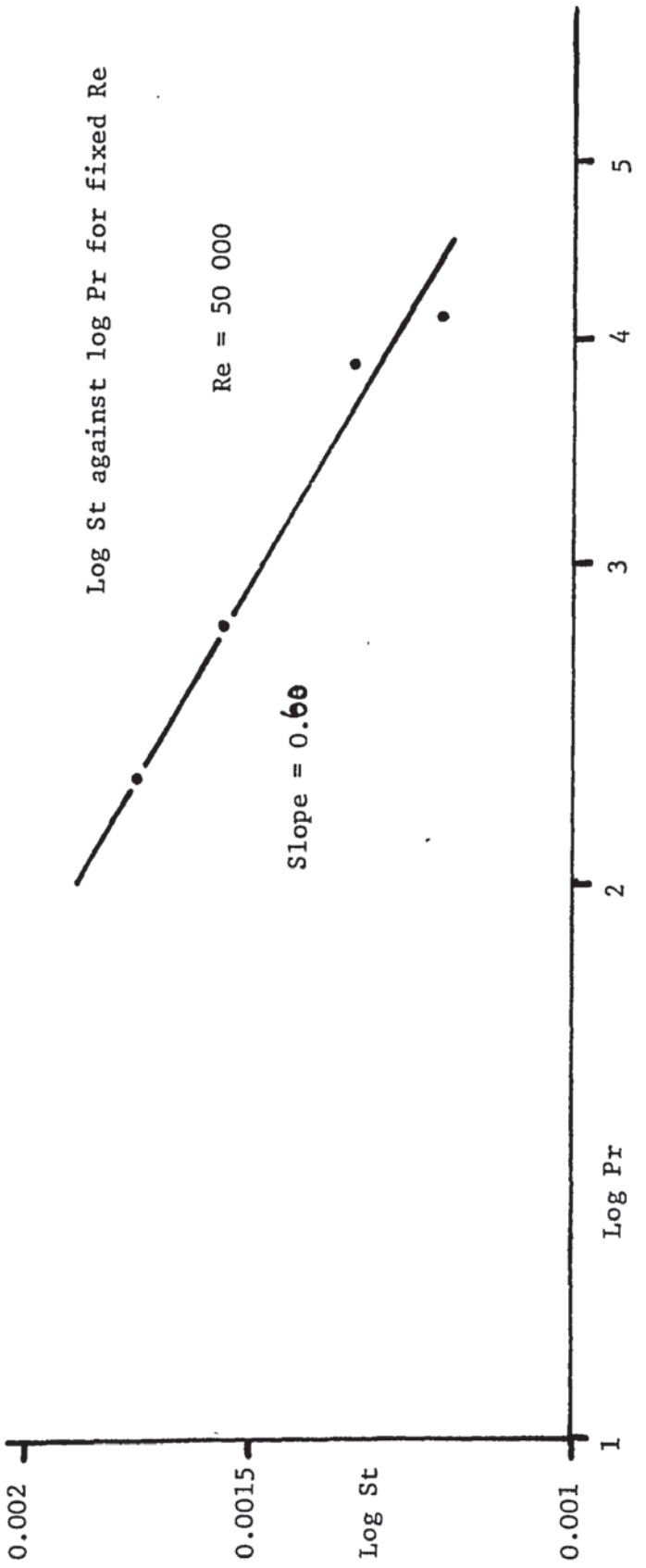
Log St against log Pr for fixed Re
Re = 50 000
Slope = 0.60
Log St
Log Pr
0.002
0.0015
0.001
1
2
3
4
5

G 4.2

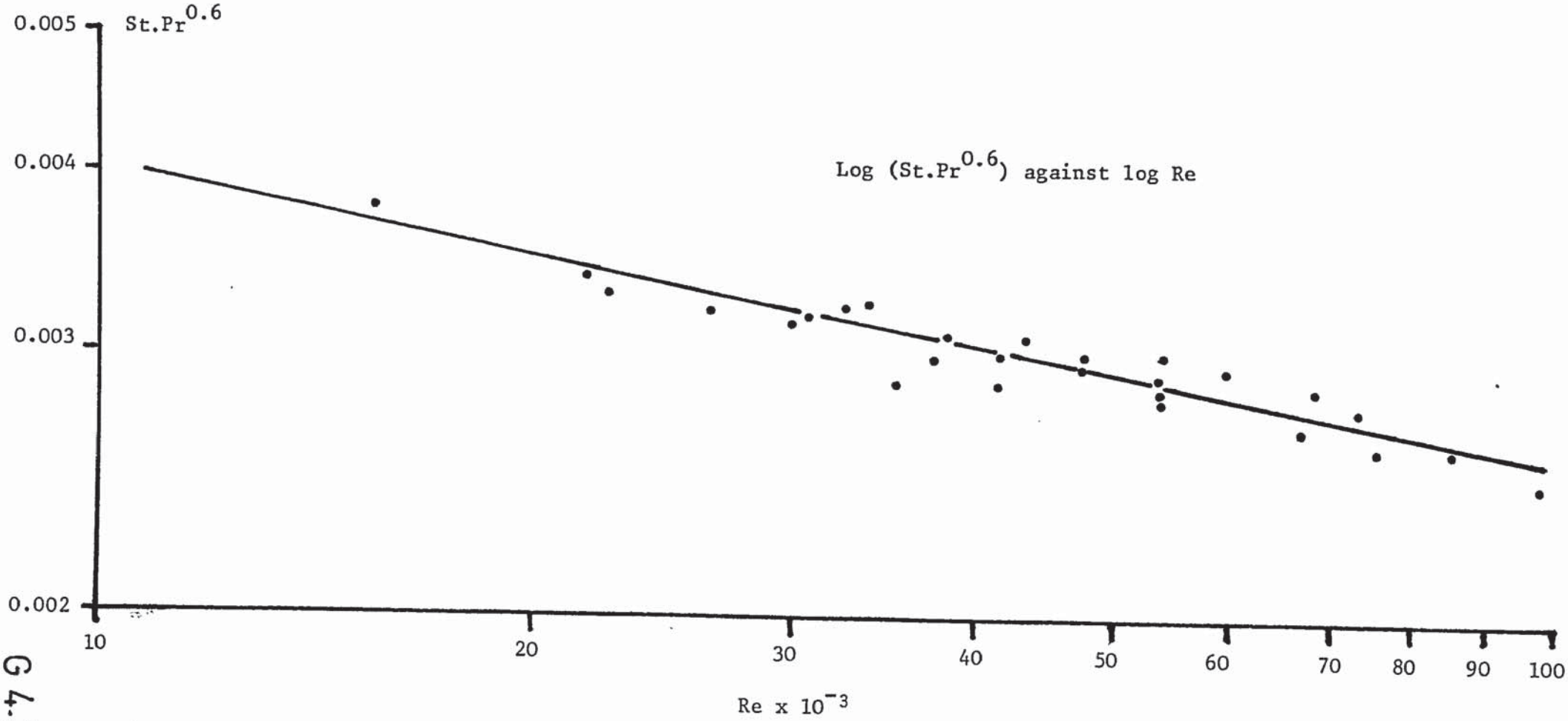
0.005
St.Pr^0.6
0.004
Log (St.Pr^0.6) against log Re
0.003
0.002
10
20
30
40
50
60
70
80
90
100
Re x 10^-3

G 4.3

POLYNOMIAL CURVE FIT

A WATSON SINGLE PHASE RUNS

DEGREE OF POLYNOMIAL 1
COEFFICIENTS
0 =0.15992398068D 01
1 =0.19920901187D 00

X	Y		DEVIATION	
Re	DATA $St.P_r^{0.6}$	EQUATION		%
15529.0000	0.0038	0.0037	0.0001	2.99
21755.0000	0.0034	0.0034	=0.0000	=1.19
30074.0000	0.0032	0.0032	=0.0001	=1.74
32753.0000	0.0032	0.0032	0.0001	1.84
38355.0000	0.0031	0.0031	0.0000	0.86
43290.0000	0.0031	0.0030	0.0001	2.99
53749.0000	0.0028	0.0029	=0.0001	=3.61
54217.0000	0.0030	0.0029	0.0002	5.28
59320.0000	0.0029	0.0028	0.0001	4.34
68238.0000	0.0029	0.0027	0.0001	4.37
73100.0000	0.0028	0.0027	0.0001	2.85
53373.0000	0.0029	0.0029	0.0000	0.43
47540.0000	0.0030	0.0029	0.0000	1.20
41612.0000	0.0030	0.0030	=0.0000	=0.79
39745.0000	0.0030	0.0031	=0.0001	=2.02
33894.0000	0.0033	0.0032	0.0001	3.49
53810.0000	0.0028	0.0029	=0.0000	=1.15
66753.0000	0.0027	0.0028	=0.0001	=2.26
75061.0000	0.0026	0.0027	=0.0001	=2.93
85000.0000	0.0026	0.0026	=0.0000	=0.87
97212.0000	0.0025	0.0026	=0.0001	=3.67
22452.0000	0.0033	0.0034	=0.0001	=3.49
26477.0000	0.0032	0.0033	=0.0001	=2.38
30745.0000	0.0032	0.0032	=0.0000	=0.06
41555.0000	0.0029	0.0030	=0.0002	=5.45
47856.0000	0.0030	0.0029	0.0001	2.01

RMS DEVIATION 0.0001

4.3 TWO-PHASE TESTS IN A PLAIN ANNULUS.

INTRODUCTION.

Following the single phase tests in the plain annulus, the next step was to increase the heating power to produce nucleate boiling in the test section. The aim of the tests was to fully test the rig under boiling conditions and to note the maximum power level for satisfactory operation of the copper braid connections from the busbars to the heating tube. The three point sliding thermocouple probe was again used to measure the inside wall temperature of the heating tube during these tests.

PROCEDURE

The first set of tests was carried out with a constant heat flux, 445 kW/m^2, and near constant inlet temperatures. The flow velocities in the test section varied between 1.7 and 0.2 m/s.

Heat balances within + 1.85 and - 0.6% were obtained but repeat tests showed the heat transfer coefficient to have a reduced value and it was noticed that a discolouration of the heating surface was taking place. The tests were discontinued and the rig was given a long run under boiling conditions to allow the heater surface to reach a stable condition.

It was noticed during these tests that the three point thermocouple probe was not always contacting with all three thermocouples and this led to the design of the six point thermocouple probe with a fully floating head D 3.18. The power supply was also improved by the addition of a boost transformer fed by a "Variac" to give fine control of the heating power.
When the surface conditions of the heating tube had stabilized a series of tests was carried out with a constant input power of 280 kW/m^2 and a constant mass flow rate of water through the annulus. During the tests results were taken to enable the heat transfer

coefficient to be calculated for different values of water inlet temperature. The tests were then repeated for different values of mass flow rate of water through the annulus. Having concluded these tests, the whole series was repeated at a higher power level, 520 kW/m^2.

The results were presented as a plot of heating tube outside wall temperature against the fluid bulk temperature, G 4.4, G 4.5, and also as a plot of $Nu/Pr^{0.4}$ against $Re^{0.8}$ with an overplot of water temperatures, G 4.6.

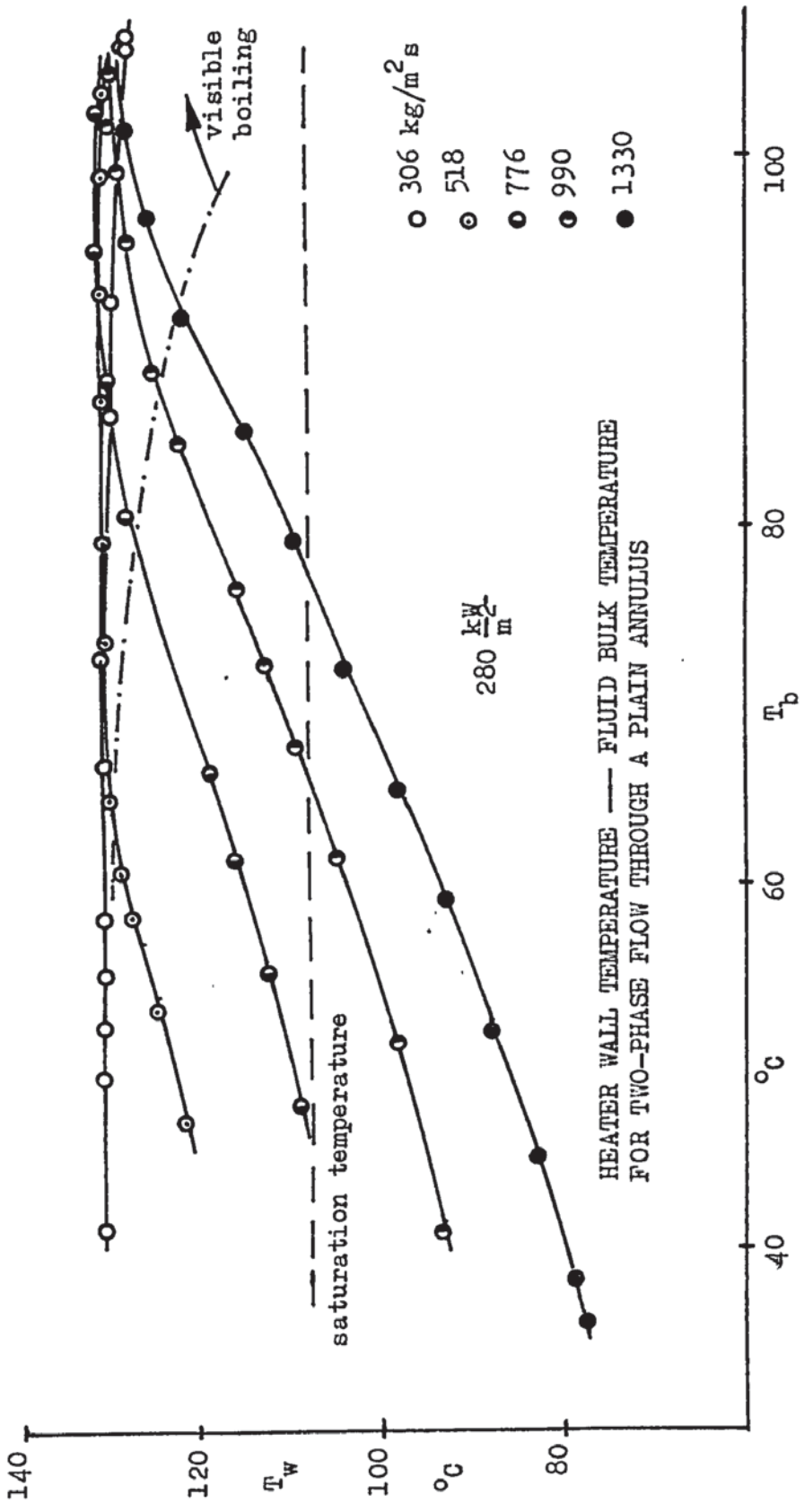
140
120
100
80
T_w
°C
40
60
80
100
T_b
°C
visible boiling
saturation temperature
280 $\frac{kW}{m^2}$
306 kg/m²s
518
776
990
1330
HEATER WALL TEMPERATURE — FLUID BULK TEMPERATURE
FOR TWO-PHASE FLOW THROUGH A PLAIN ANNULUS

G 4.4

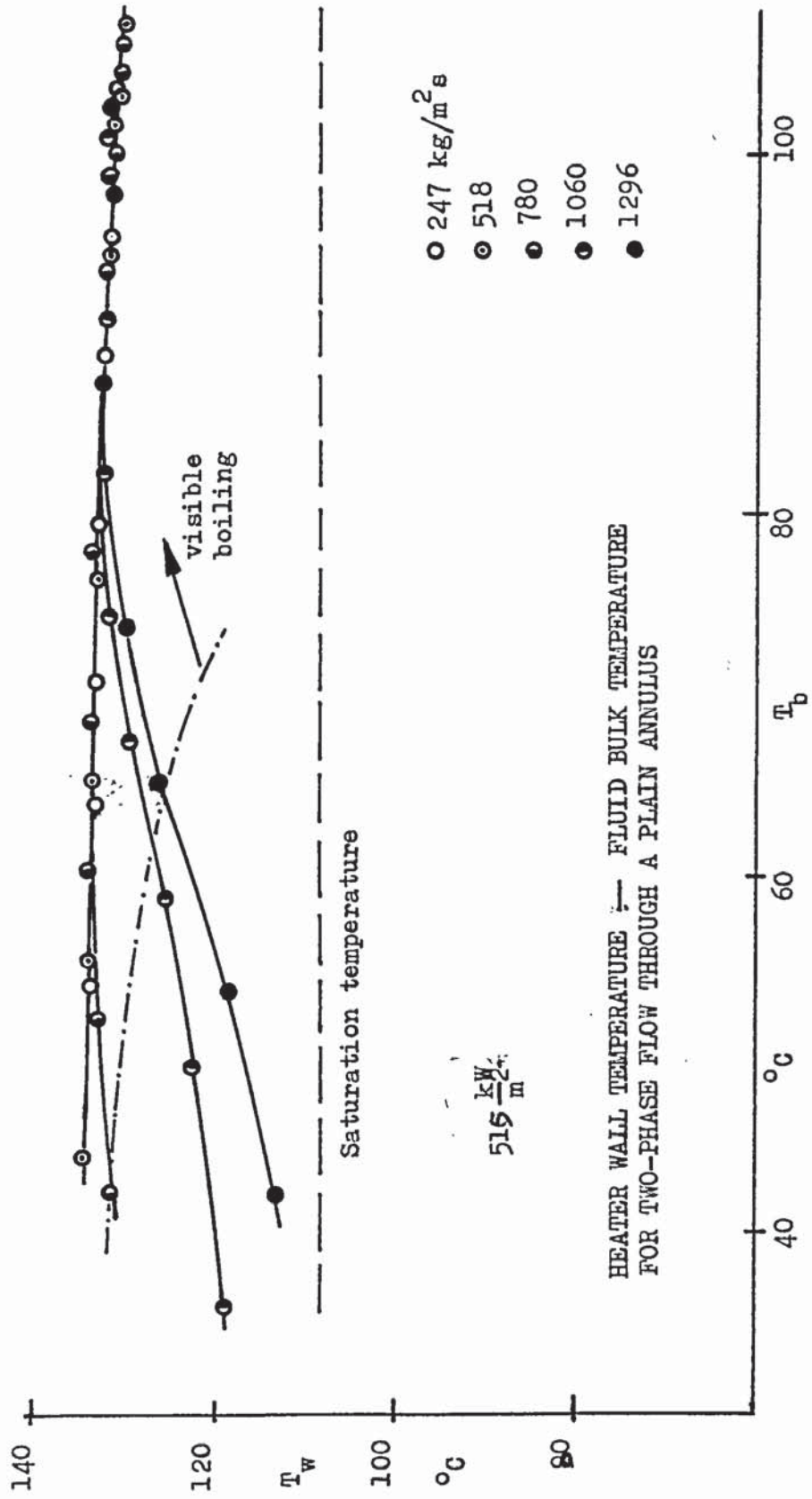

HEATER WALL TEMPERATURE ;— FLUID BULK TEMPERATURE
FOR TWO-PHASE FLOW THROUGH A PLAIN ANNULUS

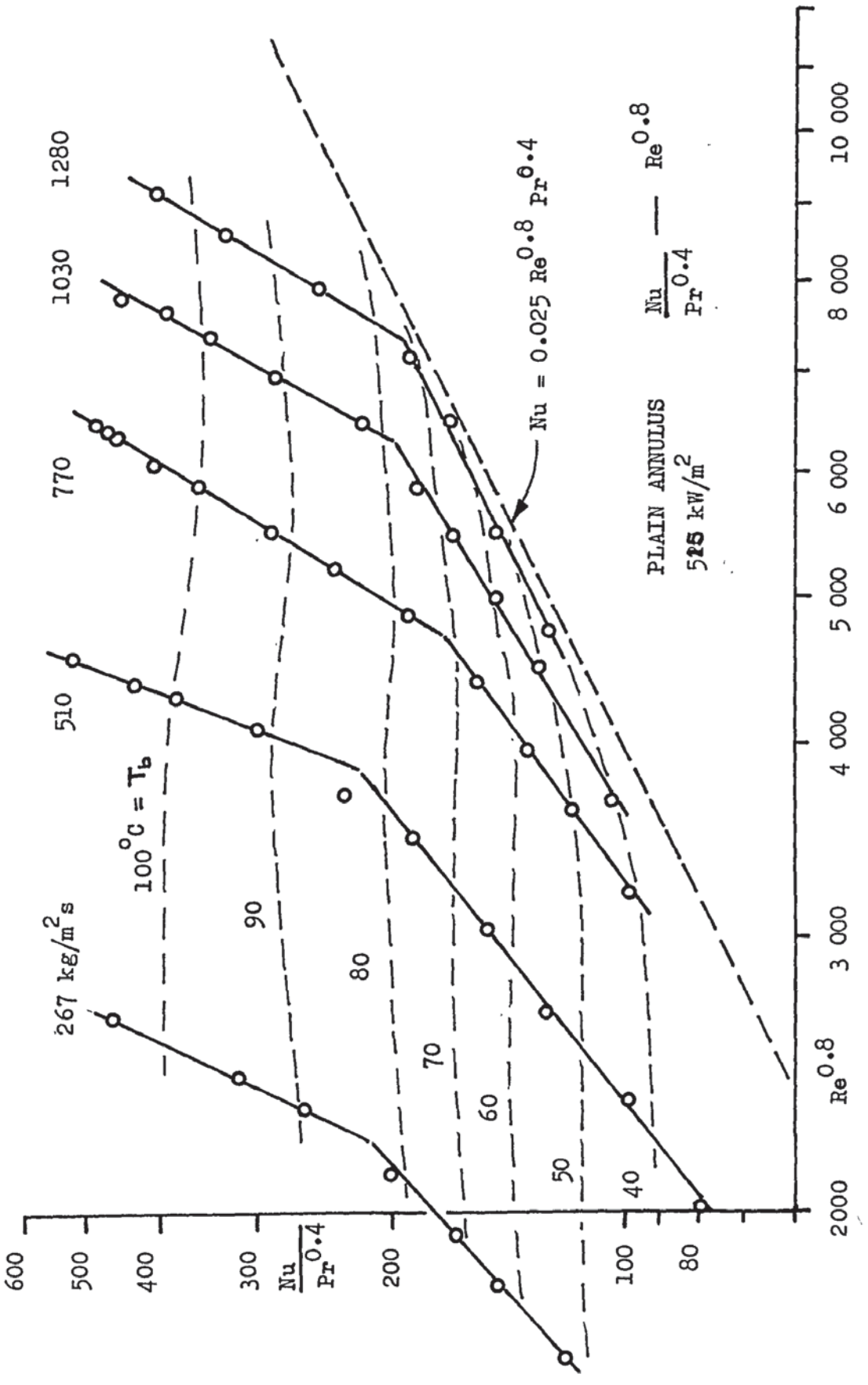
PLAIN ANNULUS
515 kW/m²
Nu = 0.025 Re^0.8 Pr^0.4
Nu/Pr^0.4 — Re^0.8
267 kg/m²s
510
770
1030
1280
100°C = Tb
90
80
70
60
50
40
Nu/Pr^0.4
Re^0.8
600
500
400
300
200
100
80
2000
3 000
4 000
5 000
6 000
8 000
10 000

G 4.6

4.4 SINGLE AND TWO-PHASE TESTS WITH WATER FLOWING THROUGH AN ANNULUS WITH A HEATED INNER WALL AND A STEP REDUCTION IN SECTION.

INTRODUCTION.

Considering a smooth reduction in diameter of an annular flow channel, the fundamental flow pattern of the fluid would be as drawn, D 4.2, and since no re-expansion occurs then the pressure losses would be minimal. The heat transfer coefficient for the inner wall to the fluid could be expected to increase smoothly from the value in the large section to that in the small section.

If however the reduction in diameter is abrupt then it could be expected that a vena contracta would be present downstream of the step in section and that since this would be followed by an uncontrolled divergence then an additional pressure loss would occur and also an improvement in the heat transfer coefficient would be expected to exist in this length of channel at the vena contracta and just beyond.

PROCEDURE.

Tests were carried out with water flowing upwards through a step reduction in flow section, D 4.3, both for single phase and boiling conditions, additionally a careful pressure traverse, D 3.24, G 4.13, was taken along the axis of the test section without heating. Four different flow rates were used and for each one a test was performed for a number of constant water inlet temperatures.

The outside wall temperature of the heating tube was calculated from the inside temperature as measured by the radiation thermocouple probe. The temperature of the bulk fluid was calculated from the measured temperature at inlet to the test section and the measured heat release to the water up to the measuring point on the axis of the test section.

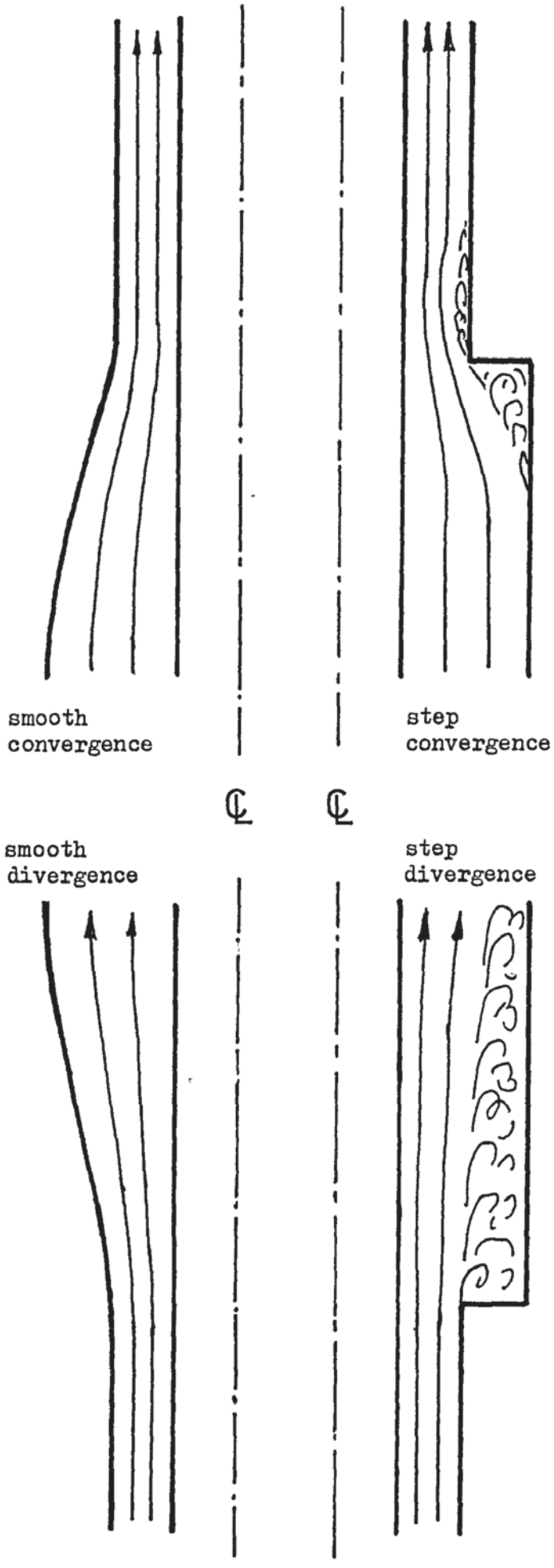

BASIC FLUID FLOW PATTERN IN AN ANNULUS WITH A SMOOTH/STEP CHANGE IN SECTION

1/4 FULL SIZE

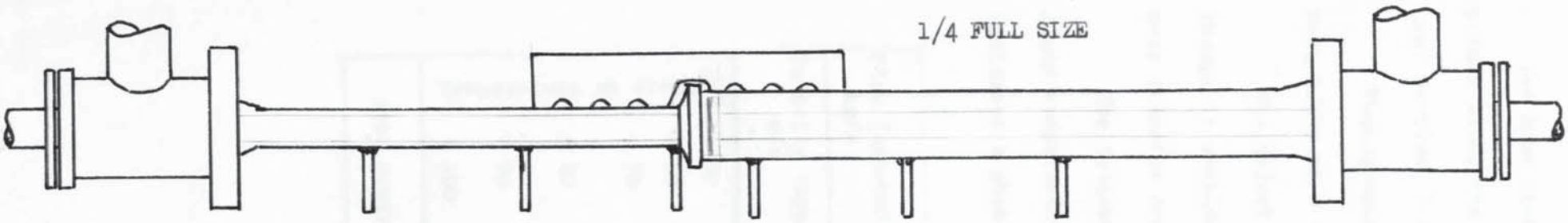

TEST SECTION ($1\frac{1}{2}$"/1" glass tube with $\frac{3}{4}$" heating element)
Tube clamps ommitted, and only one stiffening rib shown

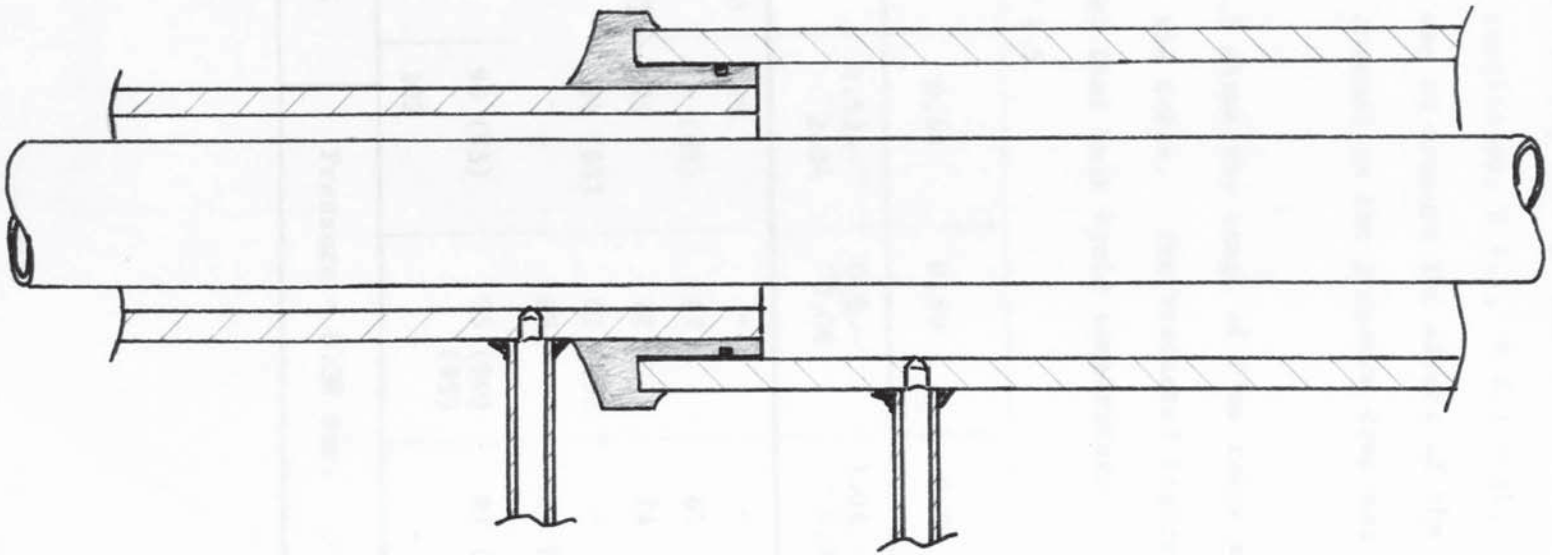

SECTION THROUGH THE STEPPED ANNULUS - FULL SIZE

D 4.3

The heat transfer coefficient was calculated at a number of points along the axis and plotted against axial distance along the test section, D 4.4, G 4.7 - 12.

Photographs of the water flowing through the test section were taken at a range of test conditions, D 4.5, P 4.1 - 11.

The object of the tests was to measure the effect of the step change in section of the flow channel on the pressure drop and the heat transfer coefficient.

The following table T 4.5 shows the range of flow rates and fluid temperatures covered by the tests. The bracketed figure indicates a photograph taken at that bulk fluid temperature.

T 4.5

Flow (approx) kg/s		0.22	0.44	0.66	0.88
Velocity (approx) m/s		0.27 / 1.02	0.53 / 2.04	0.8 / 3.06	1.06 / 4.08
Temperature at step, °C	+ 50	- (54)	59	-	-
	+ 60	68	- (65)	67	61
	+ 70	76 (75)	75	72	74
	+ 80	- / 87	84 (85) / -	82 (80) / 88	- / 87 (85)
	+ 90	- (90)	90 (95)	95 (90) (95)	97 (93)
	+ 100	-	102	-	-
Area contraction 1:3.86			Pressure = 0.38 bar.		

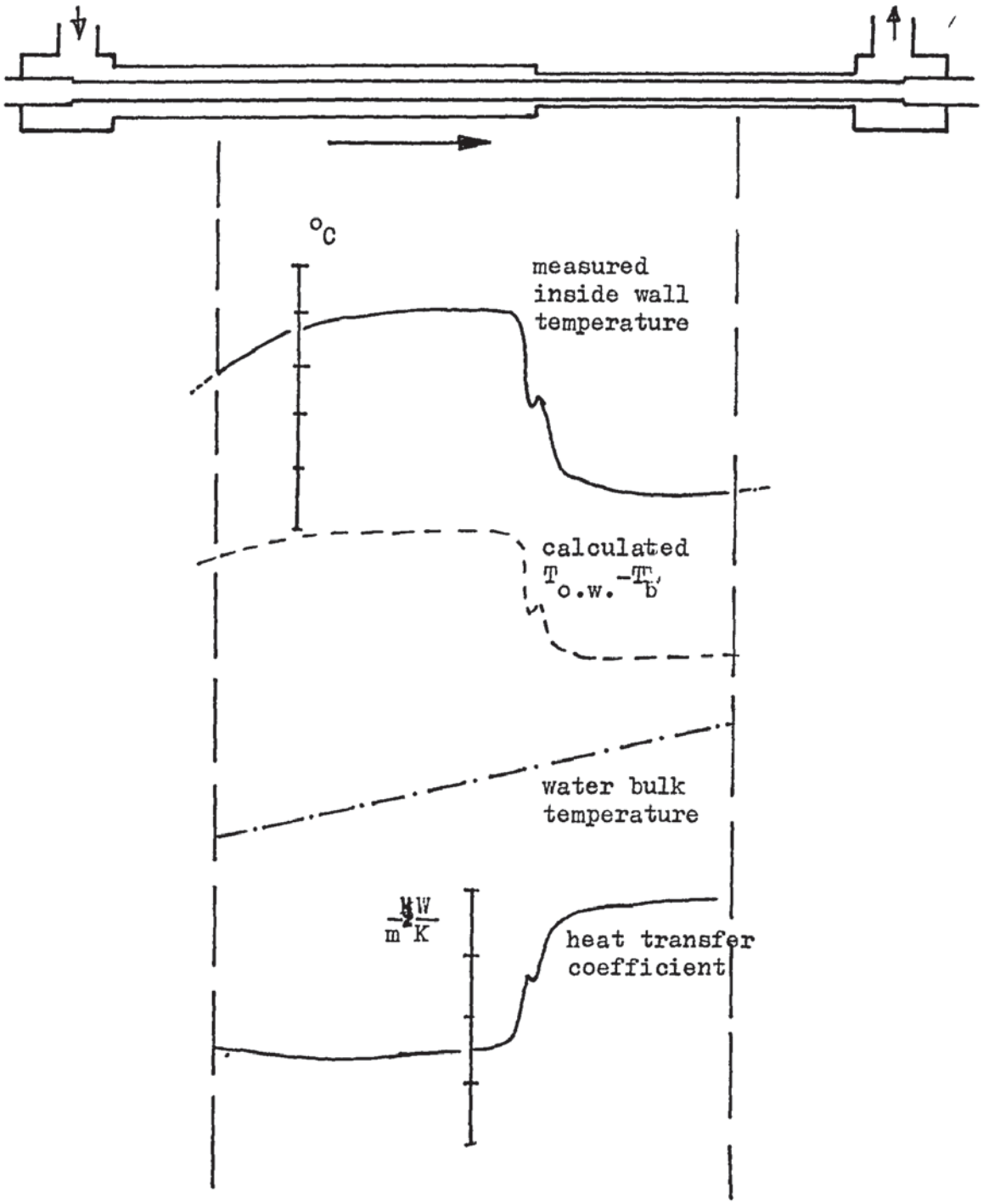

GRAPHICAL PRESENTATION OF RESULTS

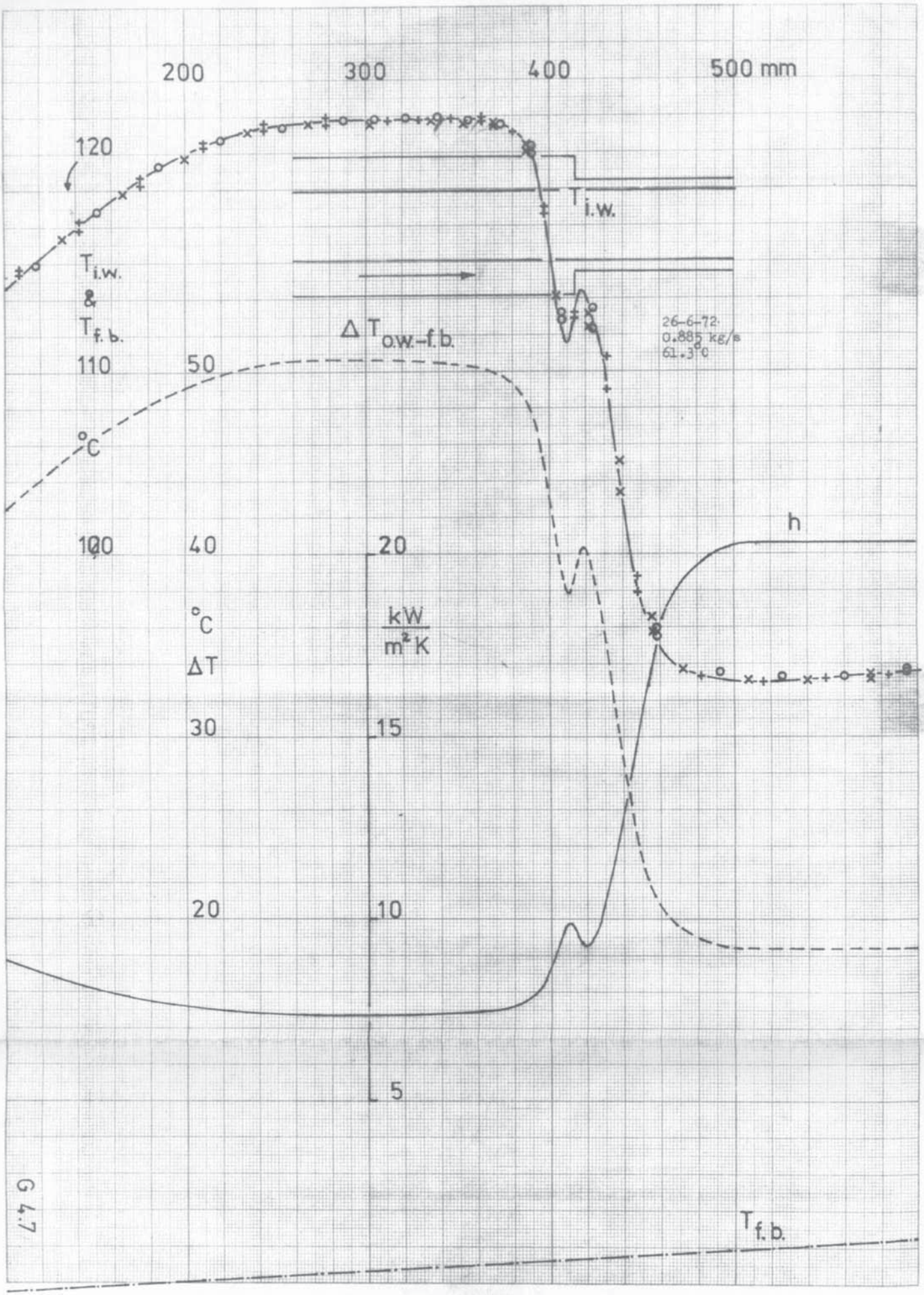
200
300
400
500 mm
120
$T_{i.w.}$
$T_{i.w.}$ & $T_{f.b.}$
110
°C
$\Delta T_{o.w.-f.b.}$
50
26-6-72
0.885 kg/s
61.3°C
100
40
°C
ΔT
30
20
20
$\frac{kW}{m^2 K}$
15
10
5
h
$T_{f.b.}$
G 4.7

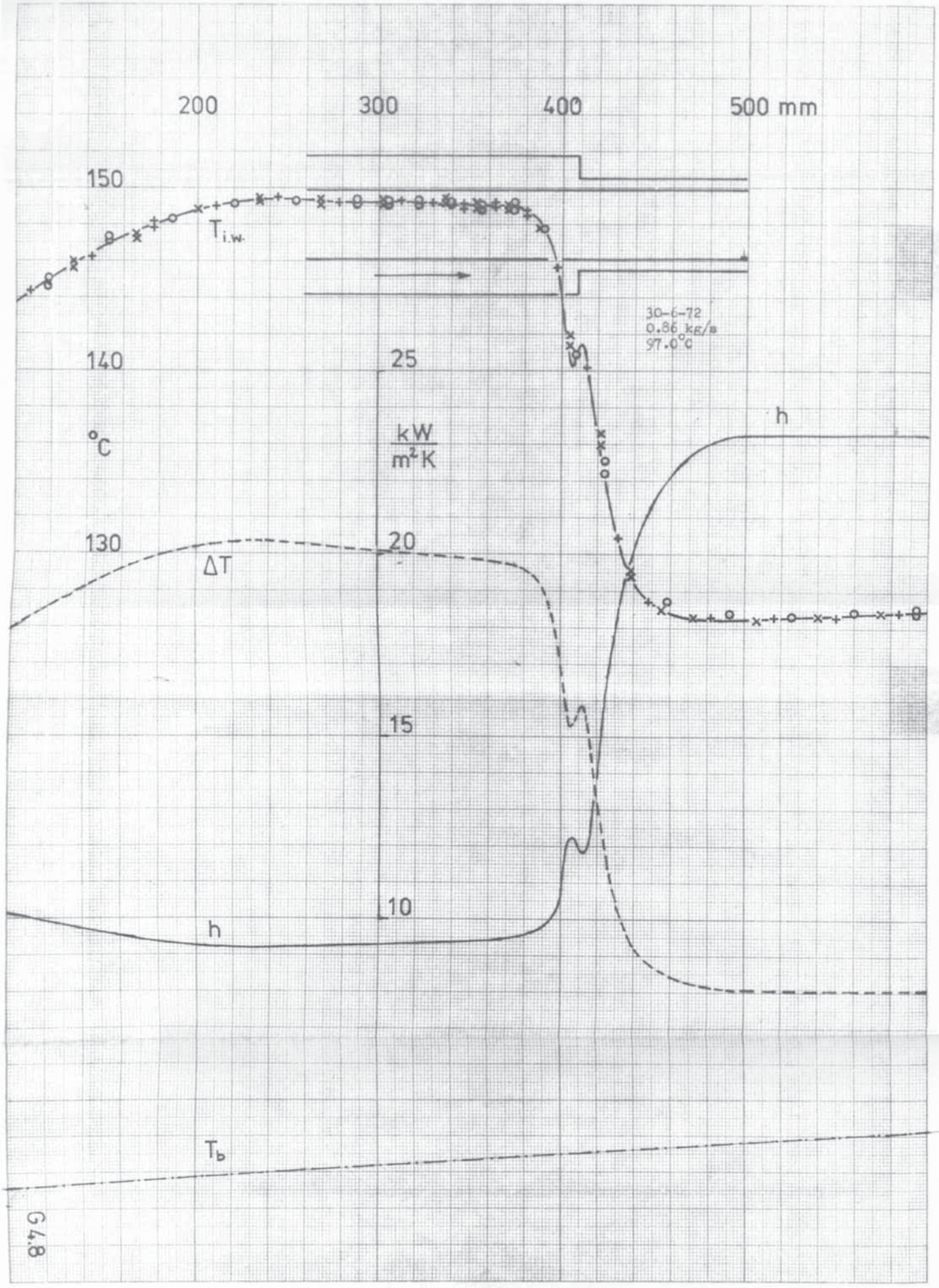
200
300
400
500 mm
150
140
130
°C
$T_{i.w.}$
30-6-72
0.86 kg/s
97.0°C
25
20
15
10
$\frac{kW}{m^2K}$
h
ΔT
h
T_b
G 48

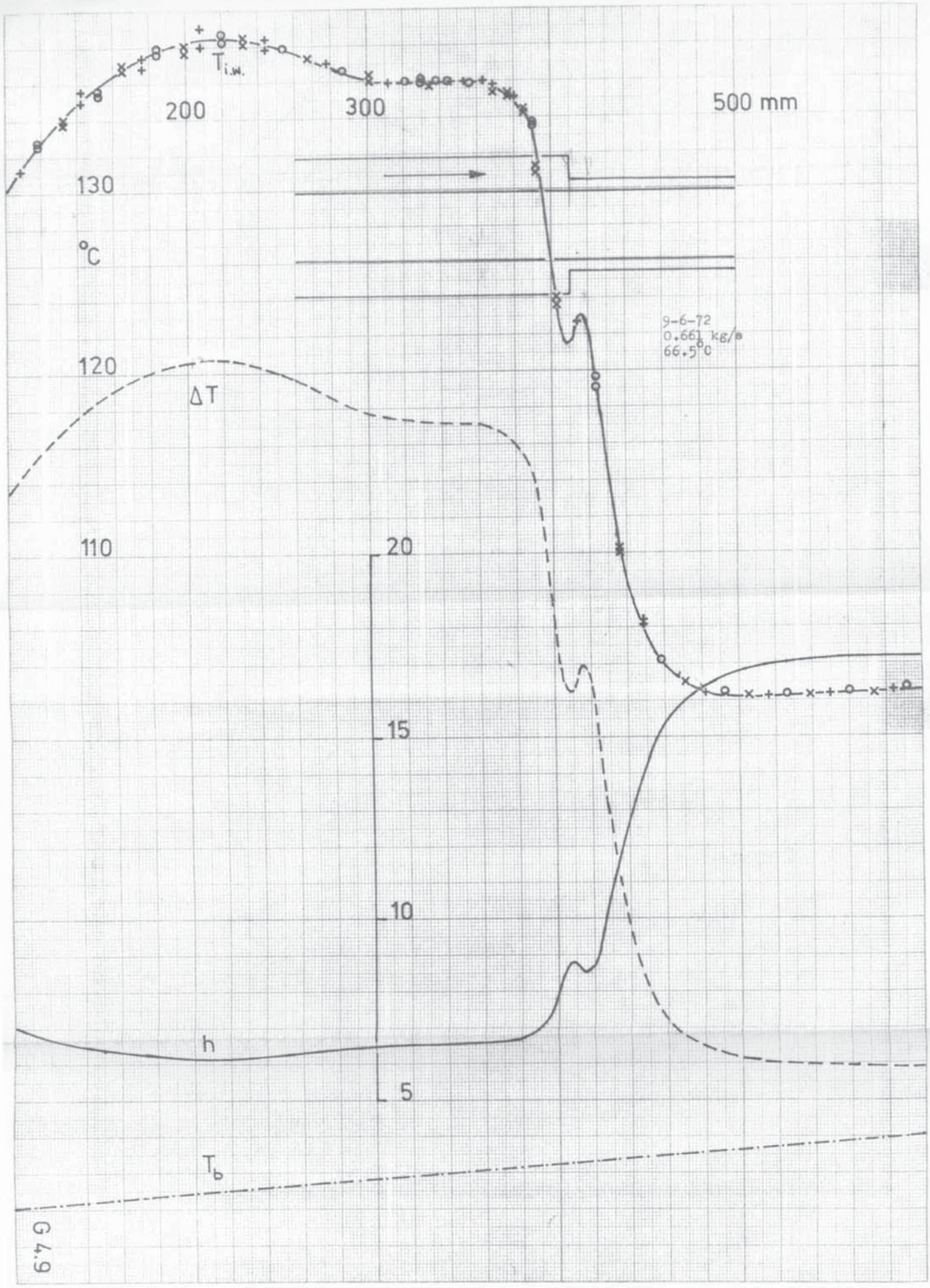
$T_{i.w.}$
200
300
500 mm
130
°C
120
ΔT
110
9-6-72
0.661 kg/s
66.5°C
20
15
10
5
h
T_b
G 4.9

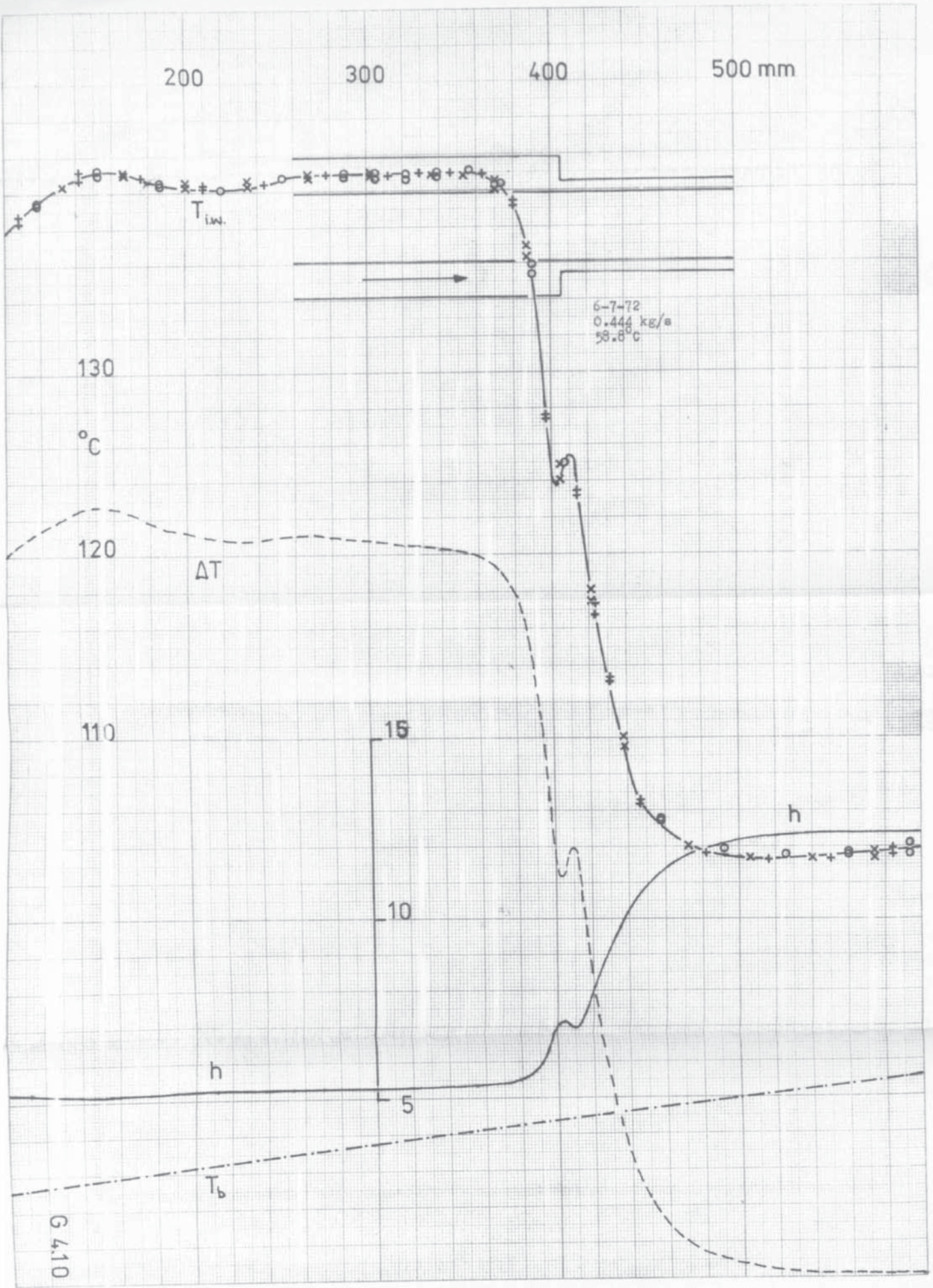
200
300
400
500 mm
$T_{i.w.}$
6-7-72
0.444 kg/s
58.8°C
130
°C
120
ΔT
110
15
10
5
h
h
T_b
G 4.10

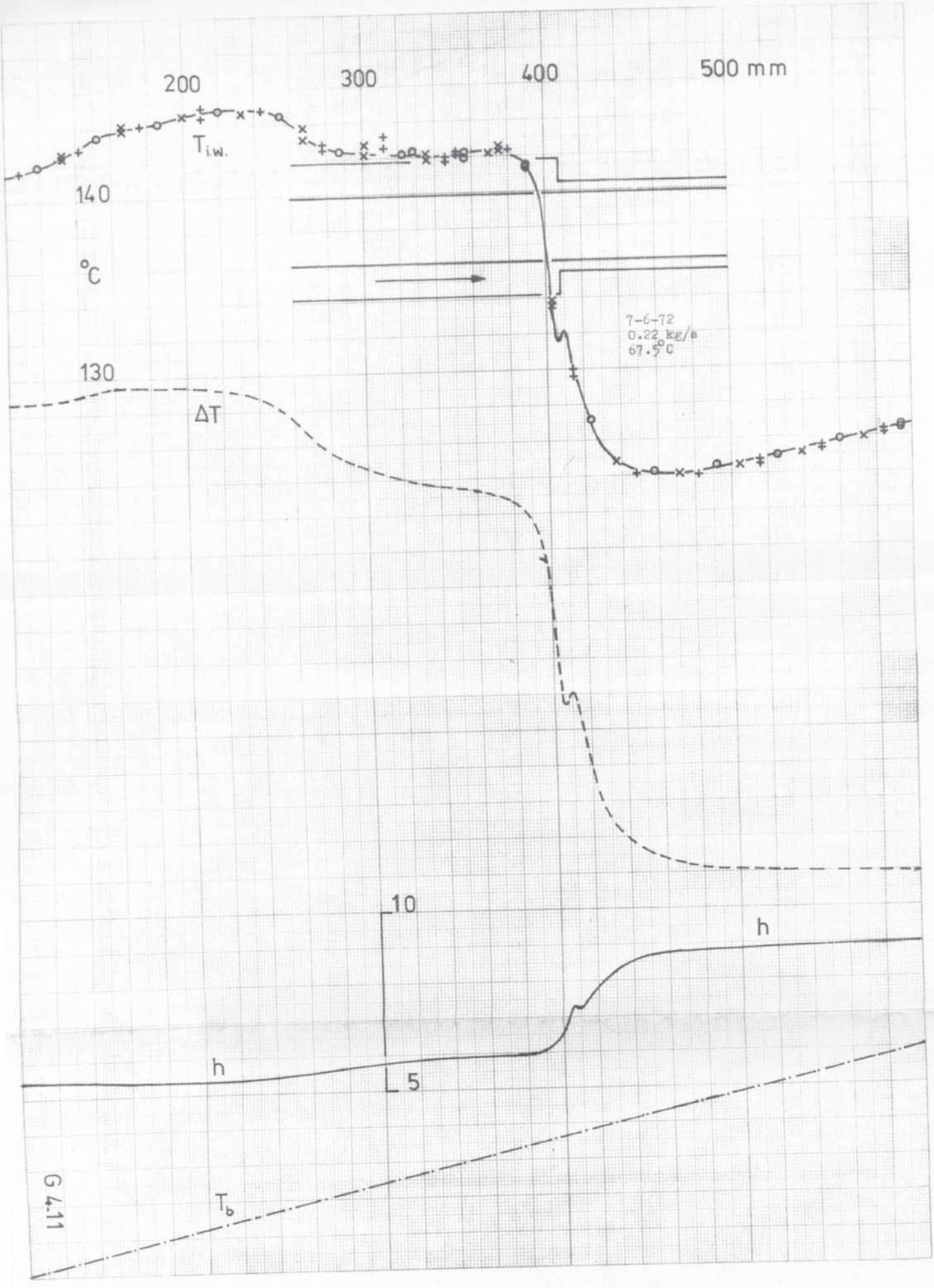
200
300
400
500 mm
$T_{i.w.}$
140
°C
130
ΔT
7-6-72
0.22 kg/s
67.5°C
10
5
h
h
T_b
G 4.11

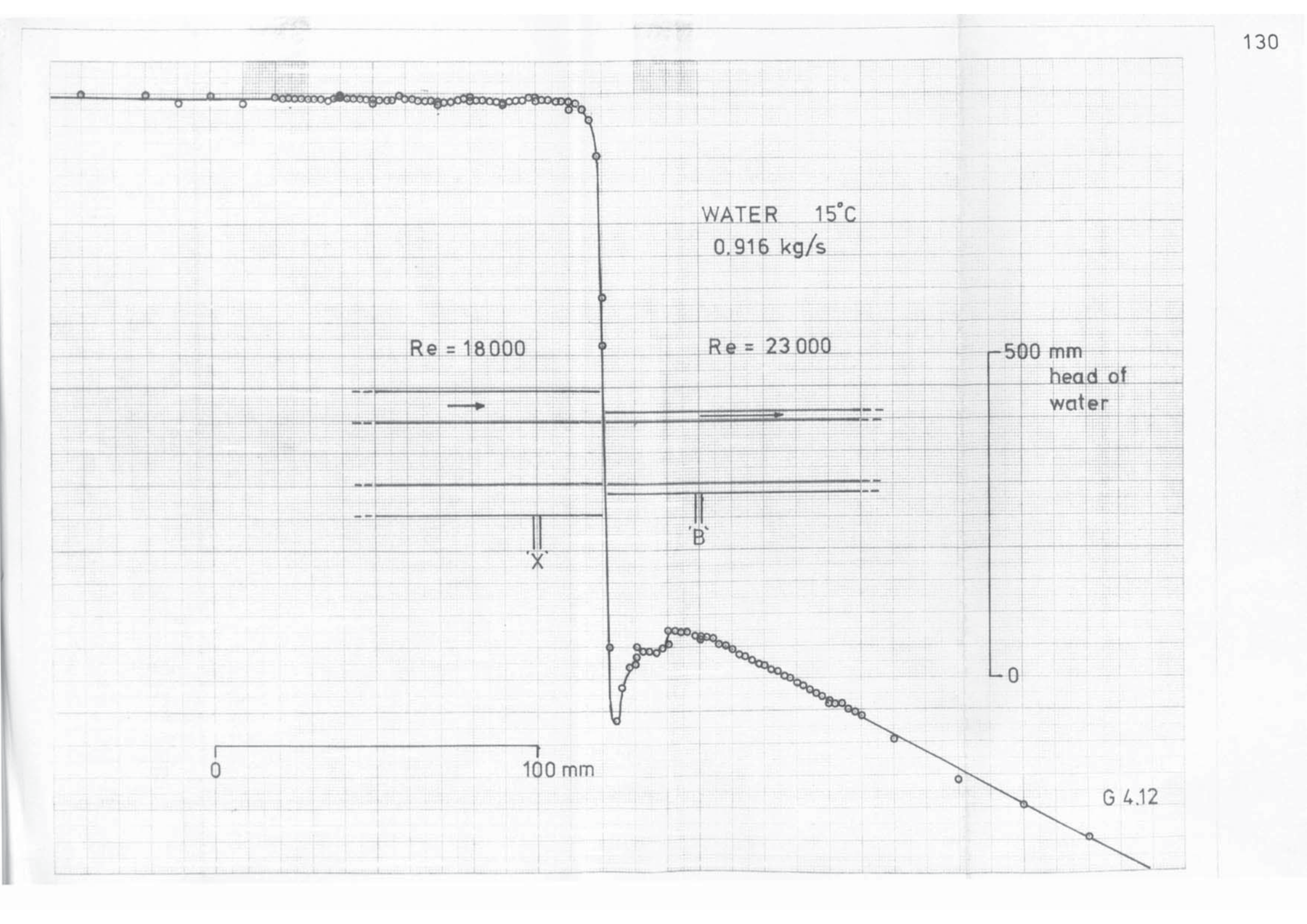
WATER 15°C
0.916 kg/s
Re = 18000
Re = 23000
500 mm
head of
water
0
'X'
'B'
0
100 mm
G 4.12

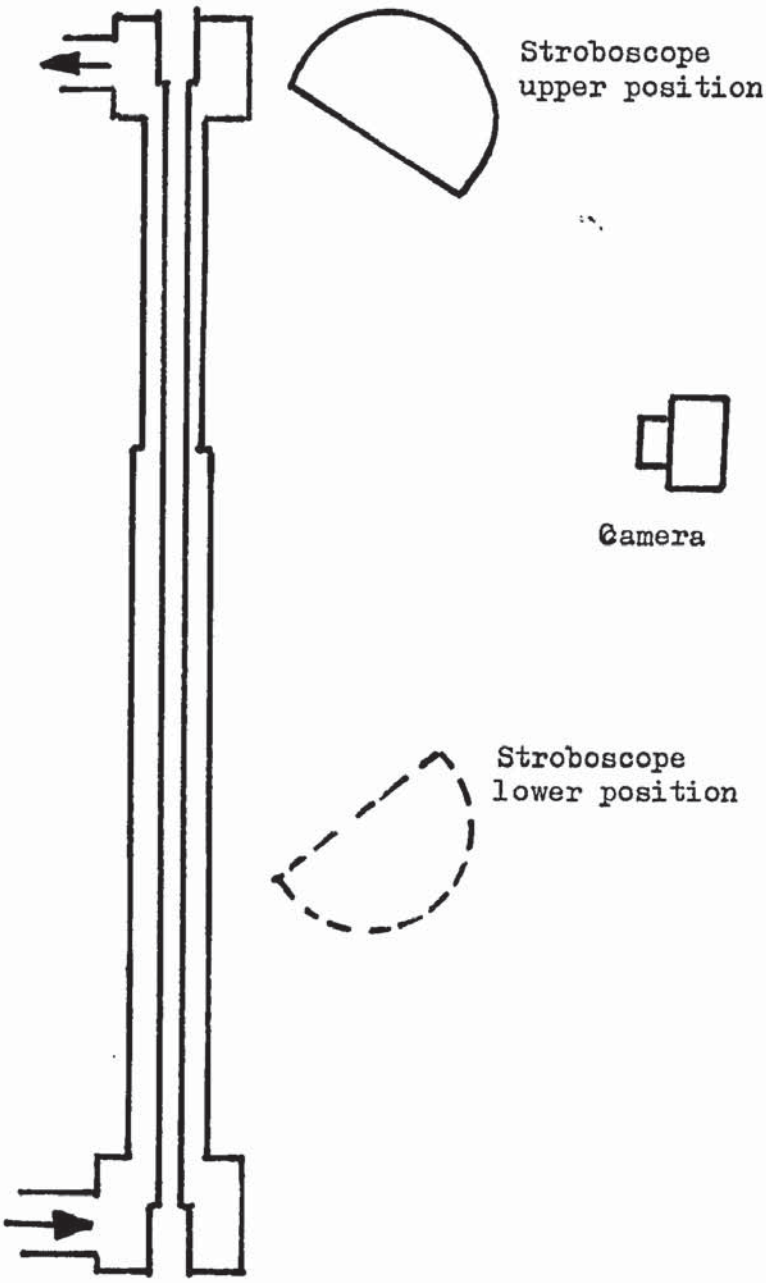

Two exposures taken at each flow rate and water inlet temperature

Kodak Tri-X 35mm film, f 11, 1/25 s.

Patersons Acuspeed developer, 6 min.

Dawe stroboscope Model 120 3 B

0.86 kg/s 93°C

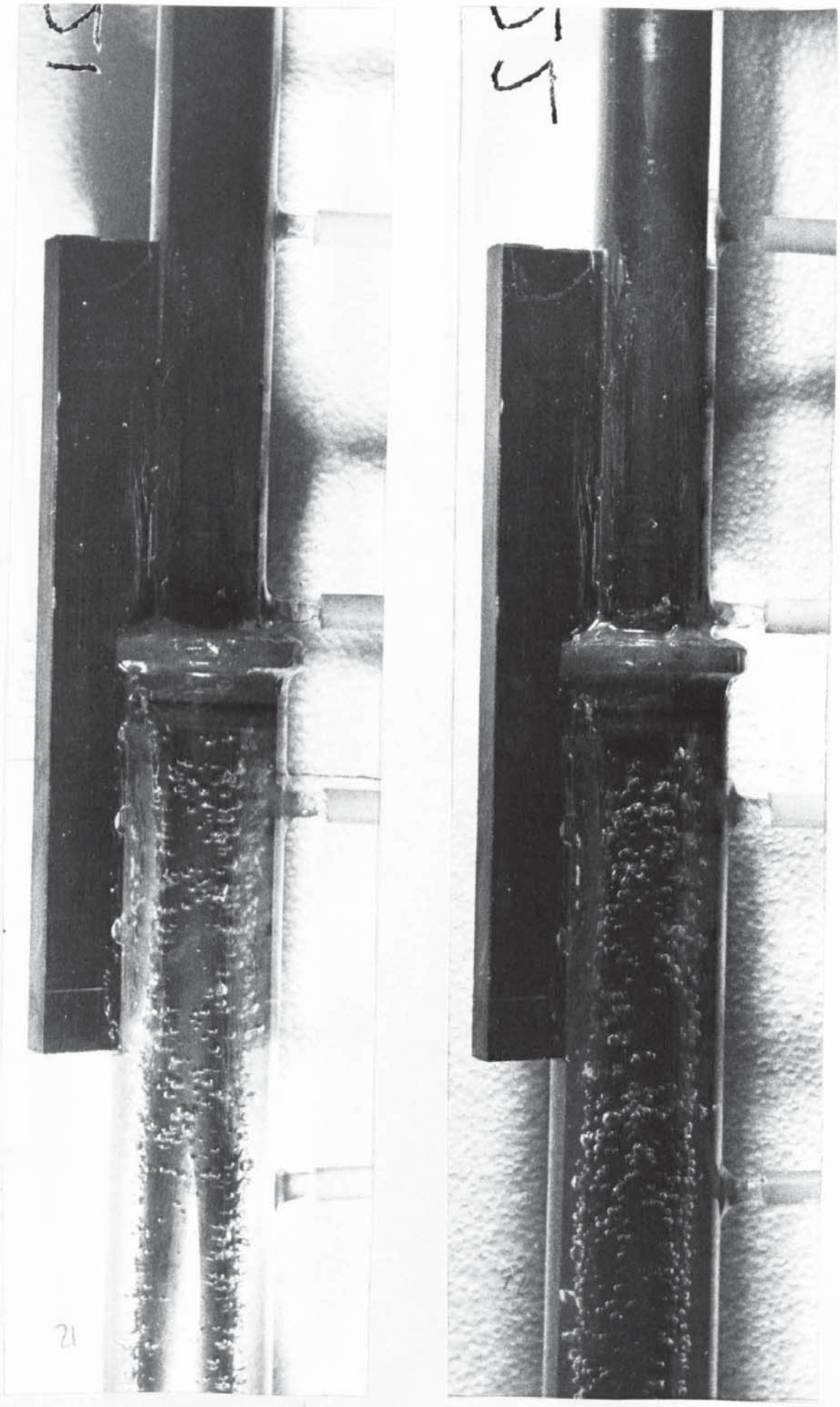

P 4.1

0.87 kg/s 85°C

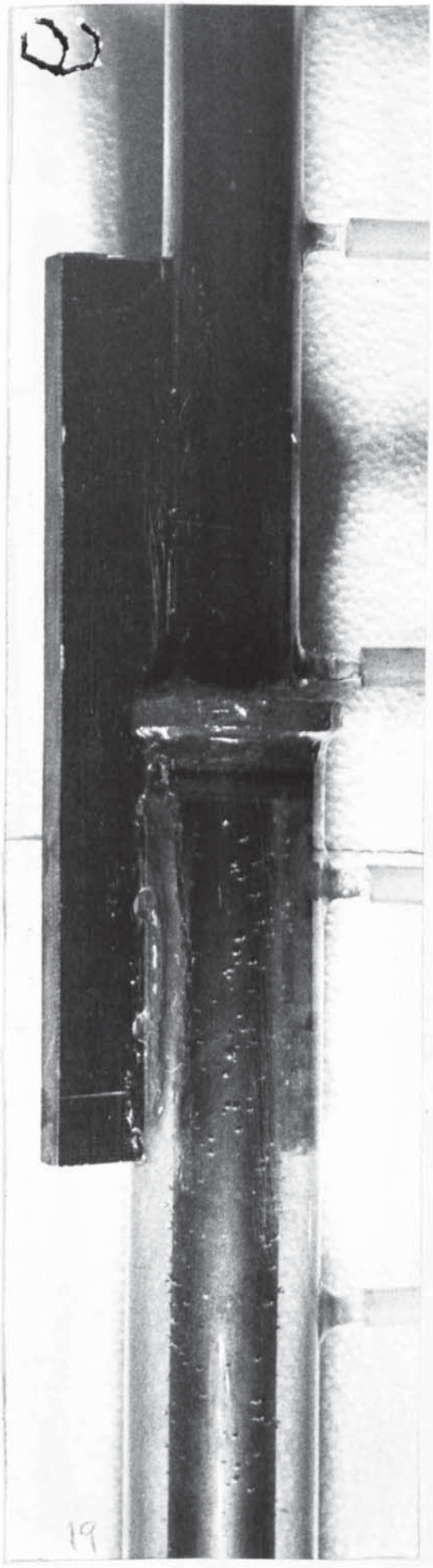

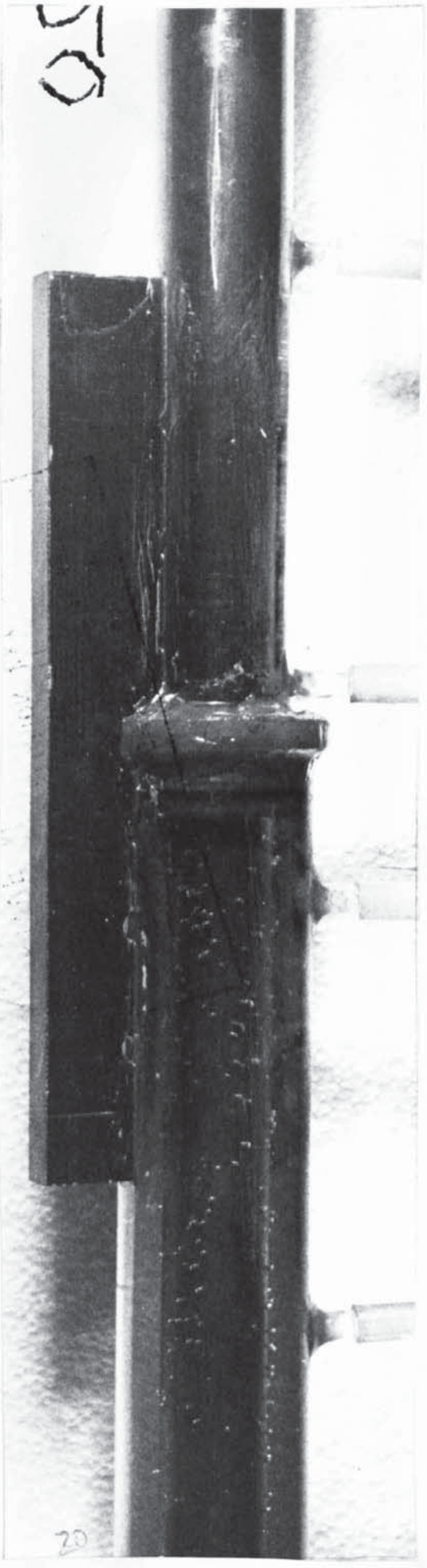

0.65 kg/s 95°C

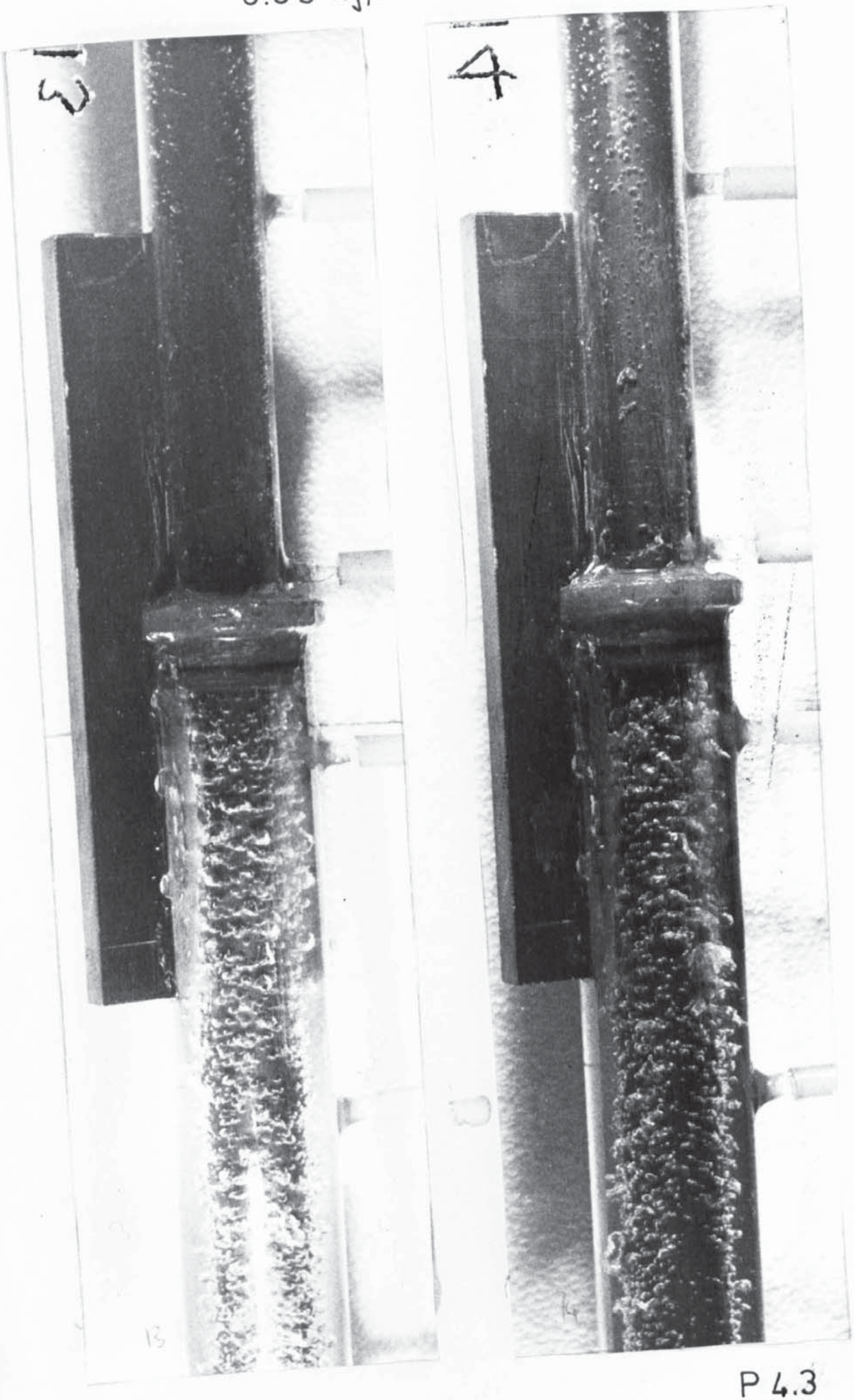

P 4.3

0.66 kg/s 90°C

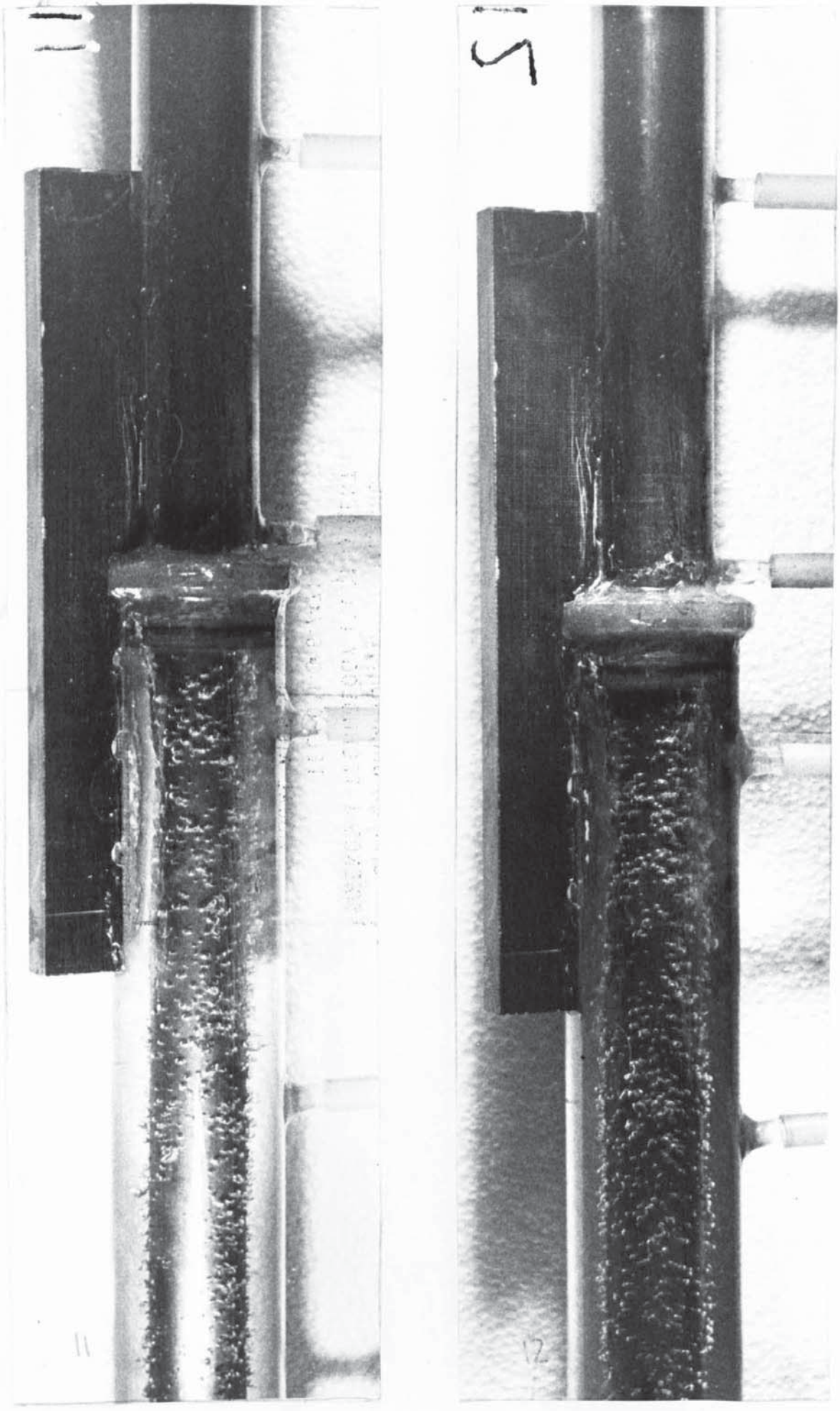

P 4.4

0.66 kg/s 80°C

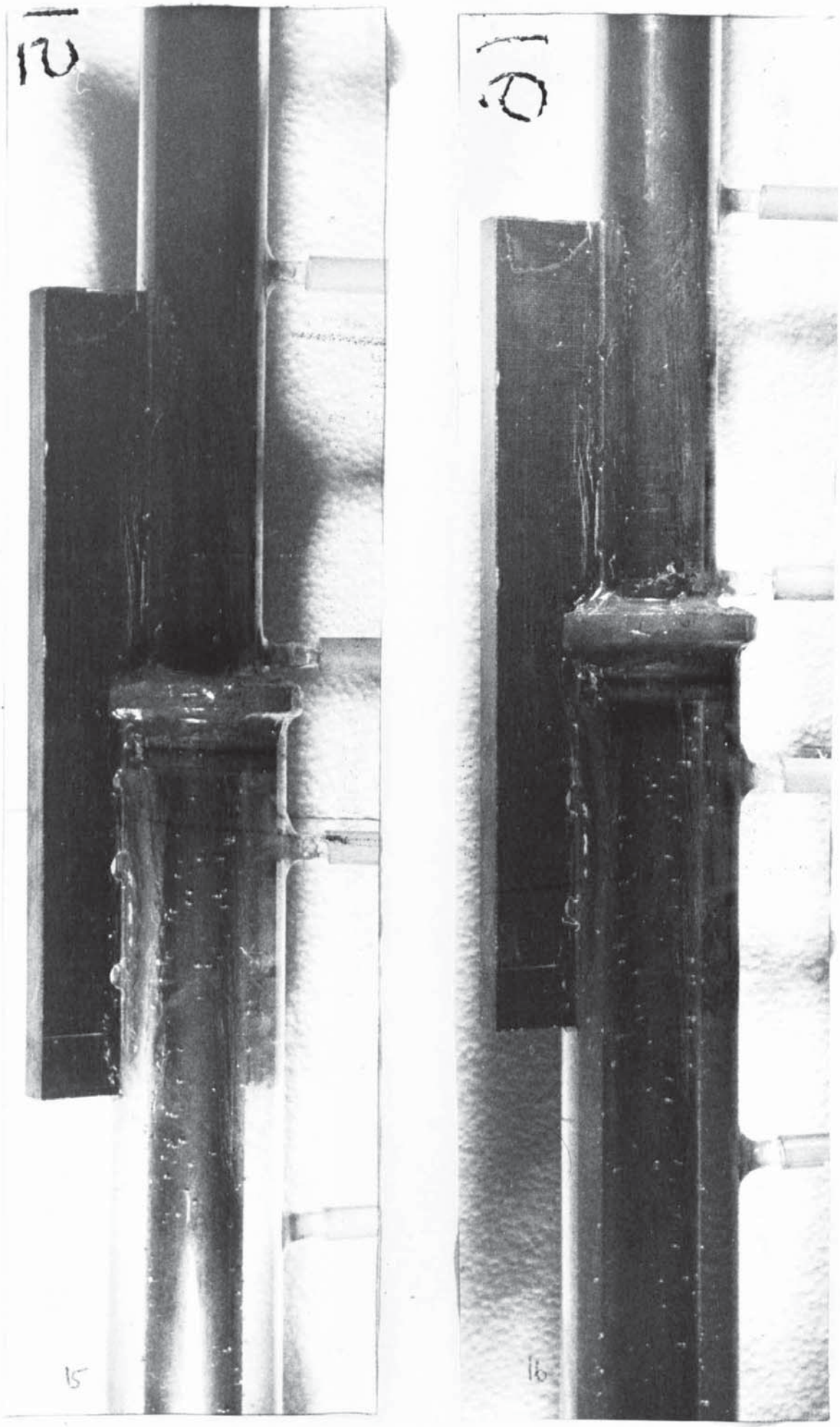

P 4.5

0.43 kg/s 95°C

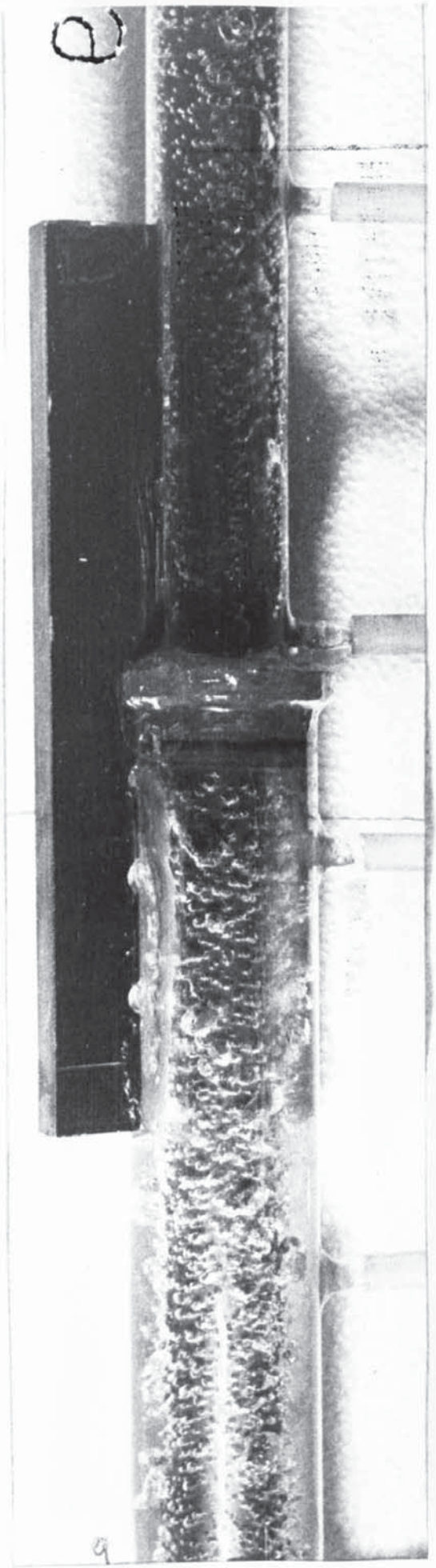

P 4.6

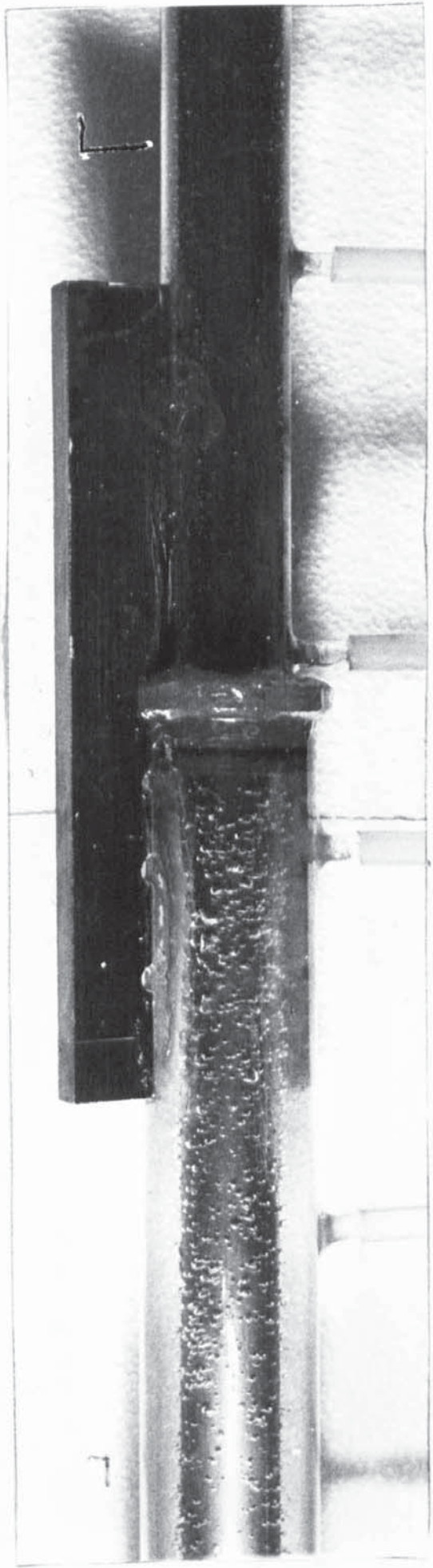

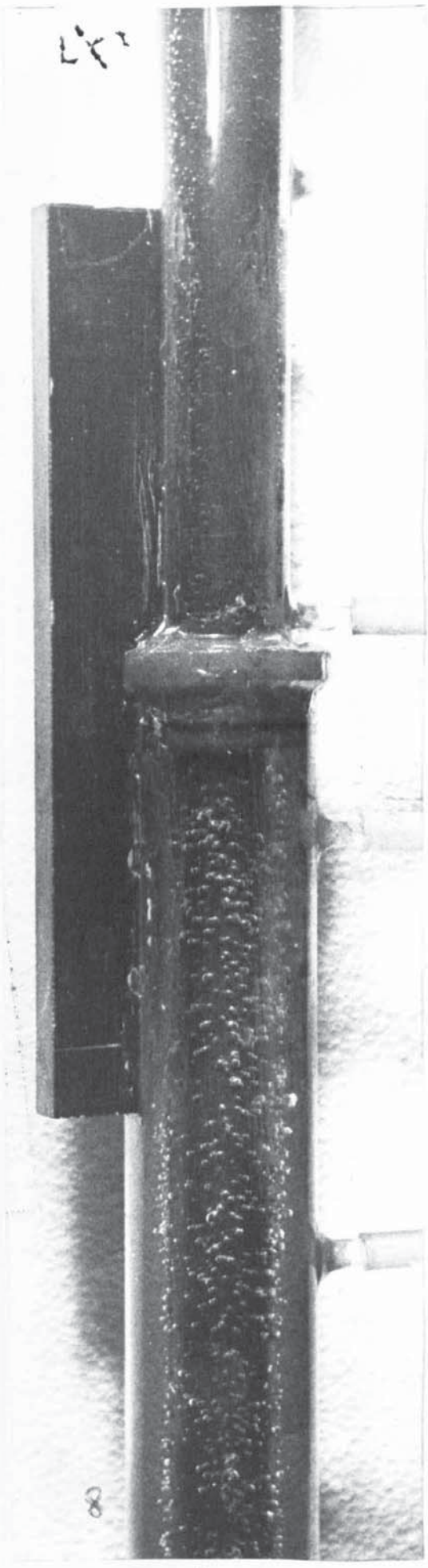

P 4.7

0.44 kg/s 65°C

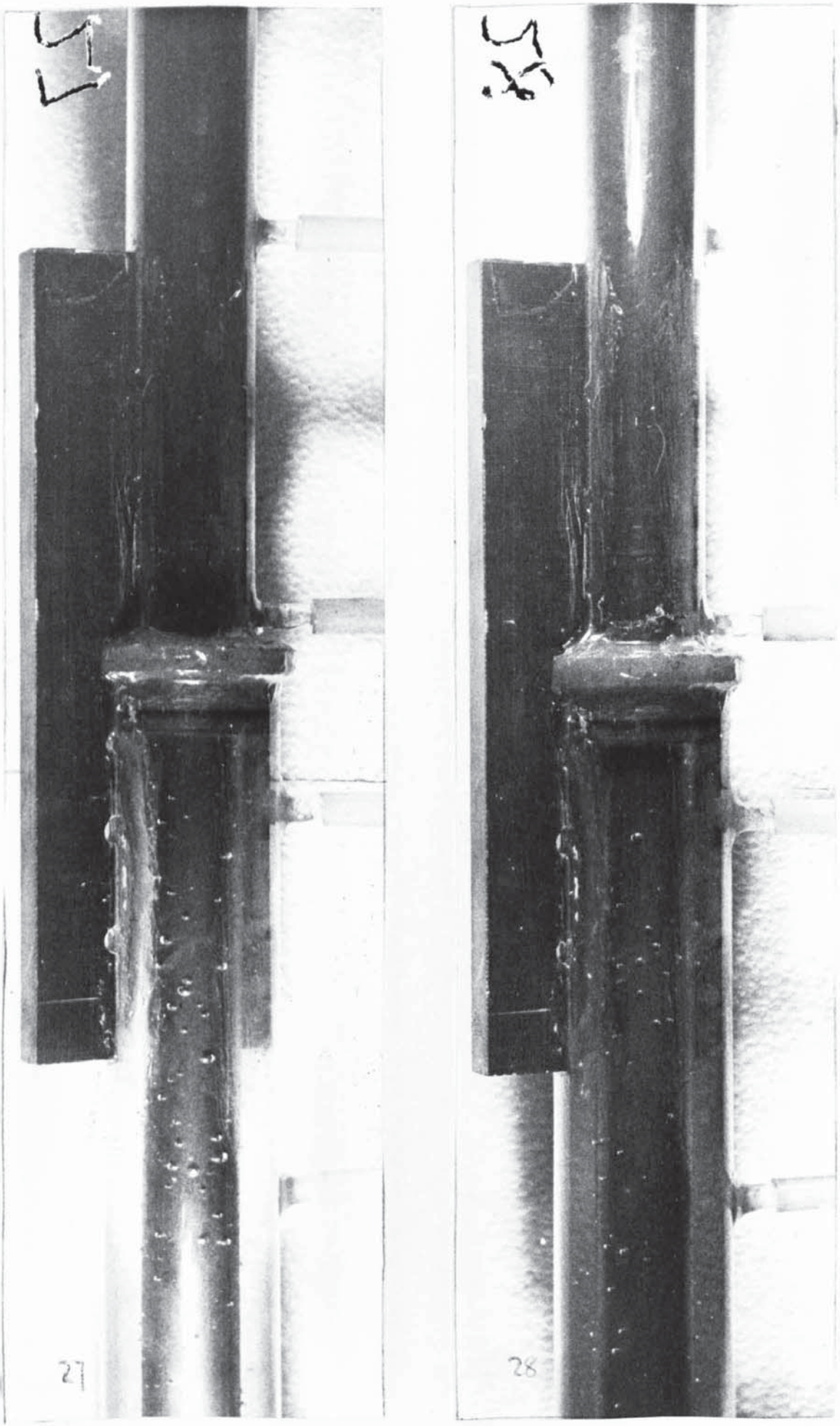

P 4.8

0.21 kg/s 90°C

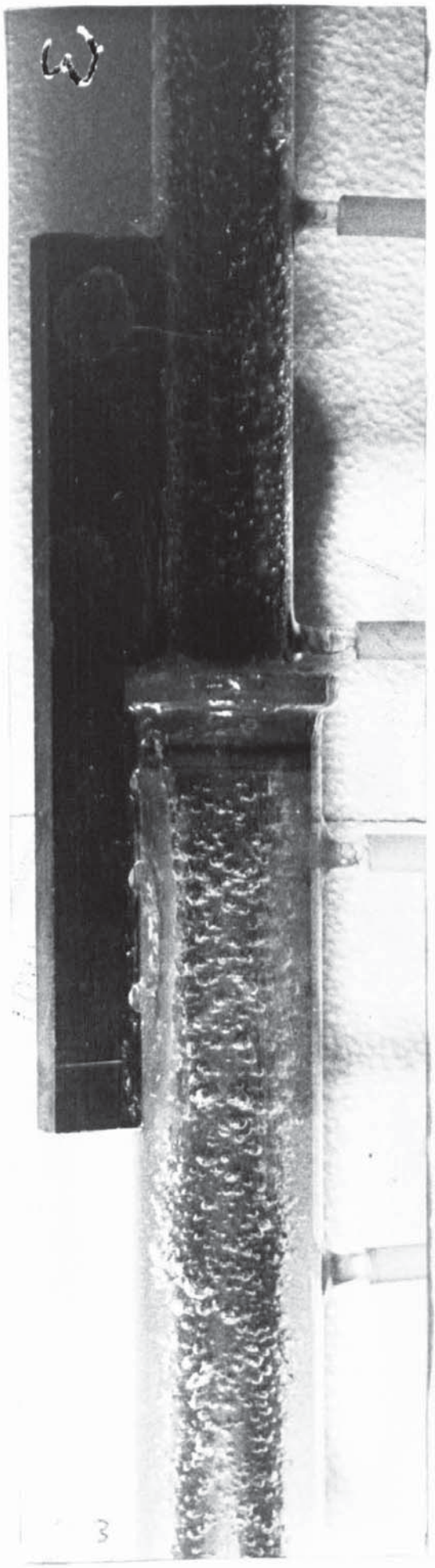

P 4.9

0.22 kg/s 75°C

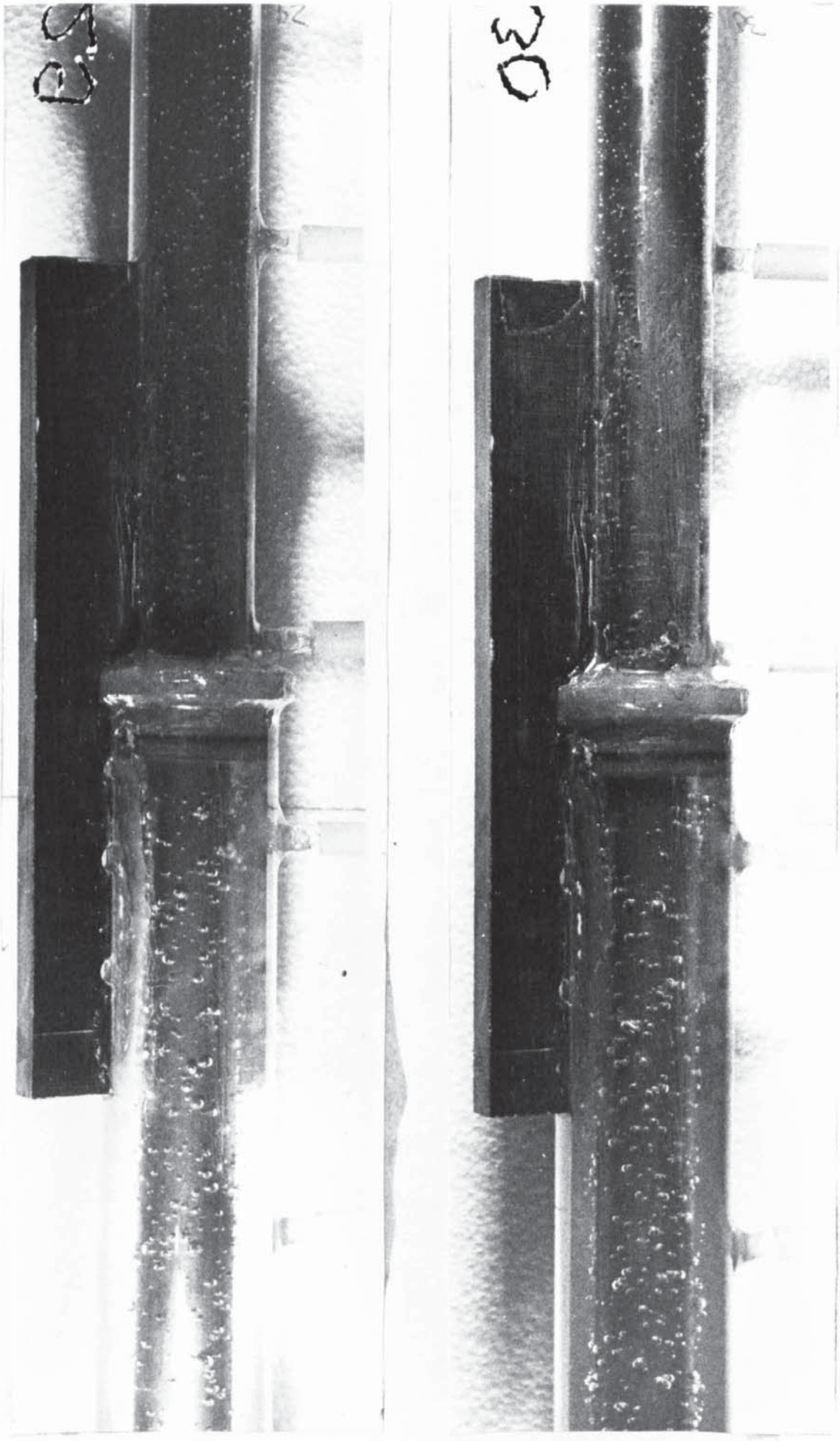

P 4.10

0.22 kg/s 54°C

4.5 SINGLE AND TWO PHASE TESTS WITH WATER FLOWING THROUGH AN ANNULUS WITH A HEATED INNER WALL AND A STEP INCREASE IN SECTION.

INTRODUCTION.

If a smooth transition from one flow section to a larger section were possible then the fundamental flow pattern of the fluid would be as drawn, D 4.2. The heat transfer coefficient would reduce smoothly from the value in the small section to that in the larger section. If the change in section was abrupt then a secondary flow pattern would be present which could alter the heat transfer coefficient.

PROCEDURE.

Tests were carried out with water flowing upwards through a step increase in flow section, both for single phase and boiling conditions, additionally a careful pressure traverse. D 3.24, G 4.19, was taken along the axis of the test section without heating. Four different flow rates were used and for each one a test was performed for a number of constant water inlet temperatures.

The outside wall temperature of the heating tube was calculated from the inside temperature as measured by the radiation thermocouple probe. The temperature of the bulk fluid was calculated from the measured fluid temperature at inlet to the test section and the measured heat release to the water up to the measuring point on the axis of the test section. The heat transfer coefficient was calculated at a number of points along the axis and plotted against axial distance along the test section, D 4.6, G 4.14-18.

Photographs of the water flowing through the test section were taken at a range of test conditions, D 4.5, P 4.12 - 22.

The object of the tests was to measure the effect of the step change in section of the flow channel on the pressure drop and the

heat transfer coefficient.

The following table T 4.6 shows the range of flow rates and fluid temperatures covered by the tests. The bracketed figure indicates a photograph taken at that bulk fluid temperature.

T 4.6

Flow (approx) kg/s		0.22	0.44	0.66	0.88
Velocity (approx) m/s		1.02 / 0.27	2.04 / 0.53	3.06 / 0.80	4.08 / 1.06
Temperature at step °C	+ 50°C	–	–	57	53
	+ 60°C	63 (67)	61	68	63
	+ 70°C	72	–	–	76
	+ 80°C	86 (81)	86 (86) (89)	81	86
	+ 90°C	94 (93)	98 (97)	95 (90) (95)	96 (93)
	+ 100°C		105	103 (101)	105 (100)

Area enlargement = 3.86:1 Pressure = 0.38 bar

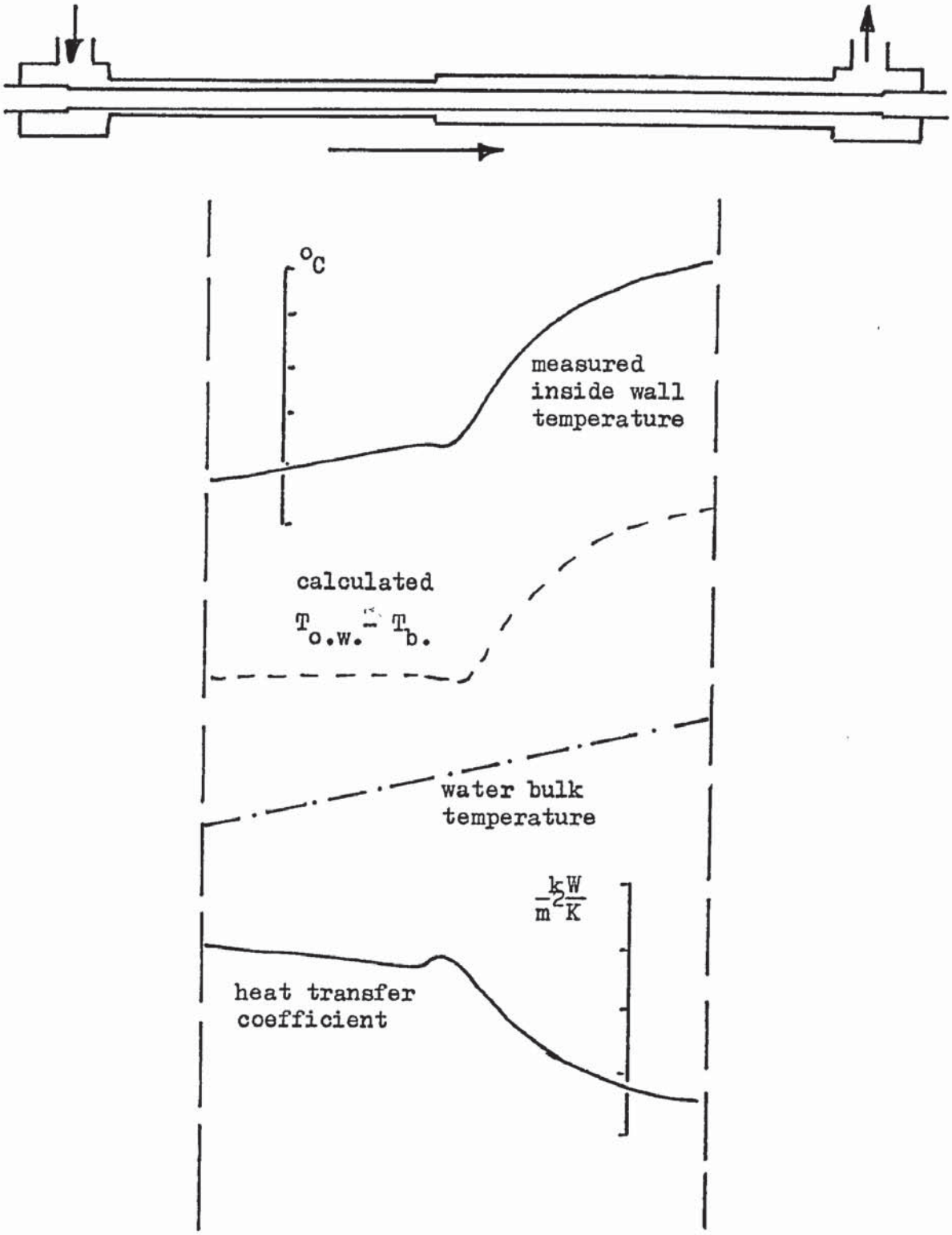

GRAPHICAL PRESENTATION OF RESULTS

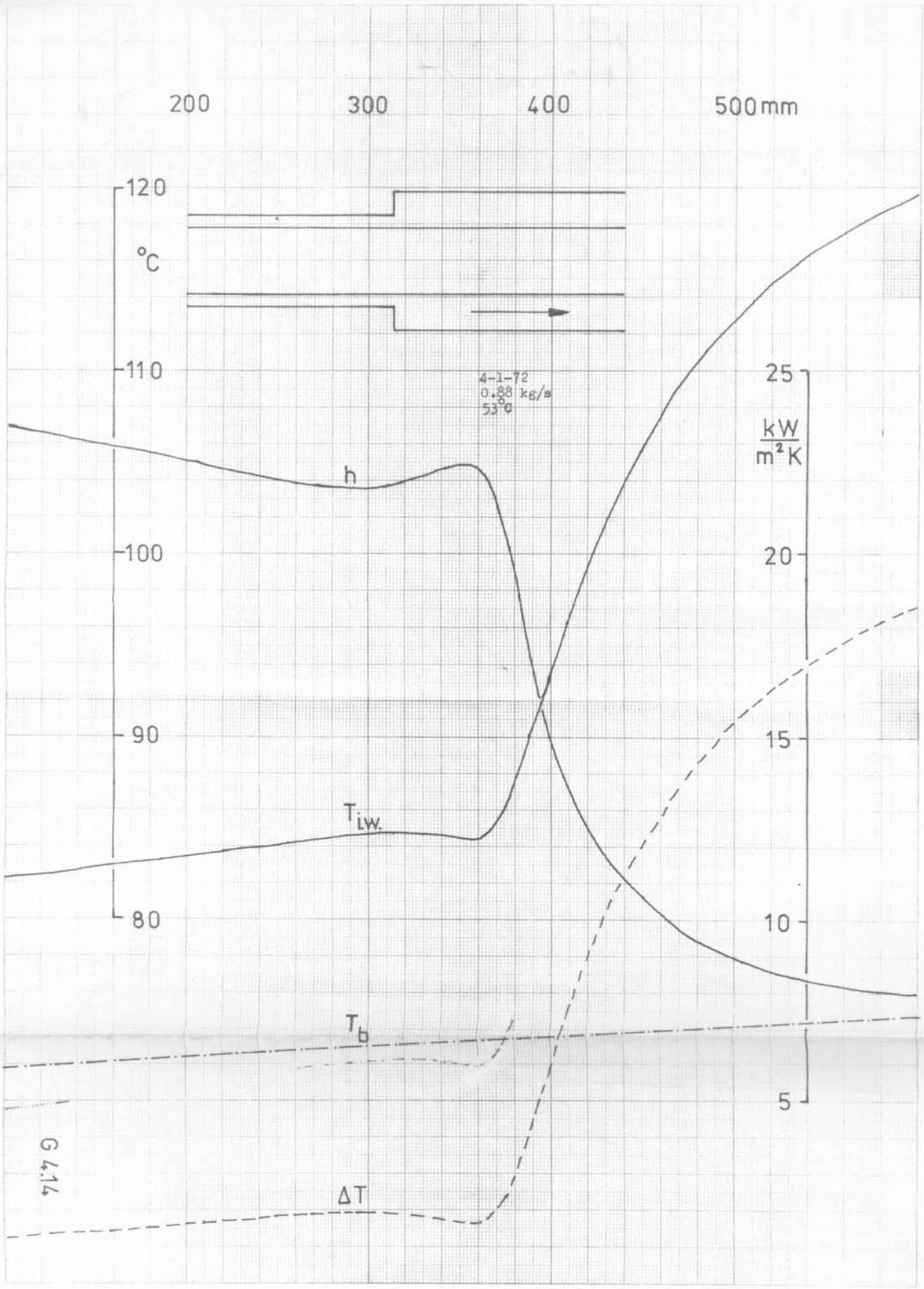
200
300
400
500 mm
120
°C
110
100
90
80
4-1-72
0.88 kg/s
53°C
h
$T_{iw.}$
T_b
ΔT
25
kW/m²K
20
15
10
5
G 4.14

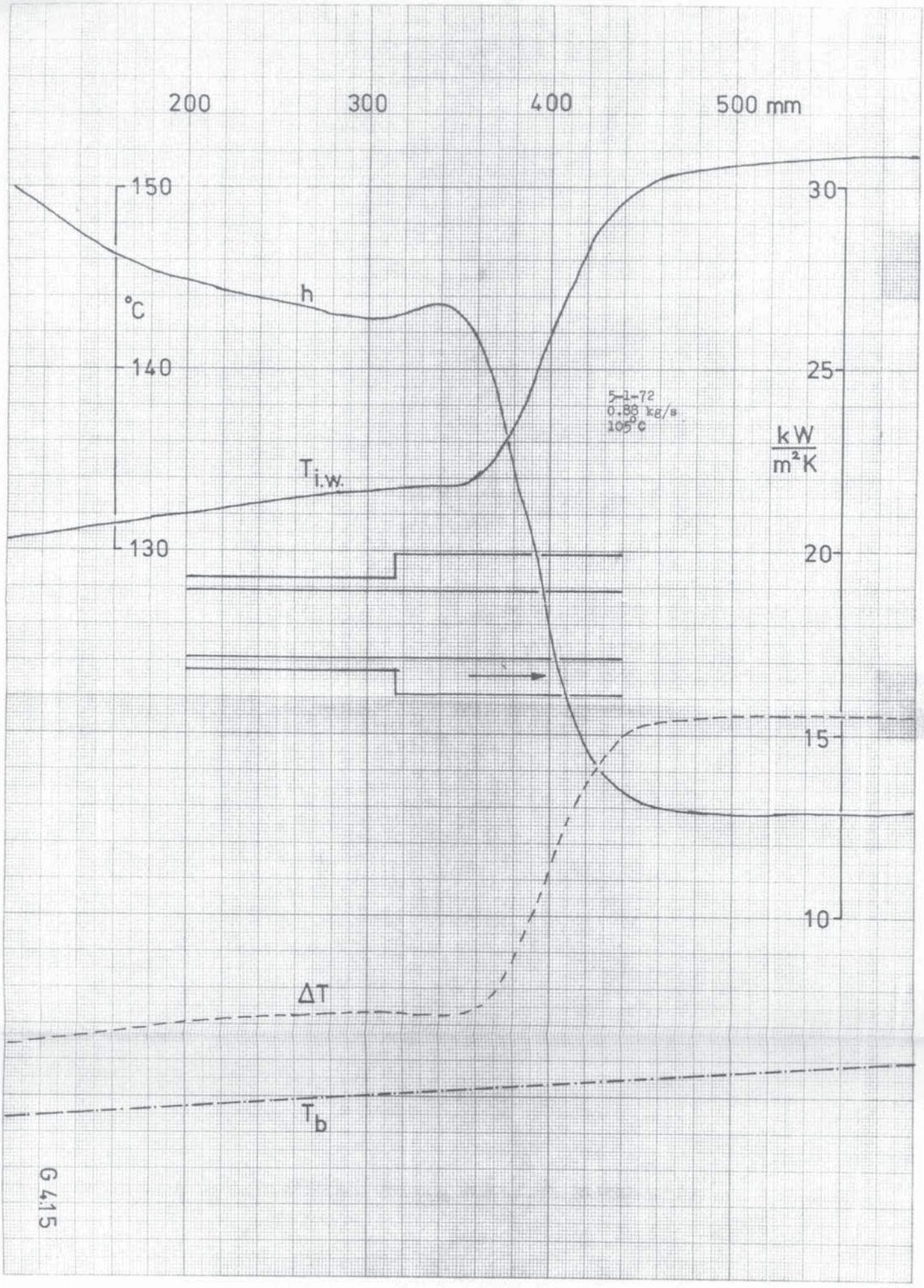
200
300
400
500 mm
150
°C
140
130
h
$T_{i.w.}$
5-1-72
0.88 kg/s
105°C
30
25
20
15
10
kW
m^2K
ΔT
T_b
G 4.15

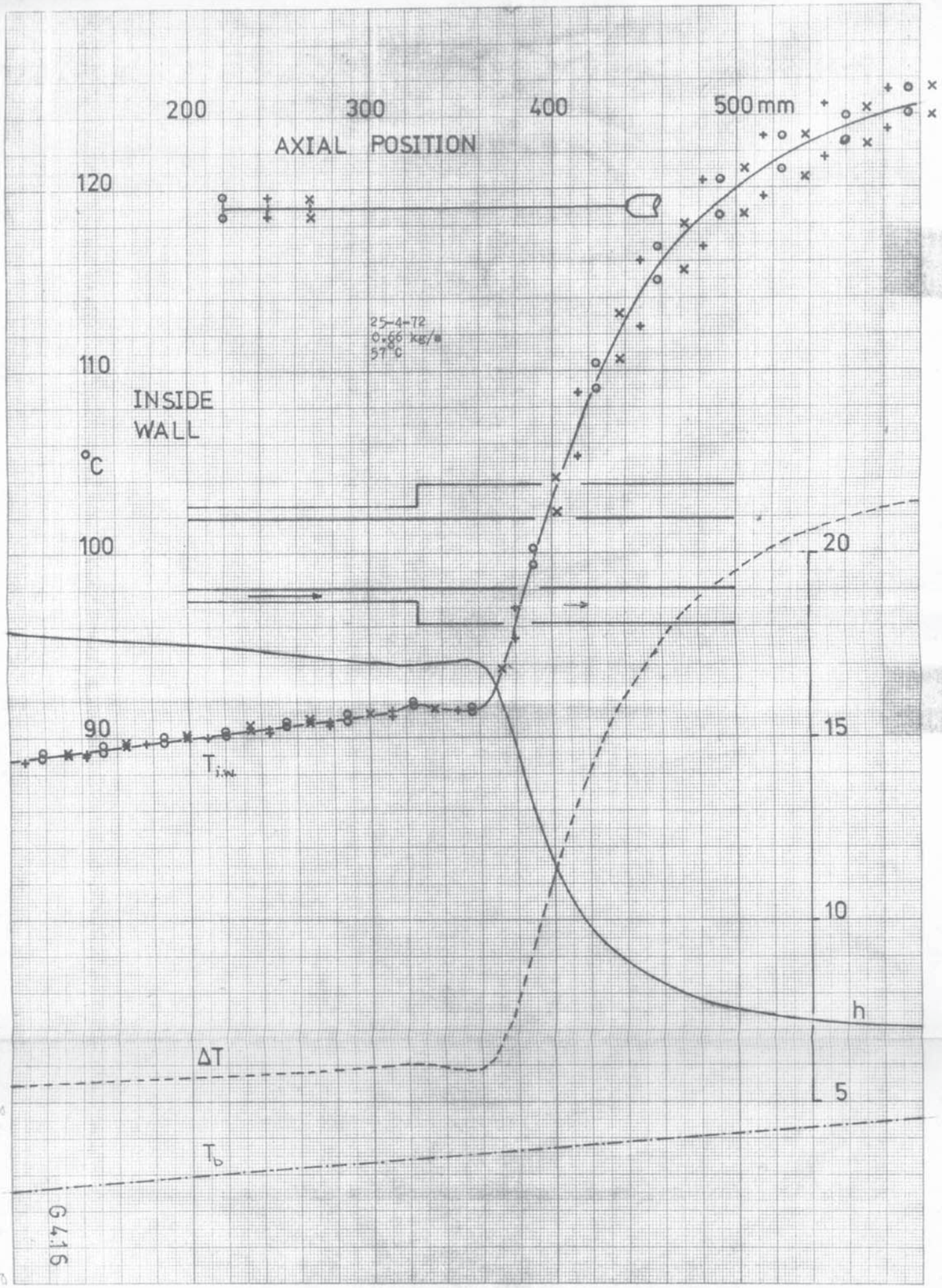
200
300
400
500 mm
AXIAL POSITION
120
110
100
90
INSIDE
WALL
°C
25-4-72
0.66 kg/s
57°C
20
15
10
5
h
ΔT
$T_{i.w}$
T_b
G 4.15

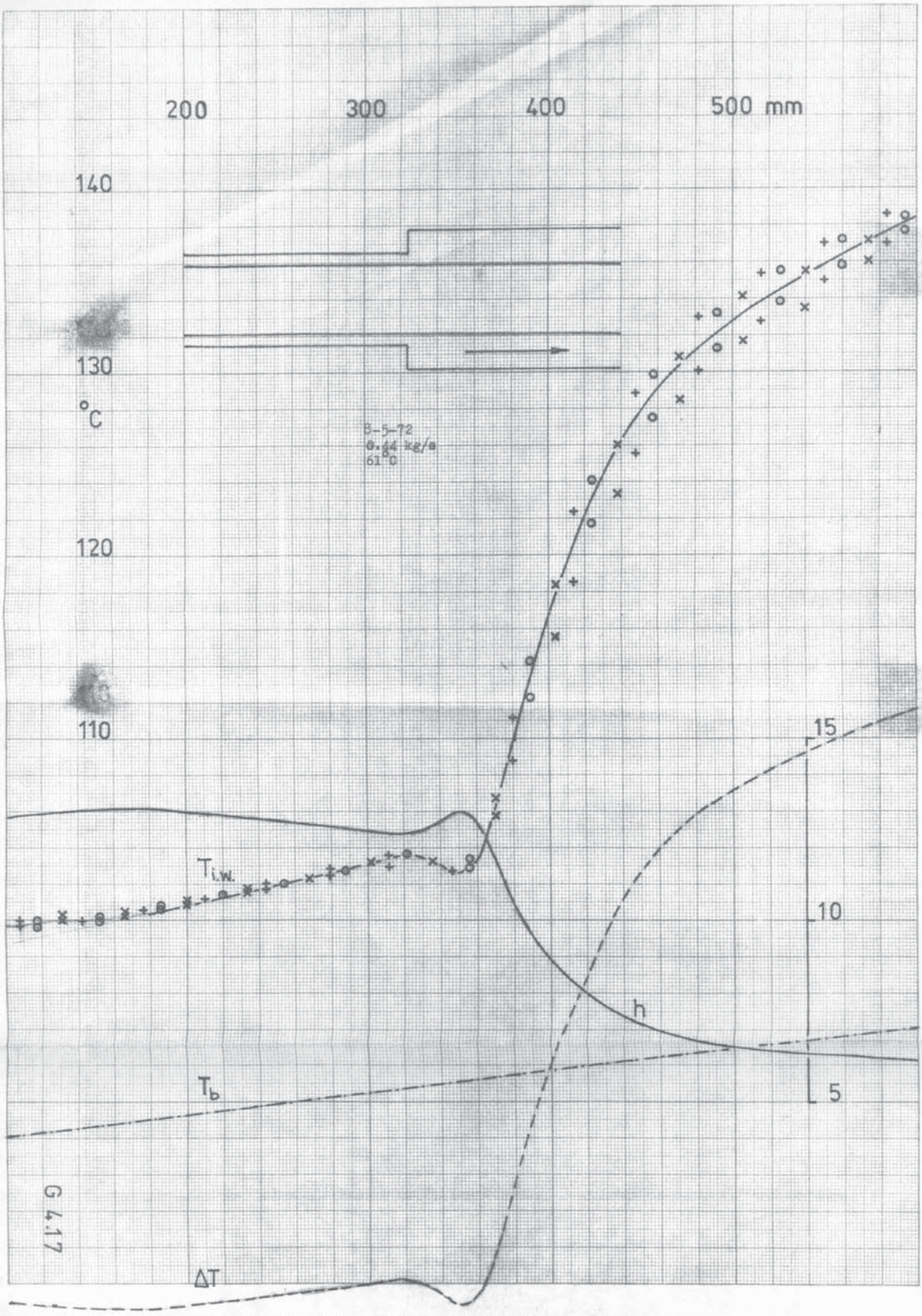
200
300
400
500 mm
140
130
°C
120
110
8-5-72
0.44 kg/s
61 °C
15
10
5
$T_{i.w.}$
T_b
h
ΔT
G 4.17

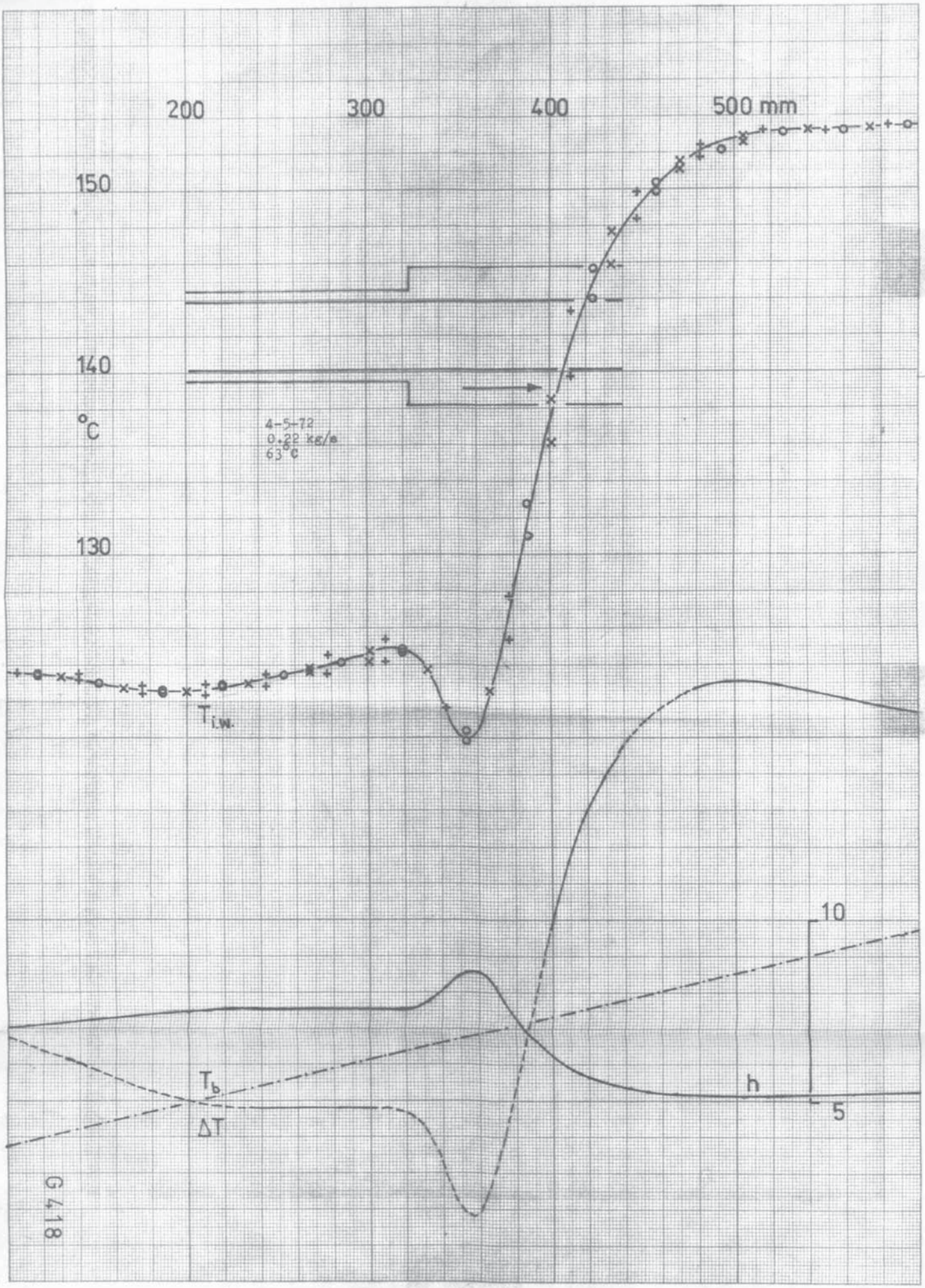
200
300
400
500 mm
150
140
°C
130
4-5-72
0.22 kg/s
63°C
T i.w.
10
h
5
T b
ΔT
G 418

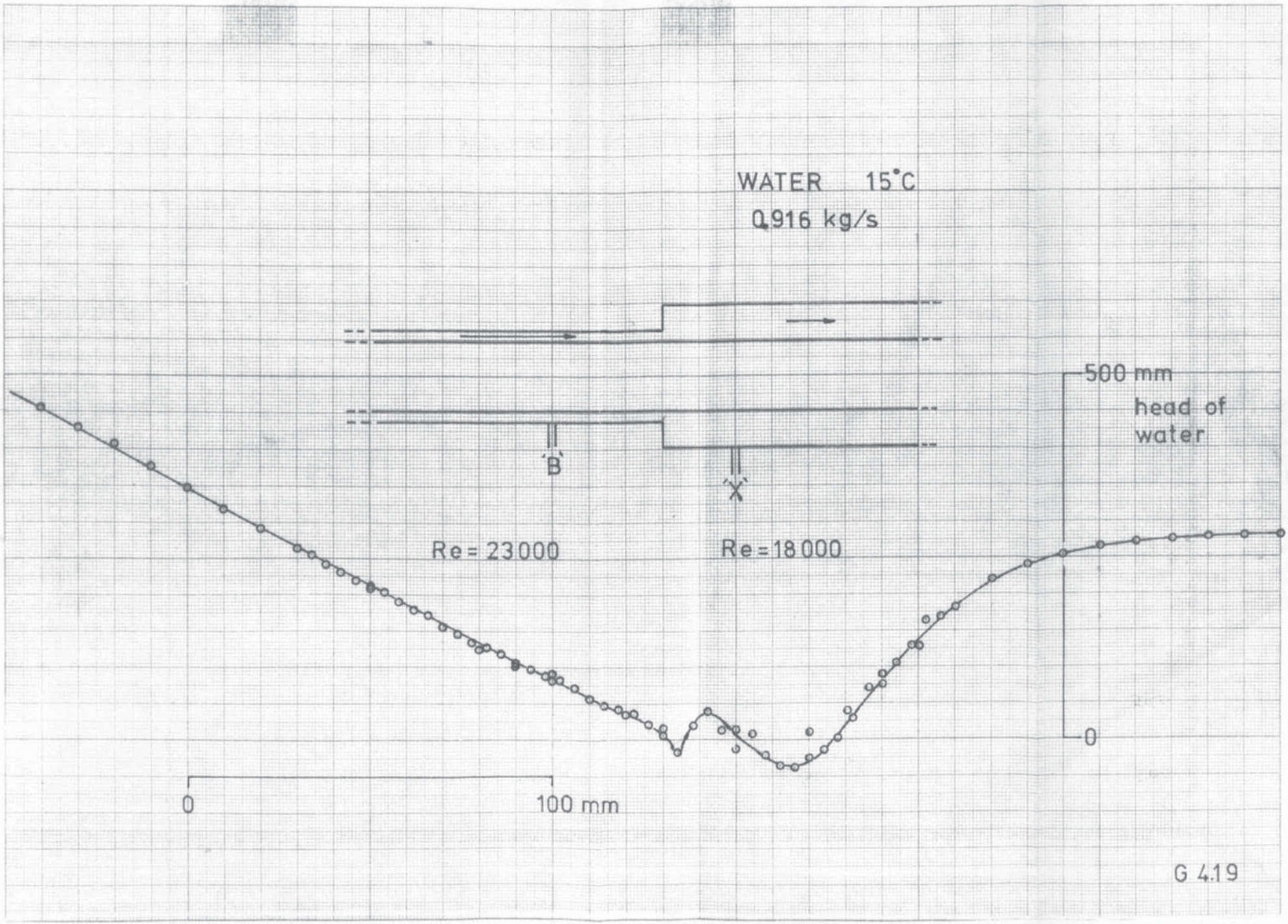
WATER 15°C
0.916 kg/s
'B'
'X'
Re = 23000
Re = 18000
500 mm
head of
water
0
0
100 mm
G 4.19

0 85 kg/s 100°C

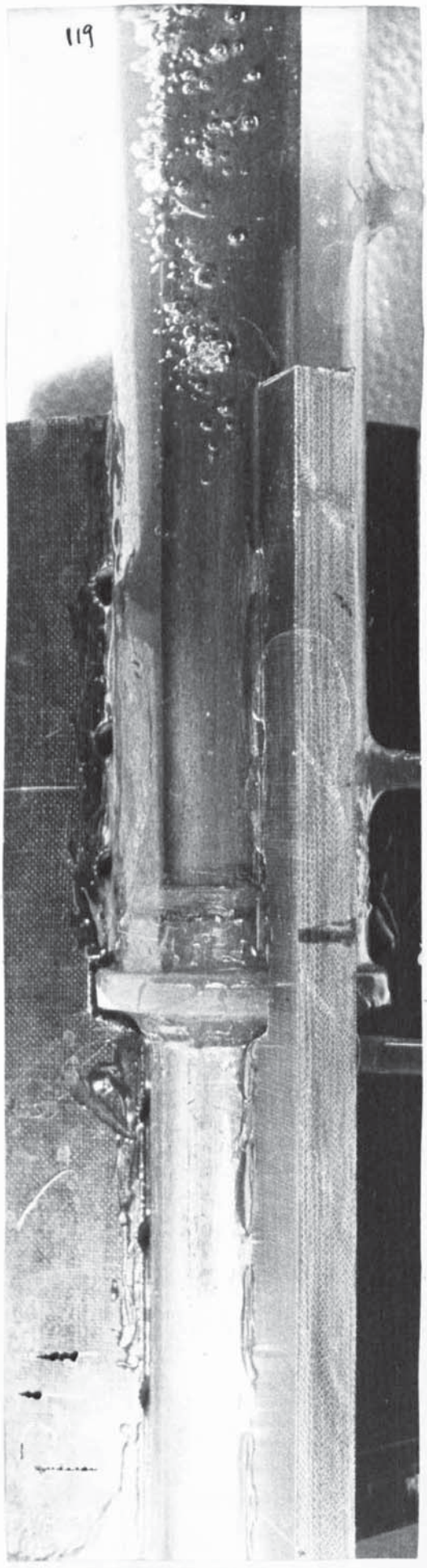

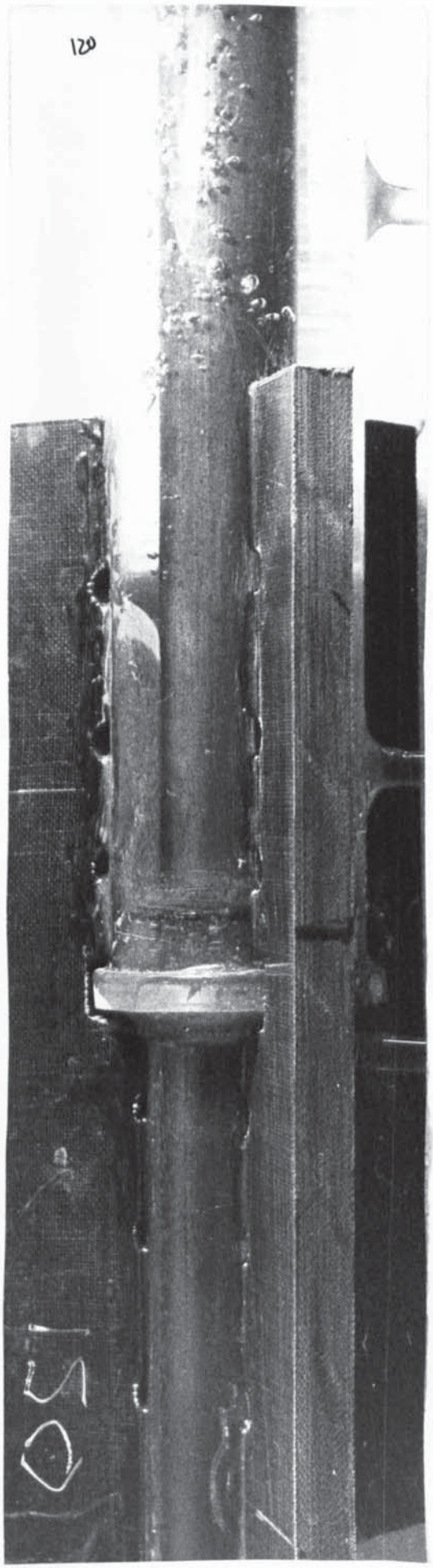

P 4.12

0.85 kg/s 93°C

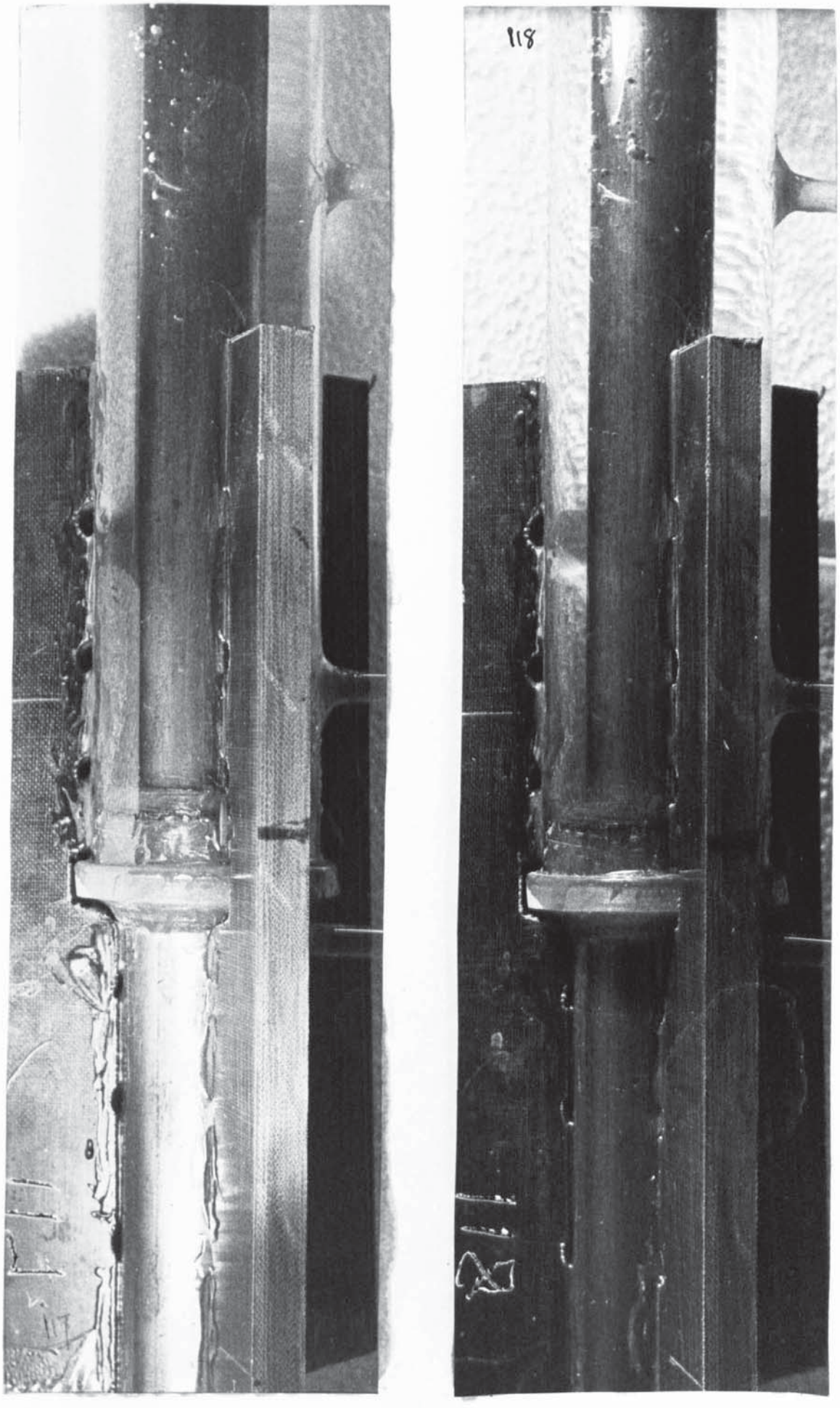

P 4.13

0.64 kg/s 101°C

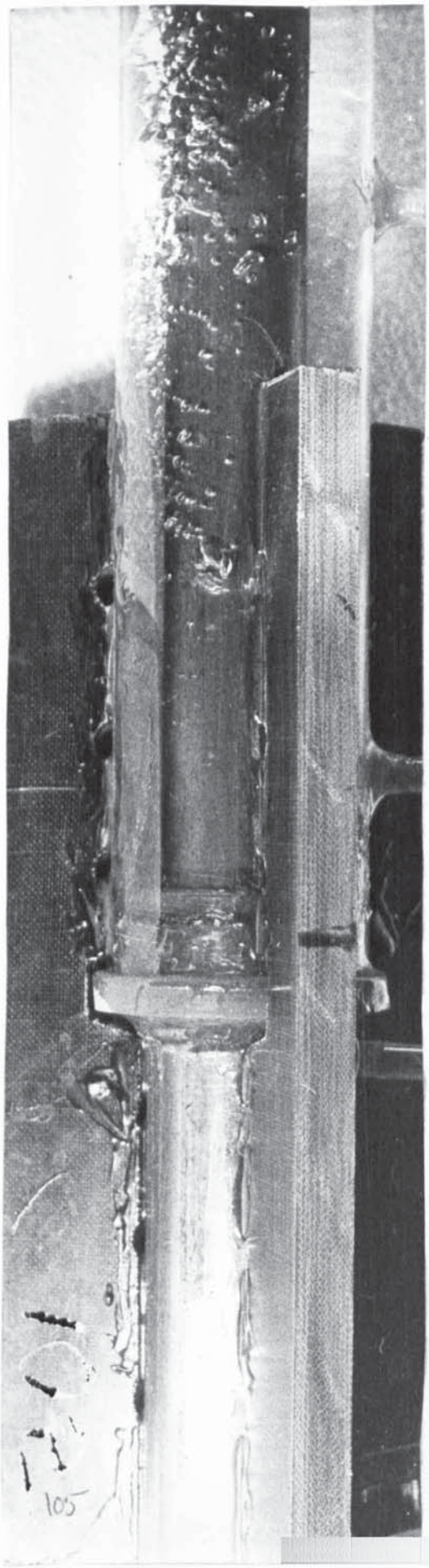

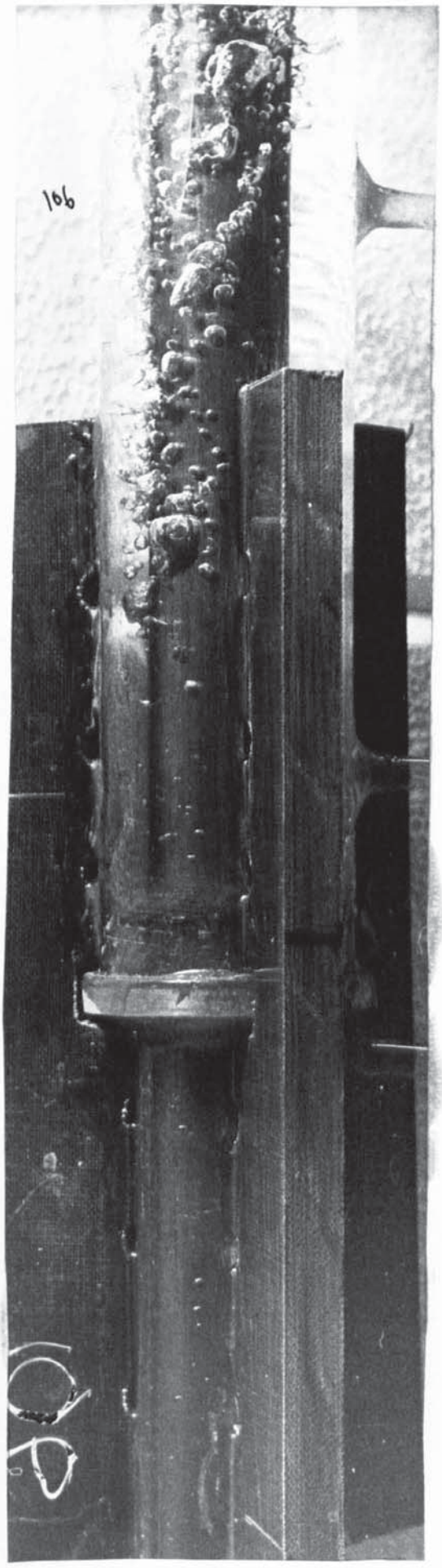

P 4.14

0.64 kg/s 95°C

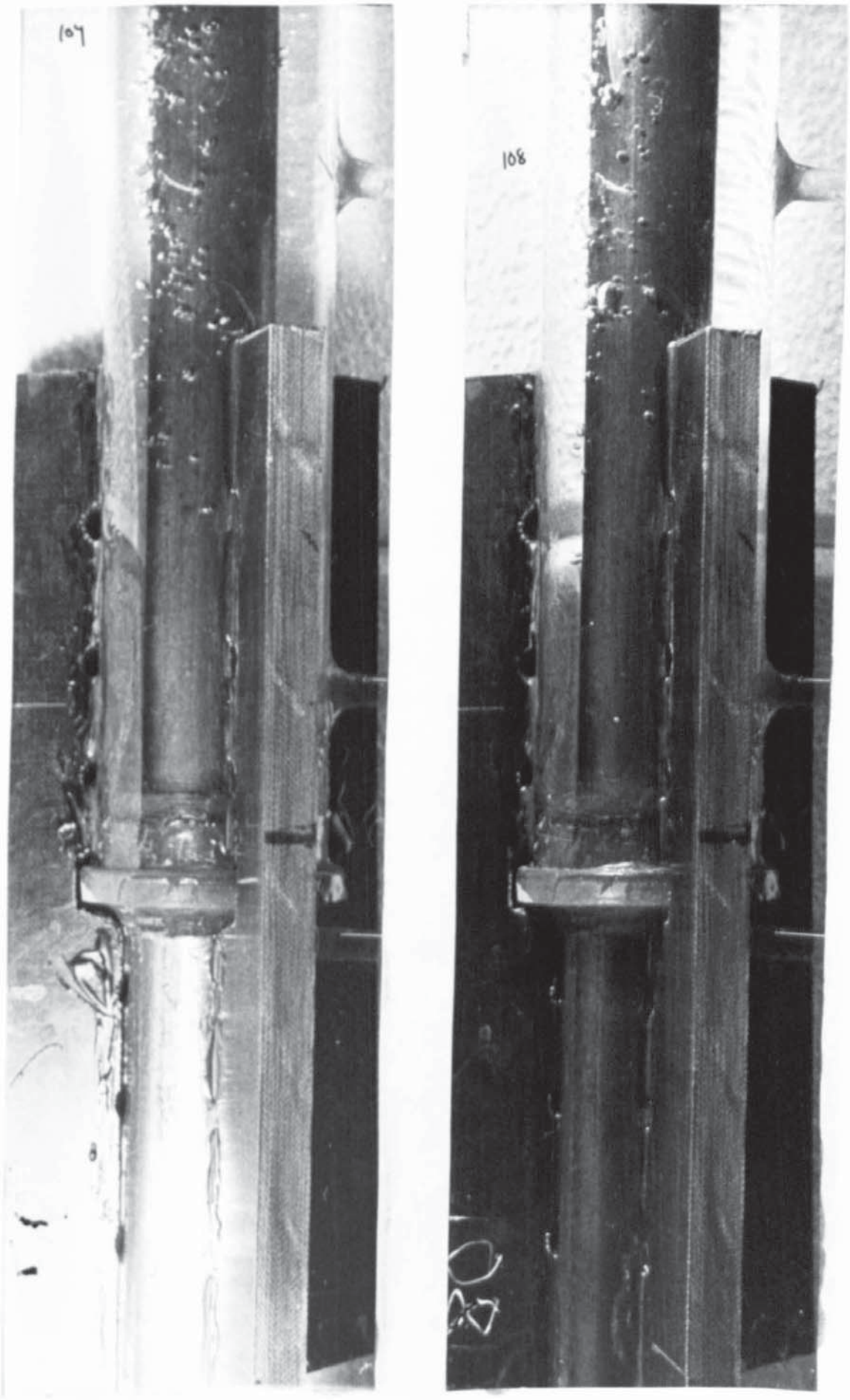

P 4.15

0.64 kg/s 90°C

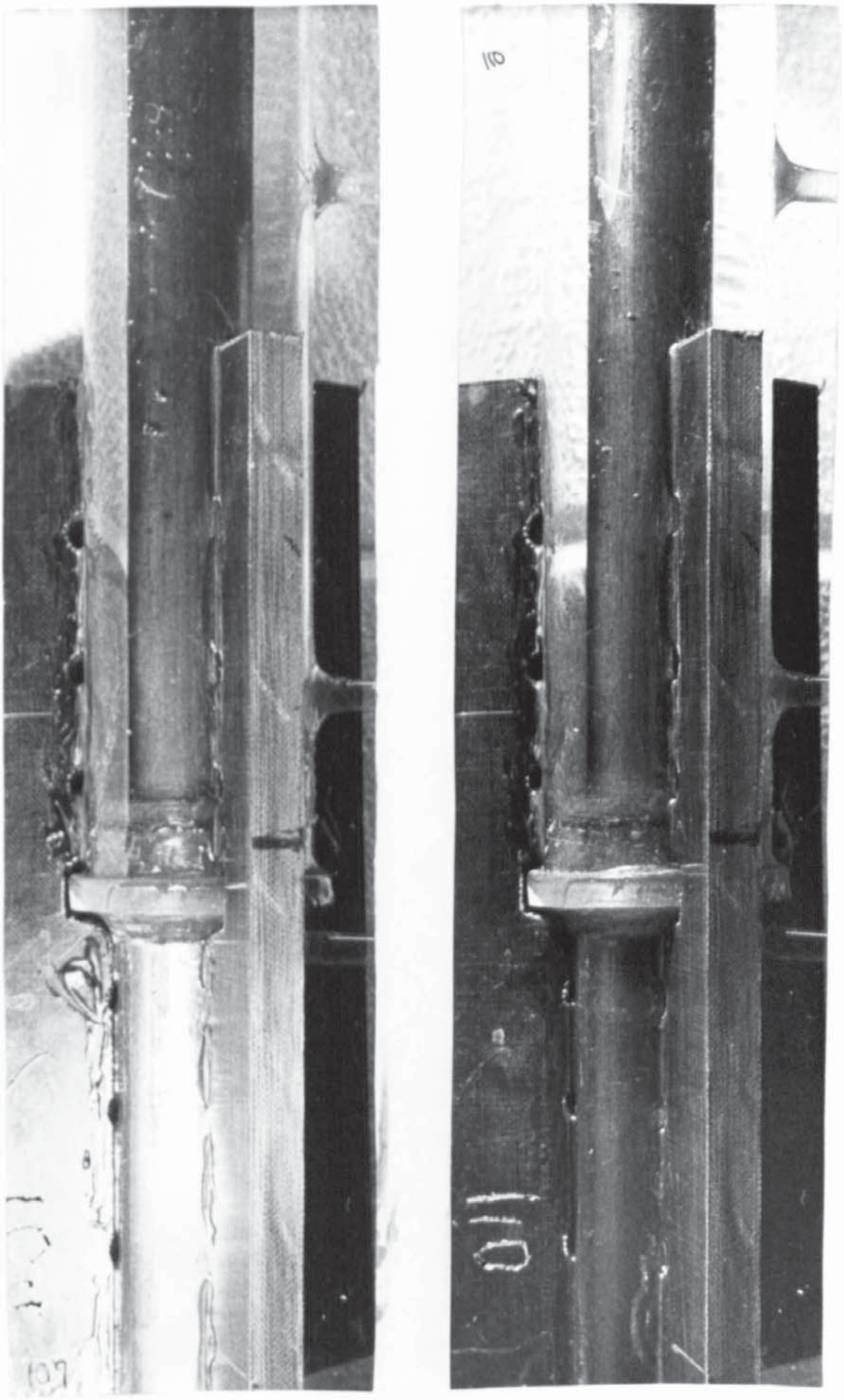

P4.16

0.43 kg/s 86°C

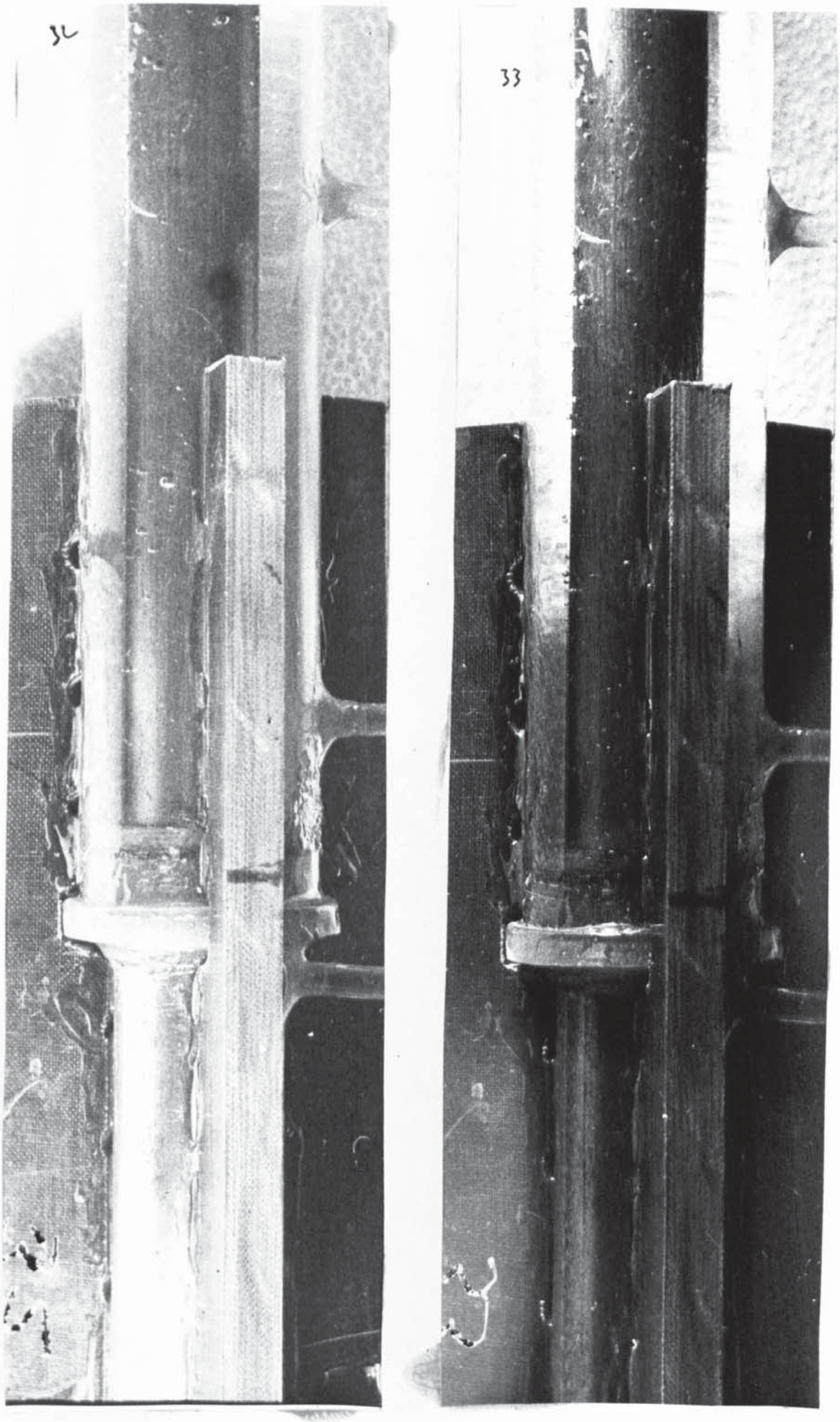

P 4.17

0.43 kg/s 89°C

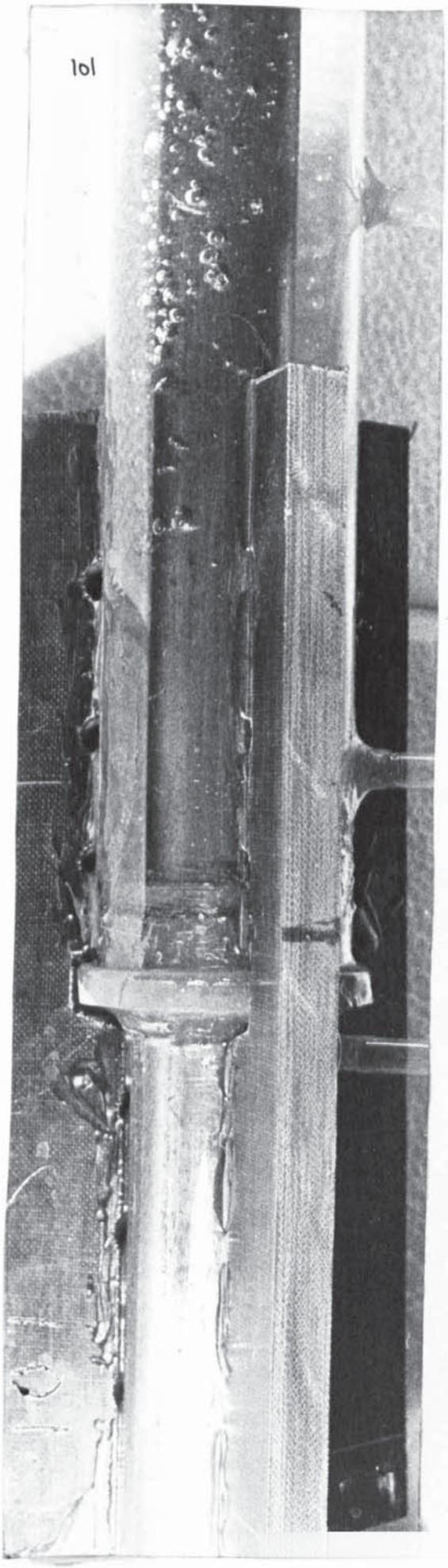

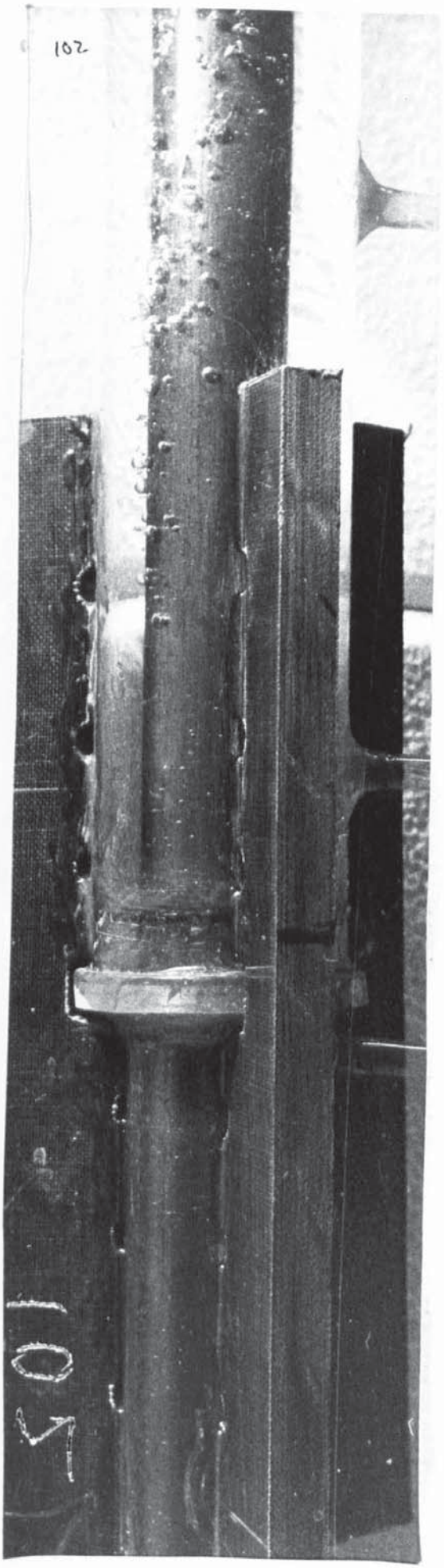

P 4.18

0.43 kg/s 97°C

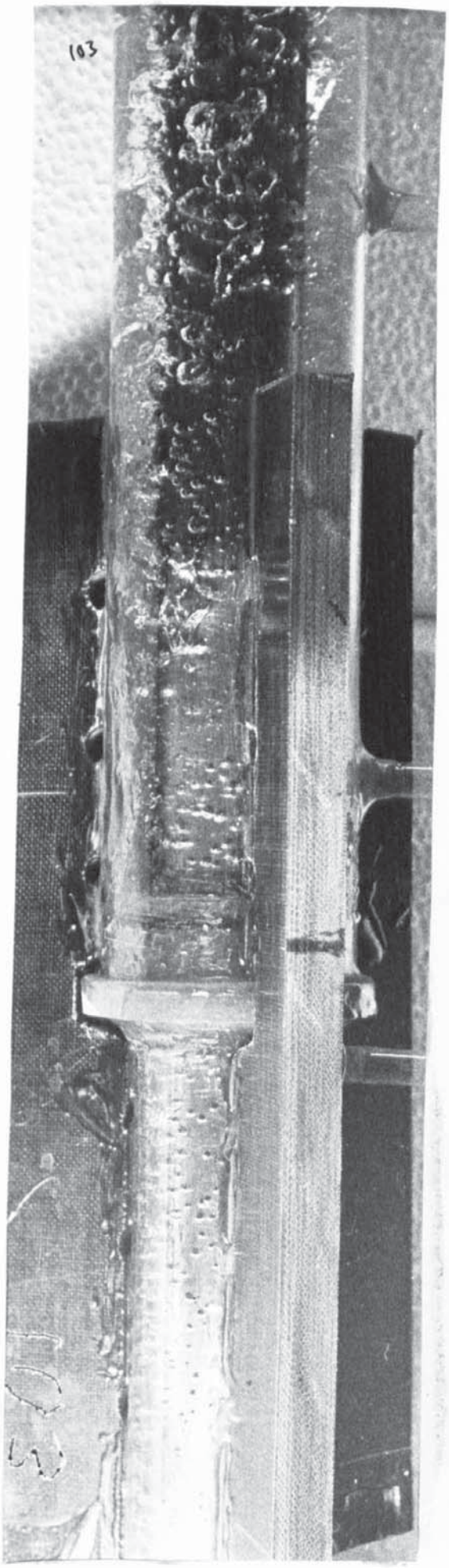

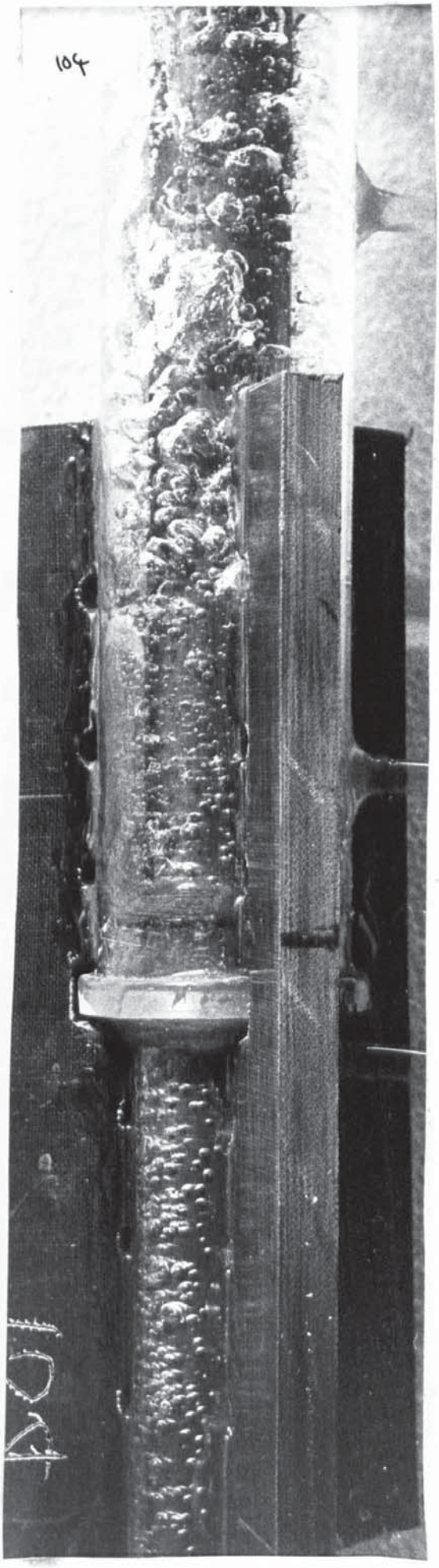

P 4.19

0.21 kg/s 93°C

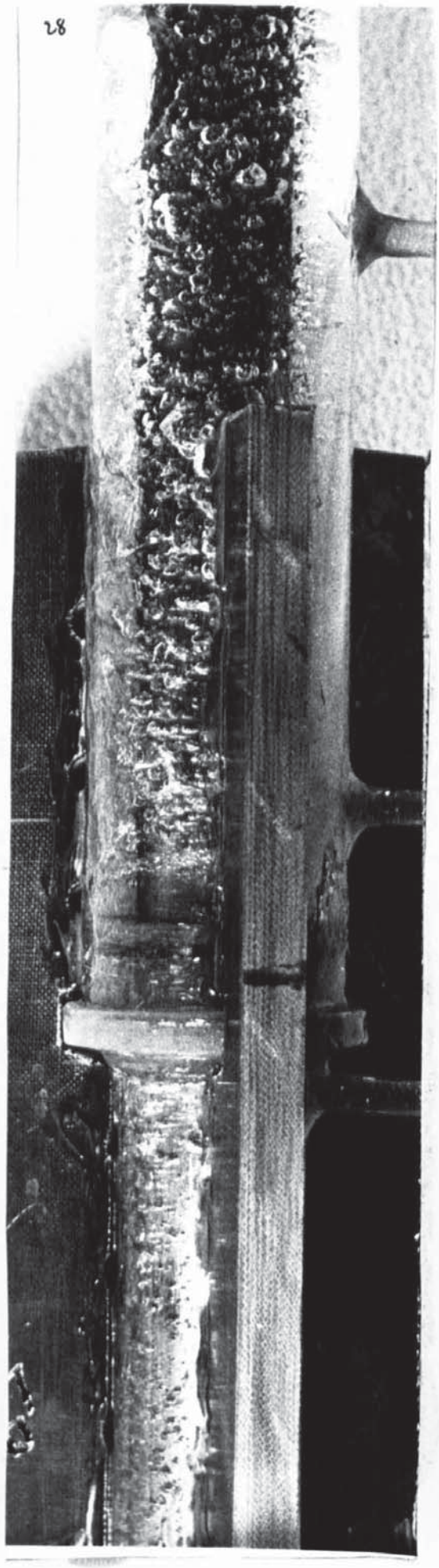

P 4.20

0.21 kg/s 81°C

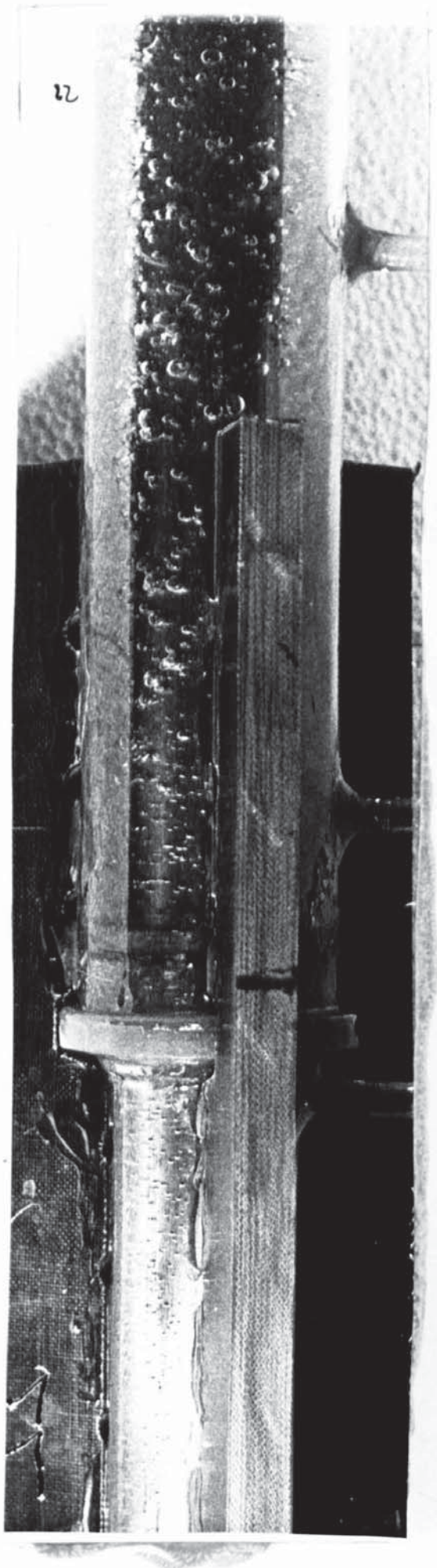

P 4.21

0.21 kg/s 67°C

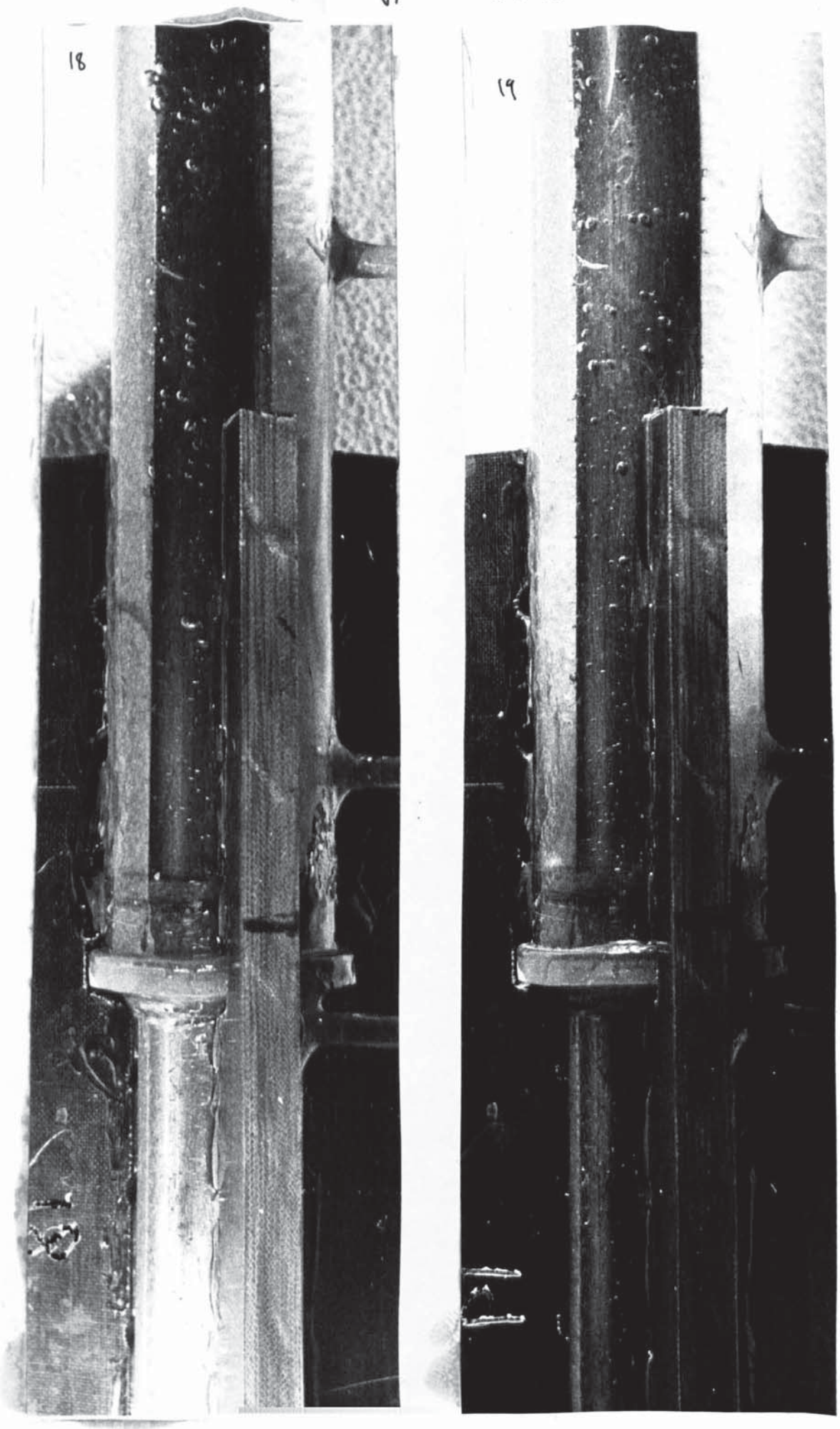

4.6 THE EFFECT OF SWIRL ON THE HEAT TRANSFER COEFFICIENT FOR SINGLE AND TWO PHASE FLUID FLOW THROUGH AN ANNULUS WITH A HEATED INNER WALL.

INTRODUCTION.

When a fluid passing through a heated tube is caused to swirl by helical guide vanes then the centrifugal force on the fluid particles due to the swirl motion will intensify the buoyancy of hot fluid relative to cold fluid. The relative buoyancy will speed the rate of mass transfer of hot fluid from the heating surface into the bulk of the fluid and thus increase the heat transfer rate from the hot surface. An additional pressure loss however will be incurred by giving the fluid a swirl motion and this may not be acceptable not withstanding the reduction in heat surface area for a given duty. The same reasoning can be applied to fluid flowing through an annular section provided that the hot surface is the outside wall of the annulus.

If the heat transfer rate is increased sufficiently to produce surface boiling then since the buoyancy of the vapour bubbles relative to the cold fluid is very much greater than the relative buoyancy of the hot fluid to the cold fluid, the heat transfer should be improved by the swirl action to an even greater extent. The increased force directing the cold fluid to the heating surface should also increase the value of the critical heat flux.

In many practical cases of fluid flow through an annular section the heating surface is the inner wall of the annulus, e.g. nuclear fuel rods, and in this case it would seem that the effect of producing swirl in the fluid flowing along the annulus would be to inhibit the mass transfer rate of hot fluid from the heating surface. It was thought that although this would certainly be the case for a single phase fluid, however if the hotter boundary layer would allow

nucleate boiling to develop at a lower bulk fluid temperature, then the result could be an improvement in the heat transfer rate for unit surface area of the hot surface.

Three series of tests were planned to investigate this possibility, in each series the swirl rate had a different value.

The test section consisted of a glass outer tube (38 mmID) and a plain central heating tube(19.1 mmID), three guide vanes of triangular section were spaced at 120° round the annular flow area formed. In the first series of tests they were straight and in the second and third series of tests they were of helical form with different lead angles in each case.

The tests were arranged to enable comparisons to be made between them on the basis of a constant 'Re' number for the flow section and flow rates through the annulus were adjusted to achieve this.

THE EFFECT OF ALTERING THE HELIX ANGLE ON THE SHAPE OF THE FLOW CHANNEL CROSS SECTION.

For straight axial vanes, helix angle = 0, the channel section, one of three, is of the shape shown in, D 4.7. As the helix angle is increased then, since the inside angle of the helix is less than the outside angle, the effective cross-sectional area of the flow normal to the direction of flow assumes a more nearly rectangular shape. Increasing the helix angle further gives the shape shown and in the limit will reduce to a triangular section when the outside of the vanes contact.

The helix angles, P 4.23, used in the tests were:

	Test 1	Test 2	Test 3
Inside	0 (axial)	10.0°	20.0°
Outside	0 (axial)	13.5°	27.0°

and the angle of the apex of the vane section was 60° in all cases.

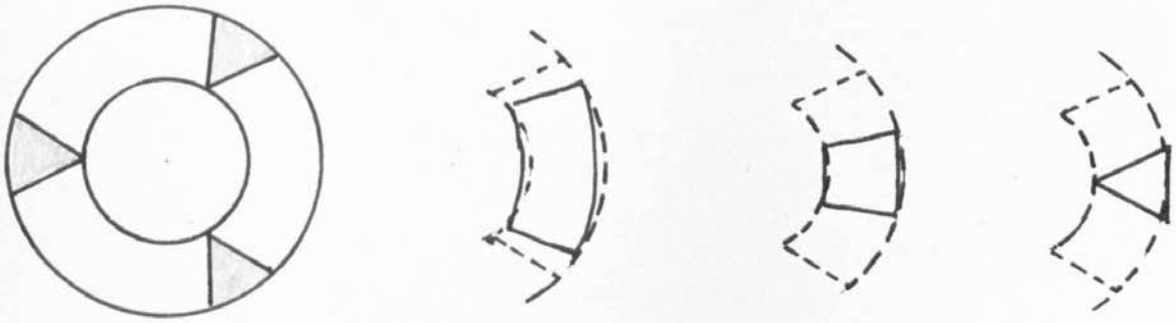

CHANGE IN SECTION WITH INCREASING HELIX ANGLE

TEST 1

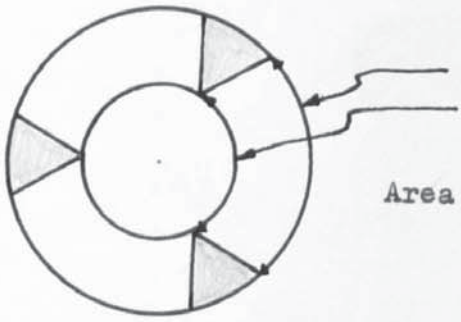

29.6 mm
20.0 mm

$$\text{Area} = \frac{855 - 3(49.1)}{3} = 236 \text{ mm}^2$$

TEST 2

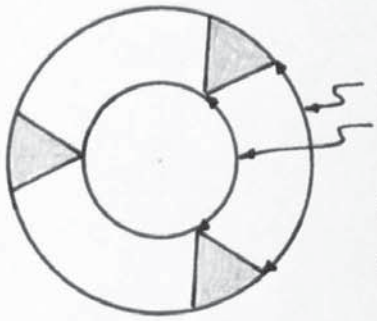

29.6 cos13.5 = 28.8 mm (-2.8%)
20.0 cos10.0 = 19.6 mm (-1.5%)

Reduction in area is ≏ 2%

Area = 236 × 0.98 = 231.4 mm^2

TEST 3

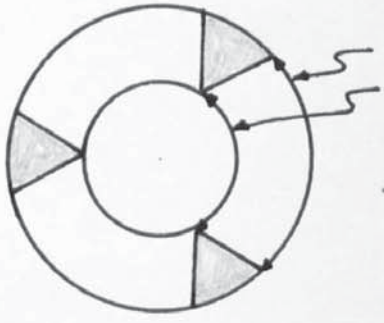

29.6 cos27.0 = 26.4 mm (-10.9%)
20.0 cos20.0 = 18.73 mm (-6.0%)

Reduction in area is ≏ 8.5%

Area = 236 × 0.915 = 215 mm^2

D 4.7

PERCENTAGE REDUCTION IN SECTIONAL AREA WITH INCREASING HELIX ANGLE

The cross-sectional area of one vane was 49.1 mm^2 in each case and the cross-sectional area of the plain annulus i.e. without vanes was 855 mm^2. When the vanes were of helical form the new effective sectional area of the flow path, i.e. normal to the direction of flow, was calculated by considering the reduction of the length of the inside and outside boundaries of the flow channel, D 4.7.

REYNOLDS NUMBER COMPARISONS FOR THE THREE SECTIONS USED.

From the section drawn, D 3.23, it can be seen that shapes of the section normal to the direction of fluid flow are near identical, sufficiently so for the conditions in each test to be dynamically similar for a single phase fluid if the Re number is kept constant for comparative tests. Comparing the sectional areas 236, 231.4 and 215 mm^2 it can be seen the velocity of flow, measured in the direction of the helical path, must be set in the ratio, 1.00, 0.98 and 0.915 for tests 1 2 and 3 respectively while the temperature is kept to the same value for each test and thus the values of ρ and μ are constant for the comparisons.

Tests were carried out for six values of flow rate in each case.

PROCEDURE.

It had been established that, for a plain annulus without guide vanes, the entrance effect became negligible after twenty two equivalent diameters downstream of the entrance G 4.20. With the vanes in position the geometry was somewhat more complicated due to the necessary presence of three spacing bands along the axis P 4.23, and it was necessary to take both an axial pressure transverse G 4.29-31, and an axial wall temperature tranverse G 4.21, to demonstrate that at the measuring point selected the effect of the

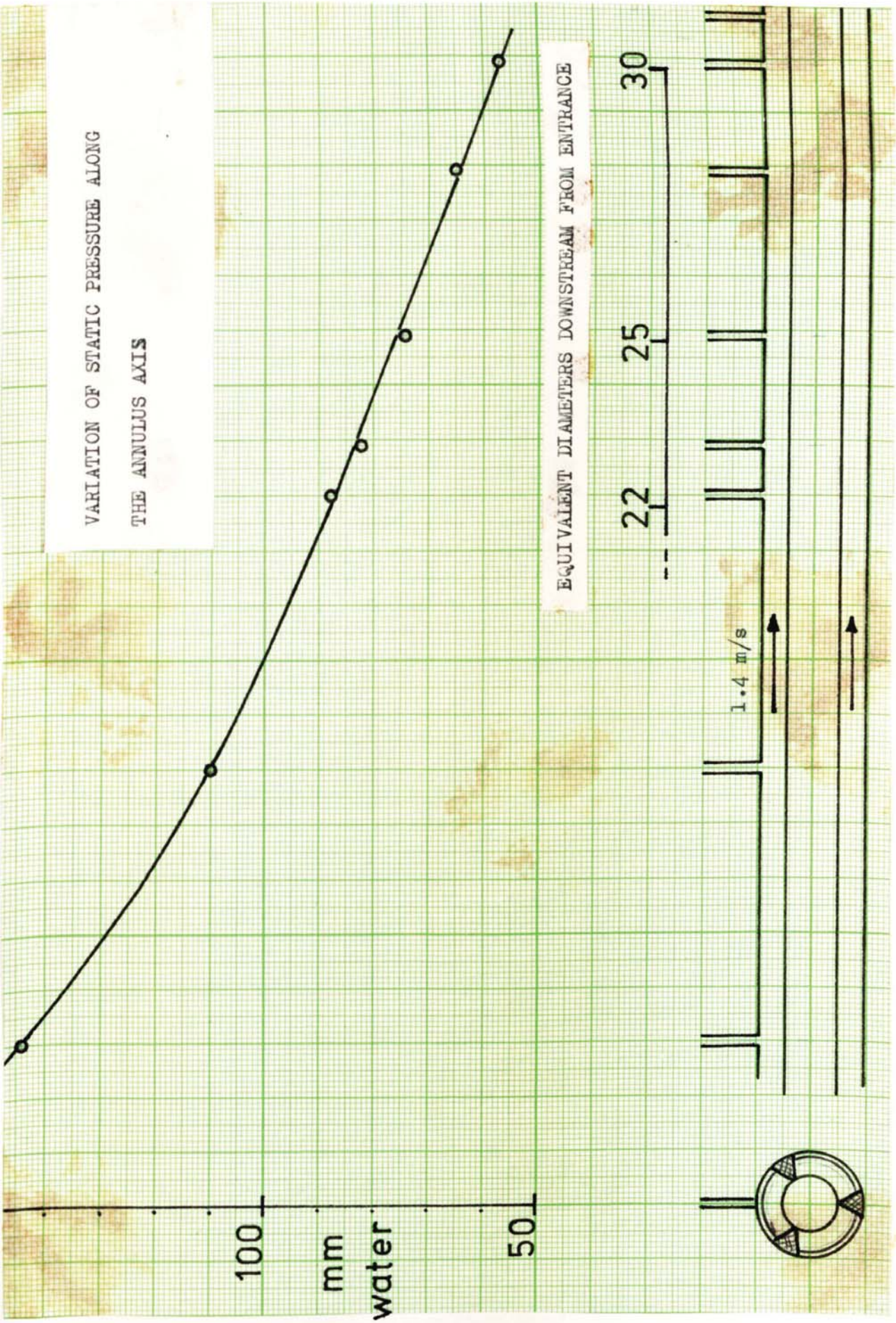
VARIATION OF STATIC PRESSURE ALONG
THE ANNULUS AXIS
100
mm
water
50
EQUIVALENT DIAMETERS DOWNSTREAM FROM ENTRANCE
22
25
30
1.4 m/s

G 4.20

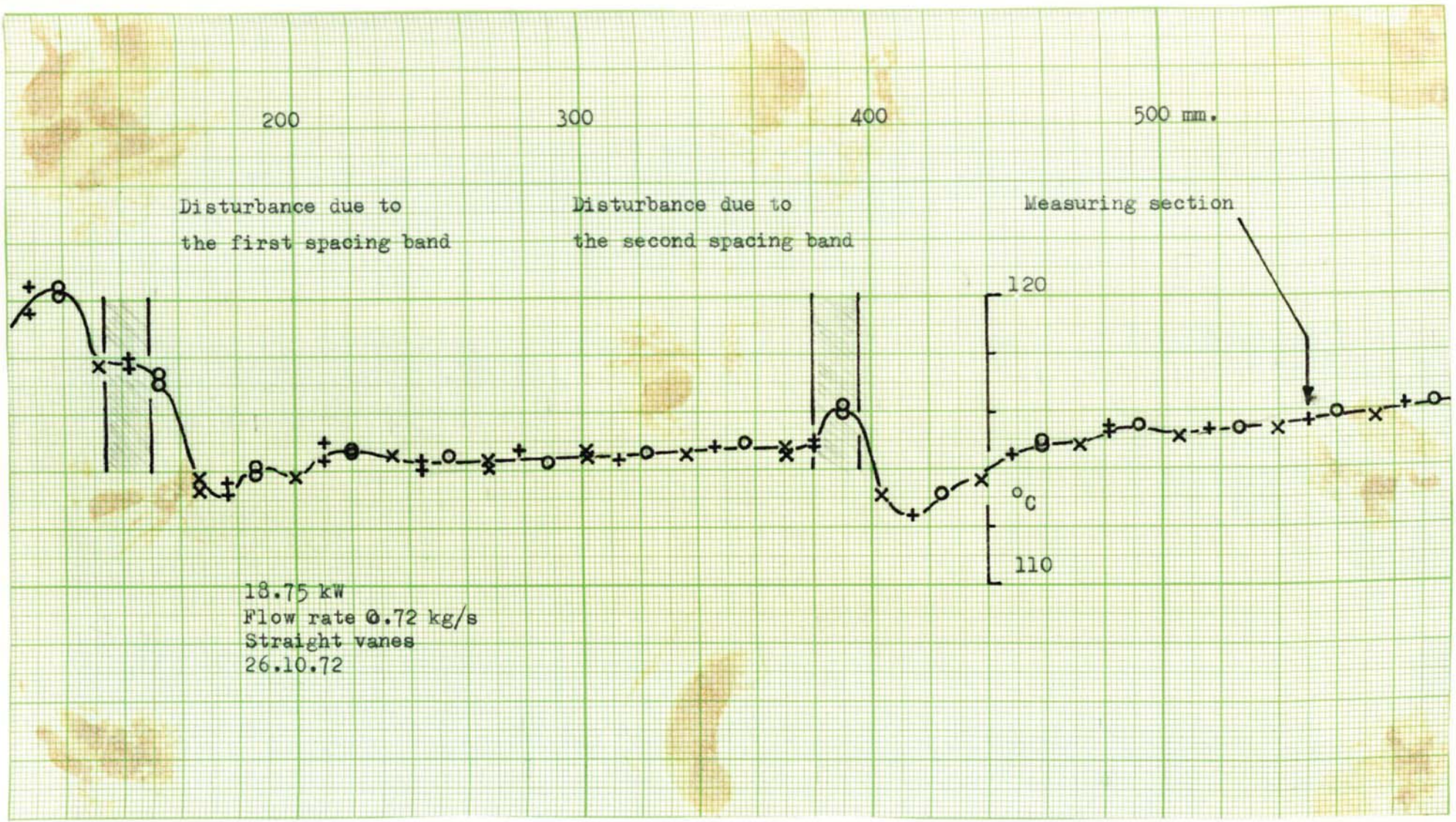

INSIDE WALL TEMPERATURE PROFILE ALONG THE AXIS OF THE HEATING TUBE

G 4.21

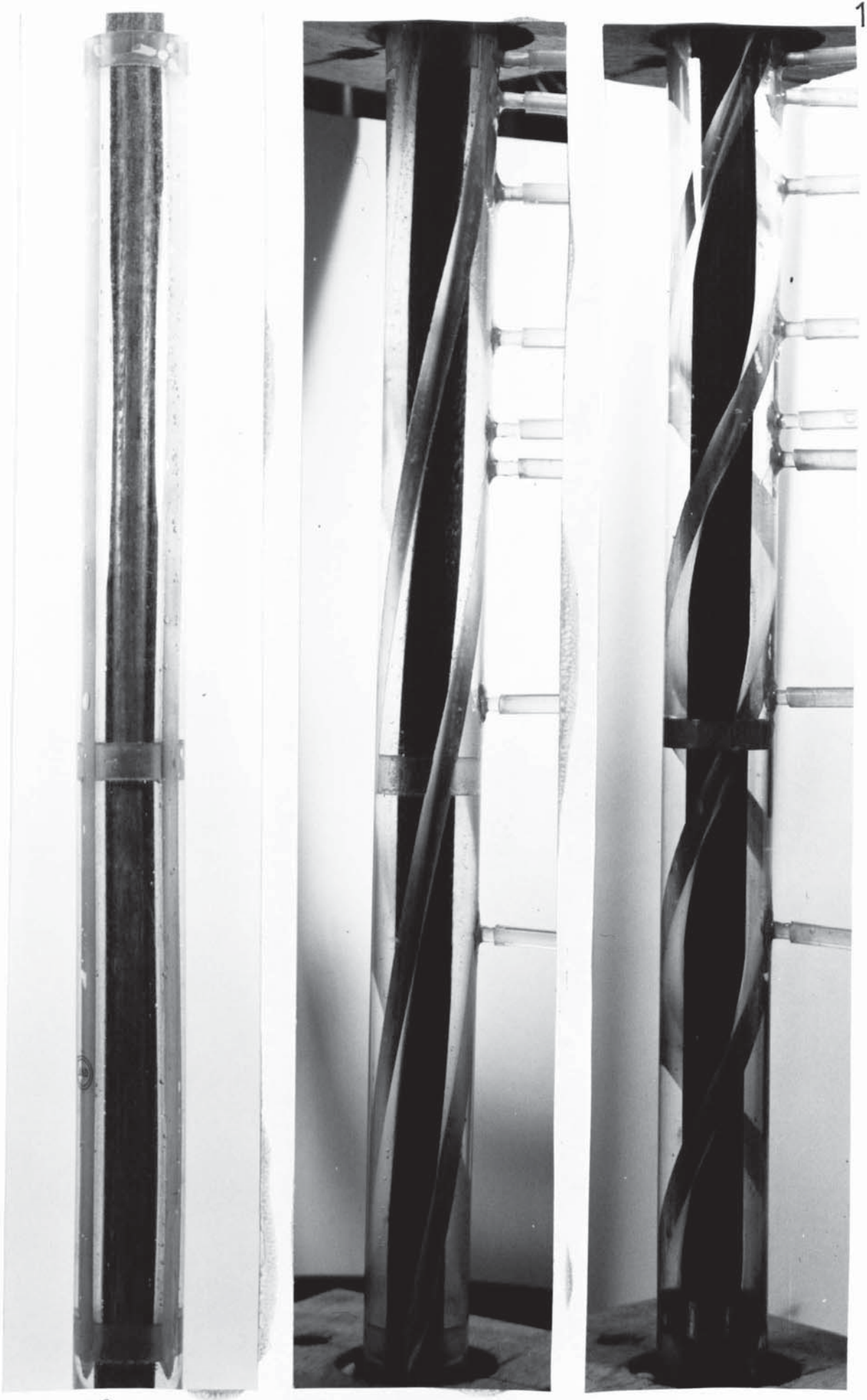

0/0°

10/13.5°

20/27°

P4.23

bands was negligible.

With a particular set of swirl vanes in position the flow rate was set at a fixed value and, when the temperature at inlet to the section had stabilized at a constant value, a set of temperature and flow values was recorded. This was repeated for a number of constant inlet temperature values and then the whole procedure was repeated with a new value of meter flow rate.

The bulk temperature of the water at the measuring section was calculated, and thus from the measured heating tube surface temperature, the heat transfer parameters were calculated. Heat balances were taken on the first tests in each series which used a low value of inlet water temperature and were thus single phase tests.

To support these tests a series of photographs P 4.24-26 of the test section were taken to show the flow pattern of vapour bubbles. Photographs were taken at selected tests, one of them illuminated by a spotlight and with a 0.02 second exposure gave a vector indication of the flow direction. The second photograph was taken using a microsecond flash tube for illumination and this effectively "froze" the boiling to show the location of the nucleation sites and the bubble sizes.

Following the heat transfer tests the heating tube was replaced by a brass tube containing pressure tappings, D 3.24, which were connected to a water manometer. The variation in the static pressure of cold water flowing up the annulus was measured, without heating. The brass tube was constructed to slide axially in the glass tube as this enabled a number of overlapping pressure sampling locations to be obtained and the axial range was extended. The pressure values at particular axial locations could be verified by comparing readings taken at the same location but through different

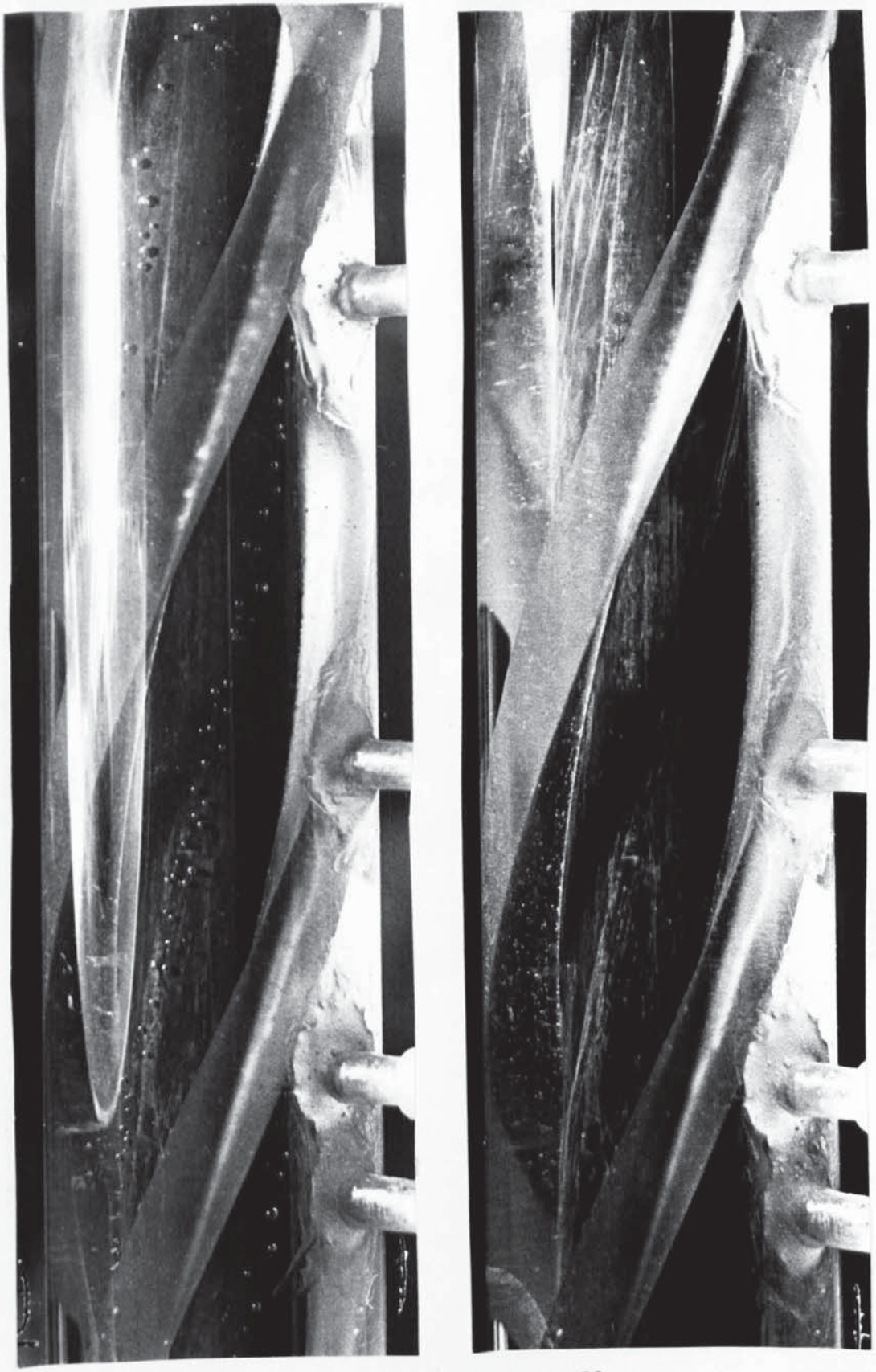

Flash

20 ms.

1.3 m/s , 92°C , 374 kW/m²

TEST 3

P 4.24

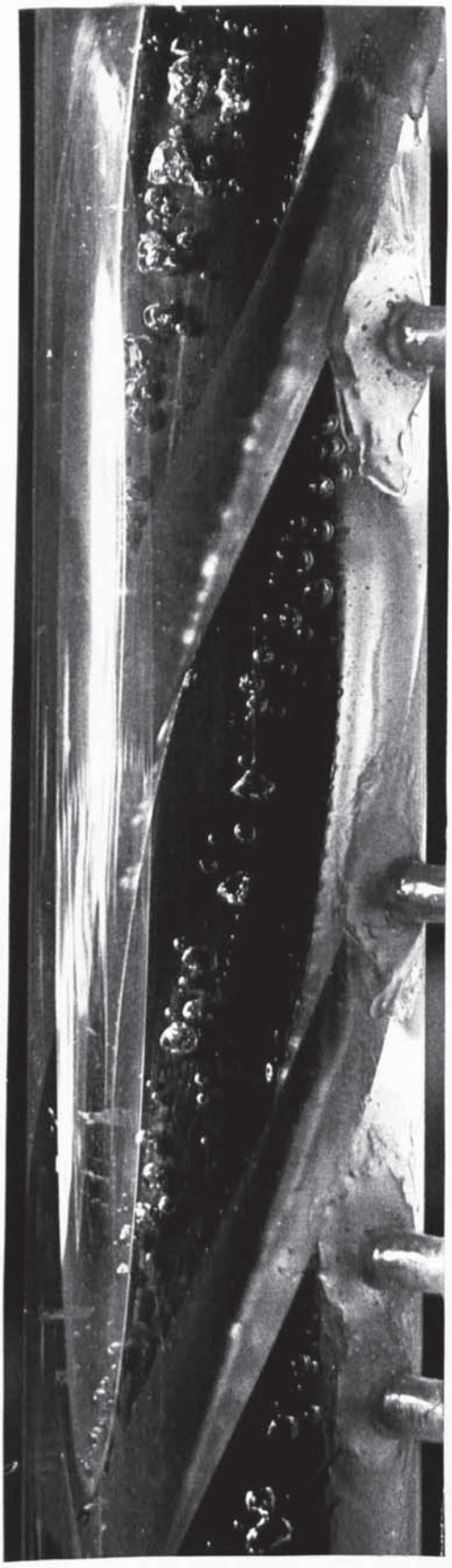

Flash 20 ms.

1.3 m/s , 100°C , 374 kW/m²

TEST 3

P 4.25

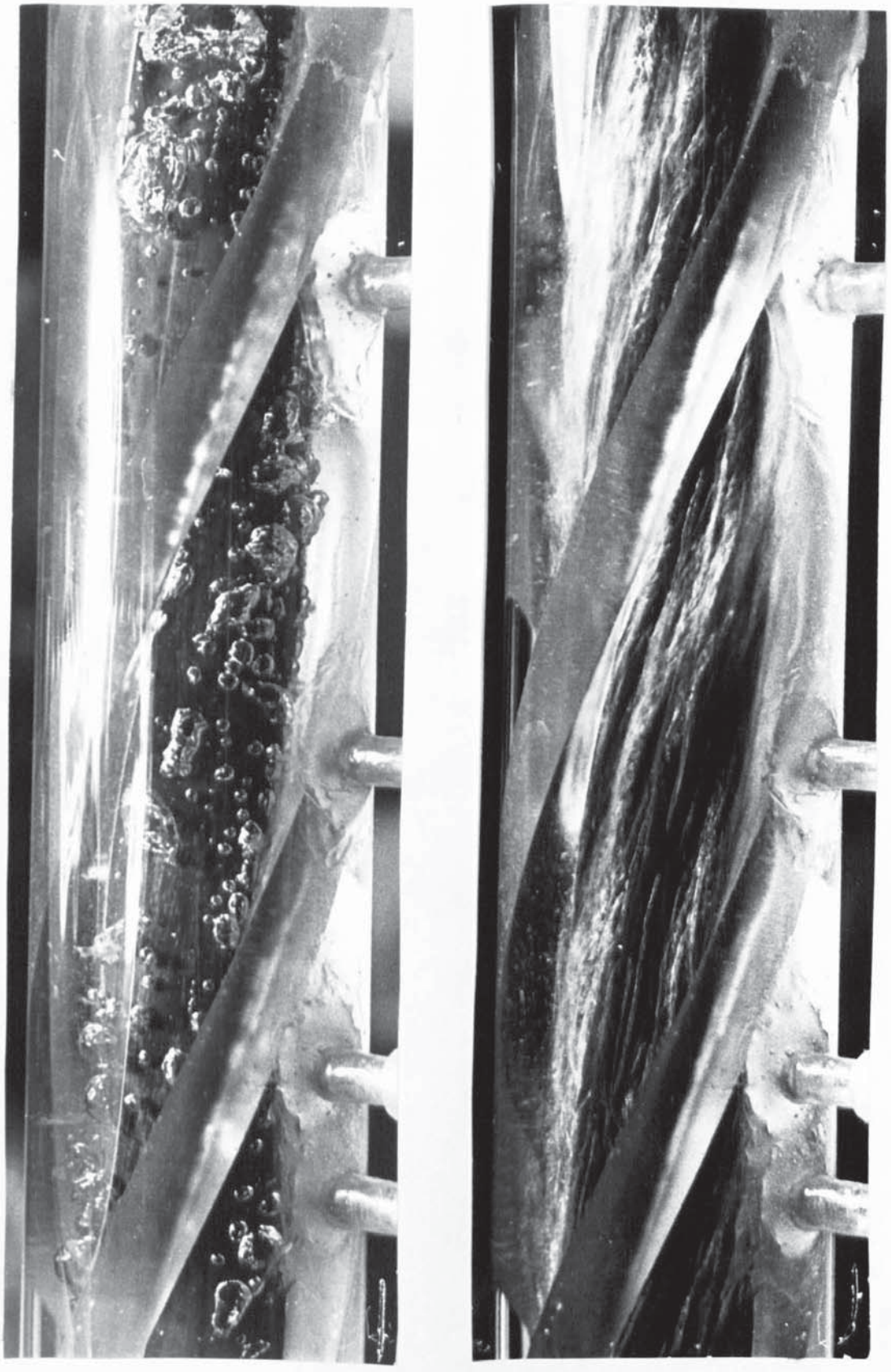

Flash

20 ms.

1.3 m/s , 105°C , 374 kW/m²

TEST 3

P 4.26

sampling holes.

The results were presented as plots of tube wall temperature against water bulk temperature G 4.22-24, and also a cross plot from this to give tube wall temperature against mass flow rate, G 4.25. Further to this a plot of $Nu/Pr^{0.4}$ against $Re^{0.8}$ was produced for each series of tests, G 4.26-28, and the axial pressure plots were drawn to compare the axial pressure variation in each test series G 4.29-31.

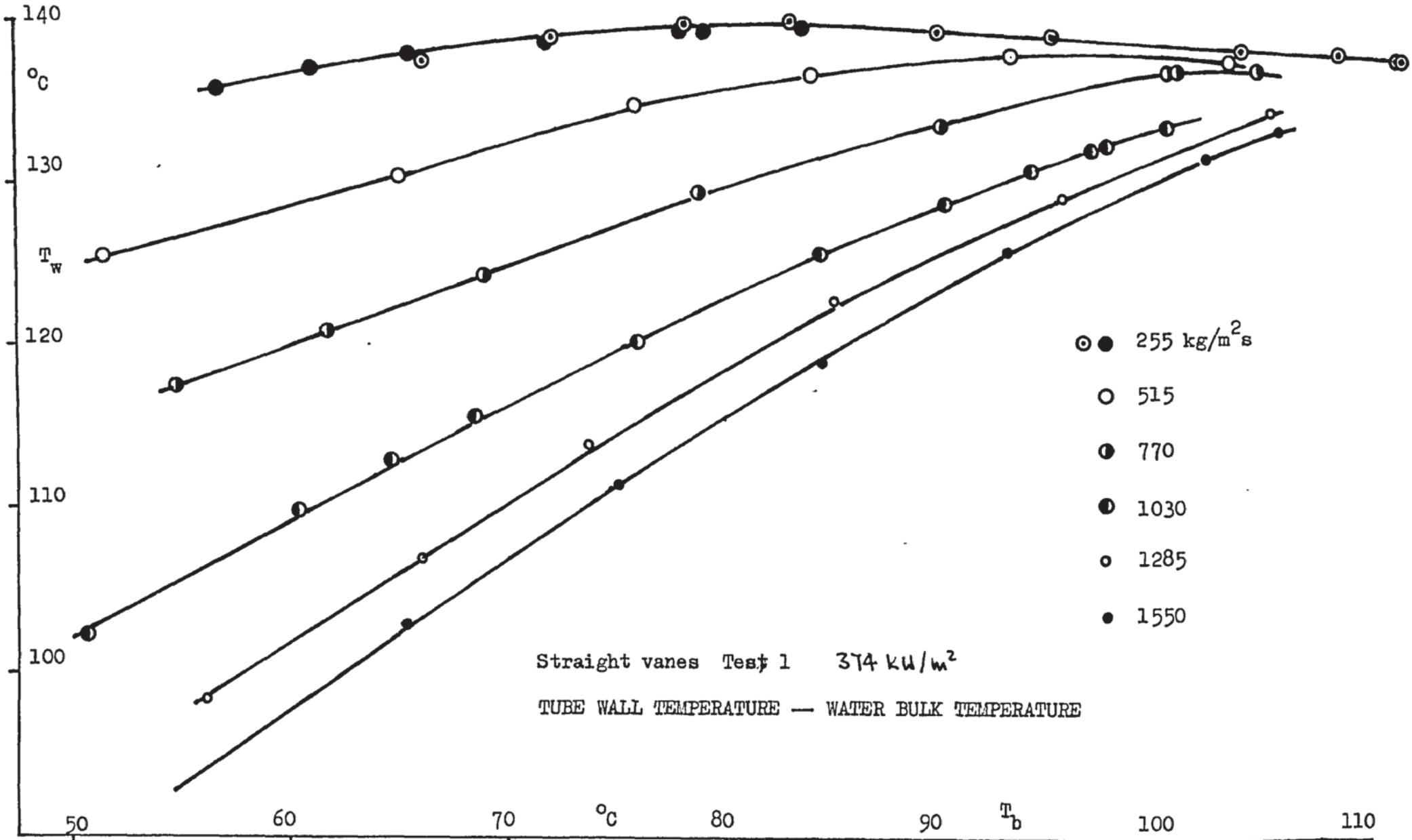
140
°C
130
T_w
120
110
100
255 kg/m²s
515
770
1030
1285
1550
Straight vanes Test 1 374 kW/m²
TUBE WALL TEMPERATURE — WATER BULK TEMPERATURE
50
60
70
°C
80
90
T_b
100
110

G 4.22

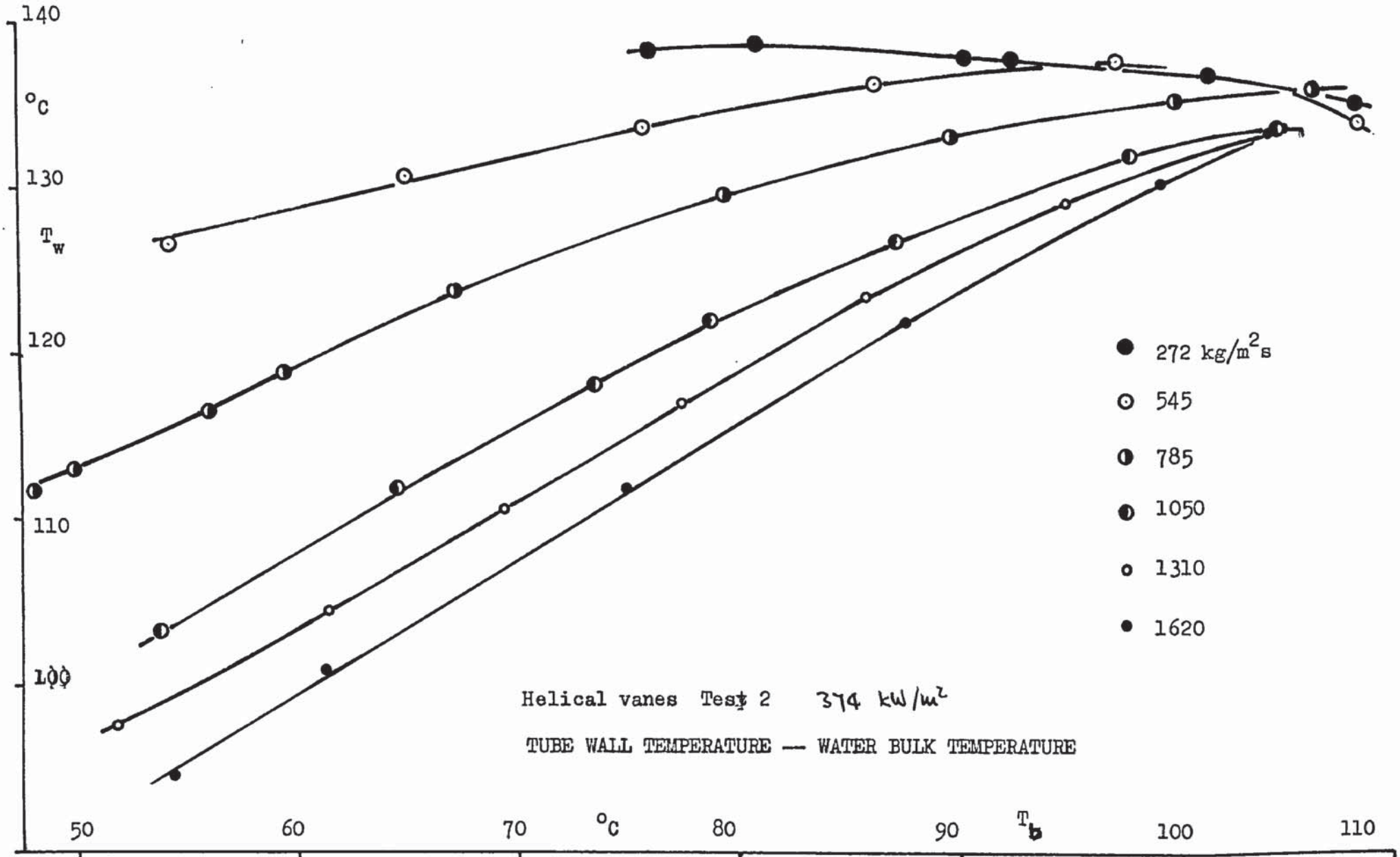
140
°C
130
T_w
120
110
100
272 kg/m²s
545
785
1050
1310
1620
Helical vanes Test 2 374 kW/m²
TUBE WALL TEMPERATURE — WATER BULK TEMPERATURE
50
60
70
°C
80
90
T_b
100
110

G 4.23

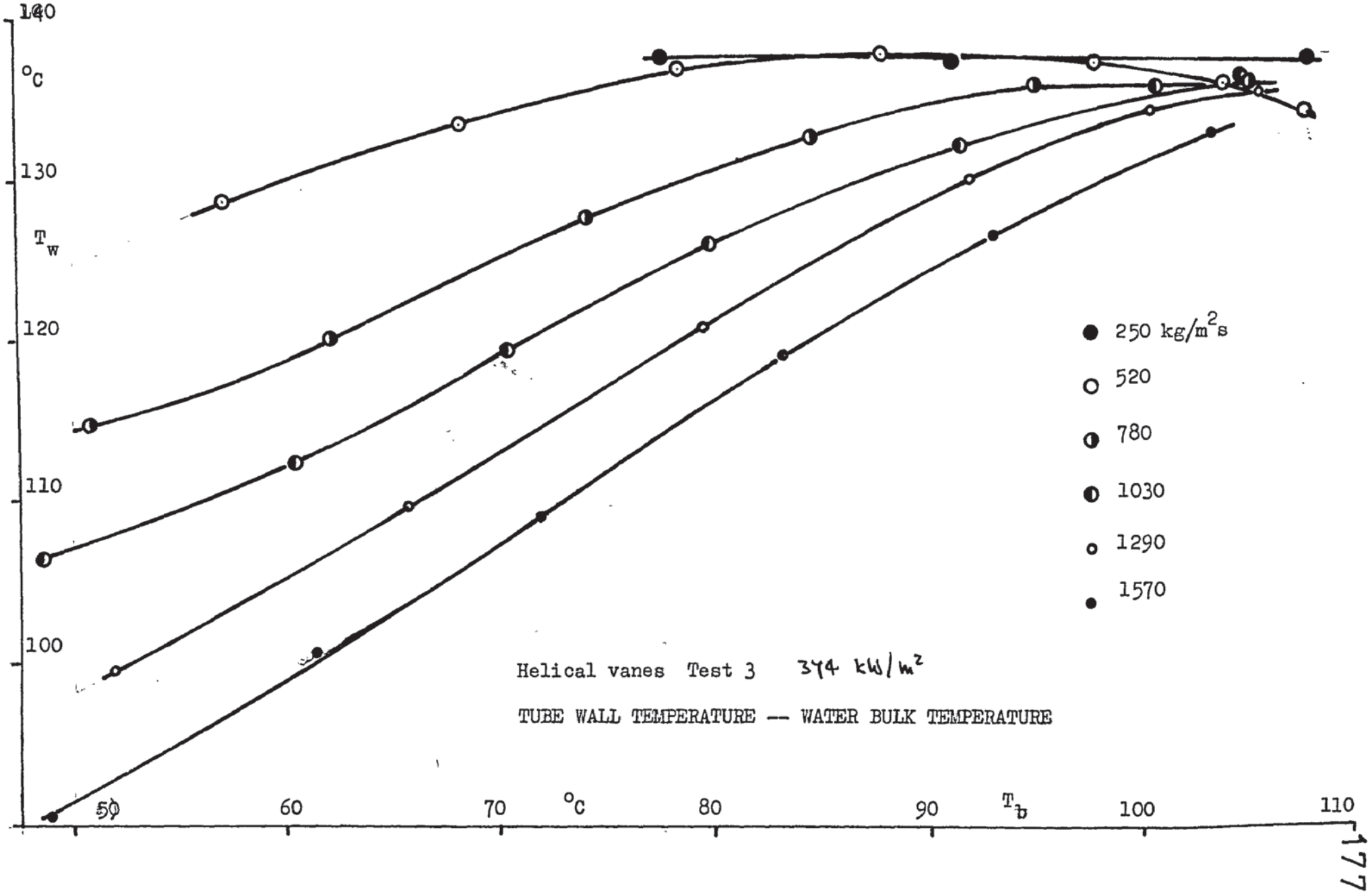
140
°C
130
T_w
120
110
100
250 kg/m²s
520
780
1030
1290
1570
Helical vanes Test 3 374 kW/m²
TUBE WALL TEMPERATURE — WATER BULK TEMPERATURE
50
60
70
°C
80
90
T_b
100
110

G 4.24

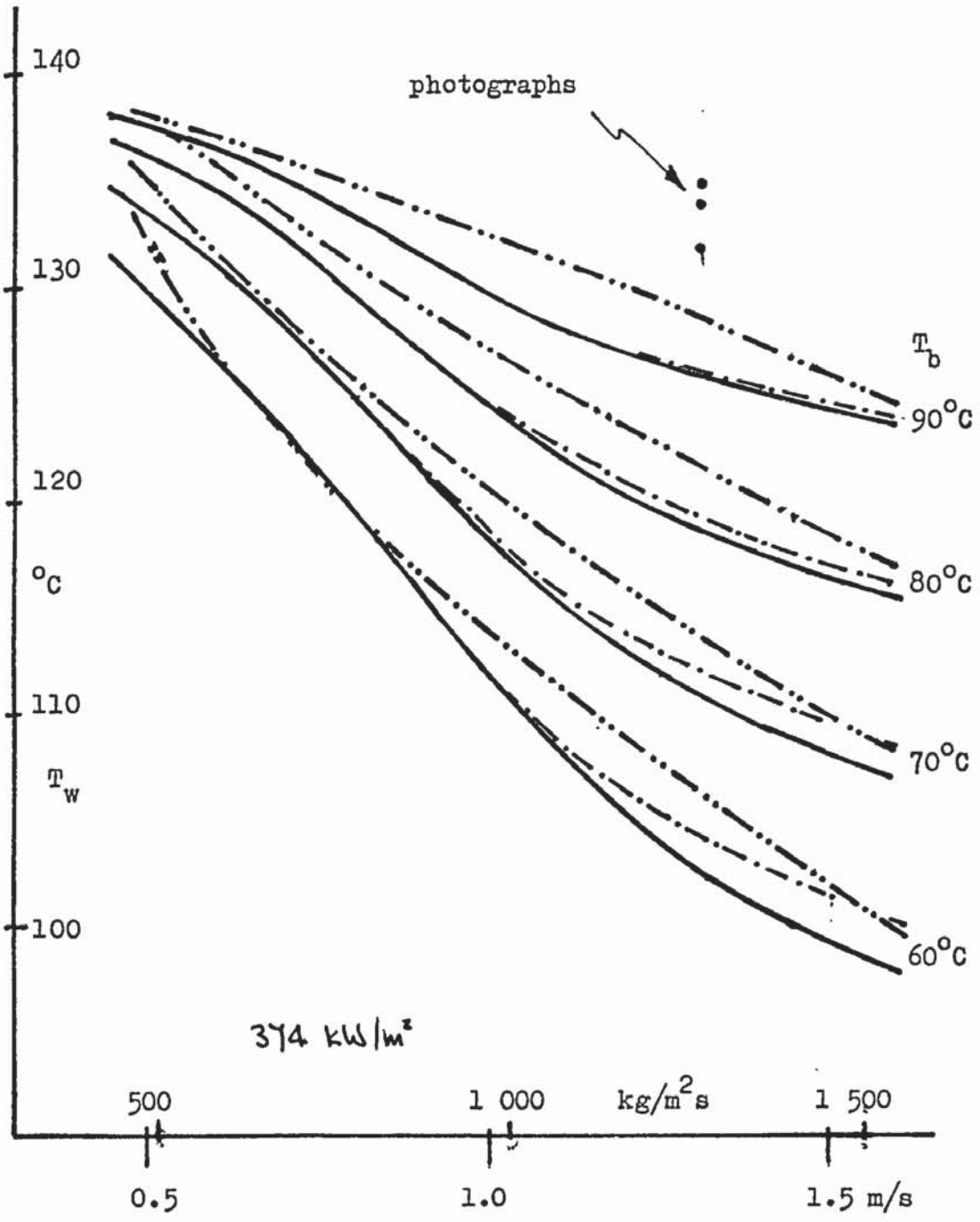

TUBE WALL TEMPERATURE — WATER MASS RLOW RATE

FOR For four set values of water bulk temperature and three types of guide vane.

Straight 1 ——————
Helical 2 —·—·—·—
Helical 3 —··—··—

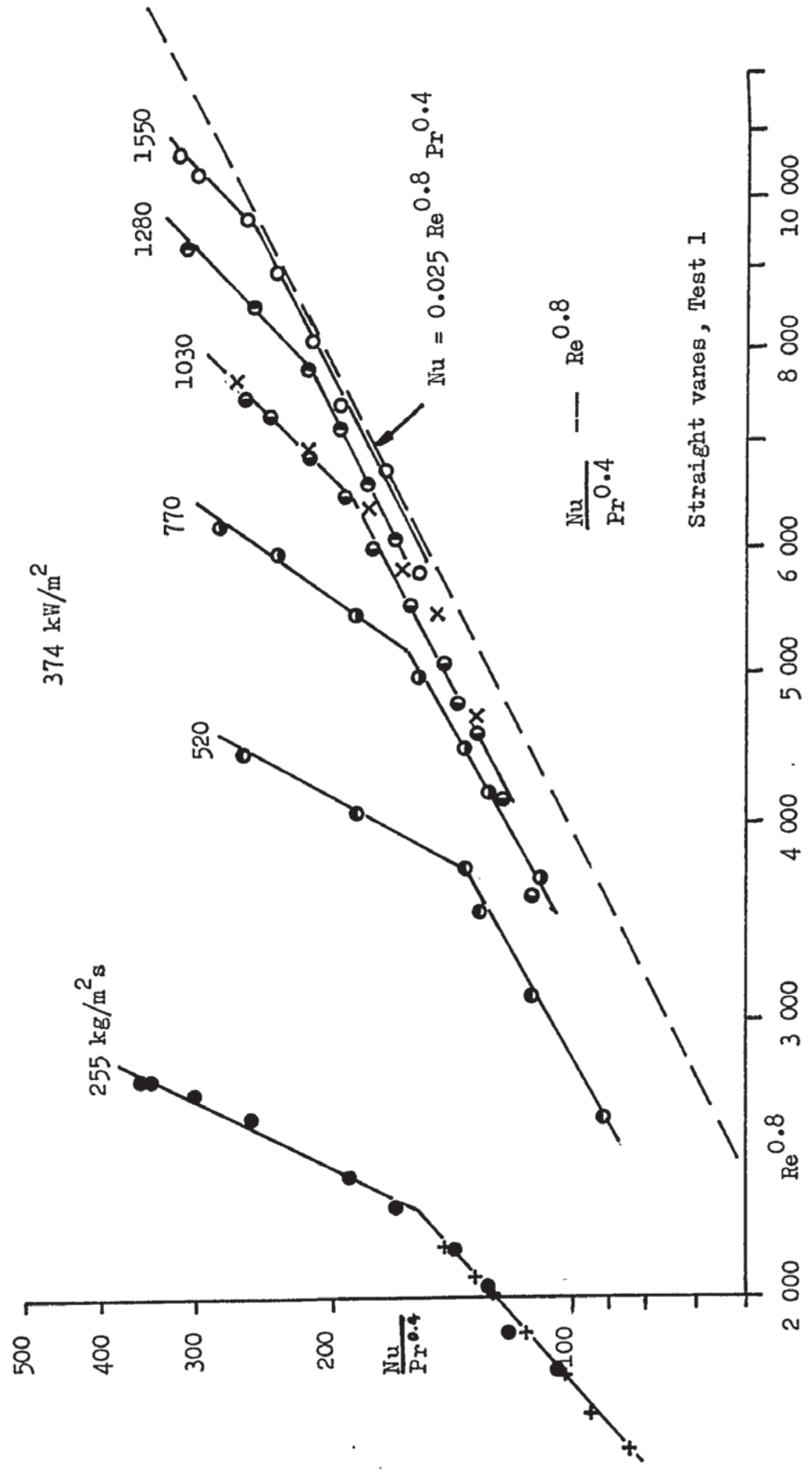
Straight vanes, Test 1
Nu = 0.025 Re^0.8 Pr^0.4
Nu/Pr^0.4 — Re^0.8
374 kW/m^2
255 kg/m^2 s
1550
1280
1030
770
520
Nu/Pr^0.4
Re^0.8
2 000
3 000
4 000
5 000
6 000
8 000
10 000
100
200
300
400
500

G 4.26

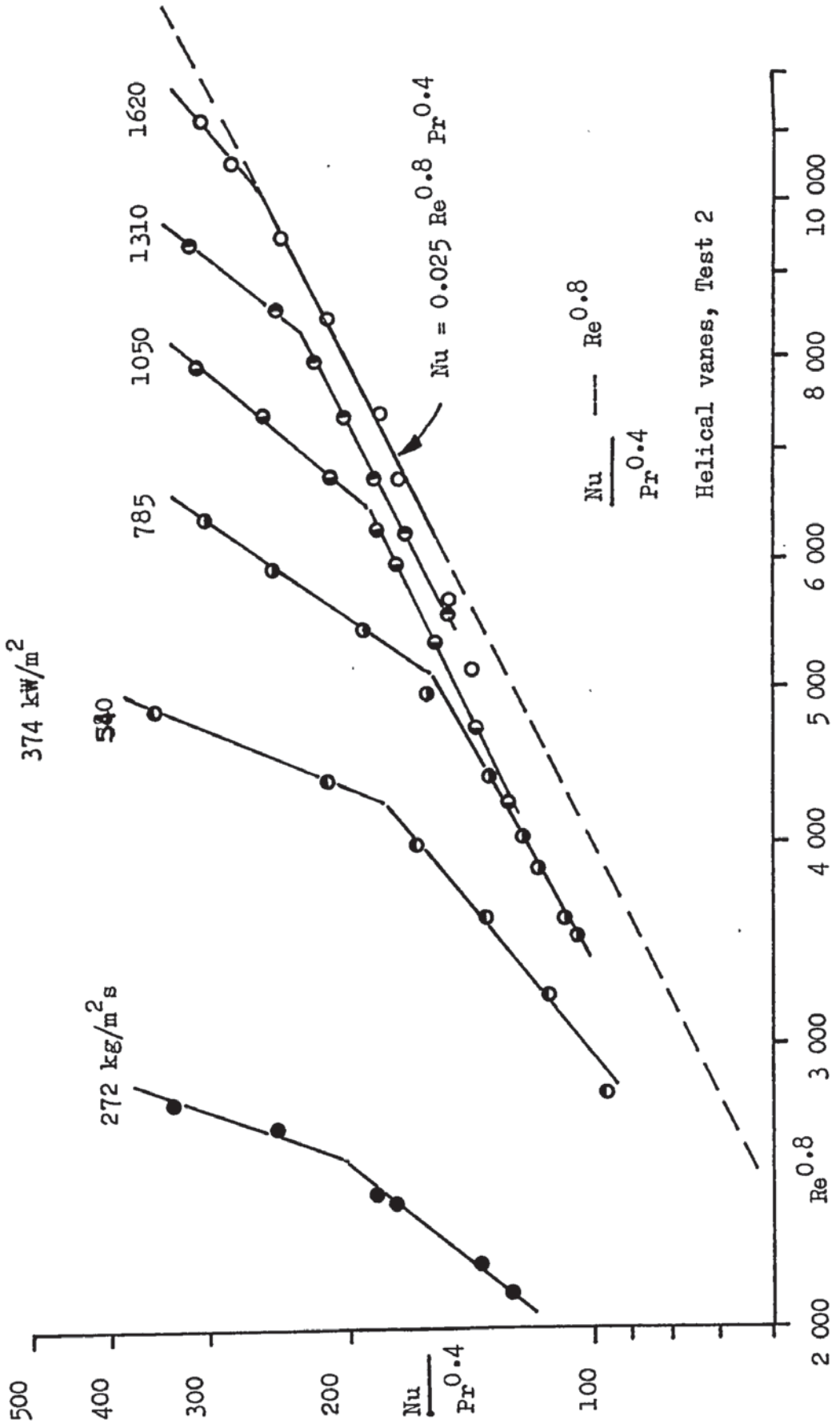
374 kW/m²
540
785
1050
1310
1620
272 kg/m²s
Nu = 0.025 Re^0.8 Pr^0.4
Nu / Pr^0.4 — Re^0.8
Helical vanes, Test 2
Nu / Pr^0.4
Re^0.8
500
400
300
200
100
2 000
3 000
4 000
5 000
6 000
8 000
10 000

G 4.27

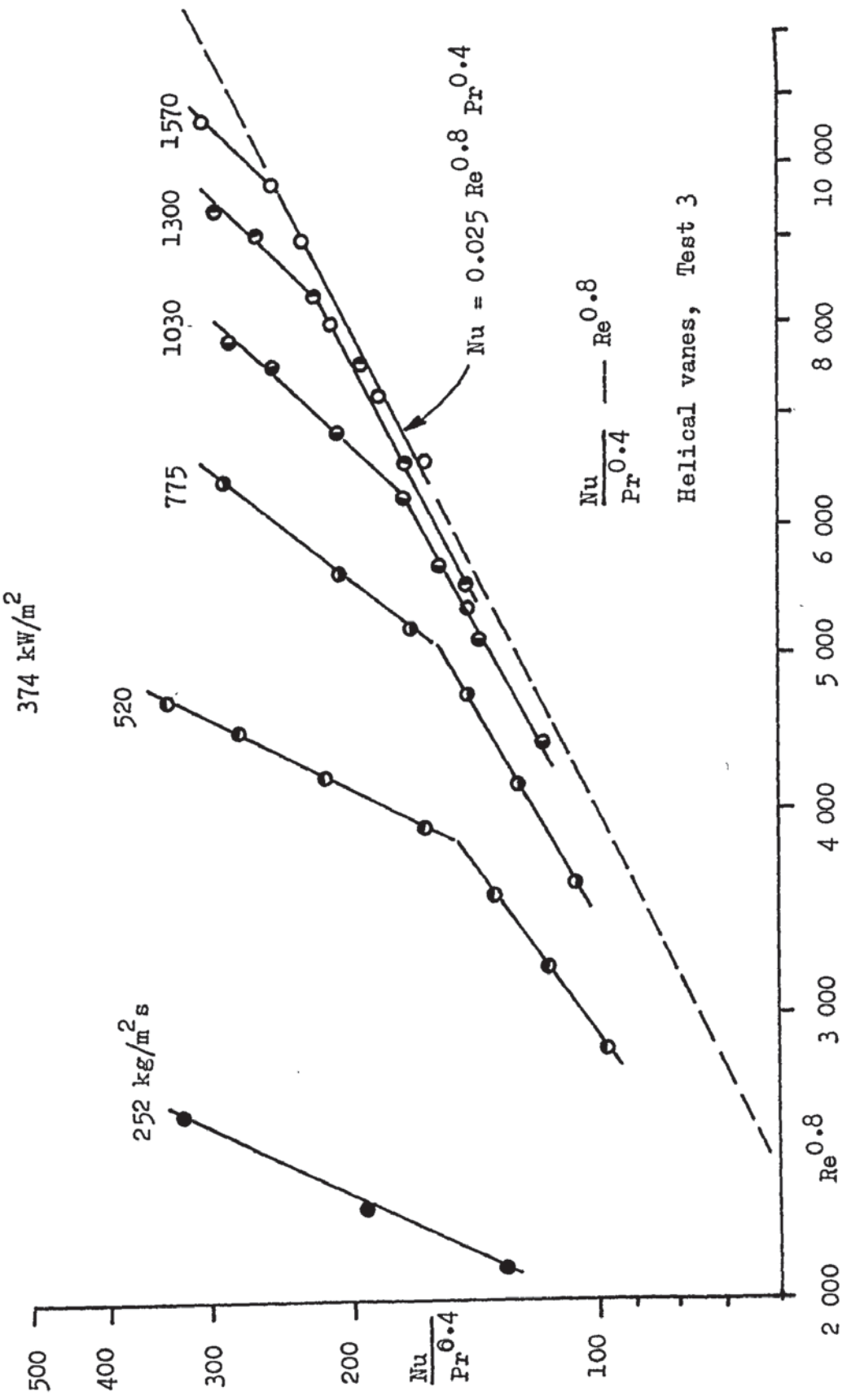
374 kW/m²
252 kg/m²s
520
775
1030
1300
1570
Nu = 0.025 Re^0.8 Pr^0.4
Nu/Pr^0.4 — Re^0.8
Helical vanes, Test 3
Nu/Pr^0.4
Re^0.8
500
400
300
200
100
2 000
3 000
4 000
5 000
6 000
8 000
10 000

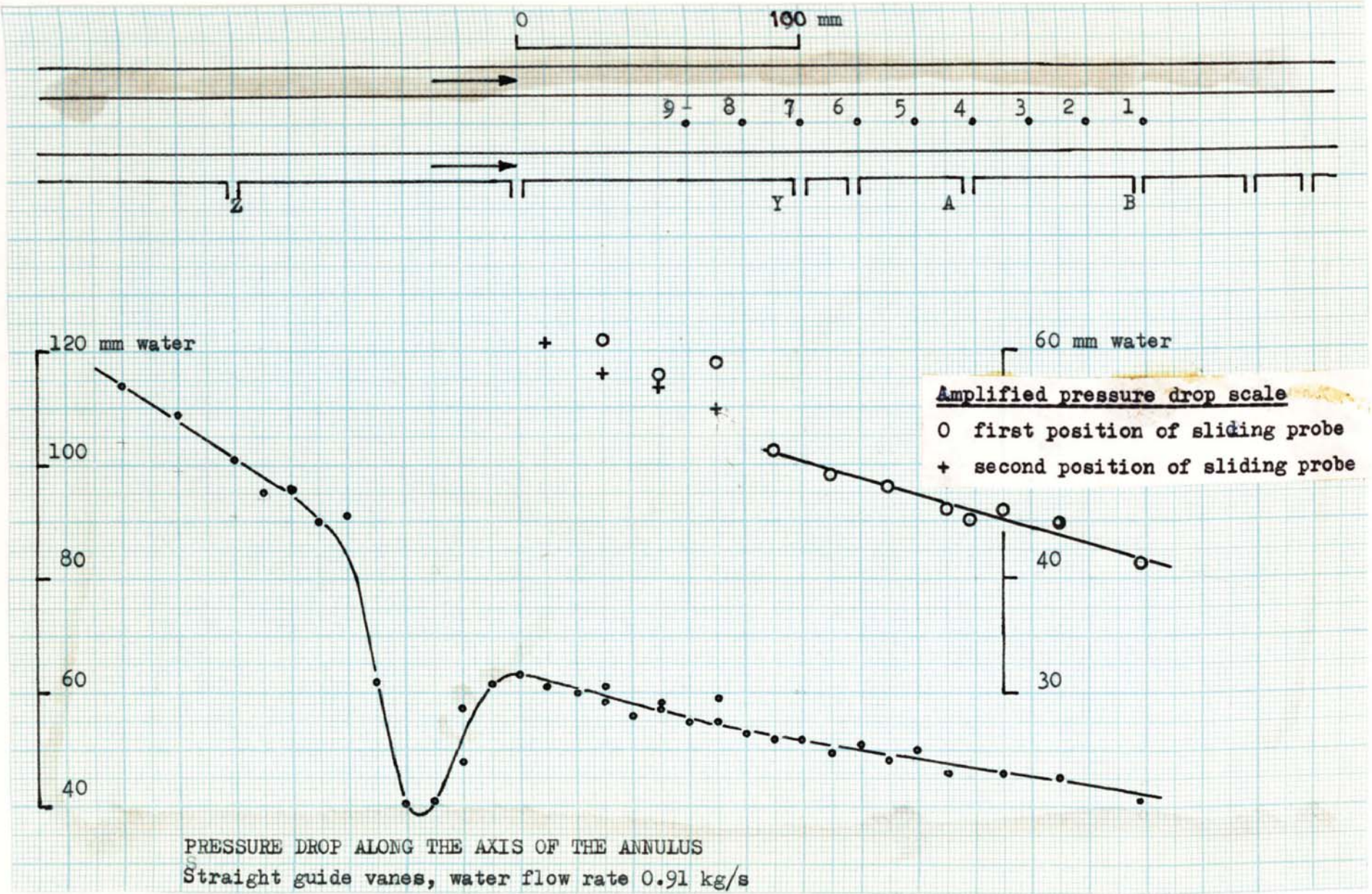

PRESSURE DROP ALONG THE AXIS OF THE ANNULUS
Straight guide vanes, water flow rate 0.91 kg/s

G 4.29

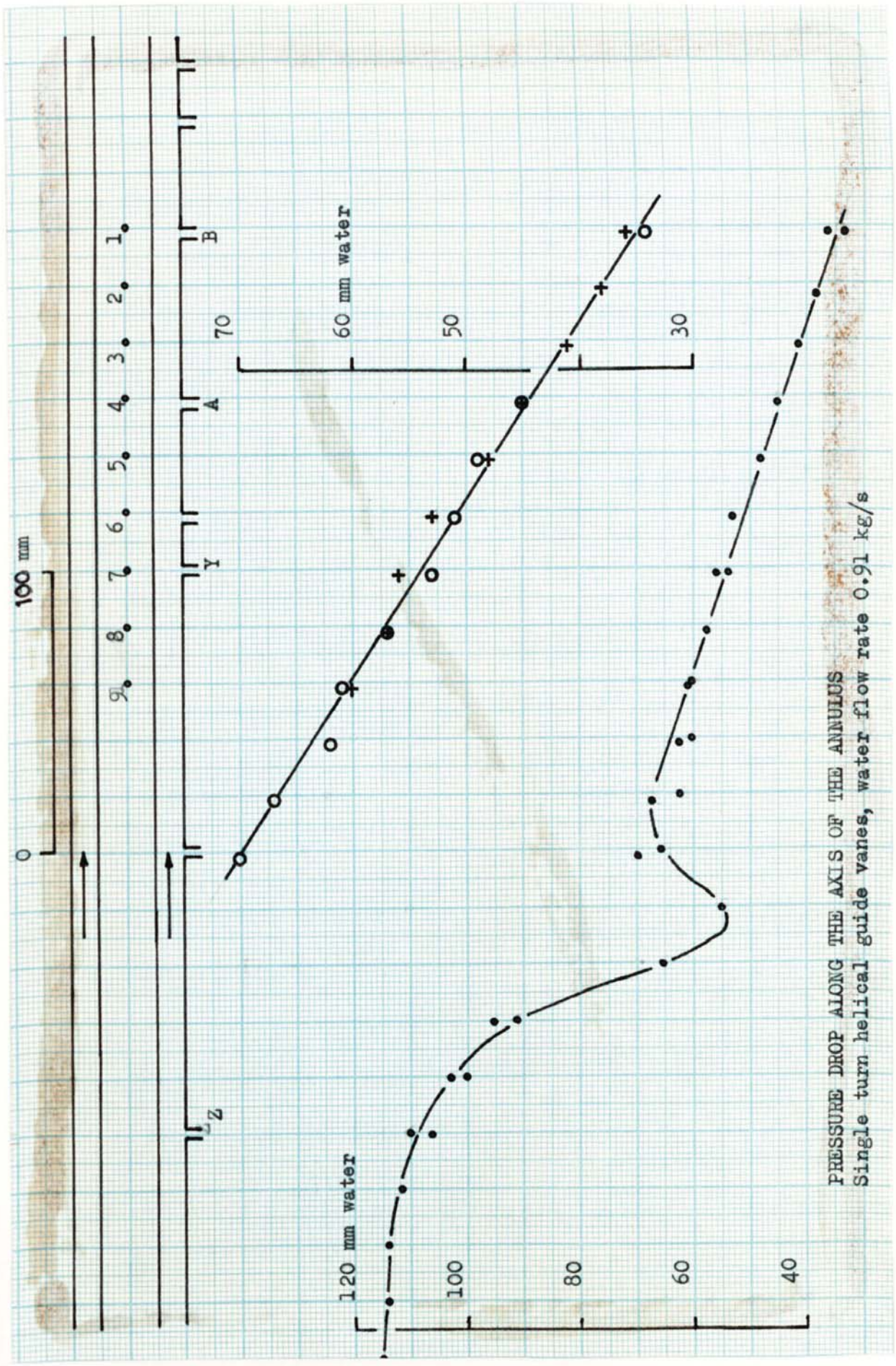

PRESSURE DROP ALONG THE AXIS OF THE ANNULUS
Single turn helical guide vanes, water flow rate 0.91 kg/s

G 4.30

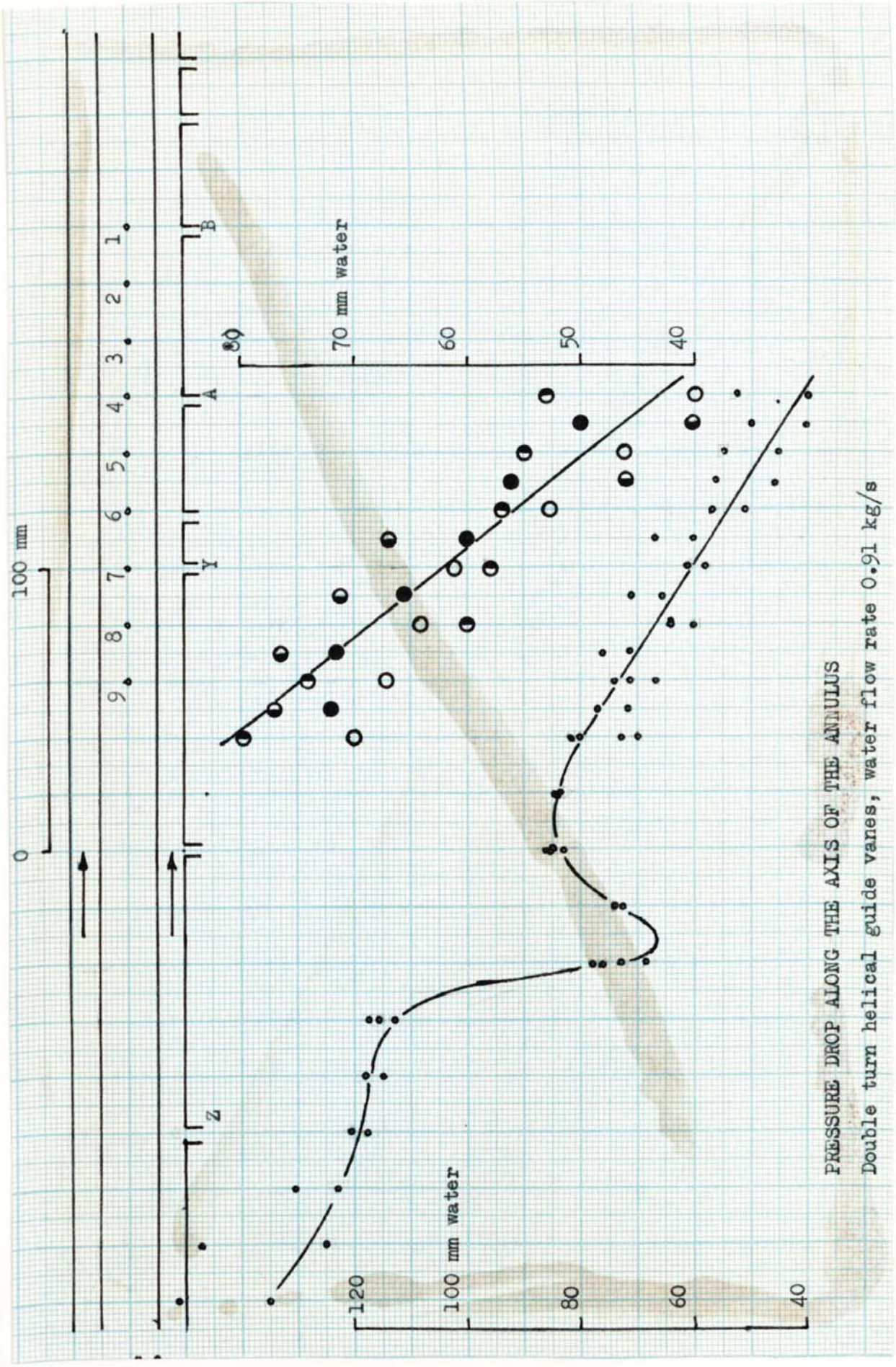

PRESSURE DROP ALONG THE AXIS OF THE ANNULUS
Double turn helical guide vanes, water flow rate 0.91 kg/s

G 4.31

4.7 FLOW VISUALIZATION.

INTRODUCTION.

Having measured the effect of a step change in flow section on the heat transfer coefficient and the pressure drop it was thought that the visualization of the flow pattern at the change of section would give some insight into the mechanism of heat transfer in that area. The photographs of the two-phase flow through the annulus had been taken using a microsecond flash light source and although they gave a picture of the vapour bubble sizes they did not give information on the fluid flow pattern. Two methods were planned, one was to use air bubbles injected into the flow and photographed with an exposure time of the order of milliseconds. The second method planned was to use a Schlieren optical system to detect the fluid boundary layer, this required the construction of a special test section.

VAPOUR BUBBLES.

The photographs of the stepped annular test section using a flash source with duration of approximately five microseconds showed the presence and size of the vapour bubbles. Two photographs were taken at each test one illuminated from above and the other from below, to give as clear a picture as possible of the flow in the large and small section of the annulus.

It can be clearly seen that the bubble size is inversely proportional to the fluid velocity and for the diverging upward flow the effect of the step enlargement is still felt for five equivalent diameters downstream as witnessed by the suppression of boiling, P 4.12. For the converging upward flow a suppression of

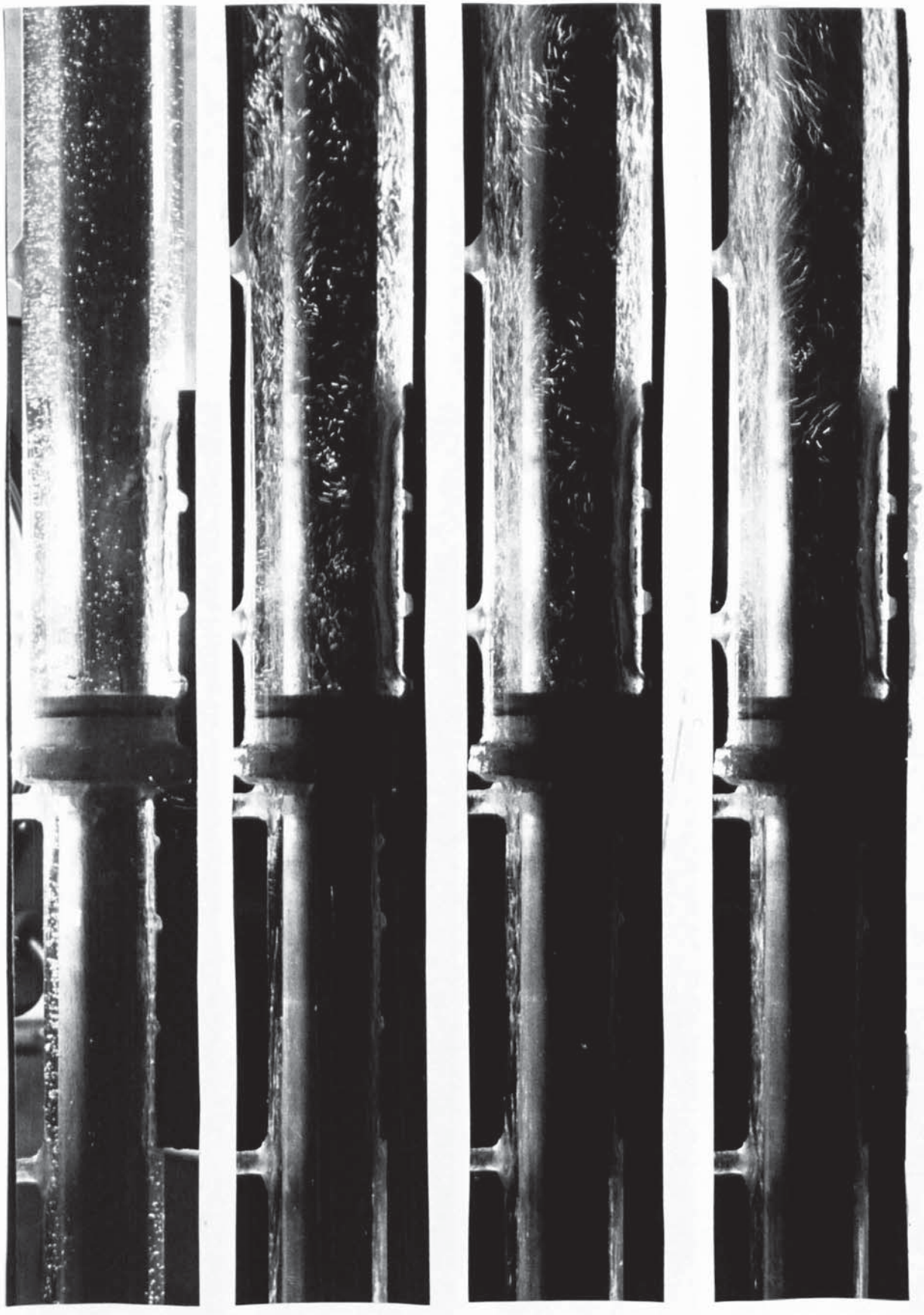

5us flash 2ms f4 4ms f4 10ms f5.6

Upward flow, Air/Water = 1/20

P 4.27

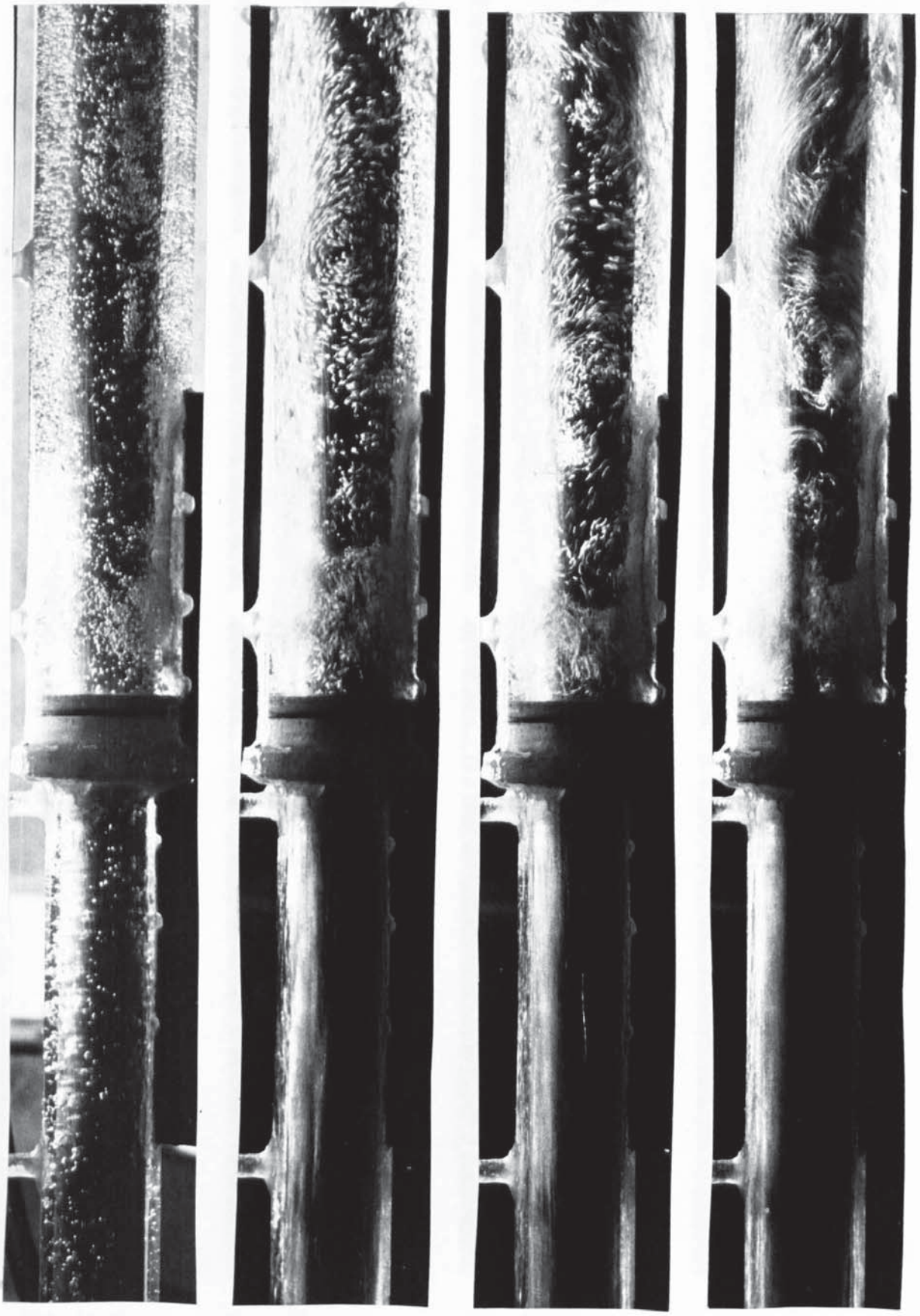

5us flash 2ms f4 4ms f4 10ms f5.6

Upward flow, Air/Water = 1/8

P 4.28

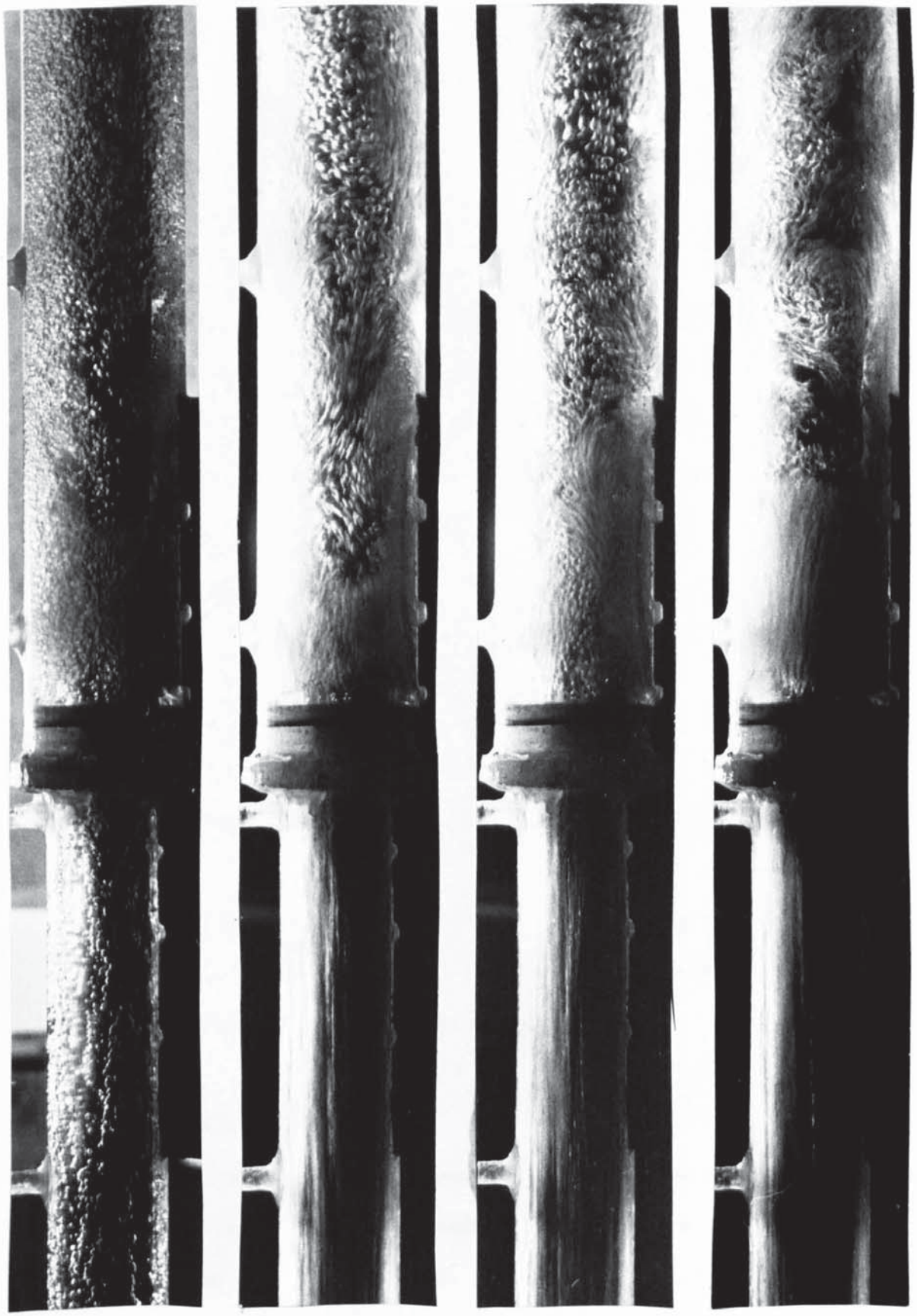

5us flash 2ms f4 4ms f4 10ms f5.6

Upward flow, Air/Water = 1/4

P 4.29

PAGE MISSING IN ORIGINAL

boiling can be seen immediately downstream of the step convergence, P 4.3.

AIR BUBBLES.

The air bubbles were injected into the water flow at the lower entrance to the test section, D 3.24, and the central tube of the annulus was not heated during these experiments. Three ratios of air to water flow were used and for each ratio photographs were taken for a range of exposure times. Only the step divergent section was used in this way since the view immediately downstream of the step convergent section was masked by the epoxy resin joint piece, D 4.3, which was translucent but not transparent.

The test conditions based on the water flow only were:

Annulus O.D mm	Flow rate kg/s	Velocity m/s	Density kg/m^3	Viscosity kg/ms	Re
25.4	0.914	4.115	1001	0.001136	23 000
38.1	0.914	1.07	1001	0.001136	18 000

and the volumetric ratios of water to air employed were 20:1, 8:1 and 4:1.

The photographs P 4.27-29 show a recirculating hold up of bubbles immediately downstream of the step enlargement and also flow vortices developing further downstream.

SCHLIEREN SYSTEM.

The flow visualization by vapour and air bubbles whilst demonstrating the fluid flow pattern cannot show the heat transfer behaviour other than by inference. If the flow could be viewed from a direction tangential to the annulus section then Schlieren or interferometry methods could be used to visualize the boundary layer

and the pattern of turbulence in the bulk fluid, D 4.8. A test section was constructed to simulate this view point and a Schlieren optical system employed to illuminate it.

The system, D 3.26, P 3.17, was operated with a black and white recording film, since this is more sensitive than colour but although prints of good definition were obtained, P 4.30-31, it was seen that a colour system would offer significant advantages in detecting the fluid boundary layer.

The colour system used was arranged to indicate hot fluid as red and cold fluid as blue this being psychologically correct for viewing, whilst any vapour bubbles showed as black areas.

Photographs were taken with water flowing through the test section both for a convergent step and a divergent step. Freon 11 was used in the test section to achieve fully developed nucleate boiling with the heating power available and photographs were taken of flow through a convergent step with nucleate boiling present.

With both water and Freon 11 the boundary layer could be clearly seen and also the turbulence in the cooler bulk fluid P 4.32-38. The illumination was produced by an electrical discharge through an argon gap and had a duration of approximately five microseconds so that all fluid movement was effectively frozen. The test section was used in the horizontal position as compared with the vertical position of the annular flow channel used for all of the previous tests so to this extent the processes of heat transfer were not absolutely the same.

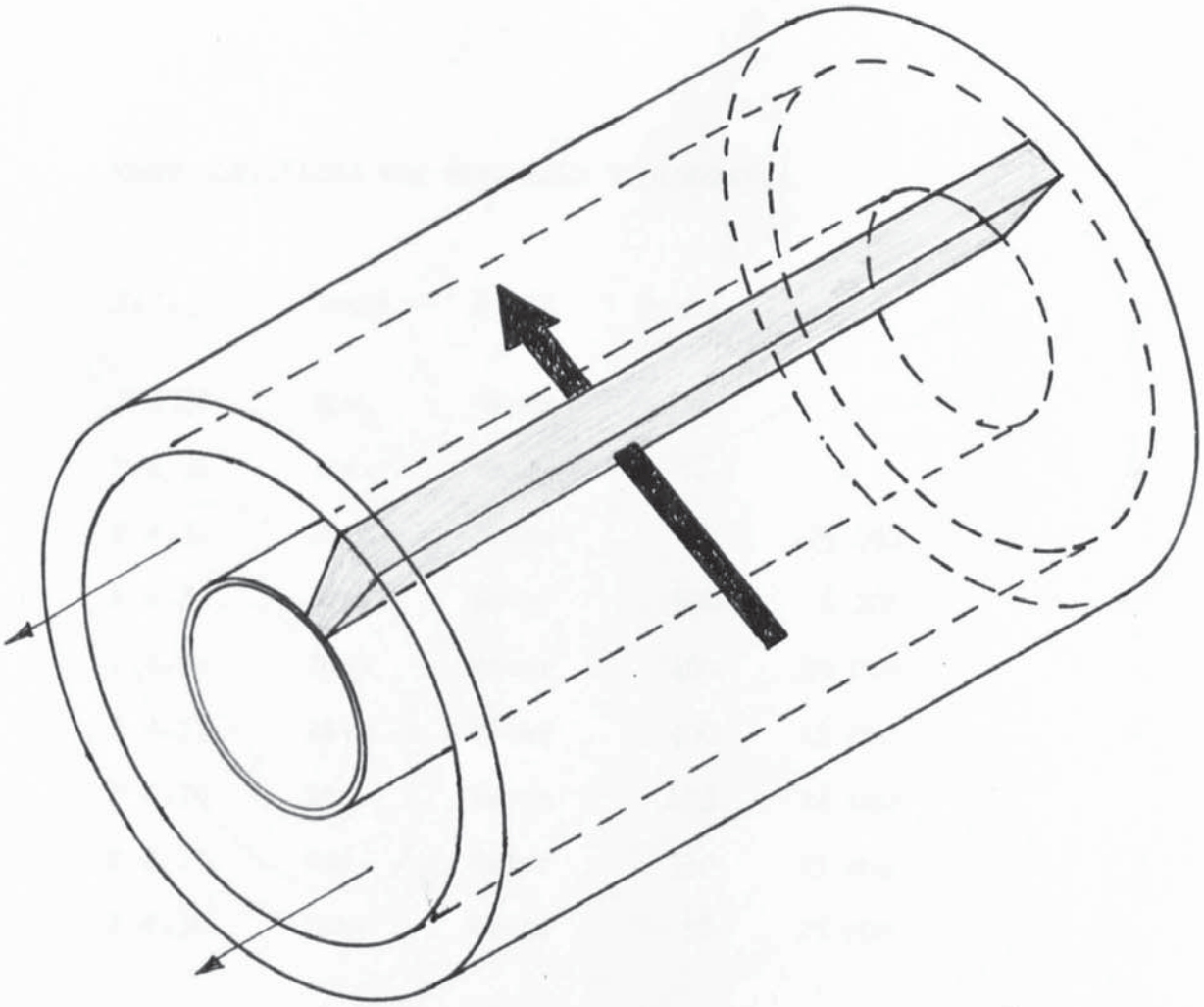

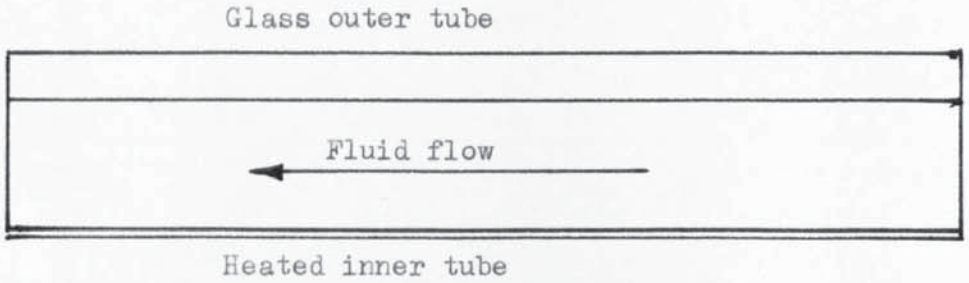

TANGENTIAL VIEWPOINT REQUIRED TO VISUALIZE THE BOUNDARY LAYER

TEST CONDITIONS FOR SCHLIEREN PHOTOGRAPHS

Ref.	Shape	Fluid	Power kW/m^2	Re
P 4.30	Div.	Water	-	-
P 4.31	Div.	Water	-	-
P 4.32	Para.	Freon	10	25 000
P 4.33	Con.	Water	530	6 200
P 4.34	Div.	Water	400	29 000
P 4.35	Div.	Water	400	19 000
P 4.36	Con.	Water	133	24 600
P 4.37	Con.	Water	530	19 800
P 4.38	Con.	Freon	58	25 000

T 4.7

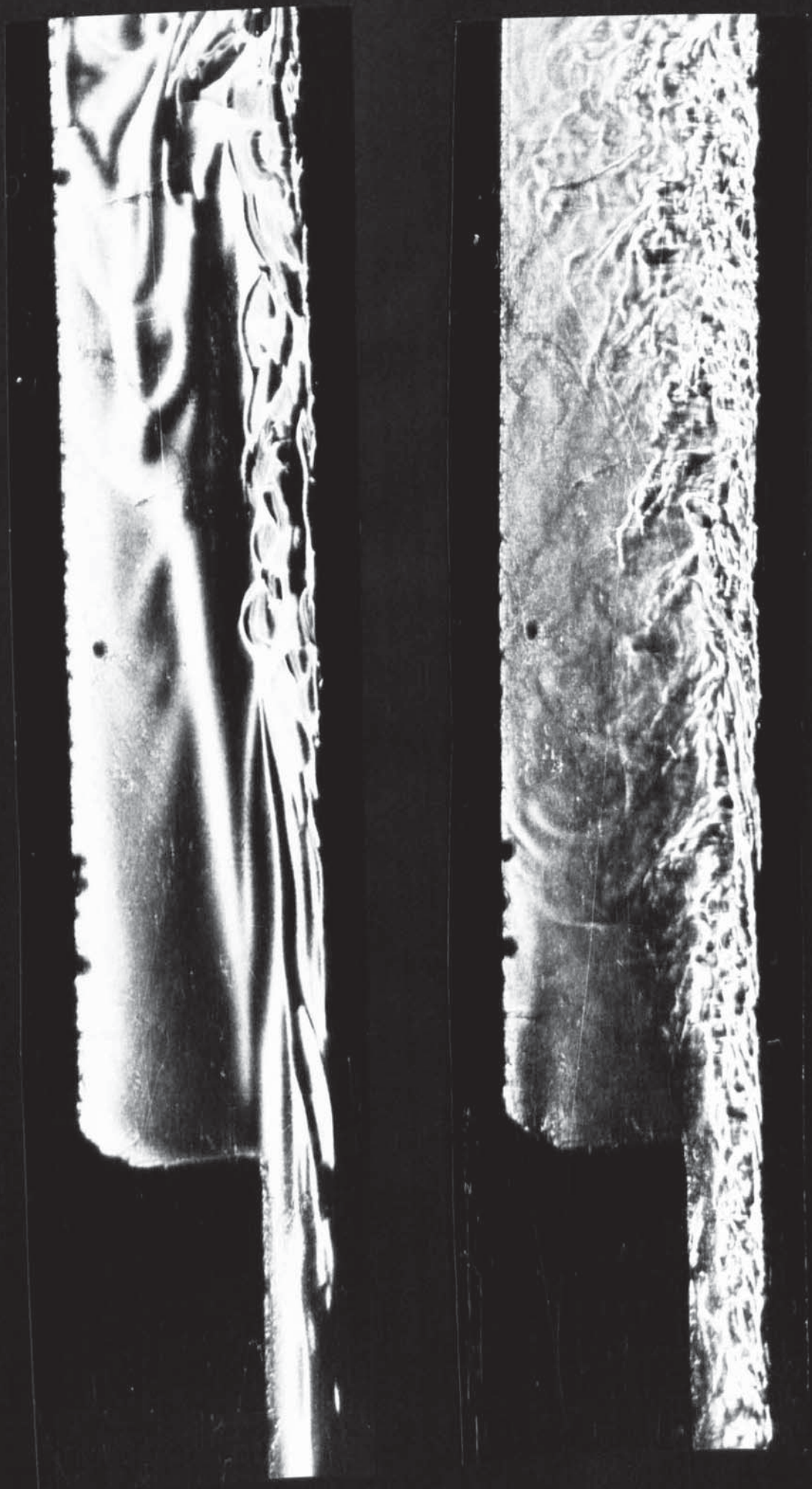

P 4 30

P 4.31

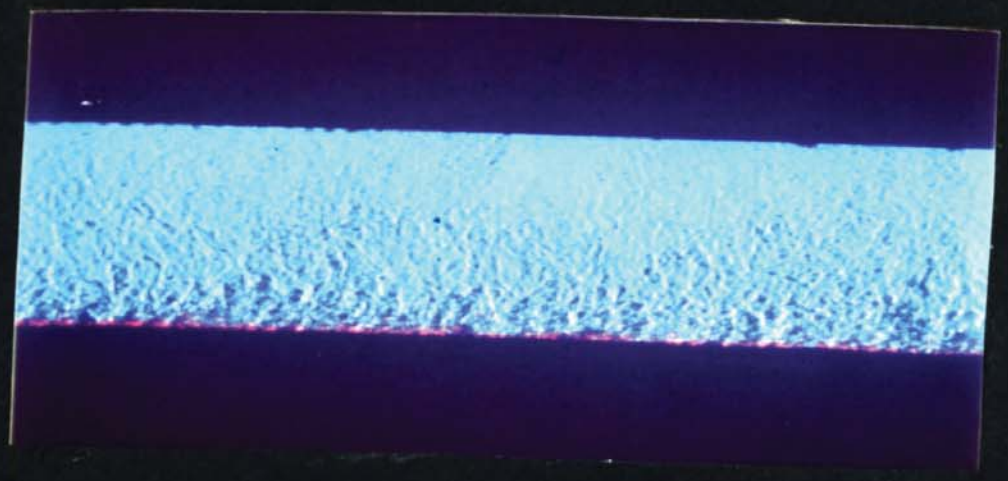

P 4,32

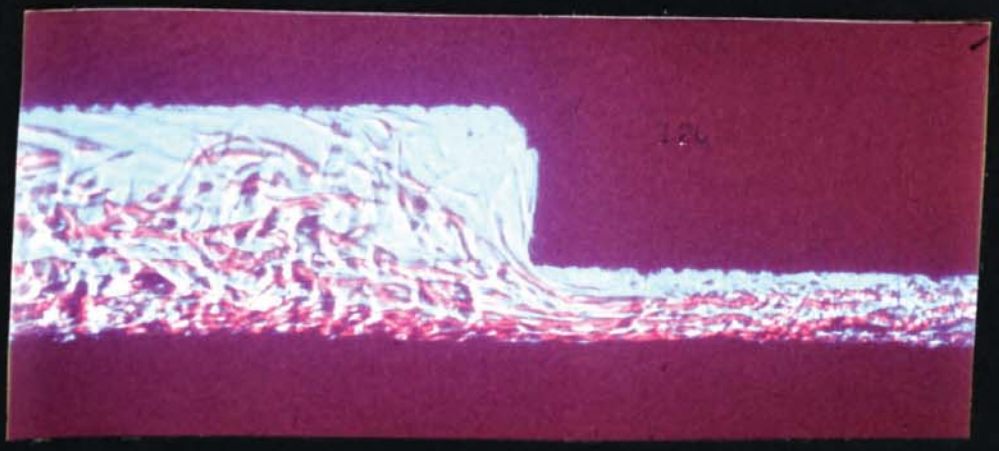

P 4,33

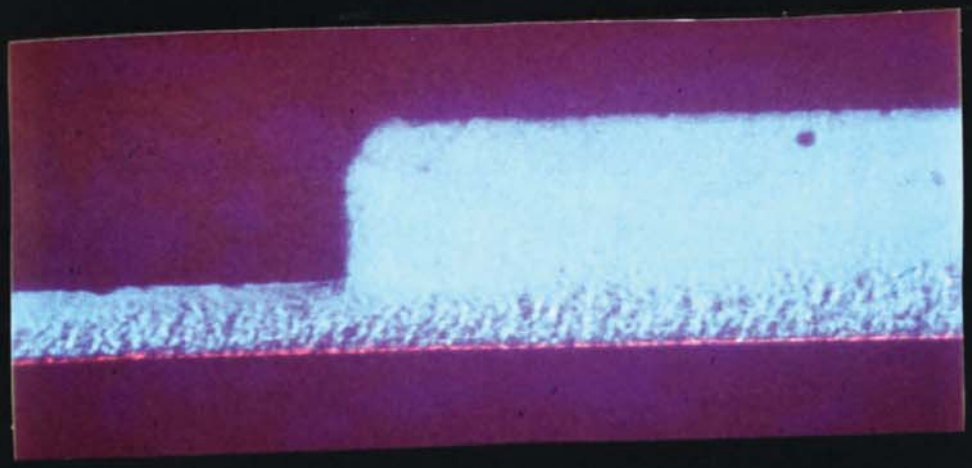

P4.34

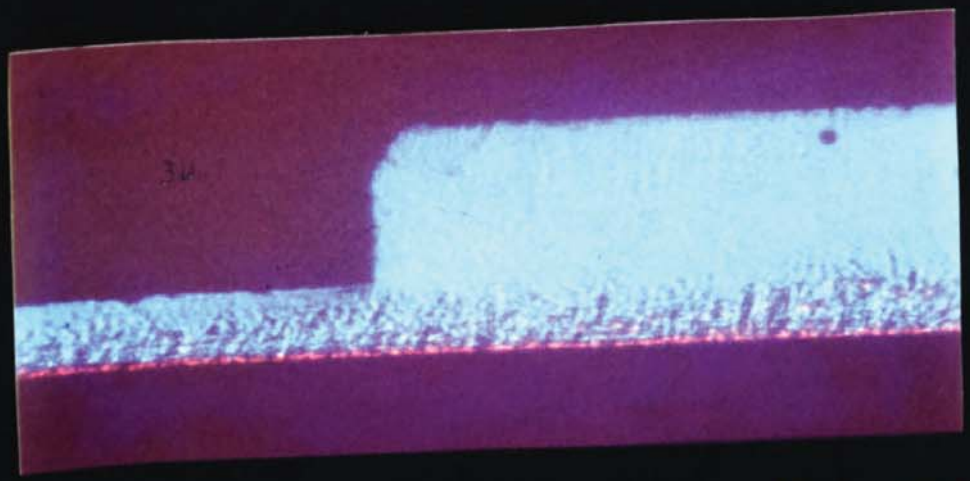

P4.35

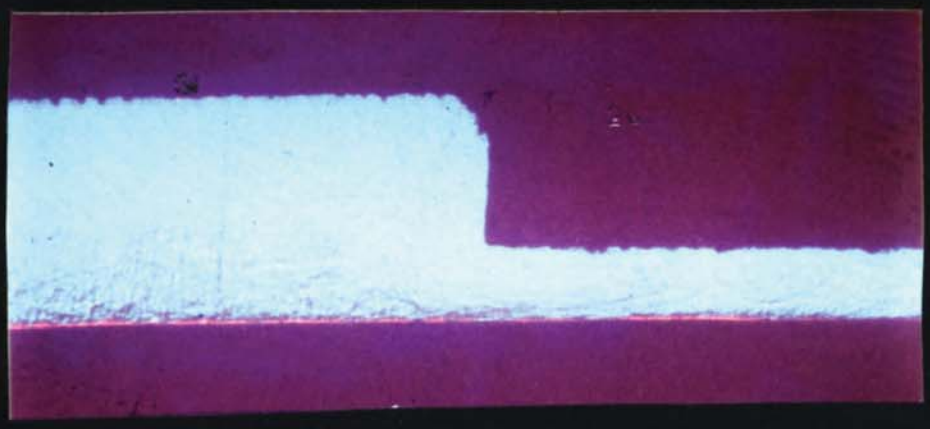

P4.36

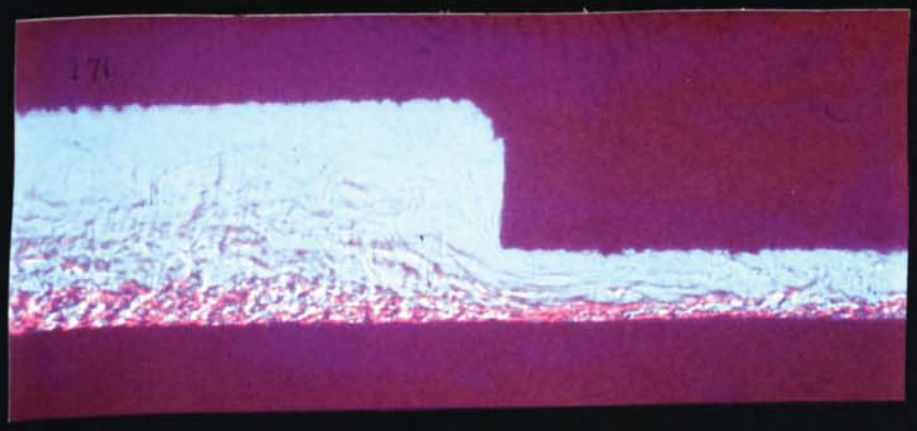

P4.37

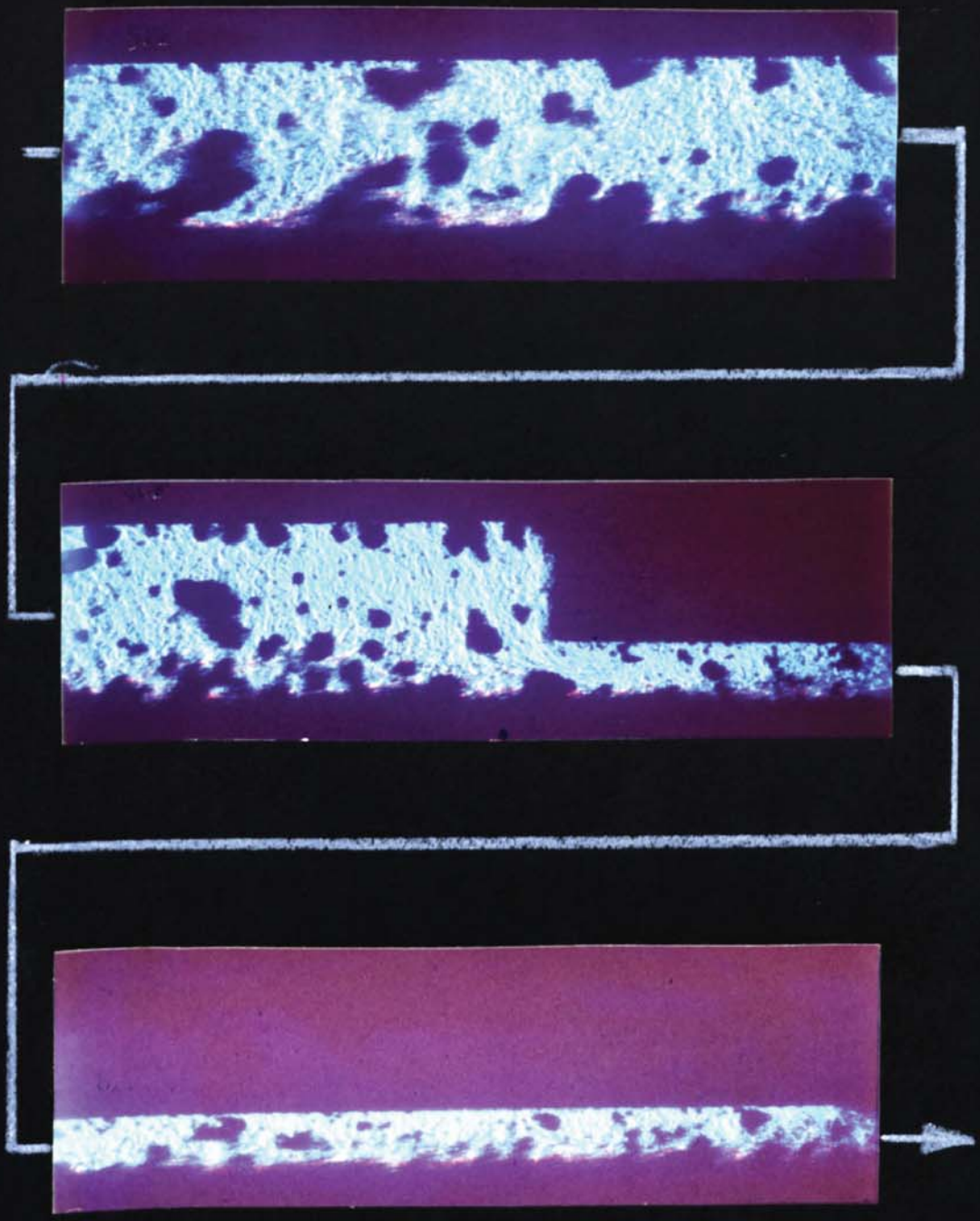

P4.38

APPLICATION OF RESULTS

PAGE NUMBERING AS ORIGINAL

5.1 SINGLE PHASE FLOW THROUGH A PLAIN ANNULUS WITH HEATING AT THE INNER WALL ONLY

The correlation derived from the experimental results,

$$St.\ Pr_b^{0.6} = 0.025\ Re_b^{-0.199}$$

can be compared with the results obtained by previous workers.

Monrad and Pelton, R 16, found that for d_o/d_i, of 1.65 and 2.45,

$$St.\ Pr^{0.66} = 0.023\ \psi\ Re^{-0.2}$$

where $\psi = 0.87\,(d_o/d_i)^{0.53}$

Substituting the value of the experimental, d_o/d_i, into this expression gives,

$$\psi = 0.84\,(2)^{0.53} = 1.257$$

and $$St.\ Pr^{0.66} = 0.029\ Re^{-0.2}$$

Wiegand and Baker, R 57, proposed that over the range of values of, d_o/d_i, between 1 and 10

$$\psi = (d_o/d_i)^{0.45}$$

thus for $d_o/d_i = 2$, $\psi = 1.414$

and $$St.\ Pr^{0.66} = 0.0325\ Re^{-0.2}$$

Thus the correlation obtained compared well with previous correlations and could be expressed as,

$$St.\ Pr_b^{0.6} = 0.0173\ Re_b^{-0.199}\ .\ (d_o/d_i)^{0.53}$$

after the form of Monrad and Pelton, to extend its use to other diameter ratios.

or as $$St.\ Pr_b^{0.6} = 0.0183\ Re_b^{-0.199}\ .\ (d_o/d_i)^{0.45}$$

after the form of Wiegand and Baker, it being understood that it is

limited in application to water between 20°C and 70°C which was the range of bulk temperatures employed in the tests.

5.2 TWO-PHASE FLOW THROUGH A PLAIN ANNULUS

The results are presented graphically, G 4.4 - 4.6, and referring to, G 4.5, it can be noted that, although the area of visible boiling is indicated, all wall temperatures are above saturation temperature. The boiling process in its inception can thus be said to be difficult to detect visually even with good lighting and close scrutiny. The lines for different values of mass velocity merge when the boiling mechanism becomes dominant over the forced convection mechanism, the wall temperature to the right of this point is reducing slightly due to the increasing liquid and vapour velocity forced by the generation of vapour.

The data of G 4.5 was re-used to plot G 4.6 showing $Nu/Pr^{0.4}$ against $Re^{0.8}$. Here the boiling mechanism appears as two regimes, the first, represented by the lower portion of the cranked line has a slope which is similar to that for the single phase conditions, the second regime has a very much steeper slope.

In the region of the first regime boiling is present but the dominant mechanism of heat transfer is by forced convection. Above the change in the slope, the dominant heat transfer mechanism is that of mass exchange due to boiling. The lines can be represented by an equation of the form,

$$\frac{Nu}{Pr^{0.4}} = B\,Re^{0.8} + C$$

where the value of C depends on whether the region is above or below the break point in the line, and on the mass flow rate. For the case of single phase flow the value of C is constant for all conditions.

The method of correlating sub-cooled boiling heat transfer data for water flowing through a round pipe by an expression of a similar form has been used by Papell, R 41, who gave the final form as

$$\frac{Nu_{bo}}{Nu_{nbo}} = 90.0\left(\left(\frac{\frac{q}{A}}{h_{fg}\,\rho_g\,V}\right)\left(\frac{h_{fg}}{c_p(t_s - t_b)}\right)^{1.2}\left(\frac{\rho_g}{\rho_f}\right)^{1.08}\right)^{0.7}$$

Since $Nu_{nbo} = C\,Re^{0.8}\,.\,Pr^{0.4}$

$$\frac{Nu_{bo}}{Pr^{0.4}} = C\left(\quad "\quad\quad "\quad\quad "\quad\right)^{0.7}.\ Re^{0.8}$$

It was thought that a comparison of the prediction of the Papell correlation with the test results would be of interest.

The correlation developed by Papell by using dimensional analysis to indicate the significant dimensionless groups had been tested against a range of data on water provided by a number of previous workers as well as his own experimental data.

The correlation is presented as a ratio of the experimental sub-cooled boiling Nu and the calculated non-boiling Nu, given by three dimensionless groups. The first group,

$$\left(\frac{\frac{q}{A}}{h_{fg}\,\rho_g\,V}\right)$$

which relates the volumetric rate of vaporization to the axial fluid velocity was first used by Sterman, R 38, and substantiated by Papell.

The second group,

$$\left(\frac{1}{t_s - t_b}\right)^{1.2} \cdot \left(\frac{h_{fg}}{c_p}\right)^{1.2} = \left(\frac{h_{fg}}{c_p(t_s - t_b)}\right)^{1.2}$$

was composed of the first term which was found empirically to correct for the subcooling effect and the second term was used as a multiplier to produce a non-dimensional group.

The third term,

$$\left(\frac{\rho_g}{\rho_f}\right)^{1.08}$$

was found to correct for the effect of pressure change.

This correlation was chosen, in preference to a more recently obtained correlation by Moles and Shaw, R 51, as it was based entirely on data for water and had not needed to be widened to accommodate other fluids. It was in fact fitted against some data from ammonia with some success. The fact that the correlation was produced for flow through a round pipe was not considered to preclude its use for annular flow although some loss of accuracy may result.

All of the experimental data presented for the two-phase flow through the annulus was taken at pressure level of 0.35 bar(gauge), (t_s = 108.2°C) and at a constant heat flux, 515 kW/m^2. Papell's expression can therefore be simplified for this application.

$\frac{q}{A} = 515\ kW/m^2$ $\qquad h_{Fg} = 2235\ kJ/kg$

$\rho_g = 0.78\ kg/m^3$ $\qquad \rho_F = 960\ kg/m^3$

$t_s = 108.2°C$ $\qquad c_p = 4.22\ kJ/kgK$

$$\frac{Nu_{bo}}{Nu_{nbo}} = 90.0\left(\left(\frac{515}{2235 \cdot 0.78 \cdot V}\right)\left(\frac{2235}{4.22(t_s - t_b)}\right)^{1.2}\left(\frac{0.78}{960}\right)^{1.08}\right)^{0.7}$$

$$\therefore\ Nu_{bo} = 0.025\, Re^{0.8}\, Pr^{0.4}\, 90.0\left(\text{" " "}\right)^{0.7}$$

$$\therefore\ \frac{Nu_{bo}}{Pr^{0.4}} = 2.25\left(0.2485 \cdot \frac{1}{V}\ \frac{1}{(t_s - t_b)^{1.2}}\right)^{0.7}$$

By first specifying the velocity, the value of $Nu_{bo}/Pr^{0.4}$ can be evaluated for a range of bulk temperatures and a graph drawn for comparison with the experimental results.

The comparison of the results predicted from the correlation with the results obtained experimentally is shown, T 5.1, G 5.1, for three values of mass velocity, 267, 770, and 1280 Kg/m^2S. The change in the slope is shown by the predicted result and it is generally of the same form as the experimental results but gives too high a value of $Nu/Pr^{0.4}$, of the order of +20% at the change region and the error increases at higher values.

Looking at the correlation it seems that in the first term the velocity in the denominator has a fixed single phase value whereas in practice the value would increase due to the formation of vapour. It seems that if a relationship could be developed to account for this velocity increase the correlation would fit the data more closely. Even as it stands the correlation is useful provided that the bulk temperature of the fluid does not approach within 20 K of the saturation temperature, and that Re_{Fo} does not exceed 50,000.

DATA USED IN PAPELL CORRELATION

Mass velocity = 1 280 kg/m^2s, Velocity = 1.33 m/s

T_b	Re	$Re^{0.8}$	t_s-t_b	$Nu/Pr^{0.4}$
40	40 100	4 800	68.2	96
50	48 100	5 500	58.2	126
60	56 500	6 300	48.2	169
70	65 400	7 100	38.2	232
80	74 500	7 900	28.2	344
90	84 100	8 600	18.2	520
100	93 600	9 300	8.2	1105

Mass velocity = 770 kg/m^2s , Velocity = 0.8 m/s

40	24 150	3 210	68.2	92
50	28 900	3 730	58.2	122
60	34 000	4 250	48.2	164
70	39 400	4 650	38.2	218
80	44 900	5 250	28.2	328
90	50 600	5 900	18.2	514
100	56 450	6 300	8.2	1080

Mass velocity = 1 280 kg/m^2s, Velocity = 1.33 m/s

40	40 100	4 800	68.2	96
50	48 100	5 500	58.2	126
60	56 500	6 300	48.2	169
70	65 400	7 100	38.2	232
80	74 500	7 900	28.2	344
90	84 100	8 600	18.2	521
100	93 600	9 300	8.2	1105

T 5.1

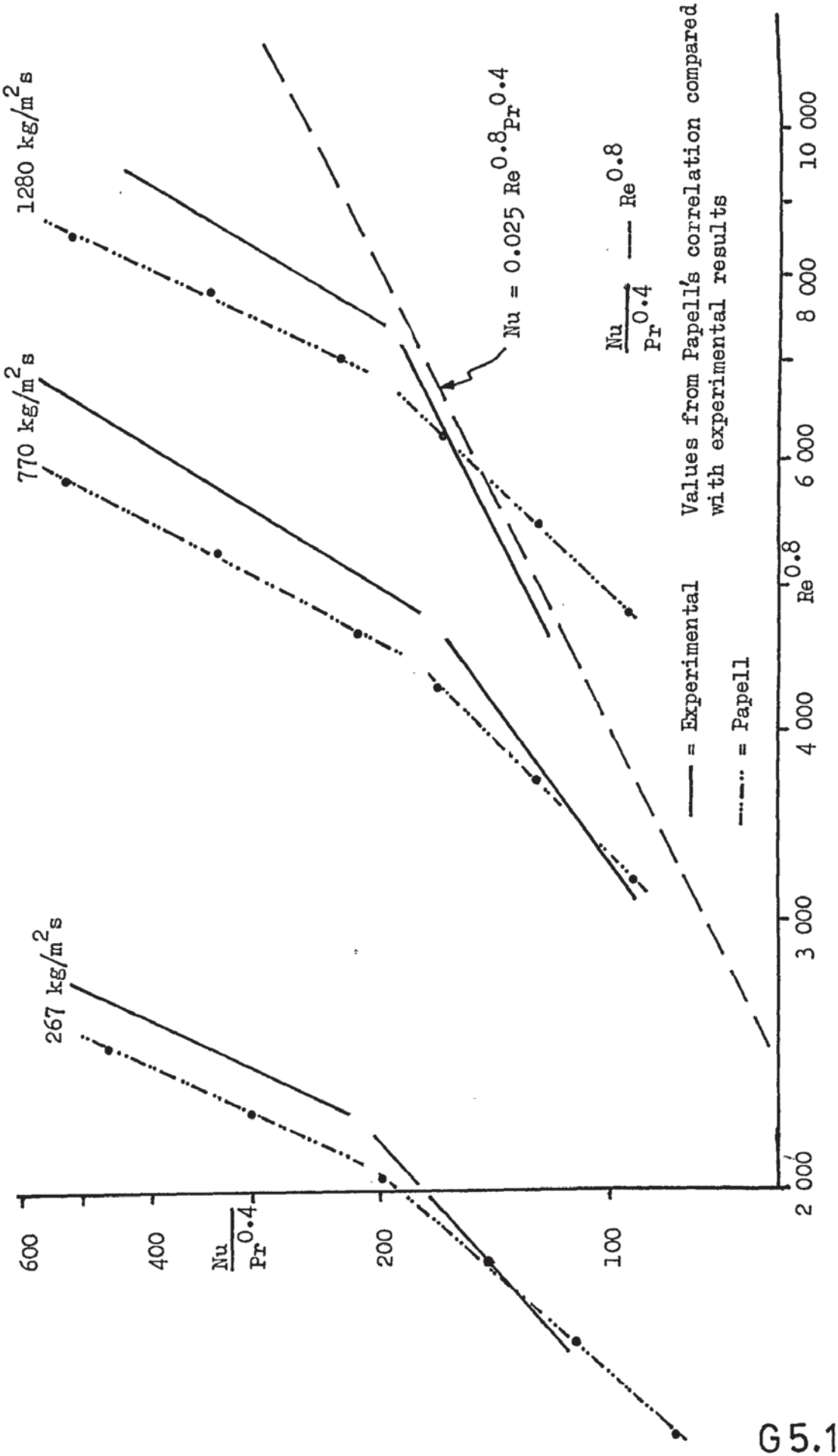
1280 kg/m²s
770 kg/m²s
267 kg/m²s
Nu = 0.025 Re^0.8 Pr^0.4
Nu / Pr^0.4 — Re^0.8
Values from Papell's correlation compared with experimental results
— = Experimental
-·-·- = Papell
Nu / Pr^0.4
Re^0.8
600
400
200
100
2 000
3 000
4 000
6 000
8 000
10 000

G5.1

5.3 SINGLE AND TWO-PHASE FLOW THROUGH A STEPPED ANNULUS

The results of the experimental work are presented as eight graphs, four for the convergent flow G 5.2 - G 5.5, and four for the divergent flow G 5.6 - G 5.9. Each graph represents a constant mass flow rate of water.

The reduction of this information to one curve for convergent flow and one curve for divergent flow would be a convenient way of presenting the results.

For the single phase flow of water through a round pipe with a step change in diameter, Ede, Hislop and Morris, R . 1, attempted to reduce their data to a single curve by using an N value where,

$$Nu = N . Pr^{0.4} . Re^{0.8}$$

for the case of flow through a straight pipe.

If the pipe contains a discontinuity in the flow area the heat transfer coefficient and hence Nu will increase (or decrease) as a result, and this increase or decrease over the value for a plain pipe can be accounted for by giving N an increased (or reduced) value. If the experiments carried out at different flow velocities and temperatures are to be reduced to one curve then the plot of,

$$N = \frac{Nu}{Pr^{0.4} . Re^{0.8}}$$

should correlate the range of results.

Ede, Hislop and Morris, were not able to reduce their data to a single curve by this method and they had to present their results as a number of curves, each representing a different value of the Re number.

PAPELL CORRELATION

In the experimental work described earlier the added complexity of sub-cooled boiling was present and any attempt to reduce the data to a single curve must rely on a sub-cooled boiling heat transfer correlation. The two available correlations are that of Papell, R 41, and that of Moles and Shaw, R 51.

The correlation of Papell,

$$\frac{Nu_{bo}}{Nu_{nbo}} = 90.0\left(\left(\frac{q/A}{h_{fg}\,\rho_g\,V}\right)\left(\frac{h_{fg}}{c_p(t_s-t_b)}\right)^{1.2}\left(\frac{\rho_g}{\rho_f}\right)^{1.08}\right)^{0.7}$$

was simplified by giving values to the fixed parameters

$q/A = 374\ kW/m^3$, $h_{fg} = 2235\ kJ/kg$, $c_p = 4.22\ kJ/kgK$

$\rho_g = 0.78\ kg/m^3$, $\rho_f = 960\ kg/m^3$, $t_s = 108.2°C$

the variable parameters were, V m/s and t_b °C

The correlation reduced to,

$$\frac{Nu_{bo}}{Nu_{nbo}} = 2.72 \cdot \frac{1}{V^{0.7}} \cdot \frac{1}{(t_s-t_b)^{0.84}}$$

Using the single phase correlation for the flow of water through an annulus,

$$Nu_{nbo} = 0.025\ Re^{0.8}\ Pr^{0.4}$$

in combination with the Papell correlation gives,

$$Nu_{bo} = 0.68\ \frac{Re^{0.8}\ Pr^{0.4}}{V^{0.7}\,(t_s-t_b)^{0.84}}$$

If for each test, with $t_w > t_s$, the experimentally evaluated Nu_{exp} is divided by the predicted Nu_{bo}, then for a straight annulus the quotient should be unity and at a change of section the effect of the disturbance to the flow pattern on the local heat transfer coefficient will be shown by a departure from unity value of the

quotient. The dimensionless ratio can then be plotted against a dimensionless axial distance expressed in equivalent diameters.

MOLES AND SHAW CORRELATION

The Moles and Shaw correlation,

$$\frac{h_{bo}}{h_{nbo}} = 78.5\left(\frac{c_p \mu}{k}\right)^{0.46}_{fil}\left(\frac{h_{fg}}{c_p(t_s-t_b)}\right)^{0.5}_{s}\left(\frac{q/A}{h_{fg}\rho_g V}\right)^{0.67}_{s}\left(\frac{\rho_g}{\rho_f}\right)^{0.7}$$

was simplified in the same manner as for the Papell correlation to give,

$$h_{bo} = 4.38\ P_r^{0.46}\cdot\frac{1}{(t_s-t_b)^{0.5}}\ \frac{1}{V^{0.7}}$$

The results from G 5.2 - G 5.5, for convergent flow were used for the analysis. The measured heat transfer coefficient two equivalent diameters upsteam of the step convergence was taken in each case and the value of the experimental Nu was calculated. This value of Nu was compared with that value predicted by, the single phase correlation, the Papell sub-cooled boiling correlation, and the Moles and Shaw sub-cooled boiling correlation.

The results are tabled, T 5.2, for comparison, and it can be seen that no sensible correlation exists to the accuracy required. The experimental results are naturally higher than the predicted single phase results since the heating tube wall surface temperature was always greater than the saturation temperature. The Moles and Shaw correlation gave a closer approach to the experimental values than the Papell correlation but both gave excessively high values at the higher values of water bulk temperature even though this remained well below the saturation value.

CORRELATION COMPARISONS

°C	m/s		Nu			
t_b	V	Re	expt	nbo	boP	boMS
97	1.06	69 000	267	234	800	352
87	1.06	61 600	246	221	445	250
74	1.06	52 300	232	209	280	192
61.5	1.06	44 800	221	199	206	163
95	0.8	52 300	259	187	685	315
81.5	0.8	42 900	225	172	346	247
82	0.8	44 800	217	176	362	220
72	0.8	37 300	199	161	251	174
66.5	0.8	35 500	191	159	221	167
102	0.53	37 000	280	135	12500	436
83.5	0.53	29 200	215	127	362	215
89.5	0.53	31 700	210	129	468	245
75	0.53	26 100	195	118	263	176
59	0.53	20 500	159	107	173	136
87	0.27	15 700	242	79	415	223
76	0.27	13 600	192	70	257	167
67	0.27	11 900	174	67	200	148

$$Nu_{nbo} = 0.025\ Re^{0.8}\ Pr^{0.4}$$

$$Nu_{boP} = 90.0\left[\left(\frac{\frac{q}{A}}{h_{fg}\,\rho_g\,V}\right)\left(\frac{h_{fg}}{c_p\,(t_s-t_b)}\right)^{1.2}\left(\frac{\rho_g}{\rho_f}\right)^{1.08}\right]^{0.7}$$

$$Nu_{boMS} = 78.5\left(\frac{c_p.M}{k}\right)^{0.46}_{fil}\left(\frac{h_{fg}}{c_p\,(t_s-t_b)}\right)^{0.5}_{s}\left(\frac{\frac{q}{A}}{h_{fg}\,\rho_g\,V}\right)^{0.67}_{s}\left(\frac{\rho_g}{\rho_f}\right)^{0.7}_{s}\cdot\frac{d_e}{k}$$

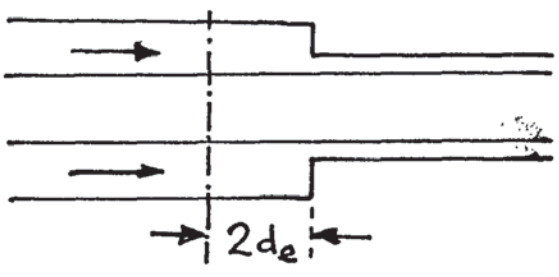

T 5.2

The problem of finding a suitable correlation to enable the variation of the heat transfer coefficient to be plotted in non-dimensional form as a single curve thus remained unresolved. A simpler but practical alternative was to plot the variation in the heat transfer coefficient as a ratio to its measured value in the appropriate straight section of the annulus. This plot is presented for convergent flow, G 5.10 and G 5.11, and also for divergent flow, G 5.12 and G 5.13.

From these plots it can be seen that the effect at a discontinuity is always smaller and of shorter length duration for two-phase flow than for single phase flow.

EFFECT OF CONVERGENCE

The effect of a convergence is to increase the heat transfer coefficient in the exit region of the large diameter section but the heat transfer coefficient in the small diameter section is reduced over the entry length. This contrasts with the effect of a convergence in a round pipe, G 2.1. The colour schlieren photographs P 4.36-.38 give an indication of the closing up of the flow pattern immediately upstream of the convergence and this increasing velocity would account for the increasing heat transfer coefficient in this region. Just downstream of the convergence there is a small drop in the heat transfer coefficient before it begins to rise to the value appropriate to the smaller diameter annulus, and looking at, P 4.37, it can be seen that in this region the boundary layer is distinctly different, appearing thicker and less turbulent. It would seem that the flow is given a strong component radially inwards at the change in section and that this inward directed flow is forcing hot fluid, which has just left the boundary layer upstream, back onto the heating surface and thus reducing the heat transfer from the surface at this point, due to the reduced temperature difference, $t_w - t_b$.

With boiling present, P 4.38, it can be clearly seen that the convergence of the flow section produces only slight change in the appearance of the boundary layer and this is corroborated by the plot of the heat transfer coefficient variation, G 5.10, where the effect of the convergence with boiling present is only half of the effect with single phase flow.

EFFECT OF DIVERGENCE

For a divergence in the flow section the heat transfer coefficient maintains its value for approximately two equivalent diameters then following a slight increase it falls gradually to the steady value appropriate to the large diameter annulus. The flow visualization photographs, P 4.27-.29, taken to support the heat transfer measurements, show a band of recirculating flow occupying approximately two equivalent diameters immediately downstream of the divergence. It is this recirculating flow which could account for the maintaining value, and improvement, of the heat transfer coefficient in this region. In the photographs of the boiling heat transfer, P 4.14 and P 4.19, it can be seen that for two equivalent diameters downstream of the step the velocity effect carries over from the smaller diameter annulus. The colour schlieren photographs, P 4.34 and P 4.35, and the black and white schlieren photograph P 4.31, confirm that in this region there is no perceptible change in the heat transfer process.

PRESSURE DROP

The variation in the static pressure was carefully measured along the axis of the annulus in the region of the step change in section, G 4.12, G 4.19, for single phase conditions without heating.

For the converging sections there was a fall in pressure to the vena - contracta, 4 mm (0.6 d_e), down stream of the step followed by a pressure recovery over the next 22 mm (3.5 d_e). The diameter of the vena-contracta was calculated as 0.985 of the annulus bore diameter. There was no obvious detailed relationship between the heat transfer variation and the pressure variation.

For the divergence the static pressure continued to fall for almost two equivalent diameters downstream of the step before making a slow recovery. This was entirely in agreement with the variation in the heat transfer coefficient and with the boundary layer pattern shown in the schlieren photographs.

For both convergent and divergent sections the static pressure variation followed the same pattern of variation over the range of flow velocities used in the tests.

5.4 SINGLE AND TWO-PHASE SWIRL FLOW THROUGH AN ANNULUS

In making these tests it was appreciated that the effect of swirl in an annulus with heated internal wall will be detrimental to the heat transfer process for the same reason that swirl improves the heat transfer coefficient when used with liquid flowing through a heated tube, R59, R60, R 61 and R 62.

With boiling swirl flow in a tube the increased bouyancy of the vapour bubbles causes them to migrate into the cooler core of the liquid and there they condense more rapidly, which can reduce the pressure drop as well as increase the heat transfer coefficient. At higher heat fluxes the swirl tends to maintain stable annular flow and raises the burn-out point.

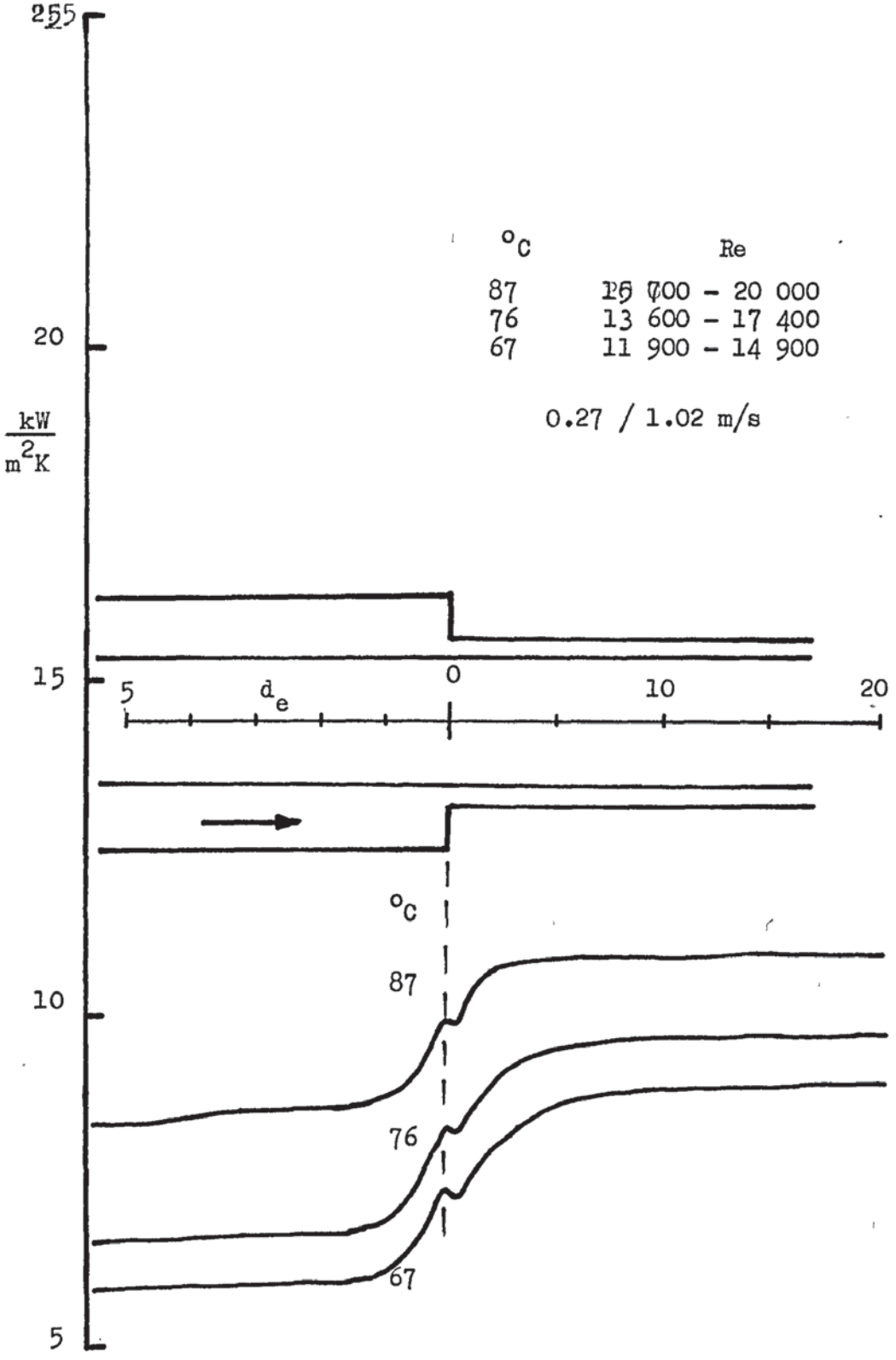

VARIATION OF THE SINGLE-PHASE HEAT TRANSFER COEFFICIENT ALONG THE AXIS OF THE ANNULUS

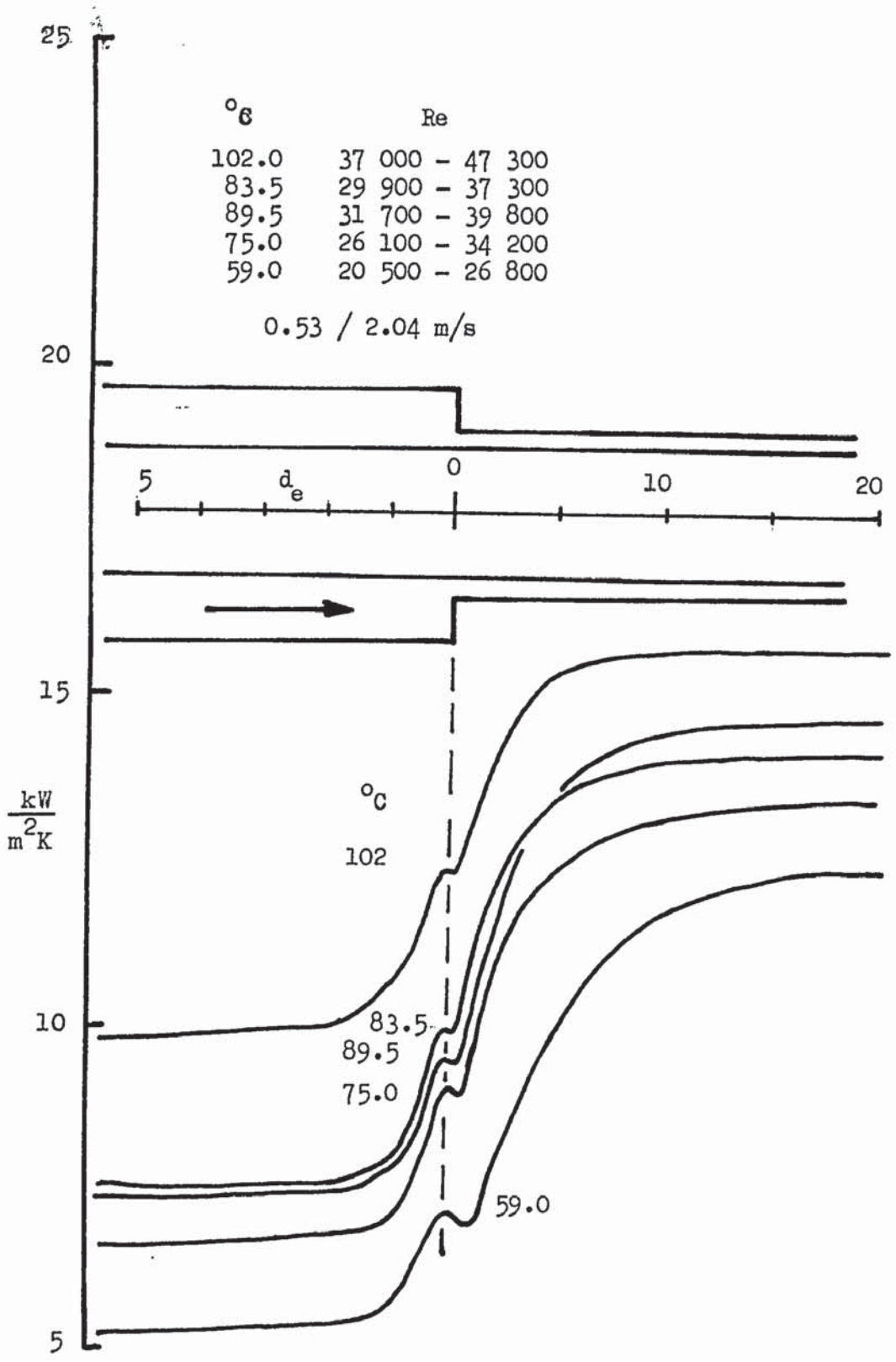

VARIATION OF THE SINGLE-PHASE HEAT TRANSFER COEFFICIENT ALONG THE AXIS OF THE ANNULUS

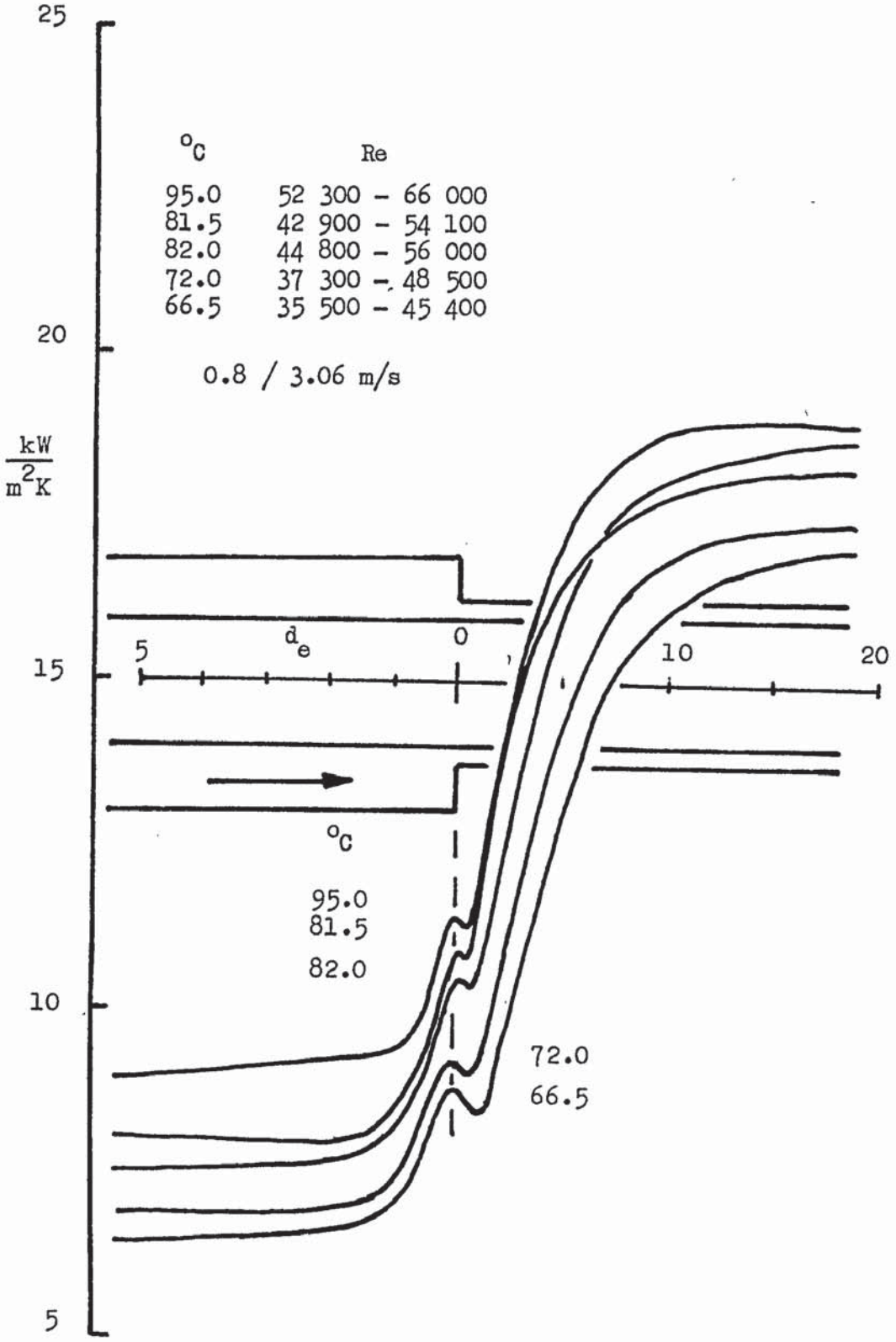

VARIATION OF THE SINGLE PHASE HEAT TRANSFER COEFFICIENT ALONG THE AXIS OF THE ANNULUS

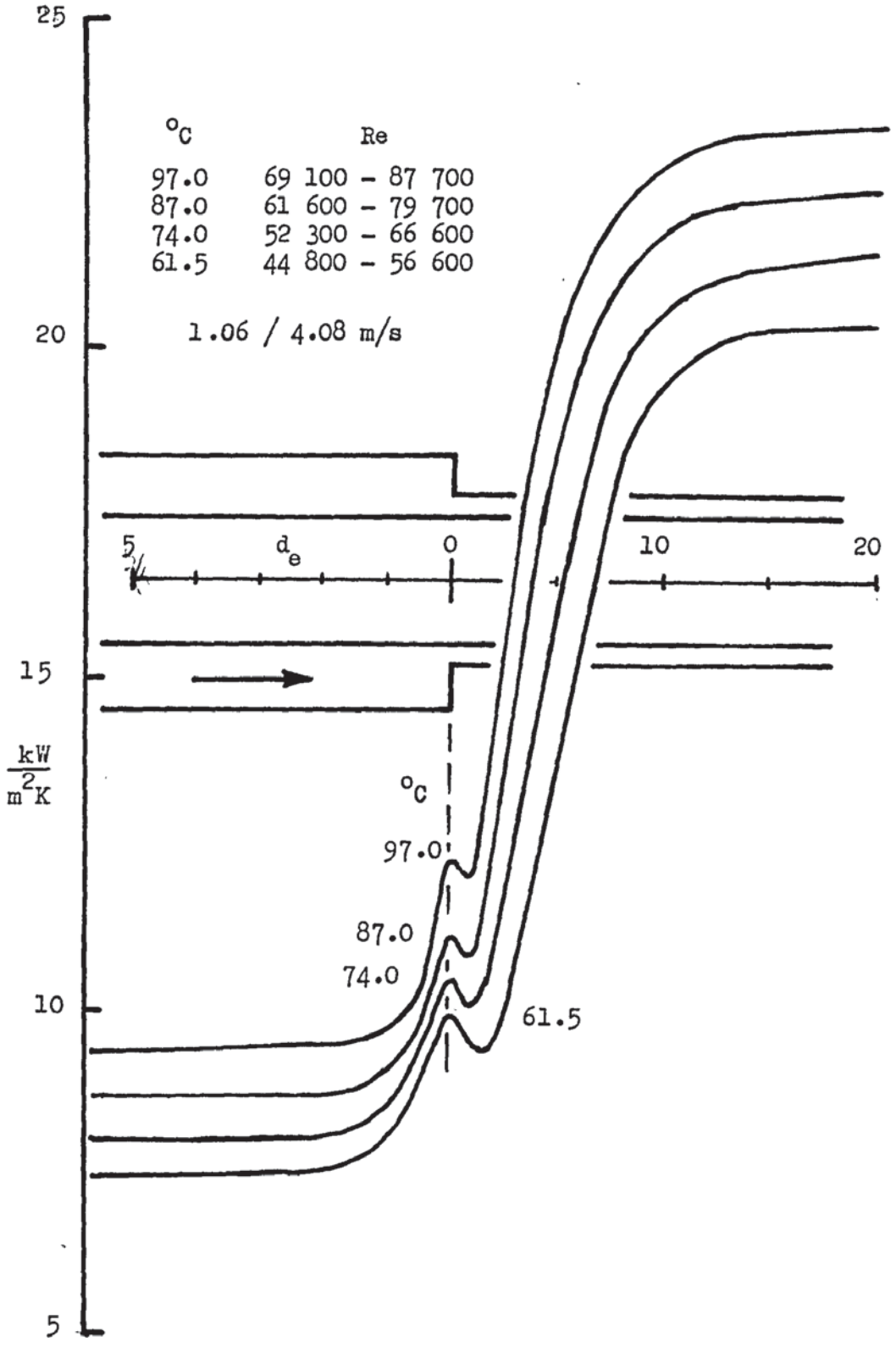

VARIATION OF THE SINGLE PHASE-HEAT TRANSFER COEFFICIENT ALONG THE AXIS OF THE ANNULUS

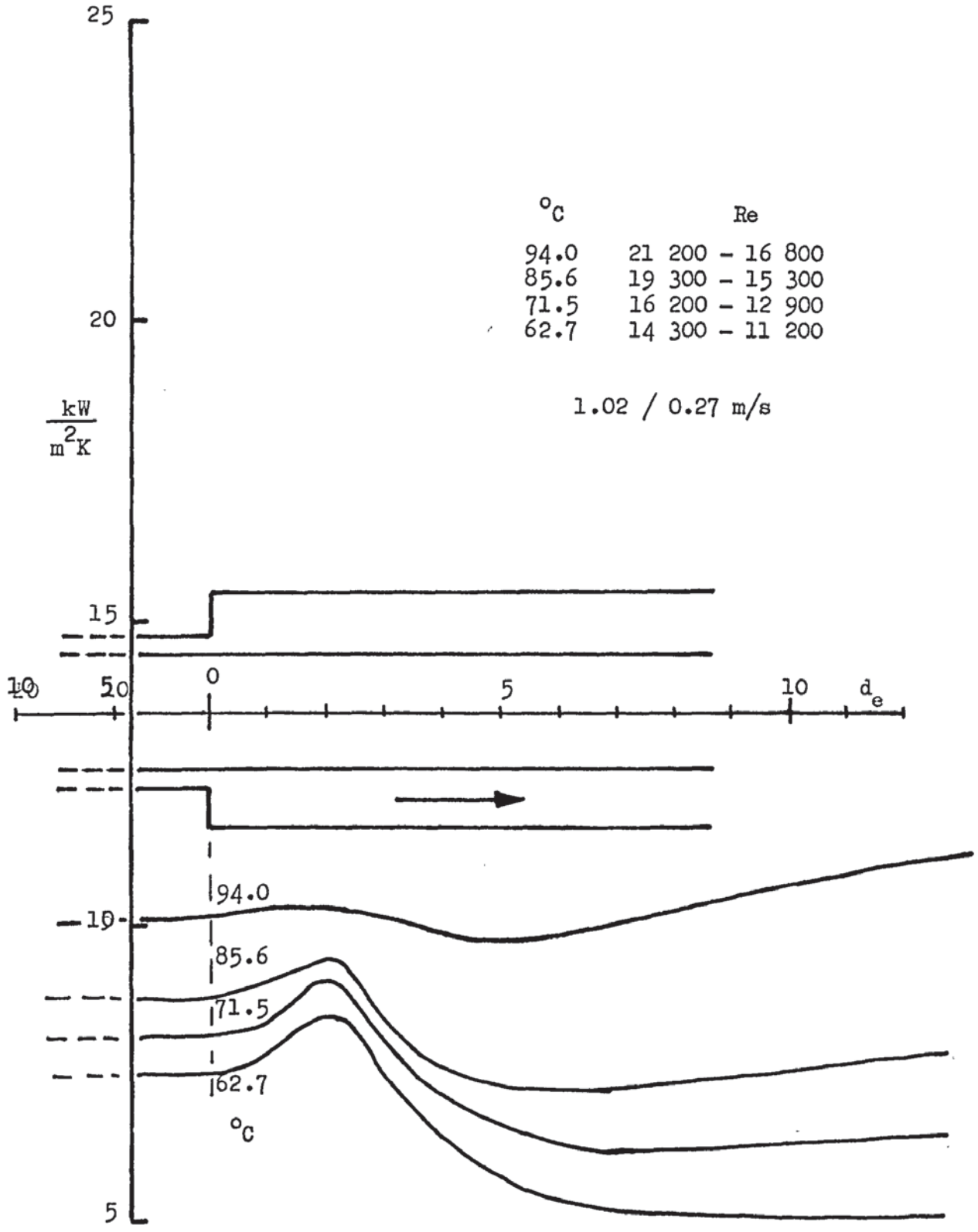

VARIATION OF THE SINGLE-PHASE HEAT TRANSFER COEFFICIENT ALONG THE AXIS OF THE ANNULUS

G 5.6

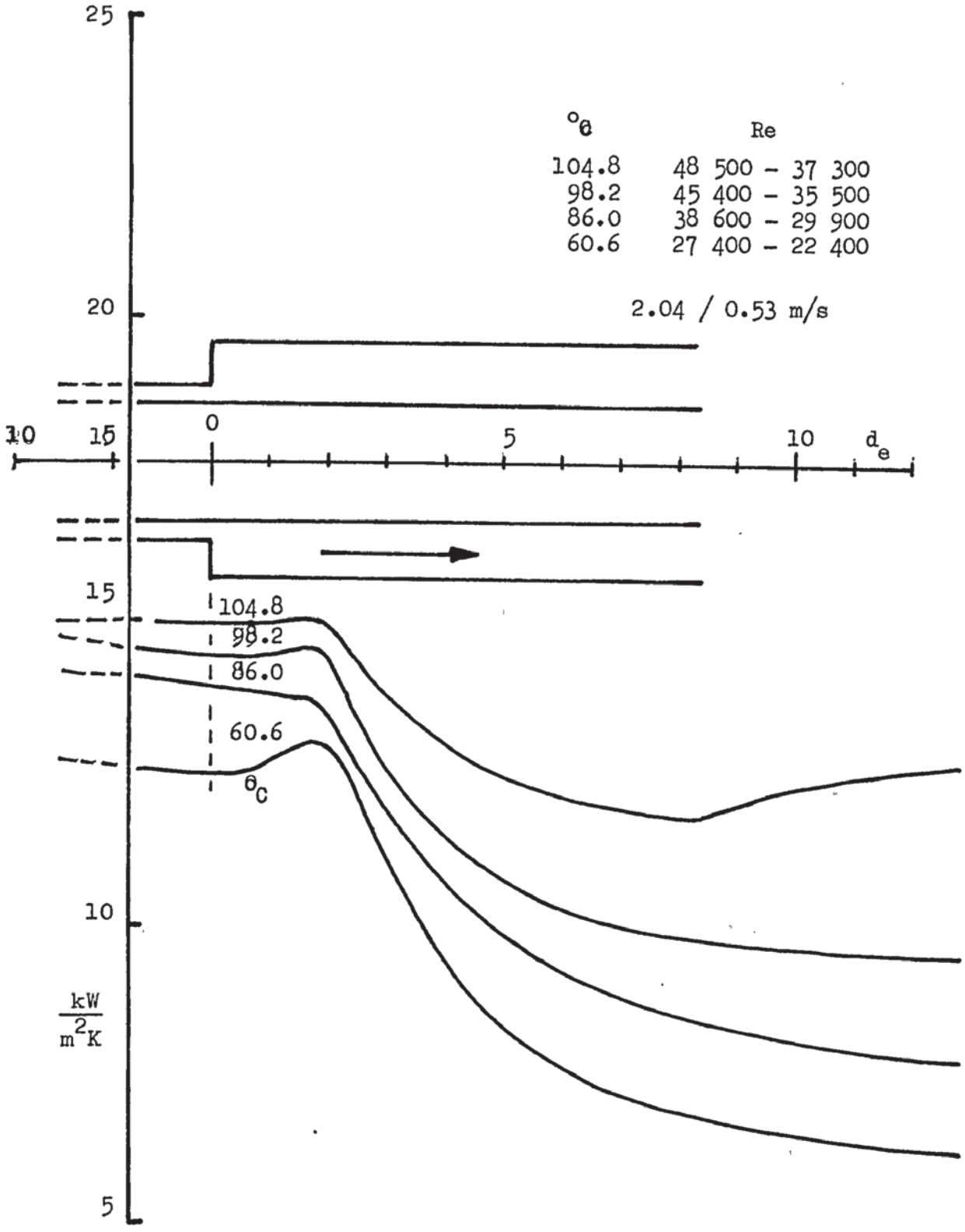

VARIATION OF THE SINGLE-PHASE HEAT TRANSFER COEFFICIENT ALONG THE AXIS OF THE ANNULUS

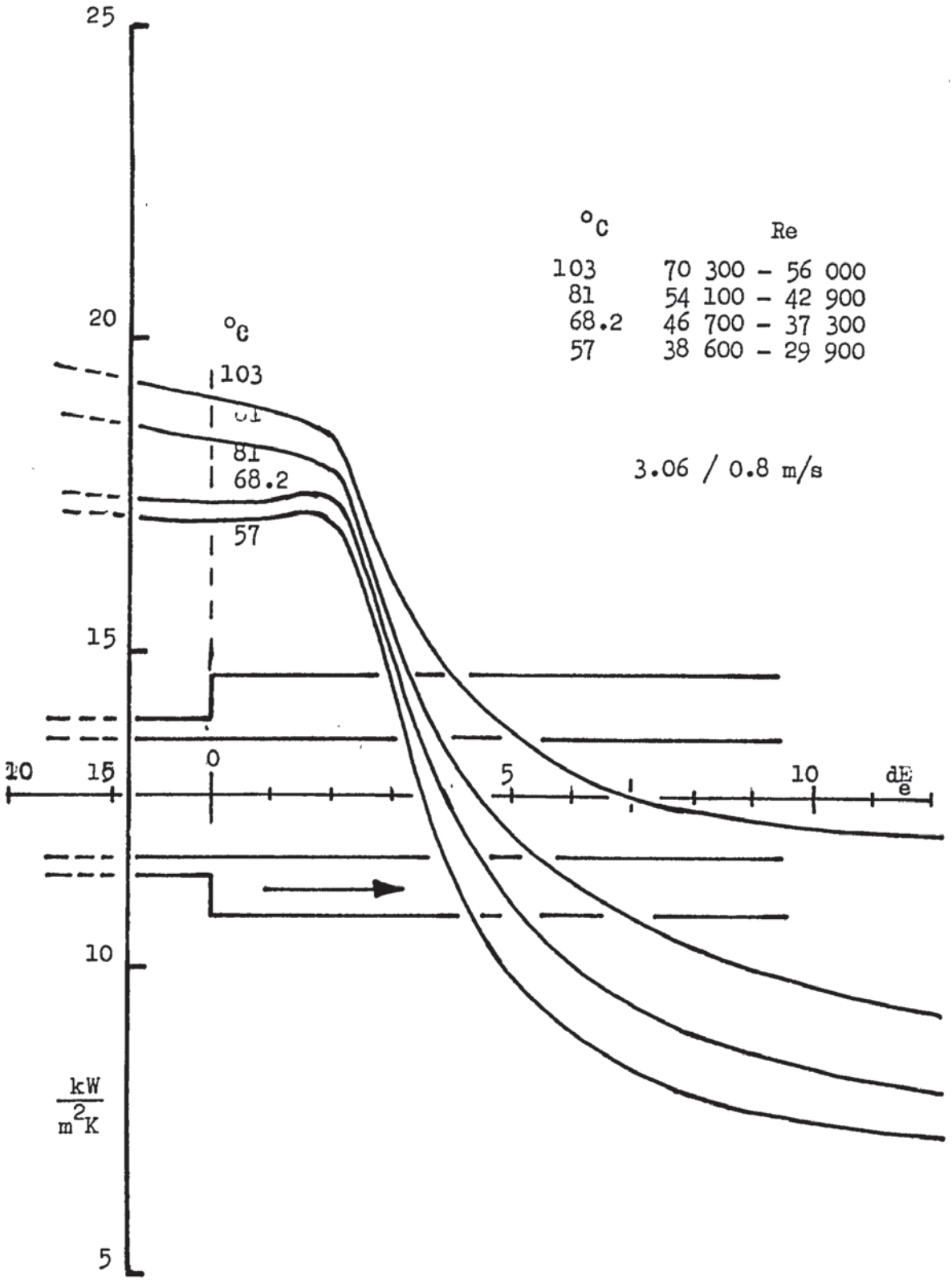

VARIATION OF THE SINGLE-PHASE HEAT TRANSFER COEFFICIENT ALONG THE AXIS OF THE ANNULUS

G 5.8

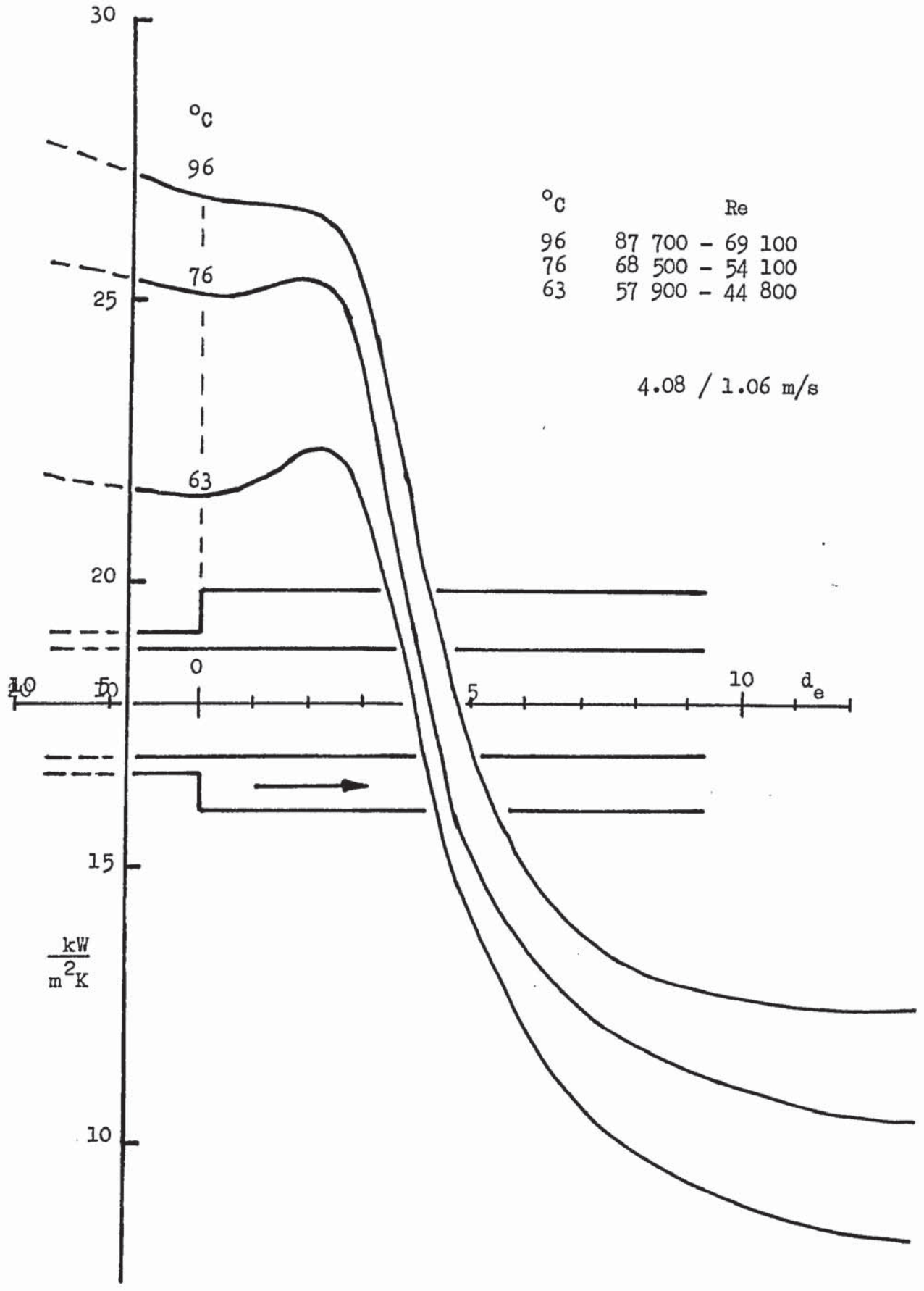

VARIATION OF THE SINGLE-PHASE HEAT TRANSFER COEFFICIENT ALONG THE AXIS OF THE ANNULUS

G 5.9

HEAT TRANSFER COEFFICIENT EXPRESSED AS A RATIO OF THE HEAT TRANSFER COEFFICIENT IN THE PLAIN ANNULUS PLOTTED AGAINST AXIAL DISTANCE EXPRESSED IN EQUIVALENT DIAMETERS

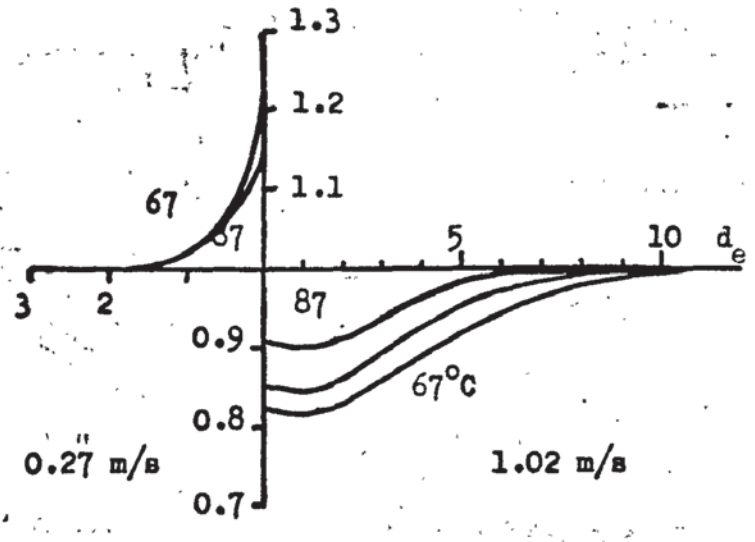

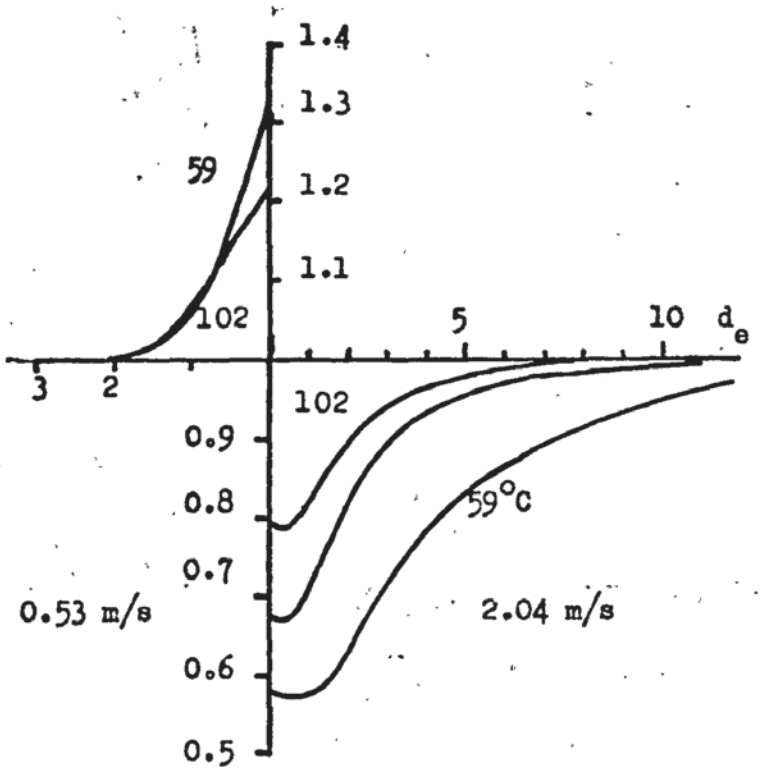

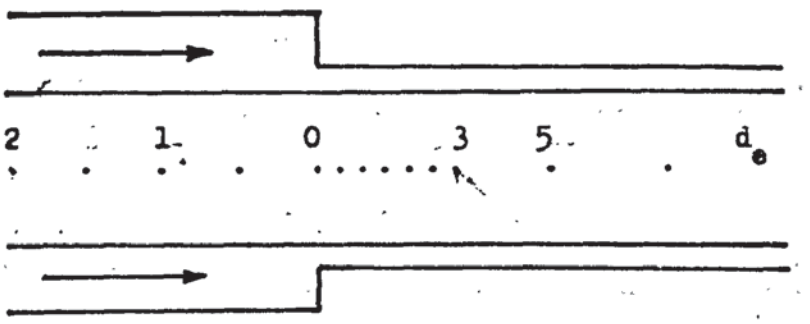

G 5.10

HEAT TRANSFER COEFFICIENT EXPRESSED AS A RATIO OF THE HEAT TRANSFER COEFFICIENT IN THE PLAIN ANNULUS PLOTTED AGAINST AXIAL DISTANCE EXPRESSED IN EQUIVALENT DIAMETERS

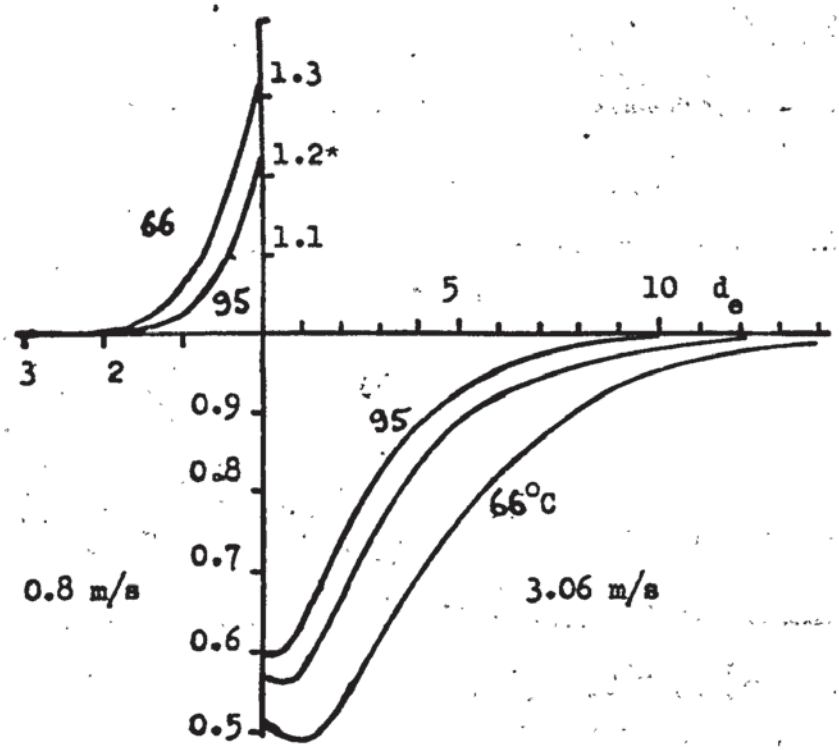

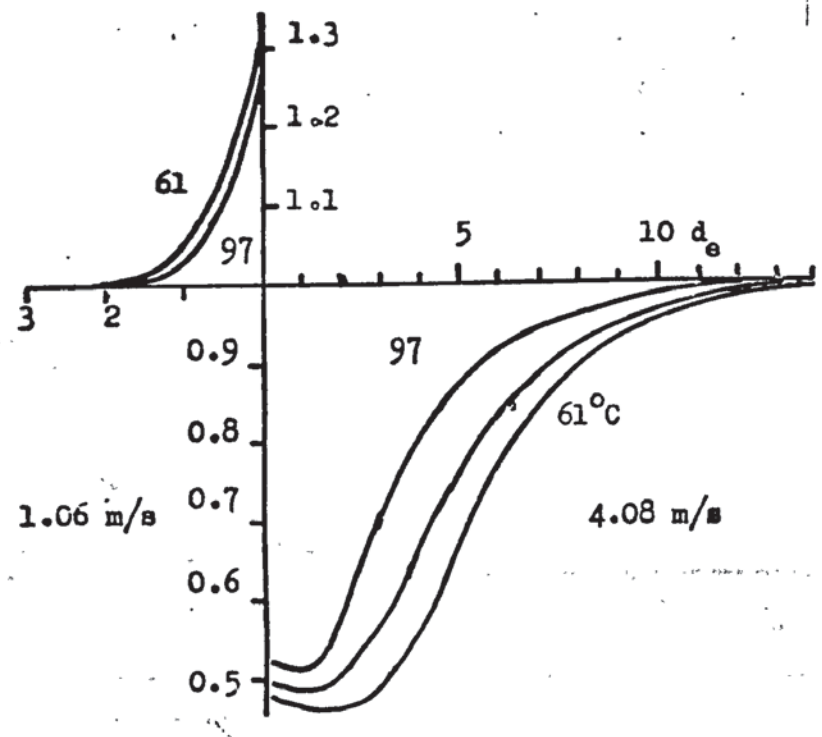

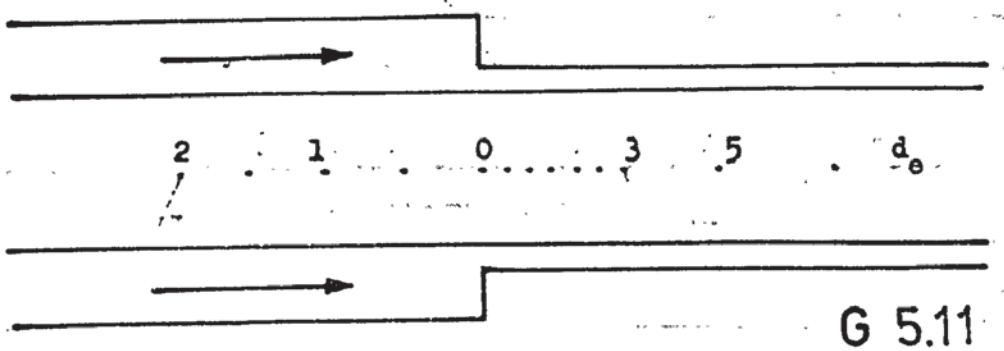

G 5.11

HEAT TRANSFER COEFFICIENT EXPRESSED AS A RATIO OF THE HEAT TRANSFER COEFFICIENT IN THE PLAIN ANNULUS PLOTTED AGAINST AXIAL DISTANCE EXPRESSED IN EQUIVALENT DIAMETERS

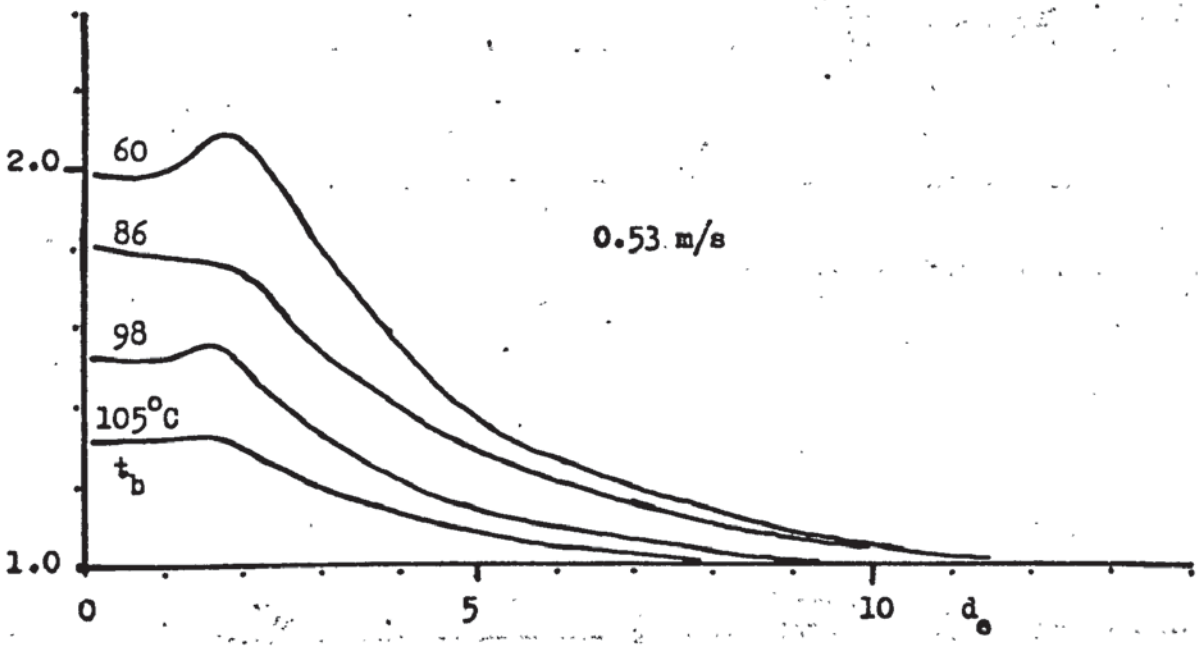

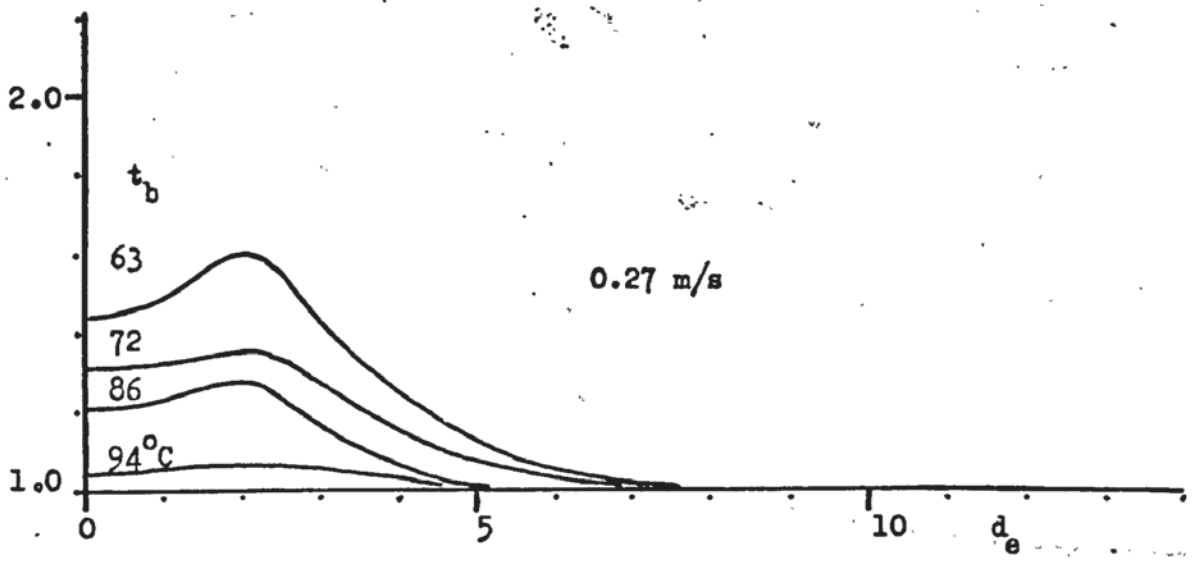

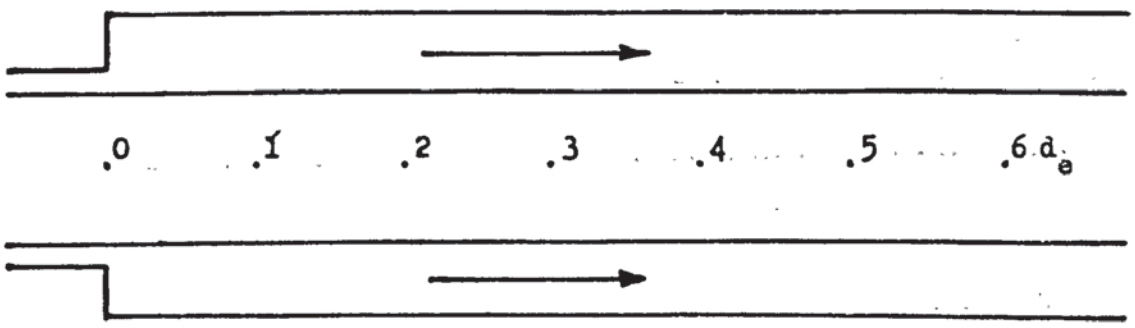

G 5.12

HEAT TRANSFER COEFFICIENT EXPRESSED AS A RATIO OF THE HEAT TRANSFER COEFFICIENT IN THE PLAIN ANNULUS PLOTTED AGAINST AXIAL DISTANCE EXPRESSED IN EQUIVALENT DIAMETERS

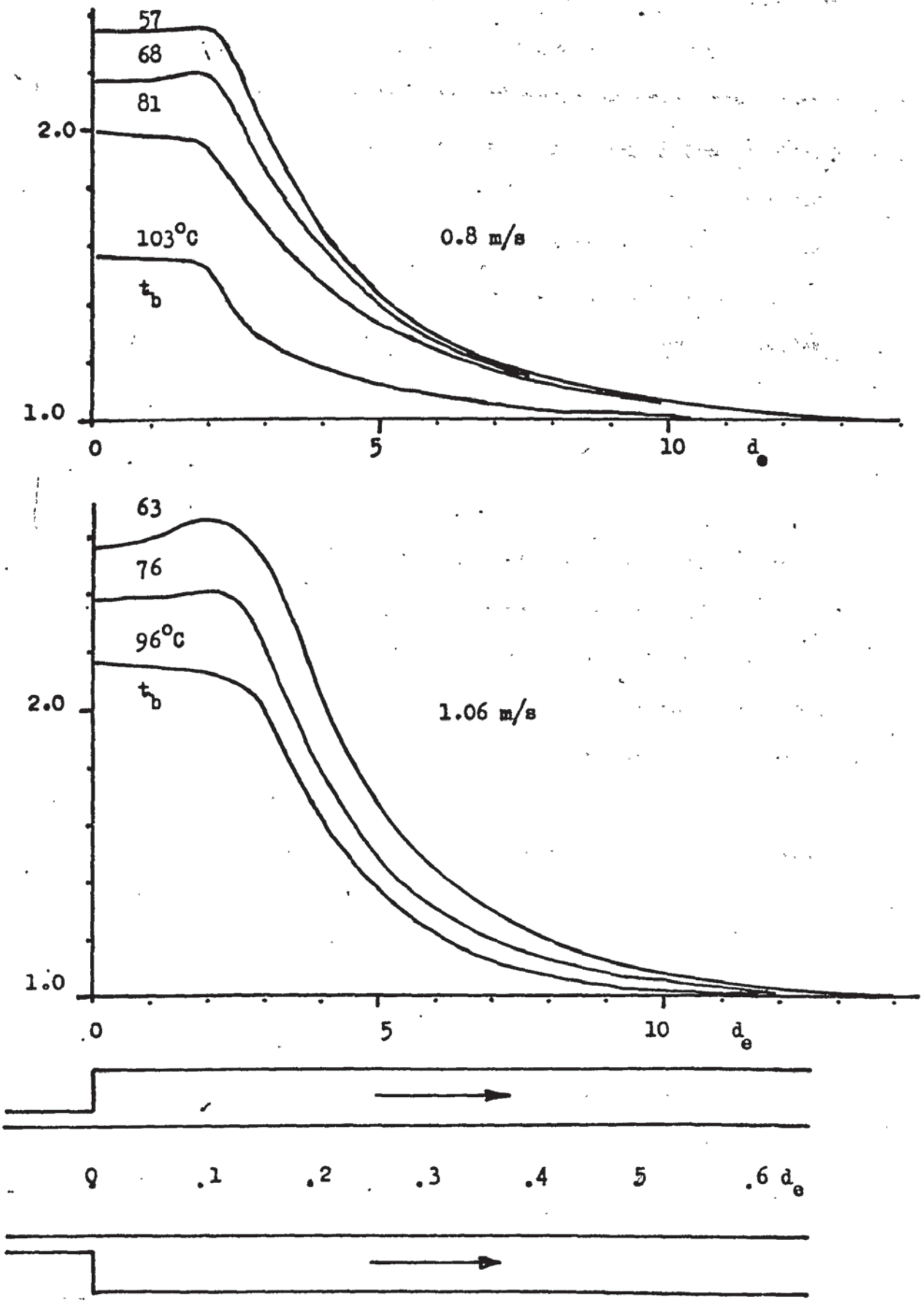

G 5.13

If the region of incipient boiling is considered, then swirl flow in an annulus could have the effect of promoting nucleate boiling at a lower fluid bulk temperature because the radial acceleration given to the liquid will inhibit the mass transfer of hot liquid from the boundary layer to the bulk of the liquid. If this is so then because of the agitation of the boundary layer due to the boiling process the effect could be an increased heat transfer coefficient without the penalty of an increased pressure drop. The effect would still be to reduce the heat transfer coefficient at higher heat fluxes and the burn-out point would be lowered, so that it must be clear that the effect was looked for only in the incipient boiling region.

TEST RESULTS

The test results were first plotted as, the heating tube wall temperature against water bulk temperature for a range of flow rates, G 4.22-.25. The graphs showed that the effect of the swirl was to increase the tube wall temperature for a given water bulk temperature and visible boiling was seen to occur at lower water bulk temperatures when swirl was present.

A cross plot was taken from these graphs, G 4.25, showing heating tube wall temperature against mass velocity for a number of water bulk temperatures. It can be seen that at high flow rates the swirl makes little difference to the tube wall temperature but as the flow reduces then the swirl adversely affects the heat transfer and then with a further reduction in flow rate the effect reduces until at 700 kg/m^2s and $t_b=60^oC$ it gives a slight advantage over straight flow. Following this, with swirl flow, the wall temperature rises rapidly to the constant level for developed boiling.

A plot of $Nu/Pr^{0.4}$ against $Re^{0.8}$, G 4.26-.28, showed no significant difference between the swirl, and straight flow.

PHOTOGRAPHS

Photographs were taken of the swirl flow in 'Test 3' with the water velocity at 1.3 m/s, P 4.24-.26, G 4.25, they clearly show that boiling develops along a narrow track in the centre of the flow area and that this fine central track of bubbles broadens as the bulk temperature increases. This is contrary to what might have been expected, in that the central area would have a higher velocity and thus be the least favourable site for boiling to develop. The direction of flow at the heating tube surface is clearly aligned to the inner helix angle and the time exposure shows no circumferential dispersal of the vapour bubbles which would indicate that circulation currents normal to the main flow are not present. The localized boiling could occur because of a band of hotter fluid or of lower pressure fluid and additional experimental data would be needed to go beyond a speculative reason for this.

PRESSURE DROP

Although the effect of swirl on the heat transfer coefficient is small, the effect on the pressure drop is substantial. Comparing the axial pressure traverses taken along the annulus axis, G 4.29-.31 for straight, single turn helix, and double turn helix, the pressure drops are in the ratio, 1:2:4, respectively.

5.5 FLOW VISUALIZATION

BUBBLES

The use of flow visualization methods was very helpful in understanding the behaviour of the fluid at changes in section. With boiling present the vapour bubbles themselves provided markers to trace the flow pattern but the size of the bubbles was dependent on the boiling conditions. With air injected into the water flow, the bubble size and number could be controlled to give the best detailed flow picture, P 4.27-.29.

SCHLIEREN

The use of a schlieren optical system gave support in studying the behaviour of the boundary layer. With black and white the system was very sensitive, P 4.30-.31, and films with very fast emulsion speeds are available to record the flow picture. The colour system has a decided advantage over black and white in that as well as indicating density changes between one macroscopic area and an adjacent area it will indicate the comparison between more widely separated areas. Thus in P 4.33 the hot fluid from the boundary layer is shown to retain its identity in the cooler bulk fluid for some time. With still photography the movement of the fluid is judged by inference from the photograph and to get full advantage from the system ciné photography is needed. With the colour film emulsion speeds now available, 500 ASA, and taking into account that for the movement of the fluid to be 'frozen', longer exposure times than the 5 μs used in these tests would be quite satisfactory, ciné is feasible.

5.6 FLOW OSCILLATIONS

At test conditions which approached the water saturation temperature, flow oscillations could develop to such a magnitude as to make data recording impossible. Flow oscillations also occurred with high heat fluxes in conjunction with large values of subcooling but these were less violent and could be passed through by making quite small adjustments to the test conditions.

An improvement would be gained by using a positive displacement pump which as previous workers have shown, R 37 provides a 'hard inlet' condition.

5.7 METASTABLE CONDITIONS

Depending on whether the heat flux was increased to reach the operating level, or reduced to the operating level, and on how long the boiling process had been operating, the stable state in the boiling process can have different parameters. This hysteresis effect has been reported by a number of workers eg.,R 63, R 47. It does seem that if the test conditions are held constant for a period of time then a stable state will be reached as the hysteresis effect disappears.

It is also possible for a small change in system parameters to precipitate the change from one mode of boiling to another, in G 5.7, with the water at 104.8°C, at the step, there is an obvious change in the heat transfer mechanism at 8.5 d_e downstream of the expansion. In G 5.3, one curve, 75°C at the step, can overtake a higher curve, 89.5°C at the step.

In obtaining test results it was invariably necessary to overshoot, ±5K, the final position while adjusting the cooling water to get a steady operating condition. After achieving a steady state operating condition the rig would be held at this condition for at least 45 minutes to verify that it had indeed stabilised and in the test which followed it would take approximately 90 minutes to complete a temperature traverse, during which time any departure from the settled position would have been noted. Experimentally it was not possible to do any more than this although a control system could be designed to be slightly overdamped and it would thus always control the test rig to approach a new operating point from a higher level (or lower level).

In considering the effect on the results, some tests were repeated after an interval of five weeks and gave identical values, which gives confidence but a more thorough approach of repeating all tests at identical approach conditions would be preferred. The ability to do this must depend on the introduction of automatic control to the test rig.

CONCLUSIONS

The accurate measurement of the temperature of the heating surface and of the fluid bulk is extremely important.

When flow oscillations were encountered they prevented the accurate measurement of the operating conditions and restricted the range of the boiling tests. The flow oscillations encountered in this work were observed visually and in severe cases the test was abandoned because of dangerous vibrations in the test rig. The impeller flow meter working over a five second period of summation had too long a time constant to indicate the presence of flow oscillations.

Data for the single phase flow of water through an annulus, 19.05/38.1 mm ID., with heat transfer from the inner surface only can be correlated by the equation,

$$St\ P_r^{0.6} = 0.025\ Re^{-0.199}$$

The presently available correlations for subcooled boiling heat transfer give predictions which are of the right order but compare only approximately with data for water at low pressure, particularly as conditions approach saturated boiling. Since no system exists to classify commercial heating surfaces on the basis of their boiling performance, this important parameter remains unspecified in some boiling correlations, except as a constant for a particular metal with a stated finish, and for others not at all.

The effect of step discontinuities in the flow section of an annulus can be usefully plotted as variations in the local heat transfer coefficient compared with the heat transfer coefficient in a plain annulus. Subcooled boiling data correlations are not available with an accuracy sufficient to permit the experimental data to be reduced to one non-dimensional curve.

As fluid conditions vary from single phase to two phase the effect of the step discontinuity progressively reduces.

In these experiments the use of swirl flow in an annulus with an inner heated wall did not improve the heat transfer coefficient (for radial accelerations up to 1 g.) but introduced a pressure drop penalty.

Flow visualization by vapour bubbles/air bubbles is a useful aid in understanding the nature of a fluid flow pattern.

Schlieren optical systems can give a useful understanding of the behaviour of a heated boundary layer. With a black and white system the difference between turbulent and laminar flow can be easily detected, P 4.30 and P. 4.31, and the general flow pattern visualized. By using colour the information produced is greatly enhanced, the local fluid temperatures can be estimated and the easy indentification of the hot and cold elements of the fluid, P 4.37, give a more detailed visualization of the convective heat transfer process. Since

photographic emulsions for colour are less sensitive than those for black and white, the colour system needs a more powerful light source if photographic recording is used. The light source can become a limiting factor if a high speed camera is used for recording the image.

APPENDICES

APPENDIX 1

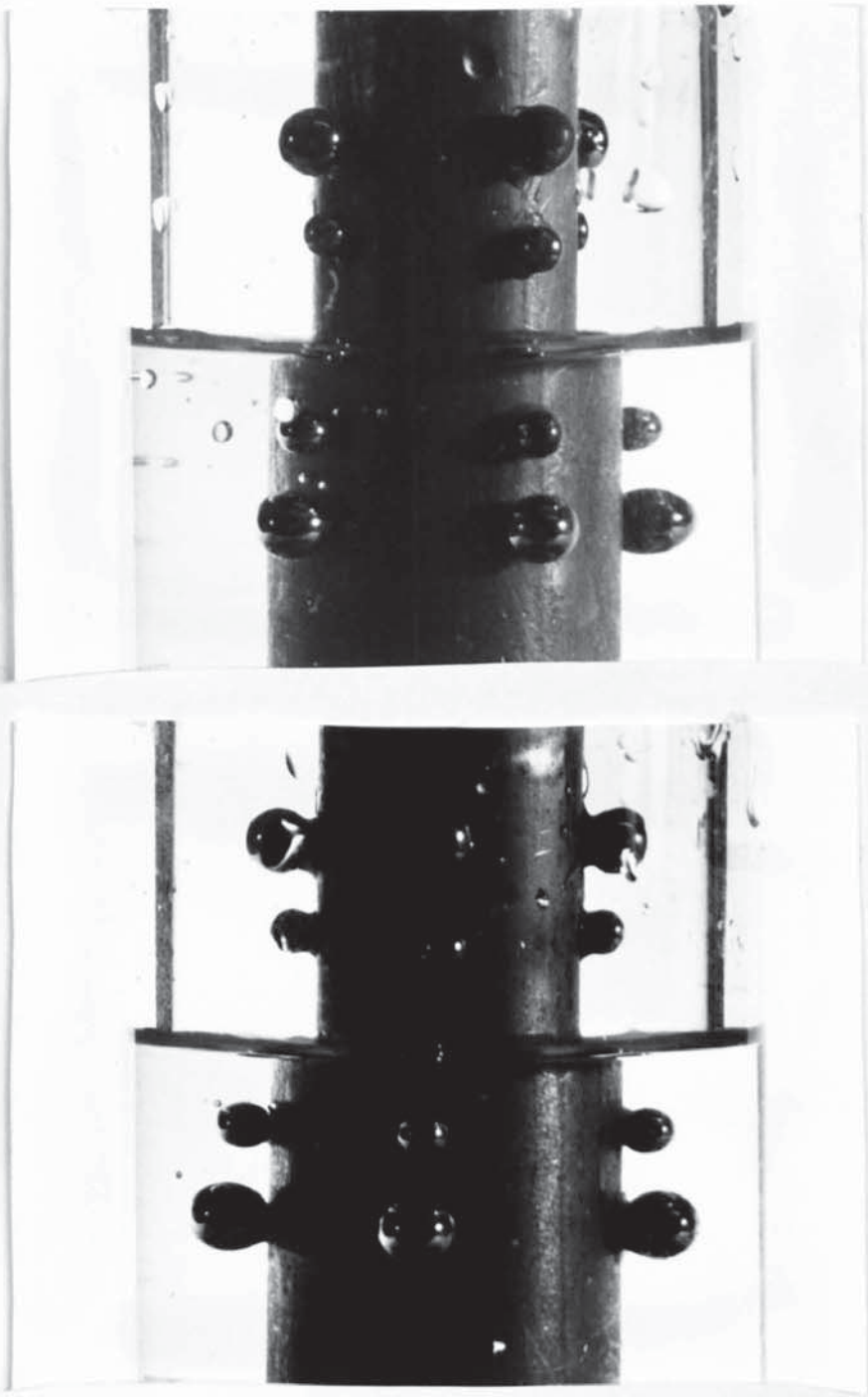

OPTICAL DISTORTION DUE TO THE LENS EFFECT OF THE WATER FILLED ANNULUS

Ball diameters ---------- 3, and 4.5 mm

Heating element diameter --------- 19.1 mm

Glass tube inside and outside dia.-38 and 46 mm

APPENDIX 2

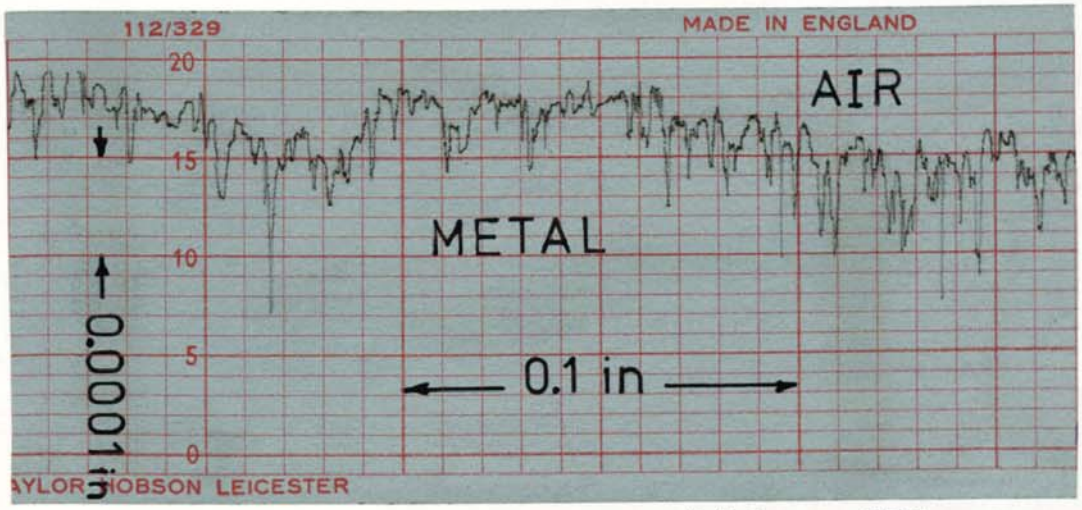

5 February 1971

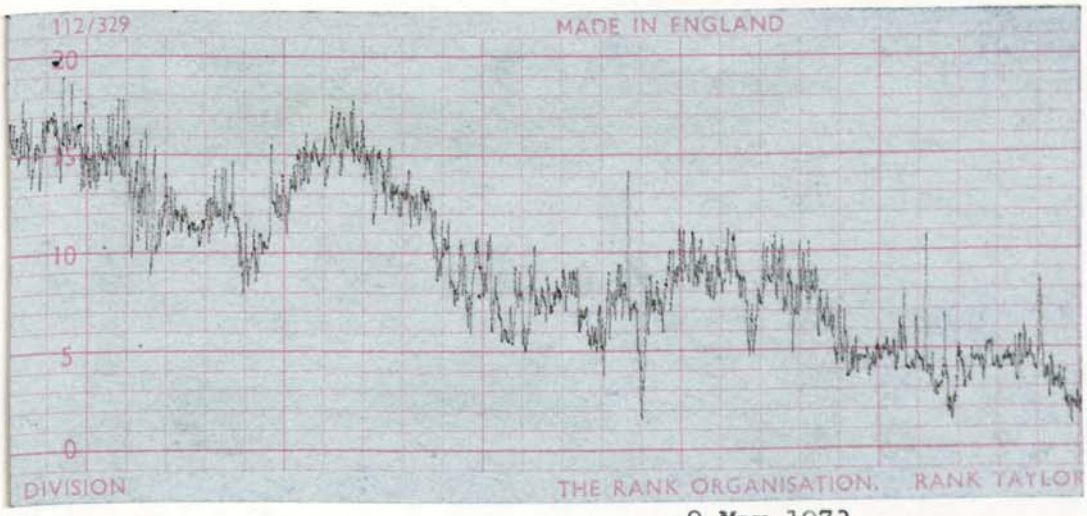

9 May 1973

SURFACE PROFILE OF THE HEATING ELEMENT MEASURED BEFORE AND AFTER THE TESTS (Talysurf)

The lower trace may be considered to be relevant to all of the tests, and shows by the upward spikes that some deposit has been laid on the heating surface during the initial commissioning period when the surface discolouration was observed to form.

APPENDIX 3

RESOLUTION OF THE DIGITAL VOLTMETER-DATA LOGGER SYSTEM USED TO RECORD THE THERMOCOUPLE OUTPUTS

The normal four figure read-out of the DVM gave tens, units, tenths, and hundredths of millivolts, but with a x2 facility this sensitivity was doubled so that the last digit moved in steps of 5 microvolts.

True	DVM indication		Reduced value	Error (mV)	
mV	x 1	x2	of x2	x 1	x2
1.400	1.40	2.80	1.400	0	0
1.401	1.40	2.80	1.400	-0.001	-0.001
1.402	1.40	2.80	1.400	-0.002	-0.002
1.403	1.40	2.81	1.405	-0.003	+0.002
1.404	1.40	2.81	1.405	-0.004	+0.001
1.405	1.41	2.81	1.405	+0.005	0
1.406	1.41	2.81	1.405	+0.004	-0.001
1.407	1.41	2.81	1.405	+0.003	-0.002
1.408	1.41	2.82	1.410	+0.002	+0.002

The x2 millivolts facility was used to give a maximum error in the read-out of ± 0.002 mV , when used with Ch/Al thermocouples this was equivalent to a temperature error of $0.05^{\circ}C$.

APPENDIX 4

CALCULATION OF THE TEMPERATURE DROP ACROSS THE HEATING STRIP

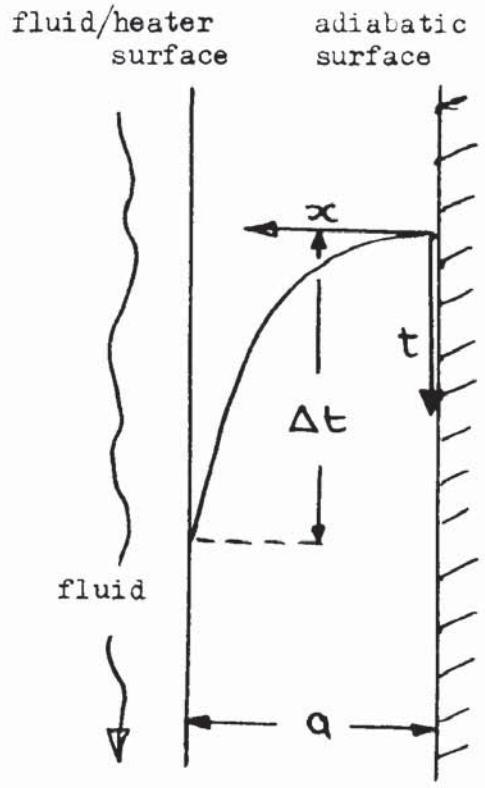

$$\frac{\partial^2 t}{\partial x^2} + \frac{q_{vg}}{k} = 0$$

$$\frac{\partial t}{\partial x} + \frac{q_{vg} x}{k} + B = 0$$

when $x = 0,\ \frac{\partial t}{\partial x} = 0,\ B = 0$

$$t + \frac{q_{vg} x^2}{k\,2} + C = 0$$

when $t = 0,\ x = 0,\ C = 0$

$$\Delta t = \frac{q_{vg}}{k} \cdot \frac{a^2}{2}$$

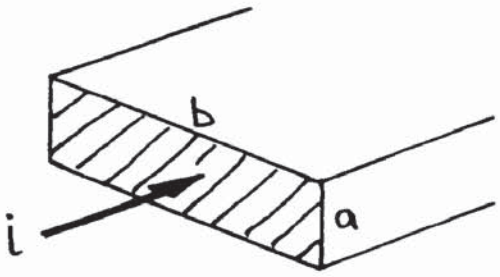

$$q_{vg} = \rho i_s^2 = \rho \left(\frac{i}{ab}\right)^2$$

$$\Delta t = \frac{1}{2b^2} \cdot \frac{\rho}{k} \cdot i^2$$

$b = 6.8\ \text{mm},\ \rho = 0.78\ \mu\Omega\text{m},\ k = 16\ \frac{W}{mK}$

$$\Delta t = \frac{1}{2 \times 6.8^2 \times 10^{-6}} \times \frac{0.78 \times 10^{-6}}{16} \times i^2$$

$$= 0.527 \times 10^{-3} \times i^2$$

e.g. for a current measured at 90 amps.

$$\Delta t = 0.527 \times 10^{-3} \times 90^2 = 4.27^\circ C$$

APPENDIX 5

CALCULATION OF THE TEMPERATURE DROP ACROSS THE HEATING TUBE

Assumptions,

No heat transfer across the inner surface

Heat flow purely radial

Uniform heat generation across the section

Constant conductivity of the tube metal

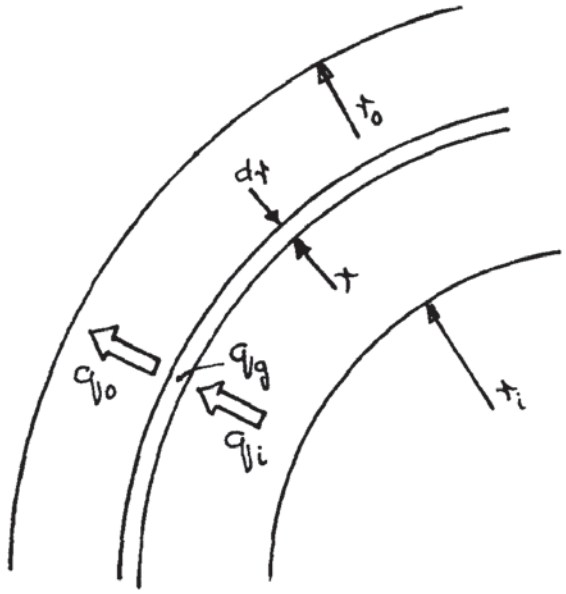

q_g = heat generated in tube metal $[W/m^3]$

q_i = heat into element = $\pi (r^2 - r_i^2) q_g$ $[W/m]$

q_o = heat out of element = $\pi ((r+dr)^2 - r_i^2) q_g$ $[W/m]$

q_m = mean heat flow through element

$= 0.5 (q_i + q_o)$

$= 0.5 \pi q_g (r^2 - r_i^2 + r^2 + 2r\,dr + dr^2 - r_i^2)$

$= 0.5 \pi q_g (2r^2 - 2r_i^2 + 2r\,dr)$

$= \pi q_g (r^2 - r_i^2 + r\,dr)$

for conduction; $q = kA \frac{dt}{dr}$

$k\, 2\pi \left(r + \frac{dr}{2}\right) \frac{dt}{dr} = \pi q_g (r^2 - r_i^2 + r\,dr)$

$$dt = \frac{q_g}{2k}\left(r\,dr - r_i^2\frac{dr}{r}\right)$$

$$t = \frac{q_g}{2k}\left(\frac{r^2}{2} - r_i^2 \ln r + C\right)$$

$$t_s = 0\,,\quad r = r_i\,,\quad C = r_i^2 \ln r_i - \frac{r_i^2}{2}$$

$$t_s = \frac{q_g}{k}\left(\frac{r^2}{2} - \frac{r_i^2}{2} - r_i^2 \ln\frac{r}{r_i}\right)$$

e.g. tube o.d. 0.75 in, 18 swg, 0.5 m long, 2000 A.

Sectional area $= 68.2\times10^{-6}\ [m^2]$

Length $= 0.5\ [m]$

Spec. res. $= 0.7\ [\mu\Omega/m]$

Resistance $= 0.7\times\frac{0.5}{10^3}\times\frac{10^6}{68.2} = 5.13\ [m\Omega]$

Power (RI^2) $= 5.13\times10^{-3}\times2000^2 = 20.52\ [kW]$

Vol. of metal $= 0.5\times68.2\times10^{-6} = 34.1\times10^{-6}\ [m^3]$

Power/volume $= 0.601\times10^9\ [W/m^3]$

$r_i^2 = (0.327\times25.4\times10^{-3})^2 = 68.7\times10^{-6}\ [m^2]$

$k = 14.6\ W/mK$

$$t = \frac{q_g\cdot r_i^2}{k}\cdot f\left(\frac{r}{r_i}\right)$$

$$= \frac{(0.601\times10^9)\times68.7\times10^{-6}}{14.6}\times0.01$$

$= 28.25\,^\circ C$ drop across the tube wall

APPENDIX 6

The following programme calculates by forward prediction the temperature profile of the outer surface from the imposed temperature profile on the inner surface which is given an axial temperature gradient equal to the maximum experimental value

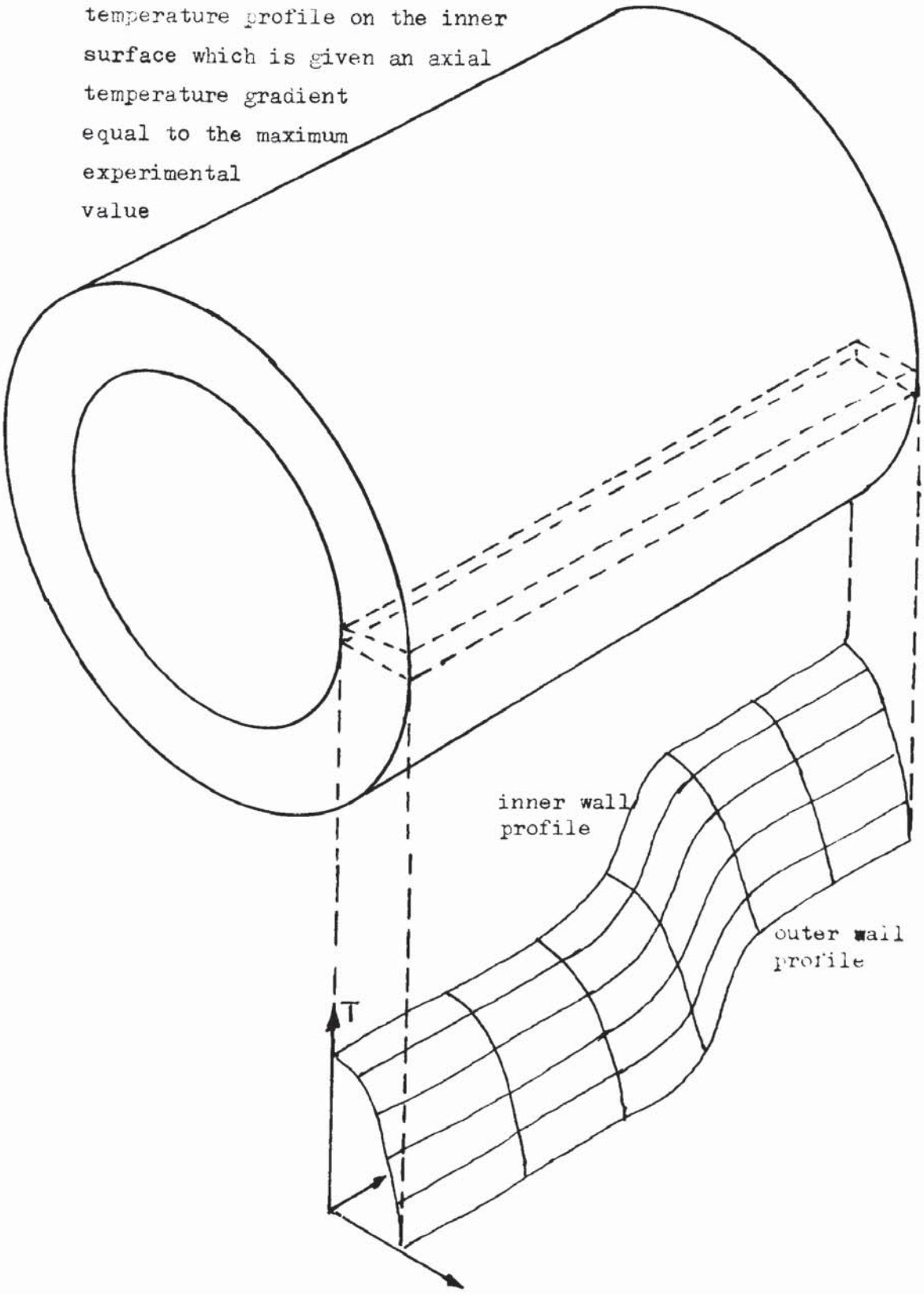

TEMPERATURE PROFILES IN THE WALL OF A ROUND TUBE

Adiabatic inner surface, Internal heat generation in the tube wall, Varying heat transfer coefficient on the cooled outer surface.

NUMERICAL METHOD TO SOLVE STEADY STATE CONDUCTION, RADIAL AND AXIAL, THROUGH A ROUND TUBE WITH INTERNAL HEAT GENERATION

FIELD POINT 1 $\uparrow I \quad \xrightarrow{J}$ $\quad J = 2,24 \; ; \quad I = 2,12$

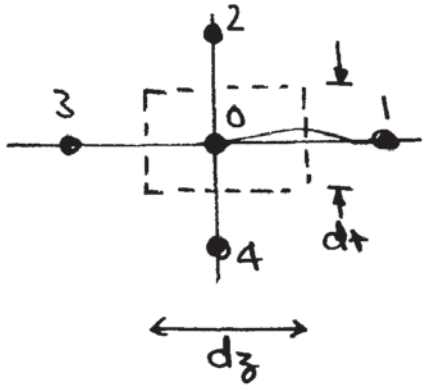

$$Q_{1-0} + Q_{2-0} + Q_{3-0} + Q_{4-0} + Q_g = 0$$

$$\frac{-k \cdot 2\pi r \cdot dr\,(t_0 - t_1)}{dz}$$

$$\frac{-k \cdot 2\pi(r+dr)\,dz\,(t_0 - t_2)}{dr}$$

$$\frac{-k \cdot 2\pi r\,dr\,(t_0 - t_3)}{dz} \quad \frac{-k \cdot 2\pi(r-dr)\,dz\,(t_0 - t_4)}{dr}$$

$$+ q_g \cdot 2\pi r \cdot dr \cdot dz = 0$$

Let $R1(I) = \dfrac{k \cdot dr}{dz}$: $R2(I) = \dfrac{k(r+dr)\,dz}{dr}$

$$\therefore R1(I)(t_1 + t_3 - 2t_0) + R2(I)(t_2 - t_0) + R3(I)(t_4 - t_0) + RQ(I) = 0$$

$$\therefore t_2 = t_0 + \frac{R1(I)(2t_0 - t_1 - t_3) + R3(I)(t_0 - t_4) - RQ(I)}{R2(I)}$$

i.e. $T(J, I+1) = T(J, I) + (R1(I) * (2.0 * J(J, I) - T(J+1, I) - T(J-1, I)) + R3(I) * (T(J, I) - T(J, I-1)) - RQ(I)) / R2(I)$

FIELD POINT 2 $\quad J = 1 \;,\quad I = 2, 12$

In this case $t_1 = t_3 = T(J+1, I) = T(2, I)$

i.e. $(1, I+1) = T(1, I) + (R1(I) * 2.0 * (T(1,I) - T(2,I)) + R3(I) * (T(1,I) - T(1,I-1)) - RQ(I)) / R2(I)$

FIELD POINT 3 $\quad J = 25 \;,\quad I = 2, 12$

In this case $t_1 = t_3 = T(J-1, I) = T(24, I)$

i.e. $T(25, I+1) = T(25, I) + (R1(I) * 2.0 * (T(25, I) - T(24, I)) + R3(I) * (T(25, I) - T(25, I-1)) - RQ(I)) / R2(I)$

FIELD POINT 4 $\quad \uparrow I \;\; \overrightarrow{J} \qquad I = 1 \qquad J = 2, 24$

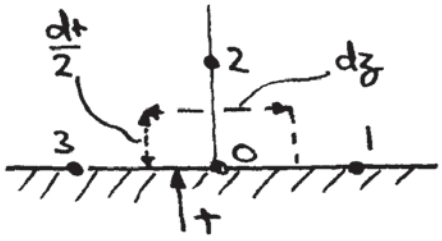

$$Q_{1-0} + Q_{2-0} + Q_{3-0} + Q_g = 0$$

$$\frac{-k \cdot 2\pi r \cdot \frac{dr}{2} (t_0 - t_1)}{dz}$$

$$- \frac{k\, 2\pi \left(r + \frac{dr}{2}\right) dz\, (t_0 - t_2)}{dr} - \frac{k\, 2\pi r \frac{dr}{2} (t_0 - t_3)}{dz}$$

$$+ q_g \cdot 2\pi r \frac{dr}{2} \cdot dz = 0$$

let $R4(I) = \dfrac{k\left(r + \frac{dr}{2}\right) dz}{dr}$

$$\therefore\ 0.5\, R1(I)(t_1 + t_3 - 2t_0) + R4(I)(t_2 - t_0) + 0.5\, RQ(I) = 0$$

$$t_2 = t_0 + \frac{0.5\left(R1(I)(2t_0 - t_1 - t_3) - RQ(I)\right)}{R4(I)}$$

i.e. $T(J,2) = T(J,1) + 0.5 * (R1(1) * (2.0 * T(J,1) - T(J+1,1) - T(J-1,1)) - RQ(1))/R4(1)$.

FIELD POINT 5 $\quad J = 1\ ,\ I = 1.$

In this case $t_1 = t_3 = T(J+1, I) = T(2,1)$

i.e. $T(1,2) = T(1,1) + 0.5 * (R1(1) * 2.0 * (T(1,1) - T(2,1)) - RQ(1))/R4(1)$

FIELD POINT 6 $\quad J = 25\ ,\ I = 1$

In this case $t_1 = t_3 = T(J-1, I) = T(24,1)$

i.e. $T(25,2) = T(25,1) + 0.5 * (R1(1) * 2.0 * (T(25,1) - T(24,1)) - RQ(1))/R4(1)$

$$= T(25,1) - 0.5 * RQ(1)/R4(1)$$

$$RD(1) = R(1) + 0.5 * DR \quad mm.$$

$$RD(I) = RD(I-1) + DR \quad mm \qquad I = 2, 12$$

$$R(I) = RD(I) - DR \quad mm \qquad I = 2, 12$$

$$R1(I) = TK * R(I) * DR / (DZ * 10**3) \quad kW/K, \quad I = 1, 12$$

$$R2(I) = TK * RD(I) * DZ / (DR * 10**3) \quad kW/K, \quad I = 2, 12$$

$$R3(I) = TK * R(I) * DZ / (DR * 10**3) \quad kW/K, \quad I = 2, 12$$

$$R4(1) = TK * RD(1) * DZ / (DR * 10**3) \quad kW/K$$

$$RQ(I) = QG * R(I) * DR * DZ / 10**9 \quad kW \qquad I = 1, 12$$

DATA, this probability function was taken to represent a typical form of temperature profile.

$TK = 0.016$ kW/m K, $QG = 320\,000.0$ kW/m^3

$R(1) = 8.33$ mm, $DZ = 2.0$ mm, $DR = 0.1$ mm

$$T(1,1) = 105.0\,^{\circ}C$$

$$B = ALOG(105.0/100.0)/900.0$$

$$T(J,1) = T(1,1)/EXP(B * ((J-1) * DZ)**2) \qquad J = 2, 16$$

$$T(J,1) = 100\,^{\circ}C \qquad J = 17, 25$$

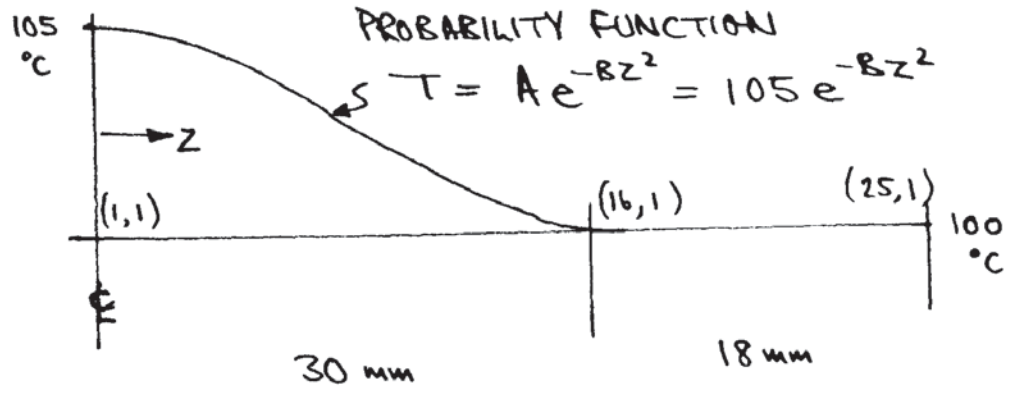

FLOW CHART FOR STEADY STATE CONDUCTION THROUGH CYLINDRICAL TUBE WITH INTERNAL HEAT GENERATION

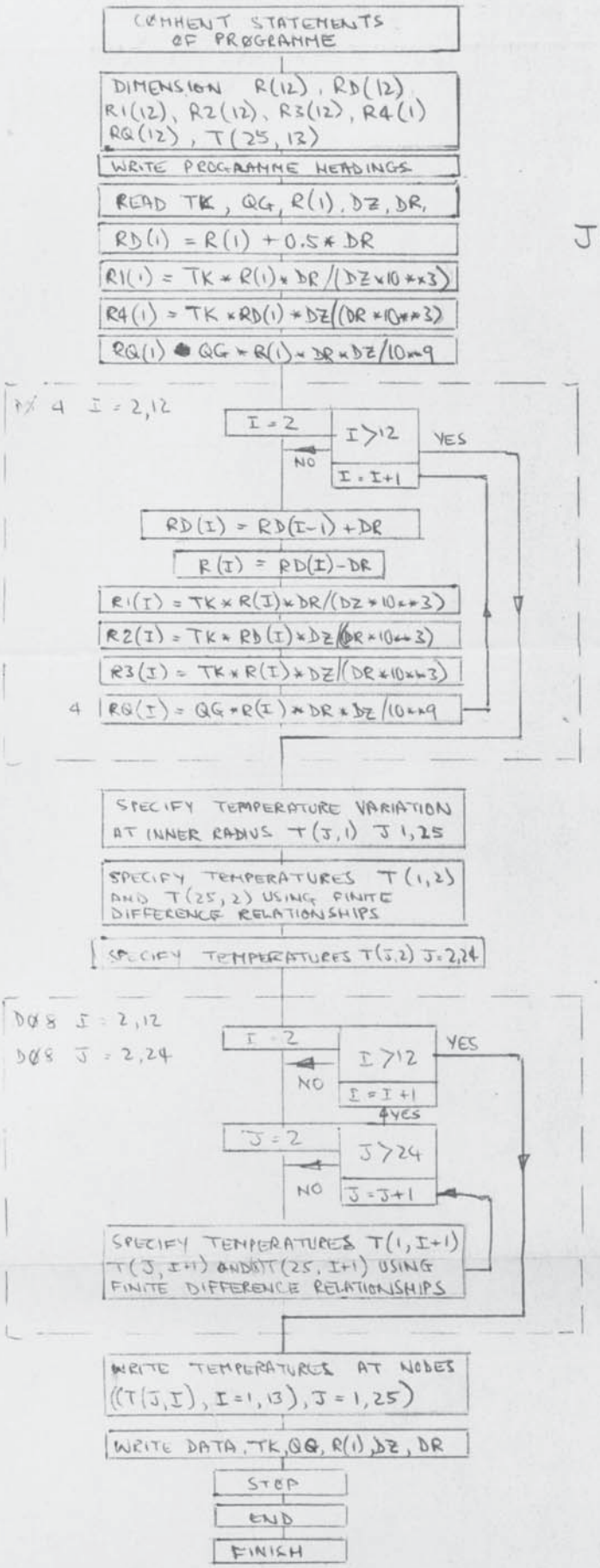

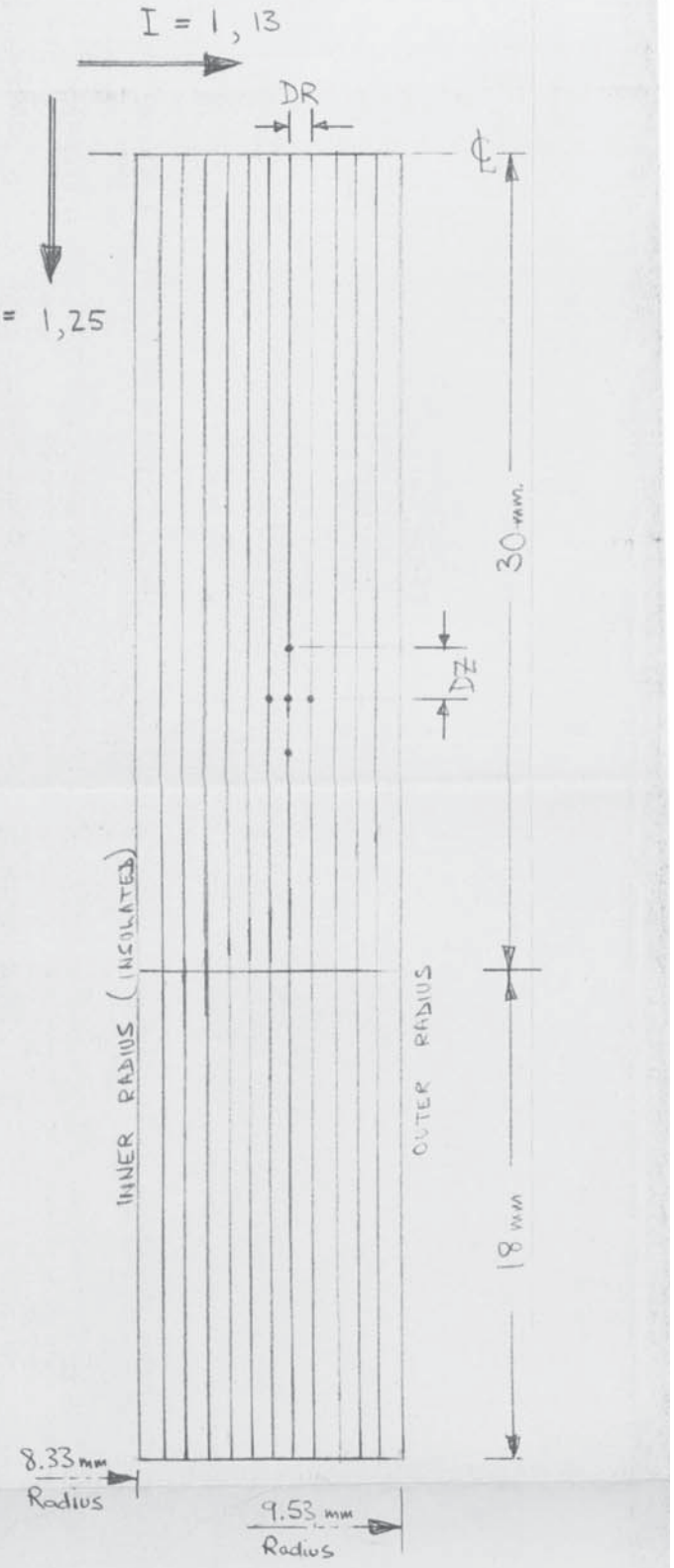

TK	QG	R(1)	DZ	DR
0.016	320000.0	8.33	2.0	0.1
kW/mK	kW/m³	mm	mm	mm

```
0012                TRACE 1
0013                READ FROM (CR)
0001                TRACE 2
0002                MASTER
0003          C     NUMERICAL METHOD TO SOLVE STEADY-STATE CONDUCTION (RADIAL AND      ATK  100
0004          C     AXIAL) THROUGH CYLINDRICAL TUBE WITH INTERNAL HEAT GENERATION      ATK  200
0005                DIMENSION R(12),RD(12),R1(12),R2(12),R3(12),RQ(12),T(25,13),R4(12)ATK  300
0006                WRITE(2,1)                                                        ATK  400
0007              1 FORMAT(1H1,20X,78HSTEADY-STATE CONDUCTION THROUGH CYLINDRICAL TUBEATK  500
0008               1 WITH INTERNAL HEAT GENERATION)                                   ATK  600
0009                WRITE(2,2)                                                        ATK  700
0010              2 FORMAT(1H0,45X,28HTEMPERATURES AT NODAL POINTS)                   ATK  800
0011                READ(1,3)TK,QG,R(1),DZ,DR                                         ATK  900
0012              3 FORMAT(5F0.0)                                                     ATK 1000
0013                RD(1)=R(1)+0.5*DR                                                 ATK 1100
0014                DZ3=DZ*1000.0                                                     ATK 1150
0015                DR3=DR*1000.0                                                     ATK 1160
0016                R1(1)=TK*R(1)*DR/DZ3                                              ATK 1200
0017                R4(1)=TK*RD(1)*DZ/DR3                                             ATK 1300
0018                RQ(1)=QG*R(1)*DR*DZ/1.0E 9                                        ATK 1400
0019                DO 4 I=2,12                                                       ATK 1500
0020                RD(I)=RD(I-1)+DR                                                  ATK 1600
0021                R(I)=RD(I)-DR                                                     ATK 1700
0022                R1(I)=TK*R(I)*DR/DZ3                                              ATK 1800
0023                R2(I)=TK*RD(I)*DZ/DR3                                             ATK 1900
0024                R3(I)=TK*R(I)*DZ/DR3                                              ATK 2000

0025              4 RQ(I)=QG*R(I)*DR*DZ/1.0E 9                                        ATK 2100
0026                T(1,1)=105.0                                                      ATK 2200
0027                B=ALOG(105.0/100.0)/900.0                                         ATK 2300
0028                DO 5 J=2,16                                                       ATK 2400
0029              5 T(J,1)=T(1,1)/EXP(B*((J-1)*DZ)**2)                                ATK 2500
0030                DO 6 J=17,25                                                      ATK 2600
0031              6 T(J,1)=100.0                                                      ATK 2700
0032                T(1,2)=T(1,1)+0.5*(R1(1)*2.0*(T(1,1)-T(2,1))-RQ(1))/R4(1)         ATK 2800
0033                T(25,2)=T(25,1)-0.5*RQ(1)/R4(1)                                   ATK 2900
0034                DO 7 J=2,24                                                       ATK 3000
0035              7 T(J,2)=T(J,1)+0.5*(R1(1)*(2.0*T(J,1)-T(J+1,1)-T(J-1,1))-RQ(1))/R4(ATK 3100
0036               11)                                                              ATK 3200
0037                DO 8 I=2,12                                                       ATK 3300
0038                DO 8 J=2,24                                                       ATK 3400
0039                T(1,I+1)=T(1,I)+(R1(I)*2.0*(T(1,I)-T(2,I))+R3(I)*(T(1,I)-T(1,I-1))ATK 3500
0040               1-RQ(I))/R2(I)                                                   ATK 3600
0041                T(J,I+1)=T(J,I)+(R1(I)*(2.0*T(J,I)-T(J+1,I)-T(J-1,I))+R3(I)*(T(J,IATK 3700
0042               1)-T(J,I-1))-RQ(I))/R2(I)                                        ATK 3800
0043              8 T(25,I+1)=T(25,I)+(R1(I)*2.0*(T(25,I)-T(24,I))+R3(I)*(T(25,I)-T(25ATK 3900
0044               1,I-1))-RQ(I))/R2(I)                                             ATK 4000
0045                WRITE(2,9)((T(J,I),I=1,13),J=1,25)                              ATK 4100
0046              9 FORMAT(/,13F9.3)                                                ATK 4200
0047                WRITE(2,10)TK,QG,R(1),DZ,DR                                     ATK 4300
0048                                                                                ATK 4400
0049             10 FORMAT(1H0,5X,4HTK =,F6.3,5X,4HQG =,F9.1,5X,17HINTERNAL RADIUS =,FATK 4500
0050               15.2,5X,4HDZ =,F4.1,5X,4HDR =,F4.1)                              ATK 4600
0051                STOP                                                            ATK 4700
0052                END                                                             ATK 4800

END OF SEGMENT, LENGTH   739, NAME  NONM

0053                FINISH                                                          ATK 4900

END OF COMPILATION -  NO ERRORS
```

STEADY-STATE CONDUCTION THROUGH CYLINDRICAL TUBE WITH INTERNAL HEAT GENERATION

TEMPERATURES AT NODAL POINTS

													ΔT
105.000	104.901	104.605	104.115	103.433	102.562	101.502	100.257	98.828	97.216	95.425	93.454	91.307	13.693
104.977	104.878	104.582	104.092	103.411	102.539	101.480	100.234	98.805	97.194	95.402	93.431	91.284	"
104.909	104.810	104.514	104.024	103.342	102.471	101.411	100.166	98.737	97.125	95.334	93.363	91.216	"
104.795	104.696	104.400	103.910	103.229	102.357	101.298	100.052	98.623	97.012	95.220	93.250	91.102	"
104.636	104.537	104.241	103.751	103.070	102.198	101.130	99.893	98.464	96.853	95.061	93.091	90.943	"
104.432	104.335	104.037	103.547	102.866	101.994	100.935	99.689	98.260	96.649	94.857	92.886	90.739	"
104.184	104.084	103.788	103.299	102.617	101.745	100.686	99.441	98.011	96.400	94.618	92.638	90.490	13.694
103.890	103.791	103.495	103.005	102.324	101.452	100.393	99.147	97.718	96.107	94.315	92.344	90.197	13.693
103.553	103.454	103.158	102.668	101.986	101.115	100.055	98.810	97.381	95.769	93.977	92.007	89.859	13.694
103.172	103.072	102.777	102.287	101.605	100.734	99.674	98.429	96.999	95.388	93.506	91.626	89.478	"
102.748	102.648	102.353	101.863	101.181	100.309	99.250	98.005	96.575	94.964	93.172	91.201	89.054	"
102.281	102.181	101.886	101.396	100.714	99.842	98.783	97.538	96.108	94.497	92.705	90.735	88.587	"
101.772	101.673	101.377	100.887	100.205	99.334	98.274	97.029	95.599	93.988	92.196	90.226	88.078	"
101.222	101.122	100.827	100.337	99.655	98.783	97.724	96.479	95.049	93.438	91.646	89.675	87.528	"
100.631	100.531	100.236	99.746	99.064	98.193	97.133	95.888	94.459	92.848	91.057	89.087	86.940	13.691
100.000	99.900	99.602	99.108	98.420	97.541	96.472	95.216	93.774	92.148	90.340	88.352	86.184	13.816
100.000	99.901	99.605	99.115	98.433	97.560	96.501	95.255	93.825	92.213	90.421	88.450	86.302	13.698
100.000	99.901	99.605	99.115	98.432	97.560	96.500	95.254	93.824	92.212	90.419	88.448	86.299	13.704
100.000	99.901	99.605	99.115	98.432	97.560	96.500	95.254	93.824	92.212	90.419	88.448	86.299	13.701
100.000	99.901	99.605	99.115	98.432	97.560	96.500	95.254	93.824	92.212	90.419	88.448	86.299	"
100.000	99.901	99.605	99.115	98.432	97.560	96.500	95.254	93.824	92.212	90.419	88.448	86.299	"
100.000	99.901	99.605	99.115	98.432	97.560	96.500	95.254	93.824	92.212	90.419	88.448	86.299	"
100.000	99.901	99.605	99.115	98.432	97.560	96.500	95.254	93.824	92.212	90.419	88.448	86.299	"
100.000	99.901	99.605	99.115	98.432	97.560	96.500	95.254	93.824	92.212	90.419	88.448	86.299	"
100.000	99.901	99.605	99.115	98.432	97.560	96.500	95.254	93.824	92.212	90.419	88.448	86.299	"

TK = 0.016 QG = 320000.0 INTERNAL RADIUS = 8.33 DZ = 2.0 DR = 0.1

BIBLIOGRAPHY

1. EDE A.J., HISLOP C.I., MORRIS R.
Effect on the local heat transfer coefficient in a pipe of an abrupt disturbance of the fluid flow.
I.Mech.E., Vol. 170, 1956, 1113-1130.

2. EDE A.J., MORRIS R., BIRCH E.S.
The effect of abrupt changes of diameter on heat transfer in pipes.
N.E.L., Report No. 73, 1962.

3. RICHARDSON B.L.
Some problems in horizontal two-phase two-component flow
Ph.D. Thesis, Purdue University, 1958.

4. FERRELL J.K., McGEE J.W.
Two-phase flow through abrupt expansions and contractions
North Carolina State University, Chem. Eng., 1966.

5. WIEGAND J.H., BAKER E.M.
Transfer processes in annuli
A.I.Chem.E., Vol. 38, 1942, 569-92.

6. MONRAD C.C., PELTON J.F.
Heat transfer by convection in annular spaces.
A.I.Chem.E., Vol. 38, 1942, 593-611.

7. DAVIS E.S.
Heat transfer and pressure drop in annuli
A.S.M.E., Vol.65, 1943, 755-9.

8. McMILLEN E.L., LARSON R.E.
Annular heat transfer coefficients for turbulent flow.
A.I.Chem.E., Vol. 40, 1944, 177-202.

9. CARPENTER F.G., COLBURN A.P., SCHOENBORN E.M.
Heat transfer and friction of water in an annular space.
A.I.Chem.E., Vol. 42, 1946, 165-87.

10. McADAMS W.H.
Heat transmission.
McGraw-Hill 1954, 242-3.

11. MOSCICKI I., BRODER J.
Roczniki Chem., Vol. 6, 1926,

12. NUKIYAMA S.,
Soc. Mech. Eng. Japan, Vol. 37, No. 206, 1934.

13. FARBER E.A., SCORAH R.L.
Heat transfer to water boiling under pressure
A.S.M.E., Chicago meeting, June 1947.

14. McADAMS W.H. et al
Heat transfer at high rates to water with surface boiling.
Ind. abd Eng. Chem., Vol. 41, No. 9, 1949, 1945-53.

15. KREITH F., SUMMERFIELD M.
Pressure drop and convective heat transfer with surface boiling at high heat flux; data for analine and n-butyl alcohol.
A.S.M.E., Vol. 72, No. 6, 1950, 869-879.

16. KREITH F., SUMMERFIELD M.
Heat transfer to water at high flux densities with and without surface boiling.
A.S.M.E., Vol. 71, No. 7, 1949, 805-815.

17. ROHSENOW W.M., CLARK J.A.
A study of the mechanism of boiling heat transfer.
A.S.M.E., Vol. 73, No. 5, 1951, 609-20.

18. GUNTHER F.C.
Photographic study of surface boiling heat transfer to water with forced convection.
A.S.M.E., H.T. Div., 1950

19. GUNTHER F.C., KREITH F.
Photographic study of bubble formation in heat transfer to subcooled water.
Jet Propulsion Lab., Cal. Inst. Tech., 1950.

20. JENS W.H., LOTTES P.A.
Analysis of heat transfer, burnout, pressure drop and density data for high pressure water.
U.S.A.E.C., A.N.L. - 4627, 1951.

21. ROHSENOW W.M.
A method of correlating heat transfer data for surface boiling of liquids.
A.S.M.E., Vol. 74, 1952, 969-76

22. JACOB M.
Heat Transfer,
John Wiley & Sons, 1949.

23. FRITZ W.
Berechnung des Maximalvolumens von Dampfblasen
Physikalische Zeitschrift, Vol. 36, 1935.

24. DONALD M.B., HASLAM F.
The mechanism of the transition from nucleate to film boiling.
Chem. Eng. Sc., Vol. 8, 1958, 287-94.

25. ADDOMS J.N.
Heat transfer at high rates to water boiling outside cylinders.
D.Sc. Thesis, M.I.T., 1948.

26. CICHELLI M.T., BONILLA C.F.
Heat transfer to liquids boiling under pressure.
A.I.Chem.E., Vol. 41, 1945, 755-787.

27. CRYDER D.S., FINALBORGO A.C.
Heat transmission from metal surfaces to boiling liquids: effect of temperature of the liquid on film coefficient.
A.I.Chem.E., Vol. 33, 1937, 346.

28. FORSTER H.K., ZUBER N.
Dynamics of vapour bubbles and boiling heat transfer.
A.I.Chem.E., Vol. 1, No. 4, 1955, 531-5.

29. DERGARABEDIAN P.
The rate of growth of vapour bubbles in superheated water.
A.S.M.E., J.App.Mech., Vol. 75, 1953, 537.

30. GRIFFITH P.
Bubble growth rates in boiling.
A.S.M.E., Paper 57-HT-2, 1958, 721-7.

31. BANKOFF G., MIKESELL R.D.
Growth of bubbles in a liquid of initially non-uniform temperature.
A.S.M.E., H.T. Div., 1958

32. LEVY S.
Generalised correlation of boiling heat transfer.
A.S.M.E., J.H.T., 1959, 37-42.

33. ENGELBERG-FORSTER K., GREIF R.
Heat transfer to a boiling liquid -- mechanism and correlations.
A.S.M.E., J.H.T., 1959, 43-53.

34. ELLION M.
Study of the mechanism of boiling heat transfer.
J.P.L., Pasadena, Calif., Memo 20-88, 1954.

35. IVEY H.J., MORRIS D.J.
On the relevance of the vapour-liquid exchange mechanism for subcooled boiling heat transfer at high pressure.
U.K.A.E.A., Reactor group, AEEW R-137, 1962.

36. AVERIN E.K.
Effect of material and machining of surface on heat transfer to boiling water.
Isv.Akad.Nauk. S.S.S.R., Otdel. Tekh., Nauk. No. 3, 1954.

37. SCHROCK V.E., GROSSMAN L.M.
Forced convection boiling in tubes
Nuc.Sc.Eng., Vol. 12, 1962, 474-81.

38. STERMAN L.S.
On the theory of heat transfer from a boiling liquid.
Zh.Tech.Fiz., Vol. 23, No. 2, 1953, 341-51.

39. HSU Y.Y., GRAHAM R.W.
An analytical and experimental study of the thermal boundary layer and ebullition cucle in nucleate boiling.
N.A.S.A., T.N. D-594, 1961.

40. BENNETT J.A.R., et.al.
Heat transfer to two-phase gas liquid systems.
Trans.I.Chem.E., Vol. 39, 1961, 113-125.

41. PAPELL S.S.
Subcooled boiling heat transfer under forced convection in a heated tube.
N.A.S.A., T.N. D-1583, 1963.

42. SHARP R.R.
The nature of liquid film evaporation during nucleate boiling.
N.A.S.A., T.N. D-1997, 1964.

43. BLATT T.A., ADT R.R.
An experimental investigation of boiling heat transfer and pressure drop characteristics of Freon-11 and Freon-113 refrigerants.
A.I.Chem.E., Vol. 10, No. 3, 1964, 369-73.

44. BERGLES A.E., ROHSENOW W.M.
The determination of forced convection surface boiling heat transfer.
A.S.M.E., J.H.T., 1964, 365-72.

45. CHEN J.C.
Correlation for boiling heat transfer to saturated fluids in convective flow.
Ind.Eng.Chem.Process Design Dev., Vol. 5, No. 3, 1966.

46. COLLIER J.G.
Convective boiling and condensation
McGraw-Hill, 1972, 214.

47. HODGSON A.S.
Forced convection subcooled boiling heat transfer with water in an electrically heated tube at 100-550 lb/in^2.
Trans.Inst.Chem.Eng., Vol. 46, 1968, 25-31.

48. ROBIN T.T., SNYDER N.W.
Bubble dynamics in subcooled nucleate boiling based on the mass transfer mechanism.
Int.J.Heat Mass Transfer, Vol. 13, 1970, 305-18.

49. JACOBS J.D., SHADE A.H.
Measurement of temperatures associated with bubbles in subcooled pool boiling.
A.S.M.E., J.H.T., 1969, 123-8.

50. VILLENEUVE J.
Visualisation of saturated and subcooled pool boiling by schlieren photography.
2nd. Joint USAEC-Euratom conference, Two-phase flow meeting, Maryland, 1964.

51. MOLES F.D., SHAW J.F.G.
Boiling heat transfer to subcooled liquids under conditions of forced convection.
Trans.Inst.Chem.Eng., Vol. 50, 1972, 76-84.

52. WALKER V., RAPIER A.C.
Errors in the measurement of surface temperature caused by perturbations of the heat flux.
I.Mech.E., Vol. 180, 1965-66.

53. MAYINGER F.
Investigations into the critical heat flux (burn-out) in boiling.
2nd. Joint USAEC-Euratom conference, Two-phase flow meeting, Maryland, 1964.

54. RAAD T., MYERS J.K.
Nucleation studies in pool boiling on thin plates using liquid crystals.
A.I.Chem.E., Vol. 17, 1971, 1260-1.

55. ZAREM et al.
An electro-optical shutter for photographic purposes.
NAVORD, Report No. 1016, Inyokern (Calif.)
U.S. Naval Ordnance Test Station, 1948.

56 BOWERSOX R.B.
Use of Kerr cells in a high speed camera.
Progress Report, No. 4-114, Pasadena.
Jet Prop. Lab. 1949.

57. HOLDER D.W., NORTH R.J.
Schlieren methods.
N.P.L., Notes on Applied Science, No. 31, 1963.

58. LINDSEY W.F., BURLOCK J.
A variable frequency light synchronised with a high speed motion picture camera to provide very short exposure times.
N.A.C.A. T.N. 2949, 1953.

59. MERTE H., CLARK J.A.
Pool boiling in an accelarating system
A.S.M.E., Paper 60-HT-22, 1960

60. GINVALA K. (Ed.)
Engineering study of vapour cycle cooling equipment for zero gravity environment.
Wright Air Dev. Div., T.R. 60-776, 1961, 37-65.

61. LOPINA R.F., BERGLES A.E.
Heat transfer and pressure drop in tape generated swirl flow.
M.I.T. Report No. 70281-47, AD-654739, 1967.

62. BERGLES A.E.
Survey and evaluation of techniques to augment convective heat and mass transfer.
Progress Heat Mass Transfer, Vol. 1, 1969.

63. BEWILOGUA L., KNONER R., WOLF G.
Heat transfer in boiling hydrogen, neon, nitrogen, and argon.
Cryogenics, Vol. 6, 1966, 36-9.

64. DENGLER C.E., ADDOMS J.N.
Heat transfer mechanism for vaporization of water in a vertical tube.
Chem.Eng.Prog.Symp.Series, Vol 52, 1953, 95-103.